frontiers | Research Topics

Case reports in infectious diseases – surveillance, prevention and treatment

Edited by
Ana Afonso and Francesco Paolo Bianchi

Published in
Frontiers in Medicine
Frontiers in Public Health

ISSN 1664-8714
ISBN 978-2-8325-3379-6
DOI 10.3389/978-2-8325-3379-6

About Frontiers

Frontiers is more than just an open access publisher of scholarly articles: it is a pioneering approach to the world of academia, radically improving the way scholarly research is managed. The grand vision of Frontiers is a world where all people have an equal opportunity to seek, share and generate knowledge. Frontiers provides immediate and permanent online open access to all its publications, but this alone is not enough to realize our grand goals.

Frontiers journal series

The Frontiers journal series is a multi-tier and interdisciplinary set of open-access, online journals, promising a paradigm shift from the current review, selection and dissemination processes in academic publishing. All Frontiers journals are driven by researchers for researchers; therefore, they constitute a service to the scholarly community. At the same time, the *Frontiers journal series* operates on a revolutionary invention, the tiered publishing system, initially addressing specific communities of scholars, and gradually climbing up to broader public understanding, thus serving the interests of the lay society, too.

Dedication to quality

Each Frontiers article is a landmark of the highest quality, thanks to genuinely collaborative interactions between authors and review editors, who include some of the world's best academicians. Research must be certified by peers before entering a stream of knowledge that may eventually reach the public - and shape society; therefore, Frontiers only applies the most rigorous and unbiased reviews. Frontiers revolutionizes research publishing by freely delivering the most outstanding research, evaluated with no bias from both the academic and social point of view. By applying the most advanced information technologies, Frontiers is catapulting scholarly publishing into a new generation.

What are Frontiers Research Topics?

Frontiers Research Topics are very popular trademarks of the *Frontiers journals series*: they are collections of at least ten articles, all centered on a particular subject. With their unique mix of varied contributions from Original Research to Review Articles, Frontiers Research Topics unify the most influential researchers, the latest key findings and historical advances in a hot research area.

Find out more on how to host your own Frontiers Research Topic or contribute to one as an author by contacting the Frontiers editorial office: frontiersin.org/about/contact

Case reports in infectious diseases – surveillance, prevention and treatment

Topic editors

Ana Afonso — NOVA University of Lisbon, Portugal

Francesco Paolo Bianchi — University of Bari Aldo Moro, Italy

Citation

Afonso, A., Bianchi, F. P., eds. (2023). *Case reports in infectious diseases – surveillance, prevention and treatment*. Lausanne: Frontiers Media SA.

doi: 10.3389/978-2-8325-3379-6

Table of contents

frontiers in Public Health

CASE REPORT
published: 22 February 2022
doi: 10.3389/fpubh.2022.849978

Emergence of Within-Host SARS-CoV-2 Recombinant Genome After Coinfection by Gamma and Delta Variants: A Case Report

*Ronaldo da Silva Francisco Junior[1], Luiz G. P. de Almeida[1], Alessandra P. Lamarca[1], Liliane Cavalcante[1], Yasmmin Martins[1], Alexandra L. Gerber[1], Ana Paula de C. Guimarães[1], Ricardo Barbosa Salviano[2], Fernanda Leitão dos Santos[2], Thiago Henrique de Oliveira[2], Isabelle Vasconcellos de Souza[3], Erika Martins de Carvalho[3], Mario Sergio Ribeiro[4], Silvia Carvalho[4], Flávio Dias da Silva[5], Marcio Henrique de Oliveira Garcia[5], Leandro Magalhães de Souza[6], Cristiane Gomes da Silva[6], Caio Luiz Pereira Ribeiro[5], Andréa Cony Cavalcanti[6], Claudia Maria Braga de Mello[4], Amilcar Tanuri[2] and Ana Tereza R. Vasconcelos[1]**

[1] Laboratório de Bioinformática, Laboratório Nacional de Computação Científica, Petrópolis, Brazil, [2] Departamento de Genética, Instituto de Biologia, Universidade Federal do Rio de Janeiro, Rio de Janeiro, Brazil, [3] Unidades de Apoio ao Diagnóstico da Covid-19, Rio de Janeiro, Brazil, [4] Secretaria Estadual de Saúde do Rio de Janeiro, Rio de Janeiro, Brazil, [5] Secretaria Municipal de Saúde Rio de Janeiro, Rio de Janeiro, Brazil, [6] Laboratório Central de Saúde Pública Noel Nutels, Rio de Janeiro, Brazil

In this study, we report the first case of intra-host SARS-CoV-2 recombination during a coinfection by the variants of concern (VOC) AY.33 (Delta) and P.1 (Gamma) supported by sequencing reads harboring a mosaic of lineage-defining mutations. By using next-generation sequencing reads intersecting regions that simultaneously overlap lineage-defining mutations from Gamma and Delta, we were able to identify a total of six recombinant regions across the SARS-CoV-2 genome within a sample. Four of them mapped in the spike gene and two in the nucleocapsid gene. We detected mosaic reads harboring a combination of lineage-defining mutations from each VOC. To our knowledge, this is the first report of intra-host RNA-RNA recombination between two lineages of SARS-CoV-2, which can represent a threat to public health management during the COVID-19 pandemic due to the possibility of the emergence of viruses with recombinant phenotypes.

Keywords: recombination, SARS-CoV-2, COVID-19, iSNVs, coinfection

OPEN ACCESS

Edited by:
Jessica L. Jones, United States Food and Drug Administration, United States

Reviewed by:
Safdar Ali, Aliah University, India
Tofazzal Islam, Bangabandhu Sheikh Mujibur Rahman Agricultural University, Bangladesh
Maharshi Pandya, Snake Research Institute, India
Setya Haksama, Airlangga University, Indonesia

****Correspondence:***
Ana Tereza R. Vasconcelos
atrv@lncc.br

Specialty section:
This article was submitted to Infectious Diseases - Surveillance, Prevention and Treatment, a section of the journal Frontiers in Public Health

Received: *06 January 2022*
Accepted: *24 January 2022*
Published: *22 February 2022*

Citation:
Francisco Junior RS, Almeida LGPd, Lamarca AP, Cavalcante L, Martins Y, Gerber AL, Guimarães APdC, Salviano RB, dos Santos FL, de Oliveira TH, de Souza IV, de Carvalho EM, Ribeiro MS, Carvalho S, da Silva FD, Garcia MHdO, de Souza LM, da Silva CG, Ribeiro CLP, Cavalcanti AC, de Mello CMB, Tanuri A and Vasconcelos ATR (2022) Emergence of Within-Host SARS-CoV-2 Recombinant Genome After Coinfection by Gamma and Delta Variants: A Case Report. Front. Public Health 10:849978. doi: 10.3389/fpubh.2022.849978

INTRODUCTION

Since the first reports of patients coinfected by two genetically-distinct lineages of SARS-CoV-2 (1–7), the scientific community raised concerns about the recombination of intra-host viral RNA sequences as a possible mechanism underlying the emergence of novel variants. Indeed, this phenomenon occurs at a relatively high frequency among betacoronaviruses (8–10). In SARS-CoV-2, signals of ongoing recombination were observed in a few sequences deposited in GISAID and circulating in North America (11, 12). Both studies showed evidence of recombination between non-variants of concern. Given the emergence and widespread dispersion of variants of concern (VOC) harboring advantageous mutation able to alter the virus phenotype around

the world, the possibility of recombination between them could represent a faster and more dangerous path to increase diversity facilitating the emergence of novel VOCs. The generation of recombinant genomes mainly requires (i) circulation of different lineages in the population, (ii) coinfection events, and (iii) intra-host recombination of the coinfected lineages. For this reason, we continuously monitored the presence of coinfected samples in the bam files of the samples originated from the state of Rio de Janeiro, Brazil. During the routine analysis across the 5,073 SARS-CoV-2 genomes generated by the Corona-ômica-RJ project (http://www.corona-omica.rj.lncc.br/#/), we identified the coinfection between Gamma and Delta reported next.

CASE DESCRIPTION

In late July, a 32-year-old male with mild flu-like symptoms of fever, headache, cough, fatigue, and sore throat was referred to the Santo Antônio de Pádua municipal health department in the northeastern region of the state of Rio de Janeiro, Brazil. After 2 days from the onset of symptoms, the diagnosis of COVID-19 was confirmed by the SARS-CoV-2 reverse transcriptase-polymerase chain reaction (RT-PCR) assay of a nasopharyngeal swab. Given the mild symptoms, no hospitalization was required and the patient was quarantined at home. No alterations in blood pressure or saturation were observed during the course of the disease. The patient did not report any comorbidities and had not been vaccinated by the time the sample was collected. The sample's relative quantification of the viral load ($RQVL = 2^{-\Delta CT}$) exhibited elevated values, with an RT-PCR cycle threshold (Ct) of 16.70 corresponding to the top 3% of samples with the highest viral load from Gamma variants in our database ($n = 1{,}881$). After 24 days from the symptoms onset, the patient presented the first negative RT-PCR test.

GENOMIC EVIDENCE OF COINFECTION AND RECOMBINATION

Whole-genome sequencing analysis detected 73 intra-host single nucleotide variants (iSNVs) with allele frequency >5% and depth >100 reads. Of these, 26 were lineage-defining mutations exclusively found in the variant of concern (VOC) Gamma (P.1) and 32 were from Delta (AY.33; **Supplementary Table 1**). By using a hypergeometric distribution approach (6), we estimate an overall haplotype frequency of approximately 16 and 82% for Delta and Gamma, respectively. Nevertheless, two iSNVs characteristics of VOC Delta (ORF1ab: I1091V—AF = 94%; and ORF7b: T40I—AF = 70%) were found with a high frequency in our analysis, suggesting that some genomic copies from Gamma haplotype could also harbor the same mutations (**Supplementary Table 1**).

We then sought to investigate the occurrence of within-host recombination events between the two lineages using next-generation sequencing. In theory, mutations characteristic of Gamma should be kept in different reads from those defining mutations of Delta. We divided the SARS-CoV-2 genome into windows with at least 100 nucleotides, which is smaller than the read length of the Illumina COVIDSeq Test (Illumina) sequencing kit used in this study. Next, we only selected windows that intersected at least two iSNVs, being one lineage-defining mutation from Gamma and the other from Delta. We aimed to detect unfragmented reads that covered the entire window harboring the iSNVs selected. A total of six recombinant candidate regions across the SARS-CoV-2 genome were found (see **Supplementary Material**), four mapped in the spike gene and two in the nucleocapsid gene (**Table 1**; **Figure 1**). We detected an average of two recombinant haplotypes supported by reads harboring a combination of the discriminating mutations from Gamma and Delta (**Table 1**; **Supplementary Figures 1–6**). In addition, the within-host recombinant sequences were formed by a single breakpoint event with a minimal and maximum interval of 15 and 75 nucleotides between two discriminate mutations where an event of recombination was observed, respectively.

From the six regions selected in our analysis, four overlapped the spike gene and two the nucleocapsid gene (**Figure 1**). All recombinant haplotypes were found at a low frequency compared to the reads supporting the sequences from each VOC (**Table 1**). Region I is located at the 5' region of the spike gene and includes three lineage-defining mutations from Gamma (S: L18F, T20N, and P26S) and one from Delta (S: T19R; **Supplementary Figure 1**). We identified two regions (II and III; **Supplementary Figures 2**, **3**) overlapping the receptor-binding domain (RBD). Region II included two amino acid residue alterations from Delta (S: L452R, T478K) and one from Gamma (S: E484K; **Supplementary Figure 2**). The T478K and E484K mutations were also present in Region III (**Supplementary Figure 3**), which harbored a second alteration from Gamma (S: N501Y). This region was the only window where three different recombinant haplotypes were observed (**Table 1**; **Supplementary Figure 3**). The last region (IV) in the spike includes only one mutation from Gamma (S: H655Y) and one from Delta (S: 681R; **Supplementary Figure 4**). At the 5′ portion of the nucleocapsid gene, we selected a window (region V; **Supplementary Figure 5**) containing a single mutation from Delta (N: D63G) and from Gamma (N: P80R). Finally, the largest region selected (VI) was also mapped in N and included four mutations from Gamma (N: S202C, S202T, R203K, G204R) and two from Delta (R203M, G215C; **Supplementary Figure 6**).

The recombination in our sample was detected during the first reports of Delta in the city of Santo Antônio de Pádua and an ongoing replacement of the variant Gamma by the Delta in the state of Rio de Janeiro. Nevertheless, genomic surveillance data from the state of Rio de Janeiro indicated a frequency of 47% of sequences from Delta and 37% from Gamma (13) in July 2021. Thus, the epidemiological, geographic, and genomic data provide a conducive scenario to SARS-CoV-2 recombination.

DISCUSSION

The designation of VOC prioritizes genome sequences harboring genetic markers with demonstrated evidence for increasing virus transmissibility, virulence, or decreasing the effectiveness of

TABLE 1 | Evidence of emergence of recombinant haplotypes within a sample coinfected by Gamma and Delta variants with the mutations characteristic of Gamma and Delta are highlighted in blue and red, respectively.

Region	Gene	Genomic interval	Number of bases	Number of defining mutations	Haplotypes	Number of reads	Protein Sequence	Classification	Amplicon ARTIC V3	Amplicon ARTIC V3 Coords	Coverage: mean (sd)
I	S	21,614–21,638	24	4	TCAT	843	18F, 19T, 20N, 26S	Gamma	71	21386 - 21716	1185 (± 308)
					CGCC	167	18L, 19R, 20T, 26P	Delta			
					CGCT	42	18L, 19R, 20T, 26S	Recombinant			
					TCAC	28	18F, 19T, 20N, 26P	Recombinant			
II	S	22,917–23,012	95	3	TCA	234	452L, 478T, 484K	Gamma	76	22821 - 23189	1197 (±232)
					GAG	35	452R, 478K, 484E	Delta			
					TAG	36	452L, 478K, 484E	Recombinant			
					TCG	20	452L, 478T, 484E	Recombinant			
III	S	22,995–23,063	68	3	CAT	533	478T, 484K, 501Y	Gamma	76	22821 - 23189	1197 (± 232)
					AGA	104	478K, 484E, 501N	Delta			
					AGT	42	478K, 484E, 501Y	Recombinant			
					CGA	30	478T, 484E, 501N	Recombinant			
					CAA	25	478T, 484K, 501N	Recombinant			
IV	S	23,525–23,604	79	2	TC	694	655Y, 681P	Gamma	78	23466 - 23822	2066 (± 715)
					CG	148	655H, 681R	Delta			
					TG	44	655Y, 681R	Recombinant			
					CC	39	655H, 681P	Recombinant			
V	N	28,461–28,512	51	2	AG	950	63D, 80R	Gamma	94	28416 - 28756	1952 (±532)
					GC	73	63G, 80P	Delta			
					GG	50	63G, 80R	Recombinant			
					AC	33	63D, 80P	Recombinant			
VI	N	28,877–28,916	39	6	TCAACG	822	202C, 203K, 204R, 215G	Gamma	95	28699 - 29041	1290 (±223)
					AGTGGT	101	202T, 203M, 204G, 215C	Delta			
					AGTGGG	40	202T, 203M, 204G, 215G	Recombinant			
					TCAACT	43	202C, 203K, 204R, 215C	Recombinant			

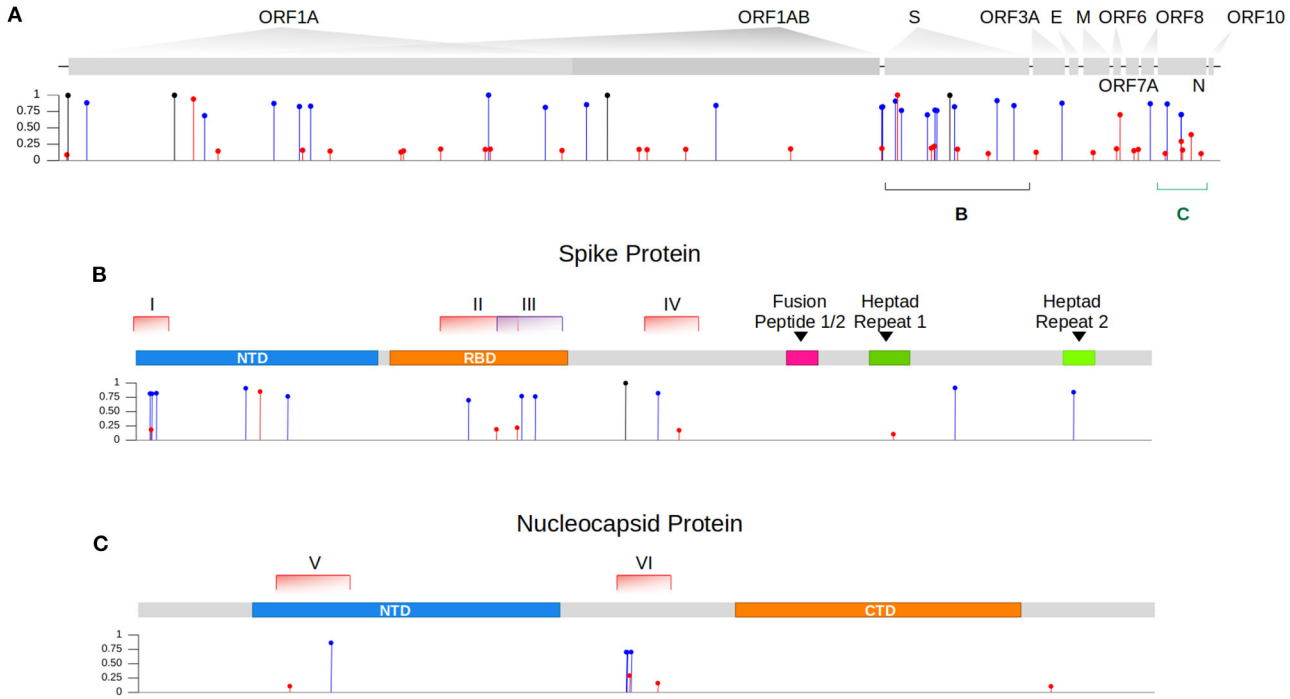

FIGURE 1 | Intra-host single nucleotide variant frequencies evidence coinfection by two genetically distinct lineages. **(A)** Identification of iSNVs across the different genes of the SARS-CoV-2 genome within our sample. In blue and red, we showed the lineage-defining mutations from the variant Gamma and Delta, respectively. iSNVs represented in black are mutations commonly found in both lineages that descend from their ancestor B.1. **(B)** Zoom in gene S showing the location of each genomic window (I-IV) where recombination events were investigated. **(C)** Zoom in gene N showing the distribution of both selected regions (V and VI) across the gene.

control measures. In this context, the VOC Gamma and Delta were notable by causing an elevated number of Covid-19 cases and deaths in Brazil and worldwide, respectively. Both VOC are known to enhance SARS-CoV-2 transmissibility and induce an immune-escape response. Therefore, recombination between both sequences could represent the emergence of novel variants of concern with new phenotypic combinations. For example, we noticed the presence of the mutation N501Y, a lineage-defining mutation from Gamma, in a haplotype carrying predominantly mutations from Delta in Region III. This mutation is widely known to increase ACE2 binding (14). We also observed the emergence of recombinant haplotypes that lost advantageous alleles such as those from Gamma harboring 484E in region II, 501N in region III, and from Delta carrying 681P in region IV.

Homologous recombination in positive-sense RNA viruses is driven by a copy-choice replication mechanism with a switch from an RNA template by the RNA-polymerase complex during replication (15, 16). Thus, the recombinant haplotypes found across the different regions selected can represent multiple events of switches occurring within a cell or a few switches from RNA templates simultaneously occurring at multiple cells. These variations could be associated with a mechanism of escaping the host's immune response and should be further investigated for the development of antiviral therapy and vaccines. Although the number of reads intersecting the discriminating iSNVs in the recombinant haplotypes seems to be small, we also observed a huge number of reads covering each mutation separately (**Supplementary Table 1**; median read depth: 1947). Thus, the read coverage and minor allele frequency in each site suggest that these mutations were not caused by low mapping quality or miscalling variant issues.

The hypothesis that the recombination might be the product of laboratory contamination is highly discouraged due to the protocol used by us. All viral particles are inactivated before RNA extraction, which stops replication and, consequently, impairs recombination from happening due to sample contamination. In addition, the high efficiency of ARTIC pool of primers utilized in our library construction rule out the possibility of the recombinant fragment being made by the initial PCR amplification step. Moreover, the 100 nucleotide window used in our genome scan and the similarity of sequence breakpoints analyzed in different genome regions make it difficult to imagine that it can be produced by the PCR step used in our library construction. One alternative speculation about the presence of mosaic reads in our sample is that the sequences could be generated by reverse mutational processes that rescue the ancestral state of the Wuhan reference sequence in each haplotype. Nevertheless, to consider an elevated number of reverse mutations happening at the same time in a coinfected sample would exceed the rate of intra-host evolution previously observed (4, 17). Even if this high rate would be accepted as real, it

is unlikely that these mutations would occur only in the "reverse direction" instead of generating a myriad of new substitutions.

Recent studies reported the detection of SARS-CoV-2 recombinant lineages circulating at a low frequency (11, 12, 18–21). Nevertheless, these studies were restricted to detecting the inter-host dissemination of genomes post-recombination events, which could be biased by spurious mutations generated due to library preparation, laboratory contamination, and unavailability of raw sequenced data. Our identification of a reliable recombination event between VOCs raises a red alert for the possible emergence of a new VOC in the future that combines advantageous mutations from independent lineages. Such an event could represent an evolutionary jump of SARS-CoV-2, immediately increasing the fitness of the VOC in a way that this hypothetical variant would fastly dominate current variants and generate a new wave worldwide (as currently seen with Omicron). While the recombination detected in this work involves mutations associated with fitness increase (L452R, E484K, N501Y), the absence of the recombinant sequences in SARS-CoV-2 samples was obtained posteriorly to this case suggests that it was not enough to supplant the circulating variants.

In summary, we report in this work the first case of intra-host SARS-CoV-2 recombination during a coinfection by the VOC Delta (AY.33) and Gamma (P.1) supported by sequencing reads harboring a mosaic of lineage-defining mutations as well as putative sequences breakpoints. We did not detect the circulation of the recombinant sequences in the state, so far. Nevertheless, such identification deeply depends on the access to raw read data from the state of Rio de Janeiro and other locations across the world. The faster detection and surveillance of recombinant SARS-CoV-2 genomes require an increase in the number of sequencing, specially in countries with an elevated number of cases, and rapid deposition of both assembled genomes and raw reads in public databases.

DATA AVAILABILITY STATEMENT

The datasets presented in this study can be found in online repositories. The names of the repository/repositories and accession number(s) can be found below: https://www.ncbi.nlm.nih.gov/, PRJNA774631.

ETHICS STATEMENT

The studies involving human participants were reviewed and approved by Ethics Committee (30161620.0.1001.5257 and 34025020.0.0000.5257). Written informed consent for participation was not required for this study in accordance with the national legislation and the institutional requirements.

AUTHOR CONTRIBUTIONS

ATRV: conceptualization. LC, ALG, APCG, RBS, FLS, and THO: DNA extraction and sequencing. IVS, EMC, MSR, SC, FDS, MHOG, LMS, CGS, CLPR, ACC, and CMBM: project administration. RSFJ, LGPA, APL, and YM: formal analysis. RSFJ and LGPA: data curation. ATRV: funding. RSFJ, APL, LGPA, and ATRV: writing – original draft. AT and ATRV: writing – review and editing. All authors contributed to the article and approved the submitted version.

FUNDING

This work was developed in the frameworks of Corona-ômica-RSFJ (FAPERJ = E-26/210.179/2020 and E-26/211.107/2021). ATRV is supported by CNPq (303170/2017-4) and FAPERJ (E-26/202.903/20). AT is supported by FAPERJ E-26/010.002434/2019 and E-26/210.178/2020. RSFJ is a recipient of a graduate fellowship from CNPq. APL is granted a post-doctoral scholarship (DTI-A) from CNPq. We acknowledge the support from the Rede Corona-ômica BR MCTI/FINEP affiliated to RedeVírus/MCTI (FINEP 01.20.0029.000462/20, CNPq 404096/2020-4).

ACKNOWLEDGMENTS

We would like to thank the patient for taking part in this study. We also acknowledge the authors and administrators of the GISAID database, which allowed this study of genomic epidemiology to be conducted properly.

SUPPLEMENTARY MATERIAL

The Supplementary Material for this article can be found online at: https://www.frontiersin.org/articles/10.3389/fpubh.2022.849978/full#supplementary-material

REFERENCES

1. Samoilov AE, Kaptelova VV, Bukharina AY, Shipulina OY, Korneenko EV, Saenko SS, et al. Case report: change of dominant strain during dual SARS-CoV-2 infection. *BMC Infect Dis.* (2021) 21:959. doi: 10.1186/s12879-021-06664-w
2. Hashim HO, Mohammed MK, Mousa MJ, Abdulameer HH, Alhassnawi ATS, Hassan SA, et al. Unexpected co-infection with different strains of SARS-CoV-2 in patients with COVID-19. *Preprints*. (2020) 1:1–17. doi: 10.20944/preprints202009.0375.v1
3. Tonkin-Hill G, Martincorena I, Amato R, Lawson AR, Gerstung M, Johnston I, et al. Patterns of within-host genetic diversity in SARS-CoV-2. *Elife*. (2021) 10:e66857. doi: 10.7554/eLife.66857
4. Lythgoe KA, Hall M, Ferretti L, de Cesare M, MacIntyre-Cockett G, Trebes A, et al. SARS-CoV-2 within-host diversity and transmission. *Science*. (2021) 372: 0821. doi: 10.1126/science.abg0821
5. Dezordi FZ, Resende PC, Naveca FG, do Nascimento VA, de Souza VC, Paixão ACD, et al. Unusual SARS-CoV-2 intra-host diversity reveals lineages superinfection. *MedRxiv [Preprint]*. (2021). doi: 10.1101/2021.09.18.21263755
6. Zhou H-Y, Cheng Y-X, Xu L, Li J-Y, Tao C-Y, Ji C-Y, et al. Genomic evidence for divergent co-infections of SARS-CoV-2 lineages. *bioRxiv [Preprint]*. (2021). doi: 10.1101/2021.09.03.458951
7. Francisco R da S Jr, Benites LF, Lamarca AP, de Almeida LGP, Hansen AW, Gularte JS, et al. Pervasive transmission of E484K and emergence of VUI-NP13L with evidence of SARS-CoV-2 co-infection events by

two different lineages in Rio Grande do Sul, Brazil. *Virus Res.* (2021) 296:198345. doi: 10.1016/j.virusres.2021.198345
8. Keck JG, Matsushima GK, Makino S, Fleming JO, Vannier DM, Stohlman SA, et al. In vivo RNA-RNA recombination of coronavirus in mouse brain. *J Virol.* (1988) 62:1810–3. doi: 10.1128/jvi.62.5.1810-1813.1988
9. Dudas G, Rambaut A. MERS-CoV recombination: implications about the reservoir and potential for adaptation. *Virus Evol.* (2016) 2:vev023. doi: 10.1093/ve/vev023
10. Hon C-C, Lam T-Y, Shi Z-L, Drummond AJ, Yip C-W, Zeng F, et al. Evidence of the recombinant origin of a bat severe acute respiratory syndrome (SARS)-like coronavirus and its implications on the direct ancestor of SARS coronavirus. *J Virol.* (2008) 82:1819–26. doi: 10.1128/JVI.01926-07
11. VanInsberghe D, Neish AS, Lowen AC, Koelle K. Recombinant SARS-CoV-2 genomes circulated at low levels over the first year of the pandemic. *Virus Evol.* (2021) 7:1–12 doi: 10.1093/ve/veab059
12. Gutierrez B, Castelán Sánchez HG, da Silva Candido D, Jackson B, Fleishon S, Ruis C, et al. Emergence and widespread circulation of a recombinant SARS-CoV-2 lineage in North America. *MedRxiv [Preprint].* (2021). doi: 10.1101/2021.11.19.21266601
13. Francisco Junior R da S, Lamarca AP, de Almeida LGP, Cavalcante L, Machado DT, Martins Y, et al. Turnover of SARS-CoV-2 lineages shaped the pandemic and enabled the emergence of new variants in the State of Rio de Janeiro, Brazil. *Viruses.* (2021) 13:2013. doi: 10.3390/v13102013
14. Starr TN, Greaney AJ, Hilton SK, Ellis D, Crawford KHD, Dingens AS, et al. Deep mutational scanning of SARS-CoV-2 receptor binding domain reveals constraints on folding and ACE2 binding. *Cell.* (2020) 182:1295–310.e20. doi: 10.1016/j.cell.2020.08.012
15. Cooper PD, Steiner-Pryor A, Scotti PD, Delong D. On the nature of poliovirus genetic recombinants. *J General Virol.* (1974) 23:41–9. doi: 10.1099/0022-1317-23-1-41
16. Worobey M, Holmes EC. Evolutionary aspects of recombination in RNA viruses. *J Gen Virol.* (1999) 80:2535–43. doi: 10.1099/0022-1317-80-10-2535
17. Voloch CM, da Silva Francisco Jr R, de Almeida LGP, Brustolini OJ, Cardoso CC, Gerber AL, et al. Intra-host evolution during SARS-CoV-2 prolonged infection. *Virus Evol.* (2021) 7:veab078. doi: 10.1093/ve/veab078
18. Jackson B, Boni MF, Bull MJ, Colleran A, Colquhoun RM, Darby AC, et al. Generation and transmission of interlineage recombinants in the SARS-CoV-2 pandemic. *Cell.* (2021) 184:5179–88.e8. doi: 10.1016/j.cell.2021.08.014
19. Varabyou A, Pockrandt C, Salzberg SL, Pertea M. Rapid detection of inter-clade recombination in SARS-CoV-2 with Bolotie. *Genetics.* (2021) 218:1–8. doi: 10.1093/genetics/iyab074
20. Yi H. 2019 novel coronavirus is undergoing active recombination. *Clin Infect Dis.* (2020) 71:884–7. doi: 10.1093/cid/ciaa219
21. Ignatieva A, Hein J, Jenkins PA. Ongoing recombination in SARS-CoV-2 revealed through genealogical reconstruction. *BioRxiv [Preprint].* (2021) 1:1–29. doi: 10.1101/2021.01.21.427579

Conflict of Interest: The authors declare that the research was conducted in the absence of any commercial or financial relationships that could be construed as a potential conflict of interest.

frontiers | Frontiers in Medicine

CASE REPORT
published: 09 May 2022
doi: 10.3389/fmed.2022.861087

Invasive Infection With *emm3*/ST15 *Streptococcus pyogenes*: The First Case Report From China and Complete Genome Analysis

Xinli Mu[1†], Yanfei Wang[1†], Lu Sun[1], Shanshan Zhao[2], Xi Jin[3], Junli Zhang[1], Yunsong Yu[1] and Xueqing Wu[1*]*

[1] Department of Infectious Diseases, Sir Run Run Shaw Hospital, Regional Medical Center for National Institute of Respiratory Diseases, Key Laboratory of Microbial Technology and Bioinformatics of Zhejiang Province, Hangzhou, China, [2] Department of Clinical Laboratory, Shangyu People's Hospital, Shaoxing, China, [3] Centre of Laboratory Medicine, Zhejiang Provincial People's Hospital, People's Hospital of Hangzhou Medical College, Hangzhou, China

OPEN ACCESS

Edited by:
Mattias Collin,
Lund University, Sweden

Reviewed by:
Andrei Nicoli Gebieluca Dabul,
University of São Paulo, Brazil
Bijit Bhowmik,
Croda, United Kingdom

***Correspondence:**
Yunsong Yu
yvys119@zju.edu.cn
Xueqing Wu
xueqing.wu@zju.edu.cn

[†]These authors have contributed equally to this work

Specialty section:
This article was submitted to Infectious Diseases – Surveillance, Prevention and Treatment, a section of the journal Frontiers in Medicine

Received: 24 January 2022
Accepted: 31 March 2022
Published: 09 May 2022

Citation:
Mu X, Wang Y, Sun L, Zhao S, Jin X, Zhang J, Yu Y and Wu X (2022) Invasive Infection With emm3/ST15 Streptococcus pyogenes: The First Case Report From China and Complete Genome Analysis. Front. Med. 9:861087. doi: 10.3389/fmed.2022.861087

Streptococcus pyogenes (GAS) may cause severe invasive disease with a high fatality rate, especially M3-type strains, which are less common in China. Here, we report the first *emm3*/ST15 invasive GAS infection case in China. The patient was diagnosed with severe skin and soft tissue infection (SSTI) and septicaemia caused by one GAS strain. Antibiotic susceptibility tests showed that the isolate was susceptible to all tested drugs. Antimicrobial therapy was then applied, and the patient fully recovered and was discharged from the hospital on Day 43. Whole-genome sequencing was carried out using the Illumina and Oxford Nanopore platforms and revealed this to be the first *emm3*/ST15-type GAS invasive infection in China. The closely related *emm3*/ST15-type GAS strains are MGAS315 from the United States and M3-b from Japan. Our finding is a warning that we should pay attention to invasive M3-type GAS infections in China and indicates the global spread of the highly virulent emm3/ST15 GAS strain.

Keywords: *Streptococcus pyogenes*, M type, *emm3*/ST15, invasive infection, whole-genome sequencing (WGS)

INTRODUCTION

Streptococcus pyogenes (Group A Streptococcus, GAS) is a common Gram-positive pathogenic bacterium that may induce various diseases, including minor ones, such as pharyngitis and scarlet fever, and serious ones, such as pneumonia and toxic shock syndrome (1). Severe GAS infections are less common but present a high fatality rate and have been reported worldwide (2–4). For example, the symptoms of GAS pharyngitis include fever, throat pain, and chills, while streptococcal toxic shock syndrome patients would develop multiorgan failure within a short time, leading to death (5, 6). It was reported a combined antibiotic therapy of penicillin and clindamycin would improve the outcomes of severe GAS infections (7).

The transmission of GAS would be through direct person-to-person *via* the inhalation of respiratory droplets, or through direct contact with contaminated objects (8). The increment in the incidence of GAS invasive infections has been associated with particular clones and varies by time

and region, which may reflect a population's susceptibility to specific strains (9, 10). GAS strains can be serologically separated into M protein serotypes based on a surface protein encoded by the *emm* gene (1). In clinical epidemiological studies, M1 and 3 are the most common GAS serotypes of invasive and toxic streptococcal diseases. Among the different sequence types of M3 strains, *emm3*/ST15-induced toxic shock syndrome and other invasive diseases have often been reported in Japan, United Kingdom, and United States (11).

In the past, we considered that M3 GAS infections were rare in China, but a recent large-scale epidemiological study indicated that M3 GAS scarlet fever has increased substantially in China since 2018 (12) and became one of the prevalent *emm* types that induced scarlet fever in 2019 (13). Here, we report the first case of a severe GAS infection caused by the *emm3*/ST15 GAS strain SHZ-1 in China. The complete genome sequence of this strain was also analyzed in the current study.

METHODS

Bacterial Isolation and Antimicrobial Susceptibility Testing

Wound secretion specimens were submitted to the clinical laboratory of Zhejiang local hospital for slide microscopy and bacterial culture using 5% sheep blood agar plates. A GAS strain was obtained and identified by matrix-assisted laser desorption ionization-time of flight mass spectrometry (Bruker Daltonics, Bremen, Germany) (14). Antimicrobial susceptibility testing (AST) of levofloxacin, chloramphenicol, clindamycin, ceftriaxone, erythromycin, penicillin, tetracycline, and vancomycin against the identified GAS strain, named SHZ-1, was performed using a disk diffusion method, and the results were interpreted according to the Clinical and Laboratory Standards Institute (15).

Whole-Genome Sequencing and Analysis

Genomic DNA of strain SHZ-1 (single colony) was prepared using a DNA mini kit (Qiagen, Valencia, CA, United States) and submitted to next-generation sequencing (NGS) and long-read sequencing using the Illumina HiSeq2000TM (Illumina Inc., San Diego, CA, United States) and Oxford Nanopore MinION platforms (Oxford Nanopore Technologies, Oxford, United Kingdom), respectively. The Illumina sequencing generated 9.1M reads with an average of ∼150 bp per read and 200 X coverage. The nanopore sequencing of this strain generated 139 contigs with an N50 of 1329619 bp and a GC content of 39.22%. Both short and long reads were used for *de novo* assembly *via* Unicycler version 1.0 (15) in a hybrid assembly model with default parameters. The genome was then used as input for *in silico* multilocus sequence typing (MLST) *via* BLAST against the PubMLST database (16), *emm* typing against the CDC emm type and subtype database tsemm (17). The annotation of SHZ-1 was performed *via* Prokka against *S. pyogenes* database (18). The annotated genome was then used for virulence factor detection against the VFDB database (19). Both SNP and cgMLST strategies were performed in the BacWGSTdb server (20) for bacterial source tracking. An *ad hoc* cgMLST scheme for *S. pyogenes* (1,170 target genes) was designed to characterize the gene-by-gene allelic profile of *S. pyogenes* strains. The identified *S. pyogenes* strain SHZ-1 was used as the reference genome in this analysis. SNP distance matrices were calculated using snp-dists 0.6.3 (21).

RESULTS

Case Presentation

A 37-year-old man injured his left foot at work 4 days prior to admission. He immediately felt pain, but it was tolerable and he had no open wounds; hence, he ignored the symptoms. The injured foot developed skin redness, swelling, and obvious tenderness 1 day later. The patient developed a conscious fever accompanied by chills, dizziness, abdominal pain, and distension. The symptoms worsened after another 2 days, and the patient was then admitted to the local hospital, Zhejiang, China. His lab results showed leukocyte counts of 22.3×10^9/L with 92.3% neutrophils, and an X-ray showed no fracture. Based on this, the diagnoses of severe skin and soft tissue infection (SSTI) was made. Three days of sulbenicillin (4 g/q12 h) and levofloxacin (0.5 g bid) treatment showed no improvement. After debridement, postoperative anti-infection treatment with vancomycin (1.0/q8 h) was applied. Leukocyte counts were still high with elevated levels of procalcitonin, and the patient was diagnosed with septicemia. X-ray confirmed no migrating lung lesions. On the fourth day of admission, a specimen culture was confirmed to be positive for GAS. AST showed that the bacterial isolate was susceptible to all tested drugs (**Supplementary Table 2**). Antimicrobial therapy was then applied with linezolid (0.6 g q12 h) and amoxicillin/clavulanate potassium (1.2 g q6 h). Declines in all inflammatory indices were then observed. Thereafter, the patient improved from GAS infection after 11 days of treatment and was transferred to debridement, suture, and skin grafting. The patient was treated with amoxicillin/clavulanate potassium (1.2 g q8 h) for another 6 days since Day 37 due to GAS culture positivity. The patient fully recovered and was discharged from the hospital on Day 43 (**Figure 1**).

Whole-Genome Analysis

Hypervirulent invasive GAS infections are rare in China. To better understand the pathogen in the current case, the strain was sent for whole-genome sequencing. The complete chromosome data of SHZ-1 were submitted to NCBI (Genbank No.CP072523.1). After the hybrid assembly, we obtained a 1819973 bp complete circular genome of GAS strain SHZ-1 with a GC content of 38.6%. We identified SHZ-1 as an *emm3*/ST15-type GAS strain *via emm* typing and MLST analysis (**Supplementary Figure**). Then we downloaded the complete genome of *emm3*/ST15 GAS strains that were isolated from different regions. Using BacWGSTdb to determine the clonal relationship among these isolates according to the pairwise comparison of the cgMLST alleles or SNP differences. In

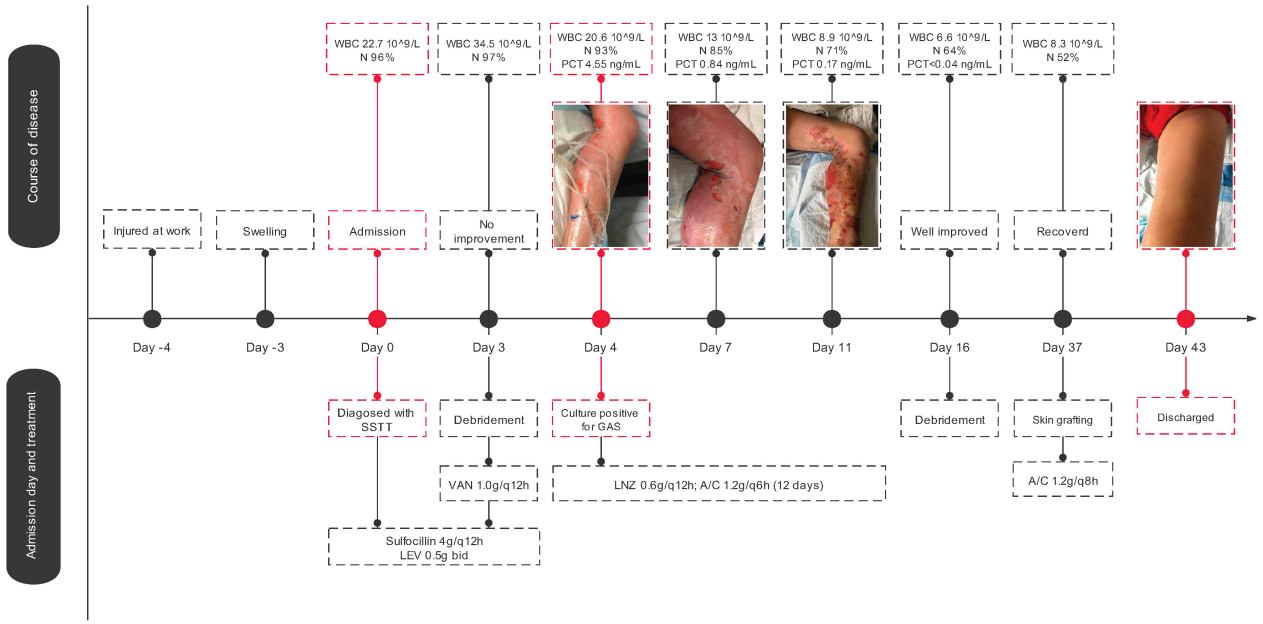

FIGURE 1 | *Streptococcus pyogenes* strain SHZ-1 infection history and genomic epidemiological analysis. The medical history of SHZ-1 infected patient. Abbreviations in the figure: SSTI, skin and soft tissue infection; LEV, Levofloxacin; VAN, vancomycin; LNZ, linezolid; WBC, white blood cell; N, neutrophils; PCT, procalcitonin; A/C, amoxicillin/clavulanate.

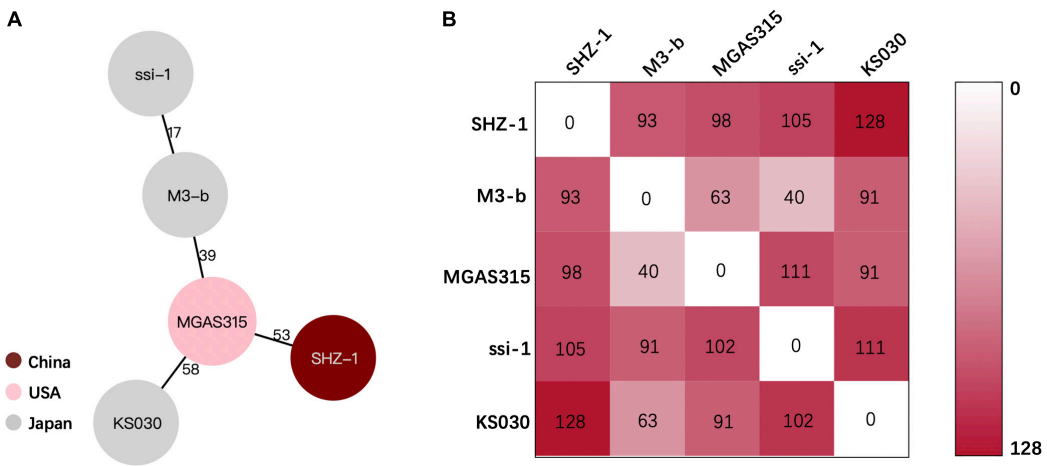

FIGURE 2 | Phylogenetic relationship between SHZ-1 and the closely related *Streptococcus pyogenes* strains. **(A)** The lines connecting the circles indicate the clonal relationship between different isolates and the digital numbers on the lines illustrate the number of allelic differences. **(B)** The single-nucleotide polymorphisms (SNPs) numbers between each *S. pyogenes* strain. The gradient of purple intensity illustrates the quantity of SNPs.

the end, the phylogenetic relatedness showed that the closest strain to SHZ-1 was MGAS315 from the United States, which has 53 core gene differences (**Figure 2A**). The SNP calling results indicated that the smallest SNP number of 93 was determined between strains SHZ-1 and M3-b from Japan (**Figure 2B**). Virulence factor detection against VFDB showed that SHZ-1 had all the virulence factors found in the other two *emm3*/ST15 strains (MGA315 and M3-b) except the streptococcal superantigen SSA-encoding gene *ssa* (**Supplementary Table 2**).

DISCUSSION

Streptococcus pyogenes serotype M3 strain-induced invasive infections have been widely reported worldwide, although they have not been common in recent years in China. We report the first case of the *emm3*/ST15 GAS strain causing severe invasive infection in China.

Recent large-scale epidemiological studies have reported an M-type shift of scarlet fever GAS isolates in China, which clearly showed that M3 GAS has become one of the most prevalent

strains in Beijing, China, since 2018 (1, 2). Our reported severe infection case indicates the emergence of widespread M3 strains in China, which belong to the most virulent strain *emm3*/ST15. Whole-genome analysis of SHZ-1 showed that the closest strain was MGAS315 from United States (22) and then M3-b from Japan (23). Both strains are invasive isolates from patients with streptococcal toxic shock syndrome in the late 1980s and 1994, respectively. Later, whole-genome analysis of these two and other *emm3*/ST15 strains showed that their association with severe infections was due to their distinct arrays of virulence factors, for example, *speA*-encoded streptococcal pyrogenic exotoxin A and *ssa*-encoded streptococcal superantigen A (22). The latter is a phage-associated streptococcal superantigen that is missing in our reported strain SHZ-1 but is encoded in both the MGAS315 and M2-b genomes. *ssa* has been detected in toxic shock syndrome-related M3 isolates (24), but only 25% of *emm3*-type GAS isolates are from Chinese patients (13). In our reported case, strain SHZ-1 that lacked the *ssa* gene still presented a strong pathogenesis in the host. We believe that genetically related *emm*/ST15 GAS strains may have geographic characteristics for their virulence, and a large-scale molecular epidemiology study of invasive GAS infection in China is needed.

In conclusion, we report the first *emm3*/ST15 invasive GAS infection in China. The complete genome analysis of pathogenic GAS strain SHZ-1 indicates the emergence of the global spread of highly virulent *emm3*/ST15-type GAS. This is a warning that attention should be paid to the epidemiology of M3-type GAS in China to prevent severe invasive GAS infections.

ETHICS STATEMENT

Written informed consent was obtained from the patient for the publication of any potentially identifiable images or data included in this article.

AUTHOR CONTRIBUTIONS

XM, JZ, and LS collected the clinical data. YW and SZ did the laboratory work. XW and YY designed the study and wrote the manuscript. All authors contributed to the article and approved the submitted version.

FUNDING

This study was supported by National Natural Science Foundation of China (No. 32000092).

ACKNOWLEDGMENTS

We acknowledge Xiaoliang He for experiments materials collection and arrangement.

SUPPLEMENTARY MATERIAL

The Supplementary Material for this article can be found online at: https://www.frontiersin.org/articles/10.3389/fmed.2022.861087/full#supplementary-material

REFERENCES

1. Cunningham MW. Pathogenesis of group A streptococcal infections. *Clin Microbiol Rev.* (2000) 13:470–511. doi: 10.1128/CMR.13.3.470
2. Wong CJ, Stevens DL. Serious group a streptococcal infections. *Med Clin North Am.* (2013) 97:721–36. doi: 10.1016/j.mcna.2013.03.003
3. Blagden S, Watts V, Verlander NQ, Pegorie M. Invasive group A streptococcal infections in North West England: epidemiology, risk factors and fatal infection. *Public Health.* (2020) 186:63–70. doi: 10.1016/j.puhe.2020.06.007
4. Leung TN, Hon KL, Leung AK. Group A *Streptococcus* disease in Hong Kong children: an overview. *Hong Kong Med J.* (2018) 24:593–601. doi: 10.12809/hkmj187275
5. Mustafa Z, Ghaffari M. Diagnostic methods, clinical guidelines, and antibiotic treatment for group a streptococcal pharyngitis: a narrative review. *Front Cell Infect Microbiol.* (2020) 10:563627. doi: 10.3389/fcimb.2020.563627
6. Belkassa K, Khelifa M, Batonneau-Gener I, Marouf-Khelifa K, Khelifa A. Understanding of the mechanism of crystal violet adsorption on modified halloysite: hydrophobicity, performance, and interaction. *J Hazard Mater.* (2021) 415:125656. doi: 10.1016/j.jhazmat.2021.125656
7. Babiker A, Li X, Lai YL, Strich JR, Warner S, Sarzynski S, et al. Effectiveness of adjunctive clindamycin in beta-lactam antibiotic-treated patients with invasive beta-haemolytic streptococcal infections in US hospitals: a retrospective multicentre cohort study. *Lancet Infect Dis.* (2021) 21:697–710. doi: 10.1016/S1473-309930523-5
8. Kemble SK, Westbrook A, Lynfield R, Bogard A, Koktavy N, Gall K, et al. Foodborne outbreak of group a *Streptococcus* pharyngitis associated with a high school dance team banquet–Minnesota, 2012. *Clin Infect Dis.* (2013) 57:648–54. doi: 10.1093/cid/cit359
9. Luca-Harari B, Darenberg J, Neal S, Siljander T, Strakova L, Tanna A, et al. Clinical and microbiological characteristics of severe *Streptococcus pyogenes* disease in Europe. *J Clin Microbiol.* (2009) 47:1155–65. doi: 10.1128/JCM.02155-08
10. O'Brien KL, Beall B, Barrett NL, Cieslak PR, Reingold A, Farley MM, et al. Epidemiology of invasive group a *Streptococcus* disease in the United States, 1995-1999. *Clin Infect Dis.* (2002) 35:268–76. doi: 10.1086/341409
11. Sekizuka T, Nai E, Yoshida T, Endo S, Hamajima E, Akiyama S, et al. Streptococcal toxic shock syndrome caused by the dissemination of an invasive emm3/ST15 strain of *Streptococcus pyogenes*. *BMC Infect Dis.* (2017) 17:774. doi: 10.1186/s12879-017-2870-2
12. You Y, Peng X, Yang P, Wang Q, Zhang J. 8-year M type surveillance of *Streptococcus pyogenes* in China. *Lancet Infect Dis.* (2020) 20:24–5. doi: 10.1016/S1473-309930694-2
13. Li H, Zhou L, Zhao Y, Ma L, Xu J, Liu Y, et al. Epidemiological analysis of group A *Streptococcus* infections in a hospital in Beijing. *China. Eur J Clin Microbiol Infect Dis.* (2020) 39:2361–71. doi: 10.1007/s10096-020-03987-5
14. Croxatto A, Prod'hom G, Greub G. Applications of MALDI-TOF mass spectrometry in clinical diagnostic microbiology. *FEMS Microbiol Rev.* (2012) 36:380–407. doi: 10.1111/j.1574-6976.2011.00298.x
15. Wayne PA, CLSI. *Performance Standards for Antimicrobial Susceptibility Testing.* 28th ed. Wayne, PA: Clinical and Laboratory Standards Institute (2018).
16. Enright MC, Spratt BG, Kalia A, Cross JH, Bessen DE. Multilocus sequence typing of *Streptococcus pyogenes* and the relationships between emm type

and clone. *Infect Immun.* (2001) 69:2416–27. doi: 10.1128/IAI.69.4.2416-2427.2001
17. CDC. *Streptococcus* Laboratory: Centers for Disease Control and Prevention. Atlanta, GA: Centers for Disease Control and Prevention (1949).
18. Seemann T. Prokka: rapid prokaryotic genome annotation. *Bioinformatics.* (2014) 30:2068–9. doi: 10.1093/bioinformatics/btu153
19. Chen L, Yang J, Yu J, Yao Z, Sun L, Shen Y, et al. VFDB: a reference database for bacterial virulence factors. *Nucleic Acids Res.* (2005) 33:D325–8. doi: 10.1093/nar/gki008
20. Ruan Z, Feng Y. BacWGSTdb, a database for genotyping and source tracking bacterial pathogens. *Nucleic Acids Res.* (2016) 44:D682–7. doi: 10.1093/nar/gkv1004
21. Seeman TKF, Page AJ. *Snp-Dists*. San Francisco, CA: GitHub, Inc (2022).
22. Beres SB, Sylva GL, Barbian KD, Lei B, Hoff JS, Mammarella ND, et al. Genome sequence of a serotype M3 strain of group A *Streptococcus*: phage-encoded toxins, the high-virulence phenotype, and clone emergence. *Proc Natl Acad Sci USA.* (2002) 99:10078–83. doi: 10.1073/pnas.152298499
23. Ogura K, Watanabe S, Kirikae T, Miyoshi-Akiyama T. Complete genome sequence and comparative genomics of a *Streptococcus pyogenes* emm3 strain M3-b isolated from a Japanese patient with streptococcal toxic shock syndrome. *J Genomics.* (2017) 5:71–4. doi: 10.7150/jgen.20915
24. Mollick JA, Miller GG, Musser JM, Cook RG, Grossman D, Rich RR. A novel superantigen isolated from pathogenic strains of *Streptococcus pyogenes* with aminoterminal homology to staphylococcal enterotoxins B and C. *J Clin Invest.* (1993) 92:710–9. doi: 10.1172/JCI116641

Conflict of Interest: The authors declare that the research was conducted in the absence of any commercial or financial relationships that could be construed as a potential conflict of interest.

Publisher's Note: All claims expressed in this article are solely those of the authors and do not necessarily represent those of their affiliated organizations, or those of the publisher, the editors and the reviewers. Any product that may be evaluated in this article, or claim that may be made by its manufacturer, is not guaranteed or endorsed by the publisher.

frontiers | Frontiers in Public Health

CASE REPORT
published: 26 May 2022
doi: 10.3389/fpubh.2022.910872

First Case Report of Human Plague Caused by Excavation, Skinning, and Eating of a Hibernating Marmot (*Marmota himalayana*)

Jinxiao Xi[1†], Ran Duan[2†], Zhaokai He[2†], Lei Meng[1], Daqin Xu[1], Yuhuang Chen[3], Junrong Liang[2], Guoming Fu[4], Li Wang[5], Hua Chun[4], Shuai Qin[2], Dongyue Lv[2], Hui Mu[2], Deming Tang[2], Weiwei Wu[2], Meng Xiao[2], Huaiqi Jing[2] and Xin Wang[2]*

[1] Gansu Provincial Center for Disease Control and Prevention, Lanzhou, China, [2] State Key Laboratory of Infectious Disease Prevention and Control, National Institute for Communicable Disease Control and Prevention, Chinese Center for Disease Control and Prevention, Beijing, China, [3] Shenzhen Nanshan Maternity and Child Health Care Hospital, Shenzhen, China, [4] Subei Mongolian Autonomous County Center for Disease Control and Prevention, Jiuquan, China, [5] Jiuquan Municipal Center for Disease Control and Prevention, Jiuquan, China

OPEN ACCESS

Edited by:
Yousef Saleh Khader,
Jordan University of Science and Technology, Jordan

Reviewed by:
Victor Suntsov,
Ishlinsky Institute for Problems in Mechanics (RAS), Russia
Joel Bozue,
United States Army Medical Research Institute of Infectious Diseases (USAMRIID), United States

***Correspondence:**
Xin Wang
wangxin@icdc.cn

[†] These authors have contributed equally to this work

Specialty section:
This article was submitted to Infectious Diseases - Surveillance, Prevention and Treatment, a section of the journal Frontiers in Public Health

Received: 01 April 2022
Accepted: 20 April 2022
Published: 26 May 2022

Citation:
Xi J, Duan R, He Z, Meng L, Xu D, Chen Y, Liang J, Fu G, Wang L, Chun H, Qin S, Lv D, Mu H, Tang D, Wu W, Xiao M, Jing H and Wang X (2022) First Case Report of Human Plague Caused by Excavation, Skinning, and Eating of a Hibernating Marmot (Marmota himalayana). Front. Public Health 10:910872. doi: 10.3389/fpubh.2022.910872

Introduction: The Qinghai-Tibet Plateau is considered the most plague-heavy region in China, and skinning and eating marmots (*Marmota himalayana*) are understood to be the main exposure factors to plague. *Yersinia pestis* is relatively inactive during marmots' hibernation period. However, this case report shows plague infection risk is not reduced but rather increased during the marmot hibernation period if plague exposure is not brought under control.

Case Presentation: The patient was a 45-year-old man who presented with high fever, swelling of axillary lymph nodes, and existing hand wounds on his right side. *Y. pestis* was isolated from his blood and lymphatic fluid. Hence, the patient was diagnosed with a confirmed case of bubonic plague. Later, his condition progressed to septicemic plague. Plague exposure through wounds and delays in appropriate treatment might have contributed to plague progression.

Conclusion: This case report reveals that excavating a hibernating marmot is a significant transmission route of plague. Plague prevention and control measures are priority needs during the marmot hibernation period.

Keywords: hibernation, plague control, *Yersinia pestis*, *Marmota himalayana*, case report

INTRODUCTION

Plague is a highly virulent zoonotic disease mainly transmitted by fleabites and contact with contaminated animal tissues (1). Skinning and eating *Marmota himalayana* is a major transmission route of plague in the *M. himalayana* plague focus, where plague is most active and virulent in China (2). During marmot hibernation, the risk of plague infection seems to be reduced owing to no marmot activity or contact with humans. However, in this case report, we show that there is a high risk of human plague when hibernating marmots are excavated.

CASE PRESENTATION

Clinical Manifestation, Diagnosis, and Treatment

The patient was a 45-year-old man who was a non-local and employed as a long-term shepherd herding sheep. On 10 December, his shoulder started to hurt, and he took some analgesic medication. One day later, the pain became unbearable, and he decided to go to a hospital, for which he spent > 7 h along a 170 - km rugged mountain road. In the county hospital, he presented with high fever, slight cyanosis, swelling of the axillary lymph nodes, and > 5 existing hand wounds measuring 2–8 mm in length on his right side, but he had no respiratory symptoms. He was suspected of having plague. A total of.3 g levofloxacin was administrated intravenously. On 12 December, the diagnosis of bubonic plague was confirmed after laboratory examination, including *Y. pestis* culturing, PCR, and the Fraction 1 (F1) antigen of s detection. At 0.720 h on 12 December, he showed symptoms of septic shock, such as mental confusion and worsened purpura, and progressed to septicemic plague. Because the patient was allergic to streptomycin, streptomycin was administrated at.25, 75, and 2 g intramuscularly (**Figure 1**). At 1100 h on 12 December, the patient went into shock, and clinical rescue failed.

Laboratory Detection

Gram staining of blood and lymphatic fluid samples showed bacilli with bipolar staining and blunt ends. The strains isolated from both samples were lysed by a *Y. pestis*-specific bacteriophage. The genes *caf1* and *pla* (3) were positive in both samples but negative in the throat swab. Consistently, the titer of the F1 antigen in both samples was 1:128 but negative in the throat swab (4). According to different region (DFR) analysis, the isolate was Genomovar 8, the main type of the local *Y. pestis* strain (5).

Epidemiological Sourcing

A total of 10 close contacts were identified: a couple that employed the patient, four herdsmen, and four medical staff (**Figure 1**). All the contacts received pre-exposure chemoprophylaxis, isolation management, and health monitoring according to the plague control guidelines of China (6, 7). The anti-F1 antibody of all the contacts was negative (titer, ≤ 1:4) (8, 9) on 12 December. On 17 December, the titer of herdsman C was 1:128, as he showed no other clinical manifestations, he was diagnosed with an asymptomatic plague infection. The titer of his three dogs were 1:32, 1:128, and 1:128, respectively.

According to epidemiology investigation and laboratory evidence, it was indicated that herdsman C was exposed to plague at the same time as the patient. According to herdsman A's statement, the patient often skinned and ate hare, which was later proven by the remains of hare fur and skin found at the patient's home, but all samples were negative for *Y. pestis*. Before 17 December, herdsman C denied coming into contact with a marmot but later cooperated with the investigation of his dogs for fear of legal punishment. After his and his dogs' antibody titers turned positive, he admitted that the patient and himself had been exposed to a hibernating marmot. They lived on adjacent pastures and had excavated, skinned, and consumed a hibernating marmot. The marmot's viscera had been fed to herdsman C's dogs at his home.

The patient was most likely infected through contact with contaminated fluid or tissue *via* his wounds, but the possibility of flea-borne transmission cannot be ruled out. Gastrointestinal infection is less likely, as the cooking was thorough. Lastly, the patient showed no signs of pneumonic plague. Thorough inspections were conducted around the two men's houses, but no marmot leftover was found. Several *Ochotona curzoniae* (commonly known as pika) but not plague hosts were caught alive around the patient's house, but all tested negative for *Y. pestis*.

DISCUSSION AND CONCLUSION

Plague infection risk is greatly increased by excavating hibernating marmots. *Y. pestis* can lie dormant in an otherwise highly susceptible host during hibernation, and it is, therefore, hard to tell whether a hibernating marmot is a plague carrier. The *M. himalayana* plague focus of the Qinghai–Tibet plateau has been constantly active and the leading source of human plague in China for decades (10, 11). Most *Y. pestis* strains were isolated from marmots found dead in the environment (2). However, marmot health cannot be assessed during hibernation. The temperature of the burrow is consistently < 10°C (12), which largely inhibits the growth of *Y. pestis*. However, in winter-sleeping animals in the torpor state, the level of innate immunity decreases, and animals are more susceptible to plague infection (13). During hibernation, marmots are in a state of heterothermia, wherein the physiological state of torpor (body temperature 5–10°C) is replaced by a state of euthermia (37°C) up to 15–20 times (14–16). When marmot body temperature restored to 28°C and then 37°C, growth and virulence expression of *Y. pestis* (17) are accumulated in marmots. In addition, marmot families hibernate together; thus, more than one marmot can be found at a time in a single burrow (18). These factors increase the risk of plague infection when hibernating marmots are excavated.

In this report, different exposure levels and antibiotic administration led to distinct outcomes. First, a shorter incubation period and a probably higher *Y. pestis* load were found in the patient than in herdsman C because of multiple existing wounds on the patient's hand. In contrast, no obvious wound was found on Herdsman C's hands, who also did less manual work as the owner of another pasture. Second, the timing and use of antibiotics were different. The patient was first administrated levofloxacin.3 g, and then after septic shock, streptomycin was prescribed, which may have further exacerbated the sepsis. Although streptomycin was administrated by gradually increasing the dose to avoid allergy, the contribution of allergy to death cannot be excluded. In contrast, the local herdsman C may have taken effective antibiotics after his special visit to the patient on 11 December. A

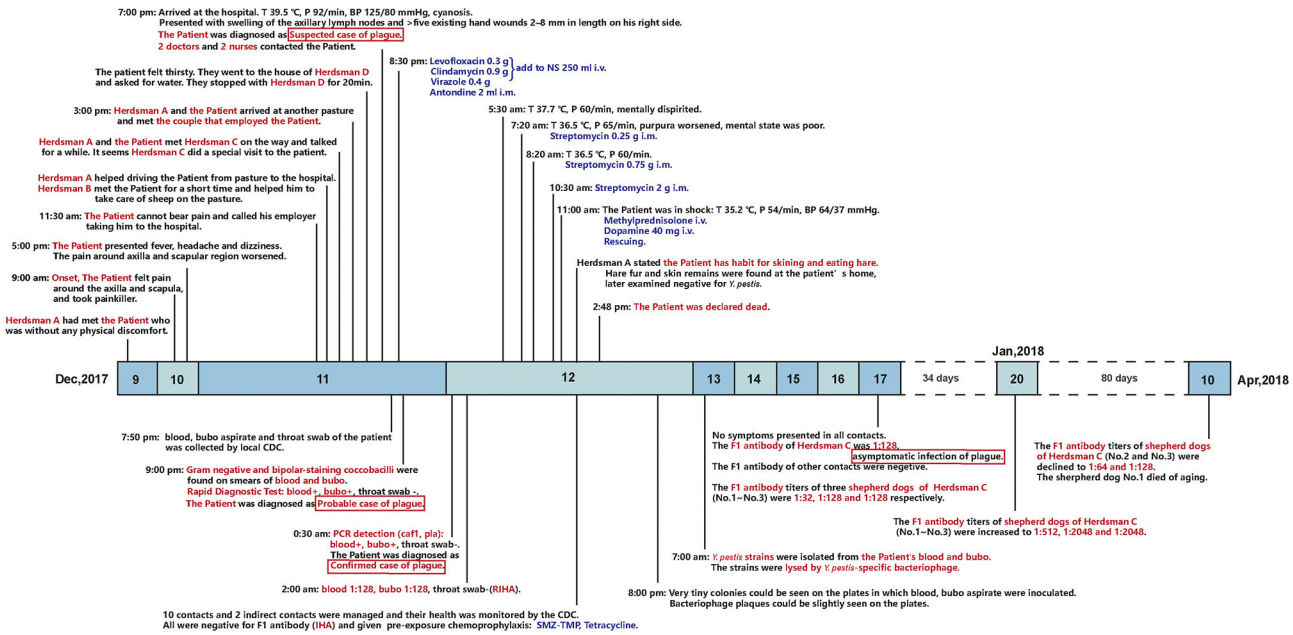

FIGURE 1 | Timeline of the outbreak and follow-up on shepherd dogs. Above the timeline: epidemiological history and clinical presentations of the patient. Below the timeline: laboratory tests of the patient and the contacts, post-exposure prophylaxis of the contacts, and follow-up on the anti-F1 antibody titer of the three shepherd dogs.

plague first-aid kit is available at each herdsman's house in China, including sulfamethoxazole-trimethoprim (SMZ-TMP) and oxytetracycline. On 12 December, herdsman C also took SMZ-TMP and tetracycline under CDC management. It was presumed that he recovered before symptoms occurred because of the antibiotics.

This case report reveals that excavating a hibernating marmot is a significant transmission route of plague. The report also dissects related risk factors and provides public health interventions. First, stronger supervision against the illegal acquisition of marmots is needed, especially during the hibernation period. With education on self-protection and ban on marmot hunting, trafficking, and sale, the infection rate in poachers and herdsmen has dropped sharply. However, employed shepherds have become the victims. These people likely receive less education on self-protection and engage in marmot consumption. In this case, the local herdsman C knew that digging a hibernating marmot was forbidden, so he denied the exposure at first. It was only when his and his dogs' antibody titers became positive that he admitted to touching and consuming a marmot. Second, there is an urgent need to improve basic medical services in the *M. himalayana* plague focus. Medical facilities are very limited in this vast focus and mostly very basic. The patient spent too much time getting to the hospital for treatment. Insufficient chemotherapy and unsuccessful use of streptomycin were the key features of this non-pneumonic case. A sharp contrast is no death from pneumonic plague in the United States in 2014 (19). A pneumonic case transferred to Beijing from *Meriones unguiculatus* plague focus was cured there, where effective treatment was adopted (20).

This case report poses new challenges to plague prevention and control of exposure to hibernating marmots. Plague infection risk is not reduced but rather increased during marmot hibernation if plague exposure is not brought under control. In addition, the ability of primary doctors is in need of urgent improvement for plague diagnosis and treatment.

DATA AVAILABILITY STATEMENT

The datasets presented in this study can be found in online repositories. The names of the repository/repositories and accession number(s) can be found in the article/supplementary material.

ETHICS STATEMENT

The studies involving human participants were reviewed and approved by Ethics Committee of the National Institute for Communicable Disease Control and Prevention of the Chinese Center for Disease Control and Prevention. The patients/participants provided their written informed consent to participate in this study. The animal study was reviewed and approved by Ethics Committee of the National Institute for Communicable Disease Control and Prevention of the Chinese Center for Disease Control and Prevention. Written informed

consent was obtained from the owners for the participation of their animals in this study.

AUTHOR CONTRIBUTIONS

JX, DX, GF, LW, HC, and HJ were engaged in the outbreak investigation. JX, LM, JL, and XW interpreted the patient data. RD, SQ, DL, HM, DT, WW, MX, HJ, and XW followed up with the shepherd dogs. JX, RD, ZH, and XW were major contributors in writing the manuscript. HJ and XW received the funding. All authors contributed to the article and approved the submitted version.

FUNDING

This study was supported by the National Science and Technology Major Project (2018ZX10713-003-002 and 2018ZX10713-001-002). The funding sources for this study had no role in the design of the study and collection, analysis, and interpretation of data, and in writing the manuscript.

ACKNOWLEDGMENTS

We thank Charlesworth Author Services for the professional editing and proofreading of our manuscript.

REFERENCES

1. Centers for Disease Control and Prevention, National Center for Emerging and Zoonotic Infectious Diseases (NCEZID), Division of Vector-Borne Diseases (DVBD). *Plague Ecology and Transmission*. (2019). Available online at: https://www.cdc.gov/plague/transmission/index.html (accessed April 9, 2022).
2. He Z, Wei B, Zhang Y, Liu J, Xi J, Ciren D, et al. Distribution and characteristics of human plague cases and *Yersinia pestis* isolates from 4 marmota plague foci, China, 1950–2019. *Emerg Infect Dis.* (2021) 27:2544–53. doi: 10.3201/eid2710.202239
3. Ge P, Xi J, Ding J, Jin F, Zhang H, Guo L, et al. Primary case of human pneumonic plague occurring in a Himalayan marmot natural focus area Gansu province, China. *Int J Infect Dis.* (2015) 33:67–70. doi: 10.1016/j.ijid.2014.12.044
4. Hai R, Yu D, Shi X, Zhang Z, Tang Y, Wang P, et al. Study on the application and evaluation of methods for gene and antigen detection in plague surveillance program. *Zhonghua Liu Xing Bing xue za zhi= Zhonghua Liuxingbingxue Zazhi.* (2007) 28:426–9. doi: 10.3760/j.issn:0254-6450.2007.05.003
5. Li Y, Dai E, Cui Y, Li M, Zhang Y, Wu M, et al. Different region analysis for genotyping *Yersinia pestis* isolates from China. *PLoS ONE.* (2008) 3:e2166. doi: 10.1371/journal.pone.0002166
6. Emergency Office of Ministry of Health, Chinese Center for Disease Control and Prevention. *Emergency Handbook for Plague Prevention and Control*. Beijing: Peking University Medical Press (2009).
7. World Health Organization. *Operational Guidelines on Plague Surveillance, Diagnosis, Prevention and Control*. (2010). Available online at: https://apps.who.int/iris/handle/10665/205593 (accessed March 19, 2022).
8. Suzuki S, Hotta S. Antiplague antibodies against *Yersinia pestis* fraction-I antigen in serum from rodents either experimentally infected or captured in harbor areas of Japan, 1971-1977. *Microbiol Immunol.* (1979) 23:1157–68. doi: 10.1111/j.1348-0421.1979.tb00548.x
9. Wang T, Qi Z, Wu B, Zhu Z, Yang Y, Cui B, et al. New purification strategy for fraction 1 capsular antigen and its efficacy against *Yersinia pestis* virulent strain challenge. *Protein Expr Purif.* (2008) 61:7–12. doi: 10.1016/j.pep.2008.05.003
10. Wang X, Wei X, Song Z, Wang M, Xi J, Liang J, et al. Mechanism study on a plague outbreak driven by the construction of a large reservoir in southwest China (surveillance from 2000-2015). *PLoS Negl Trop Dis.* (2017) 11:e0005425. doi: 10.1371/journal.pntd.0005425
11. Liu Y, Tian J, Shen E. *The Atlas of Plague and its Environment in People's Republic of China*. Beijing: Science Press (2000).
12. Wang S, Hou F. Burrow characteristics and ecological significance of Marmota himalayana in the northeastern Qinghai-Tibetan Plateau. *Ecol Evol.* (2021) 11:9100–9. doi: 10.1002/ece3.7754
13. Prendergast BJ, Freeman DA, Zucker I, Nelson RJ. Periodic arousal from hibernation is necessary for initiation of immune responses in ground squirrels. *Am J Physiol Regul Integr Comp Physiol.* (2002) 282:R1054–62. doi: 10.1152/ajpregu.00562.2001
14. Arnold W. Social thermoregulation during hibernation in alpine marmots (*Marmota marmota*). *J Comp Physiol B.* (1988) 158:151–6. doi: 10.1007/BF01075828
15. Bouma HR, Carey HV, Kroese FGM. Hibernation: the immune system at rest? *J Leukoc Biol.* (2010) 88:619–24. doi: 10.1189/jlb.0310174
16. Ortmann S, Heldmaier G. Regulation of body temperature and energy requirements of hibernating alpine marmots (*Marmota marmota*). *Am J Physiol Regul Integr Comp Physiol.* (2000) 278:R698–704. doi: 10.1152/ajpregu.2000.278.3.R698
17. Yother J, Chamness T, Goguen J. Temperature-controlled plasmid regulon associated with low calcium response in *Yersinia pestis*. *J Bacteriol.* (1986) 165:443–7. doi: 10.1128/jb.165.2.443-447.1986
18. Gong G, Shengwen W. *The Host Animal of Plague in China and its Control*. Lanzhou: Science and Technology of Gansu Press (2012).
19. Runfola JK, House J, Miller L, Colton L, Hite D, Hawley A, et al. *Outbreak of Human Pneumonic Plague With Dog-to-Human and Possible Human-to-Human Transmission—Colorado, June–July 2014*. (MMWR), Morbidity and Mortality Weekly Report. (2015) 64:429–34.
20. Liu B, Zhang D, Chen Y, He Z, Liu J, Lyu D, et al. Epidemiological characteristics of plague in the meriones unguiculatus plague focus—inner Mongolia autonomous region, China, *1950– 2019. China CDC Weekly*. (2020) 2:935–45. doi: 10.46234/ccdcw2020.256

Conflict of Interest: The authors declare that the research was conducted in the absence of any commercial or financial relationships that could be construed as a potential conflict of interest.

frontiers | Frontiers in Medicine

CASE REPORT
published: 13 June 2022
doi: 10.3389/fmed.2022.912649

Case Report: First Report of Fatal *Legionella pneumophila* and *Klebsiella pneumoniae* Coinfection in a Kidney Transplant Recipient

Maria Scaturro[1,2], *Luna Girolamini*[2,3], *Maria Rosaria Pascale*[3], *Marta Mazzotta*[3], *Federica Marino*[3], *Giulia Errico*[1], *Monica Monaco*[1], *Antonietta Girolamo*[1], *Maria Cristina Rota*[1], *Maria Luisa Ricci*[1,2] and *Sandra Cristino*[2,3]*

[1] Department of Infectious Diseases, Istituto Superiore di Sanità, Rome, Italy, [2] European Society of Clinical Microbiology and Infectious Diseases (ESCMID) Study Group for Legionella Infections (ESGLI), Basel, Switzerland, [3] Department of Biological, Geological, and Environmental Sciences, University of Bologna, Bologna, Italy

A very rare case of pulmonary *Klebsiella pneumoniae-Legionella pneumophila* coinfection in a double kidney transplanted man affected by the chronic renal disease is described. Cases of Legionnaires' disease with an incubation period of 14 days have rarely been documented. Despite the long period of hospitalization, typing of clinical and environmental *L. pneumophila* strains demonstrated that the patient's home water distribution system was the source of infection, highlighting that *Legionella* house contamination can be a hidden risk, especially for immune-compromised people.

Keywords: Legionnaires' disease, *Legionella pneumophila*, *Klebsiella pneumoniae*, coinfection, incubation period

OPEN ACCESS

Edited by:
Marwan Osman,
Cornell University, United States

Reviewed by:
Ahmad Al Atrouni,
Lebanese University, Lebanon
Markus Petzold,
University Hospital Carl Gustav Carus, Germany

***Correspondence:**
Sandra Cristino
sandra.cristino@unibo.it

Specialty section:
This article was submitted to Infectious Diseases–Surveillance, Prevention and Treatment, a section of the journal Frontiers in Medicine

Received: *04 April 2022*
Accepted: *10 May 2022*
Published: *13 June 2022*

Citation:
Scaturro M, Girolamini L, Pascale MR, Mazzotta M, Marino F, Errico G, Monaco M, Girolamo A, Rota MC, Ricci ML and Cristino S (2022) Case Report: First Report of Fatal Legionella pneumophila and Klebsiella pneumoniae Coinfection in a Kidney Transplant Recipient. Front. Med. 9:912649. doi: 10.3389/fmed.2022.912649

INTRODUCTION

Legionnaires' disease (LD) is an important public health threat caused by Gram-negative bacteria *Legionella pneumophila* (*Lp*), the species most frequently reported in infection cases (1). Most LD cases are community- or travel-acquired; however, nosocomial cases represent a great public health concern because of the high fatality rate (1). Most cases are susceptible individuals due to age, underlying diseases, abuse of alcohol, smoking, or immunosuppression (2). Water from different artificial aquatic environments, such as water systems in buildings and cooling towers, is the main reservoir of *Legionella* infection transmission by inhalation of infectious aerosols produced by showers and spa pools, as well as other devices producing aerosols. Although less common, micro-aspiration of contaminated water or direct contact with surgical wounds has been reported (3).

Here, we report an *Lp* and *Klebsiella pneumoniae* (*Kp*) coinfection case in an adult man affected by chronic renal disease.

CASE DESCRIPTION

A 59 years-old man with a background history of end-stage chronic renal failure was admitted to the hospital and on the same day underwent a double kidney transplant (7 September). Soon after surgery, he was moved to the intensive post-transplant care unit (ICU). The day after (8 September), he was transferred to the nephrology dialysis and transplant ward located in another building of the same hospital. Fourteen days after the surgery (21 September), he was transferred

to ICU where he remained until his death (1 October). The timeline of hospitalization and clinical treatments are shown in **Figure 1**. Seven days after the surgery (14 September), because of severe pain in the hypogastric area, increased inflammation indices, and the presence of clots in the bladder catheter, rectal swabs were required. Because of the positive results for KPC-producing *Kp*, the patient was isolated, and an appropriate antibiotic therapy based on co-trimoxazole (strain with MIC = 40 mg/L) and amikacin (MIC = 8 mg/L, was undertaken. Noteworthy was that the analysis of rectal swabs, performed at the time of admission, was negative. Fourteen days after the surgery (21 September), chest radiography was performed because of flu-like symptoms and breathing difficulty and detected a bilateral pulmonary infection, and chest physical examination showed reduced vesicular murmur, $SatO_2$ of 93%, and C-reactive protein of (CRP) 26. The patient was moved back to the ICU, and an antibiotic therapy based on a combination of linezolid with piperacillin/tazobactam (600 mg twice daily) was started, in association with previous treatment based on thyroglobulin (60 mg/die) plus glucocorticoids (methylprednisolone sodium succinate 40 mg twice daily).

Legionnaires' disease (LD) was suspected, and urinary antigen test (UAT) and IgG and IgM titers for *Legionella* were required. At the same time, a bronchoalveolar lavage (BAL) sample was cultured for aerobic bacteria and a real-time PCR assay for *Legionella* (*mip* gene target) was performed. The UAT and real-time PCR were positive, and the increased antibody titer was also observed (IgG = 354 U/ml; IgM= 1,153 U/ml), confirming the LD diagnosis; the health authority was immediately notified (25 September). The antibiotic therapy was then modified with meropenem (1gr/die), cotrimoxazole (3fl/die), and levofloxacin (500 mg/die). Nevertheless, the patient got worse, and 6 days after the LD diagnosis (1, October) he died.

Ten lung tissue fragments, one blood, and one bile sample were collected post-mortem for *Legionella* culture, which was performed according to the Italian and Regional Guidelines for prevention and control of legionellosis (4, 5). Direct immune-fluorescence (MonoFluo™ Kit *Legionella pneumophila*; BioRad), detecting all *Lp* serogroups, and real-time PCR assay (6), specific for the *Legionella pneumophila* serogroup 1 (*Lp*1), were also performed. The real-Time PCR assay detected *Lp*1 in all lung tissue samples, while the direct immune-fluorescence test showed *Lp* in seven out of 12 samples tested, including the blood and bile samples. The culture of ten lung tissue samples revealed the presence of *Lp* colonies in two out of the 10 fragments analyzed, while *Kp* colonies were found in almost all the fragments.

Kp colonies were tested with the broth microdilution method to determine their *in vitro* sensitivity to a panel of 16 antibiotics. According to the EUCAST 2021 breakpoints these colonies resulted resistant to ertapenem, meropenem, and tigecycline and also positive to the *blaKPC* gene by PCR (7, 8). *Lp* colonies were also tested for antimicrobial susceptibility by broth microdilution method test according to EUCAST 2021 (9). The patterns of antibiotic susceptibility testing for *Lp*1 and *Kp* from lung fragments and rectal swab samples are shown in **Table 1**. To identify the source of *Lp* infection, the environmental investigation was promptly started at the patient's home and in the hospital wards where the patient was hospitalized. Overall 75 samples were collected in accordance with ISO 19458:2006 (10) as follows: 43 from hospital wards and 32 from the patient's home, including showers, jacuzzi, and kitchen sink faucet (**Table 2**). The samples were cultured in accordance with UNI EN ISO 11731:2017 (11), and the colonies were identified

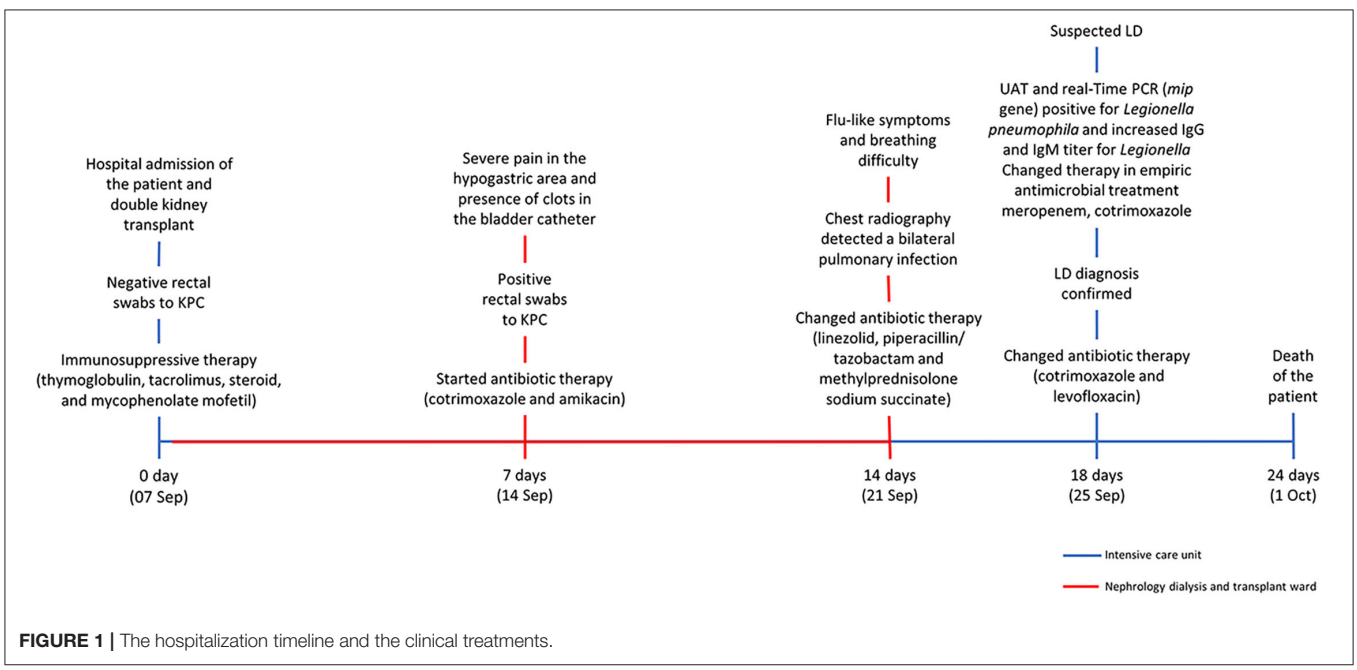

FIGURE 1 | The hospitalization timeline and the clinical treatments.

TABLE 1 | *Legionella pneumophila* serogroup 1 (*Lp*1) and *Klebsiella pneumoniae* (*Kp*) antibiotic susceptibility from (a) lung tissue fragments and (b) rectal swab sample.

	***Legionella pneumophila* (*Lp*1) (a)**		***Klebsiella pneumoniae* (*Kp*) (a)**		***Klebsiella pneumoniae* (*Kp*) (b)**	
Antibiotics pattern	**MIC (mg/L)**	**Interpretation categories (S/R)**	**MIC (mg/L)**	**Interpretation categories (S/I/R)**	**MIC (mg/L)**	**Interpretation categories (S/I/R)**
Azithromycin	0.06	S				
Amikacin			≤4	S	8	S
Amoxicillin / Clavulanic acid			≤64/2	R	≥32	R
Cefepime			>16	R	≥32	R
Ceftazidime			>64	R	≥64	R
Ceftazidime/avibactam			2/4	S		
Ceftriaxone			>4	R		
Ciprofloxacin	0.03	S	>1	R	≥4	R
Clarithromycin	0.03	S				
Colistin			1	S		
Doxycycline	4	S				
Ertapenem			>2	R	≥8	R
Erythromycin	2	S				
Gentamicin			≤1	S	≥16	R
Levofloxacin	0.03	S	>8	R		
Meropenem			8	I	≥16	R
Moxifloxacin	0.03	S				
Phosphomycin			8	S		
Piperacillin / Tazobactam			>128/4	R	≥128	R
Rifampicin	0.00046	S				
Tigecycline	32	S	1	R	4	R
Trimethoprim / Sulfamethoxazole			>8/152	R	40	S

S, sensible; I, intermediate; R, resistant; according to EUCAST criteria (8, 9).

by the *Legionella* latex agglutination test (*Legionella* latex test kit; Thermo Fisher Diagnostic, Basingstoke, United Kingdom, and Biolife, Milan, Italy).

Table 2 summarizes the *Legionella* water sample results. *Lp*1 was isolated both in the hospital and at the patient's home. *Lp*1 and *Lp*3 were discovered in the sink faucet and bidet of the patient's room toilet at concentrations ranging from 100 to 30,000 CFU/L in ICU and Nephrology wards, respectively. *Lp*1 and *L. anisa* contamination was identified throughout the patient's home, particularly in the kitchen sink faucet and in the two toilettes (10/32 positive samples).

Clinical and environmental *Lp*1 colonies were typed with monoclonal antibody (MAb) (12) and by sequence-based typing (SBT) (13). The *Lp* clinical strains, as well as the environmental strains isolated from the patient's home, specifically in the kitchen sink faucet, the shower, and the jacuzzi of one of the two toilettes, belonged to the subgroup Benidorm, Sequence Type (ST) 664, while the *Lp*1 colonies isolated from the hospital belonged to the subgroup Oxford ST1.

DISCUSSION

The case reported here is that of a very rare coinfection with *Lp* and *Kp* in a double kidney transplanted man affected by chronic renal disease. Indeed, concurrent or sequential coinfections of *Lp* with other pathogens have also been infrequently reported, mainly regarding viral coinfections (14, 15). A unique case of *Lp*-*Kp* coinfection had previously been reported in a young man who underwent a kidney transplant 4 years earlier and was healed with appropriate antibiotic therapy (16). However, according to the EU (17) and CDC (18) LD case definition, the case described by Dow and Chow was a probable case because it was diagnosed only by direct fluorescence with *Lp*-specific monoclonal antibodies, while the *Kp* infection was ascertained by culture.

Kp is an opportunistic pathogen that causes a broad spectrum of diseases and shows an increasingly frequent acquisition of antibiotic resistance. Multidrug-resistant infections have been documented worldwide as being caused by emerging major pathogens of international concern. By the production of extended-spectrum β-lactamases (ESBLs) and carbapenemases, hypervirulent *Kp* strains cause a variety of infectious diseases, including urinary tract infections, bacteremia, pneumonia, and liver abscesses (19). *Kp* colonizes various mucosal surfaces from the nasopharynx to the gastrointestinal mucosa, and in hospitalized patients, colonization rates in the gastrointestinal tract are higher (20). Additionally, *Kp*-colonized ICU patients have a higher risk of infection than non-carriers. The transition from colonization to infection is primarily due to

TABLE 2 | Environmental sampling sites of water distribution systems, and *Legionella* concentration, identification, and typing.

	Water output	Hot recirculating water	Hot water distal outlet	Cold water distal outlet	Swab samples	Total of positive sample	*Legionella* range concentration (CFU/L)	*Legionella* identification	*Lp*1 typing	
									Monoclonal antibody (MAb)	Sequence Type (ST)
Transplant ICU ($n = 18$)	2	2	10	2	2	4	300–30,000	*Lp1* and *Lp3*	*Lp*1, subgroup Oxford	1
Nephrology ($n = 25$)	2	2	11	6	4	5	100–5,000	*Lp1* and *Lp3*	*Lp*1, subgroup Oxford	1
Patient's home ($n = 32$)	2	1	10	13	6	10	100–2,800	*Lp1* and *L.anisa*	*Lp*1, subgroup Benidorm	664

impairment of host defense contributed by underlying diseases or immunodeficiency conditions. One of the factors that help to recognize a transition colonization-infection is positive culture. Although the patient's rectal swabs were negative for *Kp* at hospital admission, post-mortem examination of the lung tissue fragments revealed a massive presence of *Kp*, suggestive of lung colonization in the patient with severely immune-compromised conditions due to immunosuppressive therapy (thyroglobulin, etc.). Therefore, it is difficult to establish which of the two pathogens was the real cause of his death.

Lp could almost certainly have been the primary infection because the patient got infected at his own home. Inhalation of *Lp*-contaminated aerosols is usually followed by an incubation period ranging from 2 to 10 days before the onset of symptoms. In this case, the onset of symptoms 14 days after the admission strongly suggested a nosocomial LD case; however, only the MAb and SBT typing demonstrated that the patient acquired the *Lp*1 infection at home. These findings highlight the importance of performing *Legionella* culture on patients' respiratory secretions or postmortem lung tissues.

Although rarely observed, longer incubation periods are actually possible as already documented, mainly in immune-compromised patients (21). For this reason, according to the CDC case definition, also at the European level, the incubation period should be extended to 14 days (18).

Noteworthy, a very strange matter was that most probably the patient contracted the *Lp* infection simply by cleaning the jet breaker of the kitchen sink faucet as he used to do. Indeed, it has also been referred that the patient never used his jacuzzi or the toilette where *Lp*1 ST664 was found. In addition, home-acquired LD infections are increasingly documented (22, 23), and most likely, they could represent a high percentage of not investigated community-acquired LD cases, which remain without an identified source of infection, contributing to the underestimated rate of LD notification at Italian ad European levels.

CONCLUSION

The case reported here highlights once more the risk of LD infection at home and the importance of considering an incubation period longer than 10 days to suspect LD and consequently to ascertain and assign the true source of the infection. Besides, since the susceptibility to LD of transplanted patients is well-documented, urinary antigens should be administered immediately upon the first appearance of symptoms to promptly treat patients. If LD is confirmed, appropriate and immediate antibiotic treatments able to counteract this severe and often fatal infection must be given. In addition, physicians caring for these patients, as well as all immunocompromised or elderly patients in general, should inform these more susceptible people about the risks of contracting LD from all aerosol-producing household appliances and provide them with basic information on how to prevent it. Finally, the reported case highlights the importance of isolating and characterizing *Legionella* from clinical samples, as well as focusing on the role of other sources of infection

(e.g., home exposure) that, if not taken into account during the appropriate period of incubation, could interfere with case definition (nosocomial, travel, or community-acquired) and notification rate.

DATA AVAILABILITY STATEMENT

The raw data supporting the conclusions of this article will be made available by the authors, without undue reservation.

ETHICS STATEMENT

Ethical review and approval was not required for the study on human participants in accordance with the local legislation and institutional requirements. The patients/participants provided their written informed consent to participate in this study.

AUTHOR CONTRIBUTIONS

MS, SC, and MLR conceived and designed the study and wrote the article. LG, FM, MRP, and MMa performed the experiments on environmental samples. GE, MMo, and AG performed the experiments on human samples. MCR revised the original draft of the manuscript and provided the Italian epidemiological data. All the authors read and agreed to the published version of the manuscript.

ACKNOWLEDGMENTS

The authors would like to thank Anna Marella for the technical assistance and the patient's family for the consent to publication.

REFERENCES

1. European Centre for Disease Prevention and Control. *Legionnaires' Disease Annual Epidemiological Report for 2019*. Stockholm (2021). p. 7. Available online at: https://ecdc.europa.eu/sites/portal/files/documents/legionnaires-disease-annual-epidemiological-report.pdf (accessed March 4, 2022).
2. Phin N, Parry-Ford F, Harrison T, Stagg HR, Zhang N, Kumar K, et al. Epidemiology and clinical management of Legionnaires' disease. *Lancet Infect Dis.* (2014) 14:1011–21. doi: 10.1016/S1473-3099(14)70713-3
3. Cunha BA, Burillo A, Bouza E. Legionnaires' disease. *Lancet.* (2016) 387:376–85. doi: 10.1016/S0140-6736(15)60078-2
4. Emilia-Romagna Region. *Regional Guidelines for Surveillance and Control of Legionellosis. Delibera Della Giunta Regionale 12 Giugno 2017, N. 828. 2017. 2012*. (2017). Available online at: https://bur.regione.emilia-romagna.it/bur/area-bollettini/bollettini-in-lavorazione/n-167-del-19-06-2017-parte-seconda.2017-06-19.6161668613/approvazione-delle-linee-guida-regionali-per-la-sorveglianza-e-il-controllo-della-legionellosi/allegato-1-linee-guida-regiona.2017-06-19.1497864629 (accessed March 4, 2022).
5. Italian National Institute of Health. *Italian Guidelines for Prevention and Control of Legionellosis*. (2015). Available online at: http://www.salute.gov.it/imgs/C_17_pubblicazioni_2362_allegato.pdf guida-regiona.2017-06-19.1497864629 (accessed March 4, 2022).
6. Mentasti M, Kese D, Echahidi F, Uldum SA, Afshar B, David S, et al. Design and validation of a qPCR assay for accurate detection and initial serogrouping of *Legionella pneumophila* in clinical specimens by the ESCMID Study Group for *Legionella* Infections (ESGLI). *Eur J Clin Microbiol Infect Dis.* (2015) 34:1387–93. doi: 10.1007/s10096-015-2363-4
7. Conte V, Monaco M, Giani T, D'Ancona F, Moro ML, Arena F, et al. Molecular epidemiology of KPC-producing *Klebsiella pneumoniae* from invasive infections in Italy: increasing diversity with predominance of the ST512 clade II sublineage. *J Antimicrob Chemother.* (2016) 71:3386–91. doi: 10.1093/jac/dkw337
8. European Committee on Antimicrobial Susceptibility Testing (EUCAST). *Breakpoint tables for interpretation of MICs and zone diameters. Version 7*.1. *Break tables Interpret MICs Zo diameters Version 71*. Vaxjo (2017). p. 7.1.
9. European Committee on Antimicrobial Susceptibility Testing (EUCAST). *Guidance Document on Antimicrobial Susceptibility Testing of Legionella pneumophila*. (2021). Available online at: https://www.eucast.org/fileadmin/src/media/PDFs/EUCAST_files/Guidance_documents/Legionella_guidance_note_-_20210528.pdf (accessed March 4, 2022).
10. UNI EN ISO 19458:2006. *UNI EN ISO 19458:2006 Water Quality - Sampling for Microbiological Analysis*. (2006). Available online at: http://store.uni.com/catalogo/en-iso-19458-2006 (accessed March 4, 2022).
11. International Organization for Standardization. *ISO 11731:2017 Water quality — Enumeration of Legionella*. Geneva (2017).
12. Helbig JH, Bernander S, Castellani Pastoris M, Etienne J, Gaia V, Lauwers S, et al. Pan-European study on culture-proven Legionnaires' disease: distribution of *Legionella pneumophila* serogroups and monoclonal subgroups. *Eur J Clin Microbiol Infect Dis.* (2002) 21:710–6. doi: 10.1007/s10096-002-0820-3
13. Ratzow S, Gaia V, Helbig JH, Fry NK, Lück PC. Addition of neuA, the gene encoding N-acylneuraminate cytidylyl transferase, increases the discriminatory ability of the consensus sequence-based scheme for typing *Legionella pneumophila* serogroup 1 strains. *J Clin Microbiol.* (2007) 45:1965–8. doi: 10.1128/JCM.00261-07
14. Oggioni C, Za A, Auxilia F, Faccini M, Senatore S, Vismara C, et al. Legionnaires' disease contracted from patient workplace: first report of a severe case of coinfection with varicella-zoster virus. *Am J Infect Control.* (2016) 44:1164–5. doi: 10.1016/j.ajic.2016.03.057
15. Tan MJ, Tan JS, File TM. Legionnaires disease with bacteremic coinfection. *Clin Infect Dis.* (2002) 35:533–9. doi: 10.1086/341771
16. Dow G, Chow A. *Legionella*-associated lung abscess: critical pathogen or minor isoolate? *Can J Infect Dis.* (1992) 3:315–8. doi: 10.1155/1992/985398
17. European Centre for Disease Prevention and Control. *Legionnaires' Disease Outbreak Case Definitions*. (2022). Available online at: https://legionnaires.ecdc.europa.eu/?pid=202 (accessed March 4, 2022).
18. Centers for Disease Control and Prevention. *Legionella (Legionnaires' Disease and Pontiac Fever)*. (2022). Available online at: https://www.cdc.gov/legionella/health-depts/surv-reporting/case-definitions.html (accessed March 4, 2022).
19. Wang G, Zhao G, Chao X, Xie L, Wang H. The characteristic of virulence, biofilm and antibiotic resistance of *Klebsiella pneumoniae*. *Int J Environ Res Public Health.* (2020) 17:1–17. doi: 10.3390/ijerph17176278
20. Chang D, Sharma L, Dela Cruz CS, Zhang D. Clinical epidemiology, risk factors, and control strategies of *Klebsiella pneumoniae* infection. *Front Microbiol.* (2021) 12:1–9. doi: 10.3389/fmicb.2021.750662
21. Cassier P, Bénet T, Nicolle MC, Brunet M, Buron F, Morelon E, et al. Community-acquired Legionnaires' disease in a renal transplant recipient with unclear incubation period: the importance of molecular typing. *Transpl Infect Dis.* (2015) 17:756–60. doi: 10.1111/tid.12432
22. Ricci ML, Rota MC, Caporali MG, Girolamo A, Scaturro M. A legionnaires' disease cluster in a private building in italy. *Int J Environ Res Public Health*. (2021) 18:136922. doi: 10.3390/ijerph18136922
23. Schumacher A, Kocharian A, Koch A, Marx J. Fatal case of Legionnaires' disease after home exposure to *Legionella pneumophila*

serogroup 3 - Wisconsin, 2018. *Morb Mortal Wkly Rep.* (2020) 69:207–11. doi: 10.15585/mmwr.mm6908a2

Conflict of Interest: The authors declare that the research was conducted in the absence of any commercial or financial relationships that could be construed as a potential conflict of interest.

Publisher's Note: All claims expressed in this article are solely those of the authors and do not necessarily represent those of their affiliated organizations, or those of the publisher, the editors and the reviewers. Any product that may be evaluated in this article, or claim that may be made by its manufacturer, is not guaranteed or endorsed by the publisher.

frontiers | Frontiers in Medicine

TYPE Case Report
PUBLISHED 02 August 2022
DOI 10.3389/fmed.2022.959196

OPEN ACCESS

EDITED BY
Francesco Paolo Bianchi,
University of Bari Aldo Moro, Italy

REVIEWED BY
Fred Turner,
Curative Inc., United States
Morteza Abouzaripour,
Kurdistan University of Medical Sciences, Iran

*CORRESPONDENCE
Fumiyuki Hattori
hattorif@hirakata.kmu.ac.jp

SPECIALTY SECTION
This article was submitted to Infectious Diseases – Surveillance, Prevention and Treatment, a section of the journal Frontiers in Medicine

RECEIVED 01 June 2022
ACCEPTED 05 July 2022
PUBLISHED 02 August 2022

CITATION
Ito A, Okada T, Minato N and Hattori F (2022) Possible internal viral shedding and interferon production after clinical recovery from COVID-19: Case report. *Front. Med.* 9:959196. doi: 10.3389/fmed.2022.959196

Possible internal viral shedding and interferon production after clinical recovery from COVID-19: Case report

Asuka Ito[1], Takayuki Okada[2], Naoki Minato[2] and Fumiyuki Hattori[3]*

[1]Department of Anesthesiology, School of Medicine, Kansai Medical University, Osaka, Japan, [2]Department of Cardiovascular Surgery, School of Medicine, Kansai Medical University, Osaka, Japan, [3]Innovative Regenerative Medicine, Graduate School of Medicine, Kansai Medical University, Osaka, Japan

A 70-year-old man underwent off-pump coronary artery bypass grafting 28 days after his recovery from coronavirus disease 2019 (COVID-19), which was confirmed by a negative polymerase chain reaction (PCR) test result for severe acute respiratory syndrome coronavirus 2 (SARS-CoV-2) from a nasopharyngeal swab. The PCR test result was also negative for nasopharyngeal sampling 5 days prior to the surgery. However, his redundant saphenous vein and sputum through the endotracheal tube that was taken on the operative day showed the presence of SARS-CoV-2 by PCR. Immunohistochemical analysis of Spike and Nucleoprotein of the saphenous vein showed small clusters of each antigen-positive speckle. Ultrastructural imaging of the saphenous vein showed virus-like particles. The cell-based assay suggested that the patient's serum contained a higher concentration of type-I interferons than that of healthy control sera. These observations suggest that internal viral shedding and, to some extent, innate immune responses continue after COVID-19 recovery.

KEYWORDS

SARS-CoV-2, COVID-19, post-COVID syndrome, long-COVID, type-I interferons

Introduction

The novel coronavirus, severe acute respiratory syndrome coronavirus 2 (SARS-CoV-2), has spread worldwide and infected at least 490 million people in April 2022. Coronavirus disease 2019 (COVID-19) has several pathological features, including delayed immune response (1) and post-COVID (long-COVID) syndrome (2). SARS-CoV-2 is believed to have been transferred from bats to humans. In bats, coronaviruses do not cause any immunoresponses (remain asymptomatic), suggesting that they are tolerated, that is, the viruses can escape the audit of intracellular innate immunity (3). It

may not be a misunderstanding that at least part of this ability may work in humans as well. Actually, post-mortem histological analyses revealed a wide spectrum of tropism of SARS-CoV-2 and its long-term existence in human organs (4).

Longer asymptomatic periods accompanied by viral shedding after infections are a characteristic of SARS-CoV-2 infection. These periods are caused by the broad and efficient disruption of the host intracellular innate immune system by SARS-CoV-2, including the suppression of viral antigen presentation by MHC Class I (5). Therefore, infected cells cannot inhibit viral shedding or induce their own removal by killer T-cells. These defense systems against viral infection are normally mediated by the secretion of type-I interferons (IFNs). However, it has been suggested that type I IFN-mediated cellular immune responses are suppressed during the early phase of SARS-CoV-2 infection (1). In contrast, strong type I IFN-mediated immune responses are suggested to contribute to patient deterioration in the late phase of severe cases (6). However, to the best of our knowledge, no report regarding type I IFNs in clinically recovered patients has been published thus far.

Interferon therapy causes several side effects (7, 8). We noticed that IFN administration and post-COVID syndrome cause similar symptoms (2), including fatigue, exhaustion, weakness, dizziness, hair loss, loss of appetite, heart palpitations, depression, anxiety, high temperature, joint pain, diarrhea, stomachache, cough, headaches, sore throat, and skin rashes.

Here, we report a case in which the patient had clinically recovered from COVID-19; however, the virus continued to replicate internally, and the patient had relatively higher levels of type-I IFN in the serum. This report might be valuable for understanding the characteristics of post-COVID syndrome.

Case description

A 70-year-old man presented to our emergency hospital with dry cough and shortness of breath. He experienced gradual worsening of his symptoms for 10 days since their initiation. On physical examination, the patient's oxygen saturation was 95%. Computed tomography (CT) of the chest revealed bilateral and peripheral ground-glass opacities. The polymerase chain reaction (PCR) for SARS-CoV-2 sampling from his nasopharyngeal swab was positive. He was admitted to the intensive care unit for COVID-19 and was administered oxygen, methylprednisolone, remdesivir, and tocilizumab for 4 days, 5 days, 3 days, and 1 day, respectively, which improved his dyspnea and chest CT findings (**Figure 1**).

His medical history included diabetes mellitus and hypertension. Approximately 1 month before admission, he had experienced paroxysmal chest pain. It was transient; therefore, he did not go to the hospital. On the day of admission, an electrocardiogram demonstrated an inverted T wave in V1-3 and non-specific ST-segment depression. Serum levels of troponin I and creatine kinase MB were elevated, suggesting acute coronary syndrome (ACS). These levels decreased in 1 day. Cardiac echocardiography revealed no wall motion abnormalities and a normal ejection fraction. Although the patient complained of no chest symptoms after admission, ACS was suspected. Therefore, the patient was administered nitrates with continuous treatment for his respiratory symptoms, waiting for further cardiac investigation. The PCR test result of his nasopharyngeal swab 9 days after admission was negative. He underwent coronary angiography 14 days after admission. Coronary angiogram demonstrated three-vessel disease of the left main trunk, which required coronary artery bypass grafting (CABG) (**Figure 1**).

Coronary artery bypass grafting was scheduled using an off-pump procedure, 37 days after admission. The patient was confirmed to have a negative PCR test result with his nasopharyngeal swab 5 days before off-pump coronary artery bypass grafting (OPCAB). One hour before entering the operating room, intra-aortic balloon pump (IABP) was inserted through the femoral artery under local anesthesia. Residual blood at the time of IABP insertion was preserved for analysis. During the OPCAB procedure, the saphenous vein was harvested for grafting, and residual tissues after anastomosis were preserved for analysis. Surgery was performed uneventfully. He was transferred to the postoperative intensive care unit, intubated, and sedated. Suctioning from the endotracheal tube was performed to remove the secretions during intubation. The secretion was used for PCR testing for SARS-CoV-2. The result of the PCR test was positive.

The patient was discharged on the 12th day following the surgery without any complications (**Figure 1**). At present, the patient is in good physical condition and did not present with cardiovascular complications as well as post-COVID-19 syndrome, 18 months after OPCAB.

RNA extraction and laboratory real-time-polymerase chain reaction assay

Total RNA was extracted from the saphenous vein using Isogen® (Nippon Gene, Japan), according to the manufacturer's instructions. Reverse transcription of one microgram of RNA was performed using RiverTraAce® (Toyobo, Japan) in the presence of random hexamers and oligo(dT). To investigate virus replication, quantitative PCR was performed using the Power SYBR Green RT-PCR master mix (Applied bioystems, United States) in the presence of a nucleocapsid phosphoprotein gene-specific primer set designed by the National Institute of Infectious Diseases, Japan. The primer sequences synthesized in the 5′-to-3′ direction were CACATTGGCACCCGCAATC as the forward primer

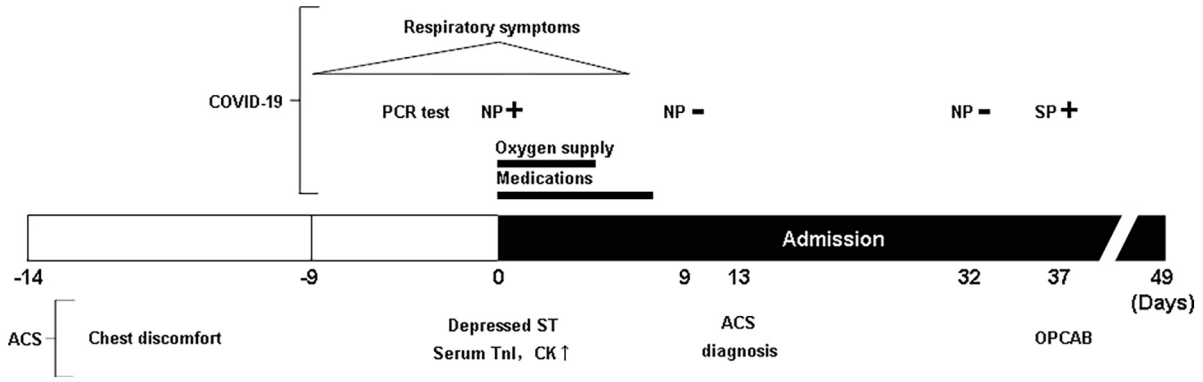

FIGURE 1
A schematic view of the patient's clinical history. NP, nasopharyngeal; SP, sputum through intubation tube; TnI, Troponin I; CK, creatine phosphokinase-MB isozyme.

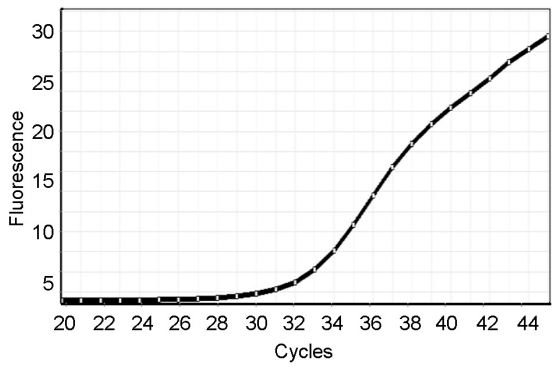

FIGURE 2
The amplification plot of the laboratory real-time RT-PCR using a nucleocapsid phosphoprotein gene-specific primer set.

(N_Sarbeco_F1) and GAGGAACGAGAAGAGGCTTG as the reverse primer (N_Sarbeco_R1). The amplification plot is shown in Figure 2.

Immunohistochemistry

Redundant tissue from the saphenous vein was fixed with 4% *para*-formaldehyde (pH 7.0). The fixed tissue was soaked in 30% sucrose (wt/vol) in Tris-buffered saline containing 0.1% tween-20 (TBS-T) and cryosectioned. Tissue sections were incubated with a primary antibody, a 1:100 diluted mouse anti-spike antibody (GeneTex, Irvine, CA, United States 6H3) or a 1:100 diluted mouse anti-nucleocapsid antibody (GeneTex, Irvine, CA, United States 1A9) at 4°C overnight. The sections were washed with TBS-T four times prior to being incubated with the secondary antibody, 1:200 diluted donkey Alexa Fluor 488 anti-mouse IgG (H + L) (Thermo Fisher Scientific, Waltham, MA, United States A21202), at room temperature for 30 min. After nuclear staining with DAPI (Thermo Fisher Scientific, Waltham, MA, United States) was performed, fluorescence signals were observed using fluorescence microscopy (Eclipse Ti2; NIKON, Tokyo, Japan). Immunohistochemistry revealed small clusters of antigen-positive speckles distinguished by autofluorescence (Figures 3A,B).

Transmission electron microscopy assay

The saphenous vein was fixed with the Karnovsky's formulation of 2% *para*-formaldehyde and 2.5% glutaraldehyde 1-mM $CaCl_2$ in a 0.1-M HEPES buffer and then post-fixed with 1.0% osmium tetroxide in a 0.1-M HEPES buffer and 0.1-M sucrose. After additional buffer washes, the samples were dehydrated with a graded ethanol series and embedded in epoxy resin. Thin sections were cut using a Leica ultramicrotome, stained with 1% uranyl acetate for 30 min, and washed with distilled H_2O. A Joel transmission electron microscope (JEM-1400A) was used for observation at 120 kV. Digital images were acquired using a Bioscan Camera Model 792 (Gatan, Inc., Japan) controlled by a digital micrograph 3.4 (Gatan, Inc.). Viral particles were observed in the saphenous vein (Figure 3C). An area devoid of viral particles was also observed (Supplementary Figure 1).

Cell-based type-I interferon assay

HepG2 cells were cultured in a 12 well plate. Cells that reached 60% confluence were stimulated with patient serum and healthy control serum from a volunteer with no history of SARS-CoV-2 infection at 10% concentration for 18 h. We performed three independent experiments. Total RNA was recovered from each well by Isogen (Nippon Gene,

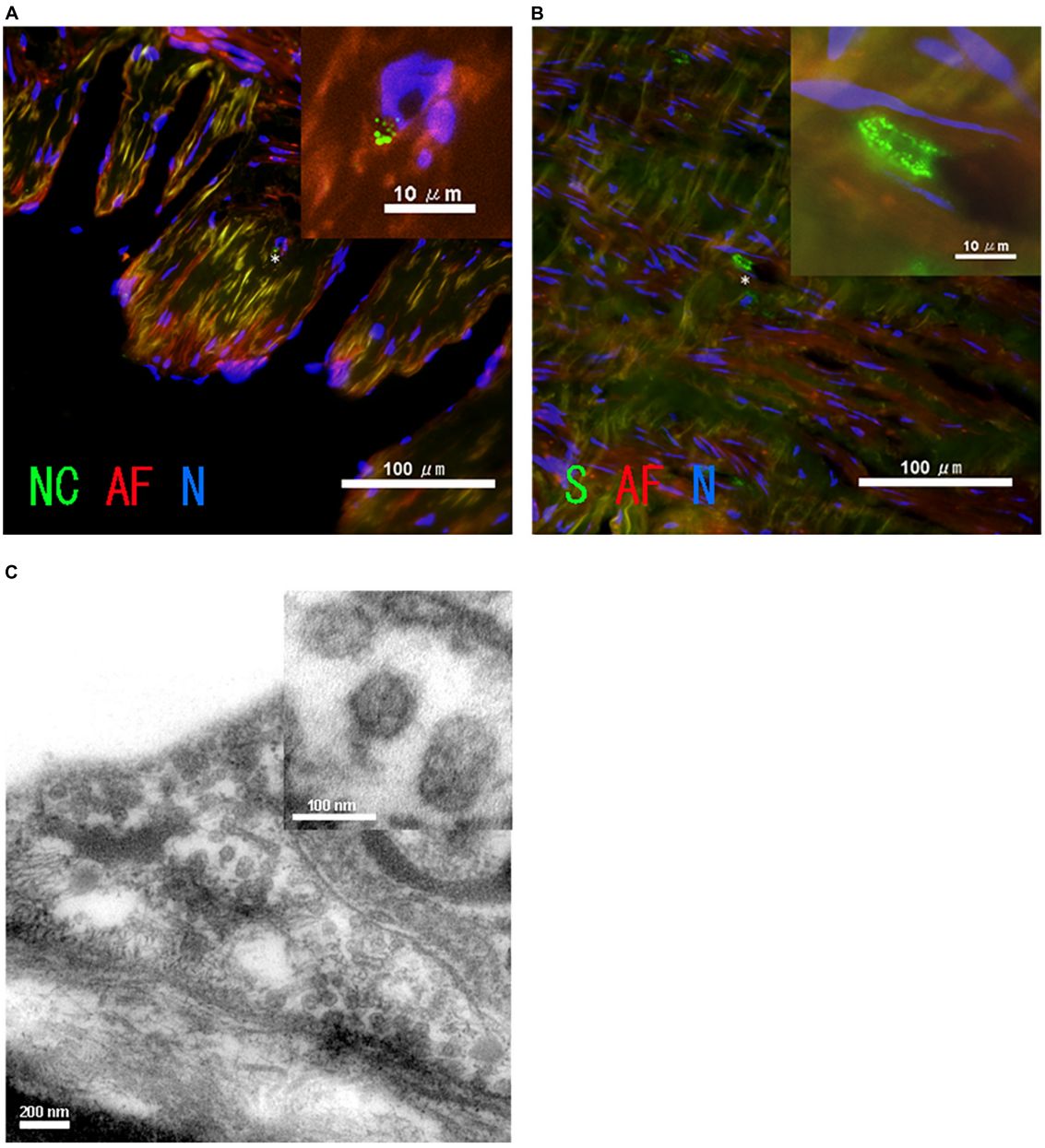

FIGURE 3
Images of SARS-CoV-2 in the patient's saphenous vein. Immunohistochemistry of the saphenous vein of **(A)** SARS-CoV-2 nucleocapsid, NC (green), and **(B)** spike, S (green). The asterisk in A indicates the position of the enlarged image shown in the inset. Autofluorescence, AF (red), and nuclear staining with DAPI, N (blue), are also shown. **(C)** Image of transmission electron microscopy of saphenous vein.

Japan). Of the total RNA, 500 ng of RNA was reverse-transcribed using the Versa cDNA Synthesis Kit (Thermo Fisher Scientific, Waltham, MA, United States). One microliter of cDNA was amplified with primers (human ISG15 Fw: CACCTGAAGCAGCAAGTGAGCGGGCTGGAG, human ISG15 Rv: CCGCAGGCGCAGATTCATGAACACGGTGCT, human MxAFw: GCCAGCAGCTTCAGAAGGCCATGCTGC AGC, human MxARv: GGGCAAGCCGGCGCCGAGCCTGCG TCAGCC, human 18S Fw: TCAACTTTCGATGGTAGTC GCCGT, human 18S Rv: TCCTTGGATGTGGTAGCCGTTTCT) using the Power Cyber Green master mix (Thermo Fisher Scientific, Waltham, MA, United States) and quantitative PCR system, Rotor gene 2 (QIAGEN, Netherlands). Serial dilutions of one of the samples were amplified using each primer pair for quantification. The quantified expression levels were normalized to the result of 18S ribosomal RNA that was used as the internal control. The data obtained from three independent wells are expressed as mean ± standard deviation. Statistical

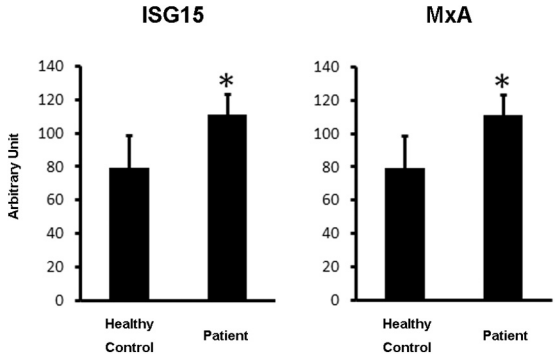

FIGURE 4
A cell-based type-I IFN assay. HepG2 cells were stimulated with the patient's serum and healthy control serum at 10% concentration for 18 h ($N = 3$). The cDNA was amplified separately. Error bars indicate standard deviations. Statistical significance ($p < 0.05$) is indicated by asterisks.

analyses were performed using the Microsoft Excel Student's *T*-test. Statistical significance was set at $p < 0.05$. As shown in **Figure 4**, type-I IFN stimulated genes (9), interferon-stimulated gene 15 (ISG 15) (10) and myxovirus resistance A (MxA) (11) expression levels were significantly higher in the HepG2 cells stimulated by the patient's serum.

Discussion

After the results of the first routine PCR test with nasopharyngeal swabs for SARS-CoV-2 were confirmed to be negative, the patient demonstrated no noticeable symptoms related to COVID-19. The patient was charged in COVID-19-free hospital until he underwent a sputum PCR test, suggesting the absence of *de novo* infection with SARS-CoV-2. Real-time PCR testing for SARS-CoV-2 performed in our laboratory using a surplus of tissue and bronchial sputum in the patient revealed possible internal, but not external, shedding of SARS-CoV-2 particles. In particular, the SARS-CoV-2 particle-like features in the immunohistochemical and ultrastructural images of the saphenous vein were strongly indicative of internal viral shedding.

It has been previously suggested that sputum PCR testing can provide clinically significant indications for persistent viral shedding (12). An increasing number of studies suggest that persistent viral shedding occurs in the lower part of the airways (13) and gastrointestinal tract (14), even after nasopharyngeal swabs demonstrate negative results. In this report, we propose the application of a PCR test to sputum samples obtained during airway intubation.

Here, we suggest the possibility of persistent viral shedding in the internal circulatory system. Although several postmortem studies of severe cases have been conducted (4), no studies have been conducted that investigate the persistence of SARS-CoV-2 particles in people who have recovered from non-severe COVID-19. Larger studies are needed to obtain sufficient information on the number of recovered patients who sustain internal viral shedding.

Persistent viral shedding may induce low-level secretion of type I IFNs; however, this may not lead to effective elimination of the infected cells. This report is the first to provide evidence of persistent type I IFN production in a patient after clinically recovering from COVID-19. Further research investigating how SARS-CoV-2 can escape detection by the immune system for prolonged periods under the partial activation of innate immunity is necessary.

We noticed a similarity between post-COVID symptoms (2) and the side effects of type I IFNs (8) and presented a possible case of this. In this report, we presented a novel theory regarding the hypothetical relationship between post-COVID-19 symptoms and the persistently low production of type I IFNs in the circulatory system.

Data availability statement

The original contributions presented in the study are included in the article/**Supplementary material**, further inquiries can be directed to the corresponding author.

Ethics statement

The studies involving human participants were reviewed and approved by the Kansai Medical University. The patients/participants provided their written informed consent to participate in this study.

Author contributions

AI, TO, NM, and FH developed the concept and design of the study. TO and NM performed the surgery and collected the surplus samples. AI and FH performed the laboratory work to obtain the data. All authors contributed to the article and approved the submitted version.

Funding

This work was supported by a grant from JSPS KAKENHI (Grant No. 21K10407).

Acknowledgments

We would like to thank the patient for agreeing to the study.

Conflict of interest

The authors declare that the research was conducted in the absence of any commercial or financial relationships that could be construed as a potential conflict of interest.

Publisher's note

All claims expressed in this article are solely those of the authors and do not necessarily represent those of their affiliated organizations, or those of the publisher, the editors and the reviewers. Any product that may be evaluated in this article, or claim that may be made by its manufacturer, is not guaranteed or endorsed by the publisher.

Supplementary material

The Supplementary Material for this article can be found online at: https://www.frontiersin.org/articles/10.3389/fmed.2022.959196/full#supplementary-material

SUPPLEMENTARY FIGURE 1
Reference image of transmission electron microscopy of saphenous vein. The area shown is near **Figure 3C**, but there are no viral particles.

References

1. Blanco-Melo D, Nilsson-Payant BE, Liu WC, Uhl S, Hoagland D, Møller R, et al. Imbalanced host response to SARS-CoV-2 drives development of COVID-19. *Cell.* (2020) 181:1036–45.e9. doi: 10.1016/j.cell.2020.04.026

2. Proal AD, VanElzakker MB. Long COVID or post-acute sequelae of COVID-19 (PASC): an overview of biological factors that may contribute to persistent symptoms. *Front Microbiol.* (2021) 12:698169. doi: 10.3389/fmicb.2021.698169

3. El-Sayed A, Kamel M. Coronaviruses in humans and animals: the role of bats in viral evolution. *Environ Sci Pollut Res Int.* (2021) 28:19589–600.

4. Hartard C, Chaqroun A, Settembre N, Gauchotte G, Lefevre B, Marchand E, et al. Multiorgan and vascular tropism of SARS-CoV-2. *Viruses.* (2022) 14:515.

5. Yoo JS, Sasaki M, Cho SX, Kasuga Y, Zhu B, Ouda R, et al. SARS-CoV-2 inhibits induction of the MHC class I pathway by targeting the STAT1-IRF1-NLRC5 axis. *Nat Commun.* (2021) 12:6602. doi: 10.1038/s41467-021-26910-8

6. Lee JS, Shin EC. The type I interferon response in COVID-19: implications for treatment. *Nat Rev Immunol.* (2020) 20:585–6.

7. Wang L, Zhao J, Liu J, Zhen C, Zhang M, Dong Y, et al. Long-term benefits of interferon-α therapy in children with HBeAg-positive immune-active chronic hepatitis B. *J Viral Hepat.* (2021) 28:1554–62. doi: 10.1111/jvh.13598

8. Konerman MA, Lok AS. Interferon treatment for hepatitis B. *Clin Liver Dis.* (2016) 20:645–65.

9. Schneider WM, Chevillotte MD, Rice CM. Interferon-stimulated genes: a complex web of host defenses. *Annu Rev Immunol.* (2014) 32:513–45. doi: 10.1146/annurev-immunol-032713-120231

10. Haas AL, Ahrens P, Bright PM, Ankel H. Interferon induces a 15-kilodalton protein exhibiting marked homology to ubiquitin. *J Biol Chem.* (1987) 262:11315–23.

11. Saber MA, Okasha H, Khorshed F, Samir S. A novel cell-based in vitro assay for antiviral activity of interferons α, β, and γ by qPCR of MxA gene expression. *Recent Pat Biotechnol.* (2021) 15:67–75.

12. Sethuraman N, Jeremiah SS, Ryo A. Interpreting diagnostic tests for SARS-CoV-2. *JAMA.* (2020) 323:2249–51.

13. Huang J, Mao T, Li S, Wu L, Xu X, Li H, et al. Long period dynamics of viral load and antibodies for SARS-CoV-2 infection: an observational cohort study. *medRxiv [Preprint].* (2020):doi: 10.1101/2020.04.22.20071258

14. Xiao F, Wan P, Wei Q, Wei G, Yu Y. Prolonged fecal shedding of SARS-CoV-2 in a young immunocompetent COVID-19 patient: a case report and literature overview. *J Med Virol.* (2022) 94:3133–7. doi: 10.1002/jmv.27694

frontiers | Frontiers in Public Health

TYPE Case Report
PUBLISHED 05 August 2022
DOI 10.3389/fpubh.2022.978200

OPEN ACCESS

EDITED BY
Francesco Paolo Bianchi,
University of Bari Aldo Moro, Italy

REVIEWED BY
A. Chandrasekaran,
SSN College of Engineering, India
Johny Kumar Tagore,
St. Joseph of Engineering, India

*CORRESPONDENCE
Parasuraman Ganeshkumar
ganeshkumardr@gmail.com

SPECIALTY SECTION
This article was submitted to Infectious Diseases - Surveillance, Prevention and Treatment, a section of the journal Frontiers in Public Health

RECEIVED 25 June 2022
ACCEPTED 22 July 2022
PUBLISHED 05 August 2022

CITATION
Madurapandian Y, Rubeshkumar P, Raju M, Janane A, Ganeshkumar P, Selvavinayagam TS and Kaur P (2022) Case report: An outbreak of viral conjunctivitis among the students and staff of visually impaired school, Tamil Nadu, India, 2020.
Front. Public Health 10:978200.
doi: 10.3389/fpubh.2022.978200

Case report: An outbreak of viral conjunctivitis among the students and staff of visually impaired school, Tamil Nadu, India, 2020

Yazhini Madurapandian[1,2], Polani Rubeshkumar[1], Mohankumar Raju[1], Aishwarya Janane[3], Parasuraman Ganeshkumar[1]*, T. S. Selvavinayagam[2] and Prabhdeep Kaur[1]

[1]ICMR-National Institute of Epidemiology, Chennai, Tamil Nadu, India, [2]Directorate of Public Health and Preventive Medicine, Chennai, Tamil Nadu, India, [3]Shri Sarradha Eye Hospital, Pudukkottai, Tamil Nadu, India

Introduction: On February 2, 2020, the head of a visually impaired school notified similar eye symptoms among the students. We investigated the cluster to confirm the diagnosis, identify potential exposures, and propose recommendations.

Methodology: We defined a case as redness/watering/discharge from any eye among the students and staff, January–February 2020. We actively searched for the cases and calculated attack rates. We drew epicurve by date of symptoms onset. We conducted a retrospective cohort study of students and staff. We collected data on potential exposures and calculated Risk Ratio (RR), 95% Confidence Interval (95%CI), and Population Attributable Risk (PAR). We sent a conjunctival swab of the three cases for microbiological analysis.

Results: We diagnosed the cases as acute conjunctivitis and identified 39 (76%) cases among 51 individuals. All the 39 cases reported watering and redness; 28 (72%) and 12 (31%) reported eye pain and discharge, respectively. The median age of the case was 11 years (range: 6–48 years). The attack rate didn't differ significantly between males [77% (20/26)] and females [76% (19/25), $p = 0.9$]. The attack rate was higher among the students [86%, (38/44)] than staffs [14%, (1/7), $p = <0.01$]. Contact with a case [RR = 2.5, 95%CI = 1.3–4.8, PAR = 51%] and staying inside campus [RR = 6.0, 95%CI = 1.0–37.3, PAR = 81%] were associated with the acute conjunctivitis outbreak. All the three conjunctival swabs were negative for bacterial growth.

Conclusion: Close contact with the case and staying inside the campus led to the outbreak of acute conjunctivitis among the students and staff of the visually impaired school.

KEYWORDS

conjunctivitis, viral conjunctivitis, disease outbreak, India, risk factors

Introduction

Conjunctivitis is one of the most common causes of red-eye and affects patients of all ages and socioeconomic classes. Viral conjunctivitis is responsible for the majority of infectious conjunctivitis, accounting for up to 75% of cases (1). Viral conjunctivitis is a highly contagious acute conjunctival infection usually caused by adenovirus (1). Epidemic keratoconjunctivitis usually results from adenovirus serotypes Ad 5, 8, 11, 13, 19, and 37 and tends to cause severe conjunctivitis (1). The diagnosis of conjunctivitis is predominantly clinical, and laboratory investigations are not indicated in all cases unless the symptoms did not subside. The conjunctivitis outbreaks are not uncommon (2–4). Such outbreaks are frequently linked to people congregation settings like hostels, classrooms, shared accommodations (2–4). On February 2, 2020, the head of a school for visually impaired children notified about the occurrence of similar eye complaints among a few students. A local team consisted of an ophthalmologist and epidemiologist to investigate the cluster of eye illnesses reported among students to confirm the diagnosis, identify the potential exposures and propose recommendations.

Methodology

We conducted an outbreak investigation of a cluster of eye complaints among visually impaired students based on the field epidemiology steps of the outbreak investigation (5, 6). An ophthalmologist examined the reported case patients and provided inputs to formulate a case definition of this cluster. We defined a case as the occurrence of any of the following eye symptoms: redness, watering, discharge, foreign-body sensation in any of the eyes among the students and staff of the visually impaired school from January 20 to February 28, 2020. We actively searched for the cases among the students and staff meeting the case definition and line-listed them. We collected demographic and clinical symptoms data in the line list. We interviewed a few key informants like case-patients and staff of the visually-impaired school about the sequence of events and illnesses to generate a hypothesis. We collected conjunctival swabs from three case-patients for microbiological analysis. We conducted a retrospective cohort study of the students and staff of the visually impaired school to test the hypothesis. We collected data on potential exposures using a semi-structured data collection tool through interviews. We used Epi Info (Ver. 7.2) for data management and analysis (7).

We described the cases by date of symptom onset as epi-curve. We described the clinical symptoms reported by the case-patients as proportions. We calculated the median age of the detected case-patients with range. We calculated the attack rates by age, gender, student/staff and place of stay with appropriate denominators and expressed as per 100 persons. We compared the attack rates of conjunctivitis between the exposed and non-exposed groups to compute Risk Ratio (RR) with 95% Confidence Interval (95%CI) and Population Attributable Risk (PAR). We considered p-value <0.05 as statistically significant.

Results

There were 51 individuals in the visually-impaired school; among them, 44 (86%) were students, and 7 (14%) were the staff. The median age of the students was 11 years and ranged between 6 and 13 years. Among the 44 students, 24 (55%) were males, and 38 (86%) were staying in the hostel within the school campus. The median age of the staff was 42 years and ranged between 34 and 48 years. Among the seven staff, five were females, and three were staying in the hostel.

The Ophthalmologist clinically diagnosed the identified cases as acute conjunctivitis. Among the 51 individuals of the visually impaired school, we identified 39 (76%) cases in which 38 (97%) were students. The median age of the case-patients was 11 years (Range: 6–48 years). The cases were reported between January 26, 2020, and February 18, 2020 (Figure 1). The pattern of the epi-curve suggested a person-to-person transmission (Figure 1). The key informants' interviews revealed that the index case had an outstation travel history and attended an inter-school competition event in Chennai, India, on Jan 20 and 21, 2020 and developed symptoms 5 days post-event. Among the 39 cases, 20 (51%) were males, and 38 (97%) stayed in the hostel. All the 39 case-patients reported watering and redness of both eyes. Eye pain and discharge in either of the eyes were reported by 28 (72%) and 12 (31%) case-patients, respectively. Almost all the cases developed the second eye infection within the 48 h of development of the first eye symptom.

The overall attack rate of acute conjunctivitis was 76% (39/51). The attack rate didn't differ significantly between males [77%, (20/26)] and females [76%, (19/25), $p = 0.9$]. The attack rate was higher among the students [86%, (38/44)] than staffs [14%, (1/7), $p = <0.001$]. Based on the descriptive epidemiology findings and key informant interviews, we hypothesized the following potential exposures for this outbreak: male gender, hostel resident and close contact with a case.

We included all 51 individuals in the retrospective cohort study. We observed that the risk for acute conjunctivitis was 2.5 times [RR = 2.5, 95%CI = 1.3–4.8, PAR = 51%] higher among those who had contact with the case [94%, (33/35)] than did not [38%, (6/16)]. We also found that being a resident of the hostel [86%, (38/44)] was six times [RR = 6.0, 95%CI = 1.0–37.3, PAR = 81%] higher risk for acute conjunctivitis than non-resident of the hostel [14%, (1/7); Table 1). All three conjunctival swabs were negative for bacterial growth. We treated all the cases and followed up till their complete recovery. We managed the case-patients with analgesics, cold compresses, and artificial tears. All the cases recovered between 7 and 10 days from the date of

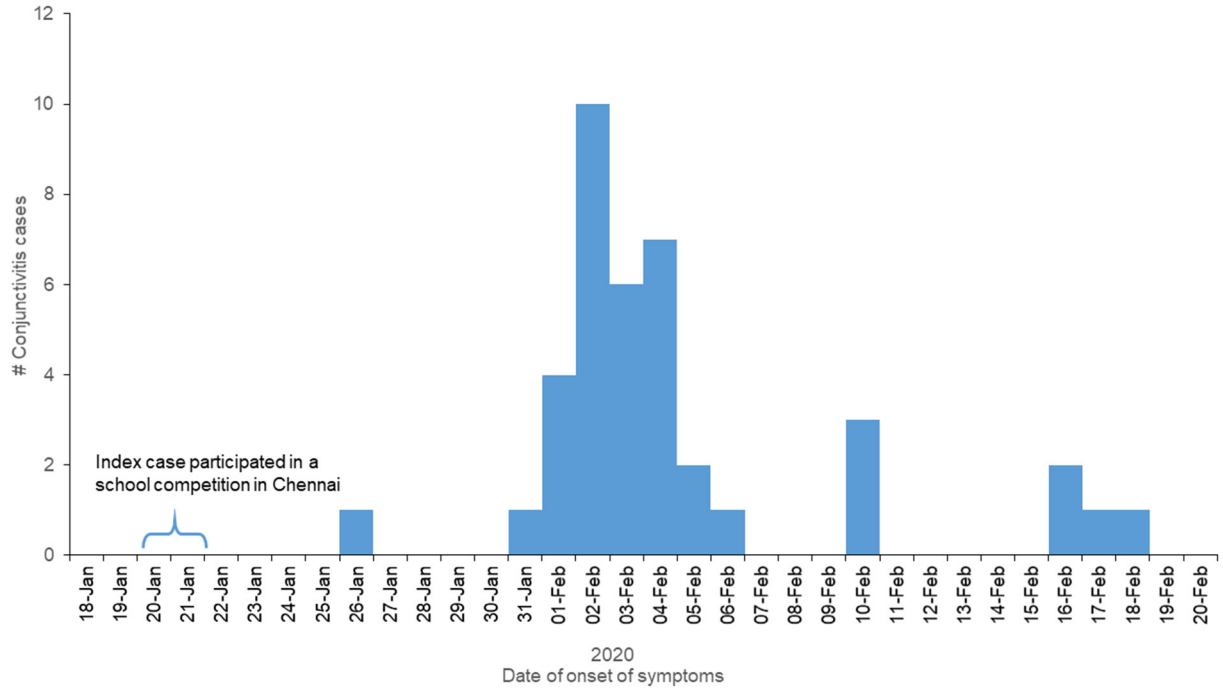

FIGURE 1
Acute conjunctivitis cases by date of onset of symptoms among the students and staff of the visually-impaired school, Tamil Nadu, India, Jan–Feb 2020.

TABLE 1 Attack rate of acute conjunctivitis by different exposures among the students and staff of a visually-impaired school, Tamil Nadu, India, Jan–Feb 2020.

	Attack rate of acute conjunctivitis									
	Exposed			Unexposed						
	#	Total	%	#	Total	%	Relative risk	95%CI	*p*-Value	PAR %
Male gender	20	26	77	19	25	76	1.0	0.7–1.4	1.0	0.6
Close contact with a case	33	35	94	6	16	38	2.5	1.3–4.8	0.00003	51
Staying in the hostel	38	44	86	1	7	14	6.0	1.0–37.3	0.0003	81
Poor hand hygiene	31	36	86	8	15	53	1.6	1.0–2.6	0.02	30

onset of symptoms. We implemented quarantine and educated personal hygiene measures.

Discussion

The outbreaks of conjunctivitis often go unreported in our routine disease surveillance system unless it draws the local media attention. Identifying the cluster of conjunctivitis and controlling the spread is vital to prevent a large community outbreak. We investigated an acute conjunctivitis outbreak in a visually impaired school with a hostel setting. In our investigation, a hoste l resident where the contact with the potential occurred was the primary source of infection. The congregation settings such as hostels, barracks, religious and social gatherings favor the transmission of disease spread through droplets (3, 8, 9). In this study, the index case, who attended the school competition with a travel history and transmitted the infection to their contacts. Isolation of the case after developing the clinical symptoms was not helpful at the time of investigation since the contacts were already exposed.

In this investigation, we could not identify the causative organism which caused the outbreak due to resource limitations. The most common causative organism of conjunctivitis is adenovirus, and it is diagnosed clinically (1). The gold standard

test for adenovirus is virus isolation and cell culture (10). In developed countries, the laboratory confirmation of adenovirus is done by detecting viral DNA by polymerase chain reaction and rapid diagnostics kits (10, 11). However, these methods are expensive and are not available in India. We established epidemiological linkage between the cases and strength of association between exposure and conjunctivitis.

Conclusion

Contact with an index case and staying in a closer congregation setting led to this outbreak of acute conjunctivitis among the students and staff of a visually impaired school. Education and awareness regarding early identification of symptoms, following personal hygiene measures and prompt isolation, would prevent such outbreaks in future in the similar settings. However, adopting such preventive measures among visually-impaired students with a closed hostel setting is challenging. We suggest the health education of the staff and caretaker of such challenging settings would identify the symptomatic individuals earliest.

Data availability statement

The raw data supporting the conclusions of this article will be made available by the authors, without undue reservation.

Author contributions

YM, PR, and AJ did the data collection. YM, PR, MR, and PG were involved in data analysis and visualization. PR, MR, PG, and PK drafted the manuscript. All the authors were involved in conceptualization, gave inputs, and accepted the final version of the manuscript.

Conflict of interest

The authors declare that the research was conducted in the absence of any commercial or financial relationships that could be construed as a potential conflict of interest.

Publisher's note

All claims expressed in this article are solely those of the authors and do not necessarily represent those of their affiliated organizations, or those of the publisher, the editors and the reviewers. Any product that may be evaluated in this article, or claim that may be made by its manufacturer, is not guaranteed or endorsed by the publisher.

References

1. Solano D, Fu L, Czyz CN. Viral conjunctivitis. In: *StatPearls*. Treasure Island, FL: StatPearls Publishing (2021). Available online at: https://www.ncbi.nlm.nih.gov/book

2. Martin M, Turco JH, Zegans ME, Facklam RR, Sodha S, Elliott JA, et al. An outbreak of conjunctivitis due to atypical streptococcus pneumoniae. *N Engl J Med.* (2003) 348:1112–21. doi: 10.1056/NEJMoa022521

3. Crum NF, Barrozo CP, Chapman FA, Ryan MAK, Russell KL. An outbreak of conjunctivitis due to a novel unencapsulated *Streptococcus pneumoniae* among military trainees. *Clin Infect Dis.* (2004) 39:1148–54. doi: 10.1086/424522

4. *Outbreak of Bacterial Conjunctivitis at a College — New Hampshire, January–March, 2002*. Available online at: https://www.cdc.gov/mmwr/preview/mmwrhtml/mm5110a1.htm (accessed April 25, 2021).

5. *Principles of Epidemiology: Lesson 6, Section 2|Self-Study Course SS1978|CDC*. (2020). Available online at: https://www.cdc.gov/csels/dsepd/ss1978/lesson6/section2.html (accessed April 25 2021).

6. Murhekar M, Moolenaar R, Hutin Y, Broome C. Investigating outbreaks: practical guidance in the Indian scenario. *Natl Med J India.* (2009) 22:252–6. Available online at: http://archive.nmji.in/archives/Volume-22/Issue-5/PDF-volume-22-issue-5/Volume-22-issue-5-How-to-do.pdf

7. Dean AG, Arner TG, Sunki GG, Friedman R, Lantinga M, Sangam S, et al. *Epi Info™, a Database and Statistics Program for Public Health Professionals*. Atlanta, GA: CDC (2011).

8. Quadri SA. COVID-19 and religious congregations: Implications for spread of novel pathogens. *Int J Infect Dis.* (2020) 96:219–21. doi: 10.1016/j.ijid.2020.05.007

9. Kennedy AM, Gust DA. Measles outbreak associated with a church congregation: a study of immunization attitudes of congregation members. *Public Health Rep.* (2008) 123:126–34. doi: 10.1177/003335490812300205

10. Elnifro EM, Cooper RJ, Klapper PE, Yeo AC, Tullo AB. Multiplex polymerase chain reaction for diagnosis of viral and chlamydial keratoconjunctivitis. *Invest Ophthalmol Vis Sci.* (2000) 41:1818–22.

11. Kaufman HE. Adenovirus advances: new diagnostic and therapeutic options. *Curr Opin Ophthalmol.* (2011) 22:290–3. doi: 10.1097/ICU.0b013e3283477cb5

frontiers | Frontiers in Public Health

TYPE Case Report
PUBLISHED 25 August 2022
DOI 10.3389/fpubh.2022.972619

OPEN ACCESS

EDITED BY
Francesco Paolo Bianchi,
University of Bari Aldo Moro, Italy

REVIEWED BY
Haroon Ahmed,
Comsats University, Pakistan
Panagiotis Karanis,
University of Nicosia, Cyprus

*CORRESPONDENCE
Xiaoju Lv
lvxj33966@126.com

SPECIALTY SECTION
This article was submitted to Infectious Diseases-Surveillance, Prevention and Treatment, a section of the journal Frontiers in Public Health

RECEIVED 18 June 2022
ACCEPTED 29 July 2022
PUBLISHED 25 August 2022

CITATION
Qu J, Xu H and Lv X (2022) Disseminated alveolar echinococcosis in a patient diagnosed by metagenomic next-generation sequencing: A case report. *Front. Public Health* 10:972619. doi: 10.3389/fpubh.2022.972619

Disseminated alveolar echinococcosis in a patient diagnosed by metagenomic next-generation sequencing: A case report

Junyan Qu[1], Huan Xu[2] and Xiaoju Lv[1]*

[1]Center of Infectious Disease, West China Hospital of Sichuan University, Chengdu, China, [2]Pathology Department, West China Hospital, Sichuan University, Chengdu, China

Background: Alveolar echinococcosis (AE) is a parasitic zoonosis with high mortality and disability rates. Diverse clinical manifestations and mimicking of differential diagnoses such as tuberculosis and malignancy pose a diagnostic dilemma. With the rapid development of molecular diagnostic techniques in recent years, metagenomic next-generation sequencing (mNGS) has become an attractive approach for the etiological diagnosis of infectious diseases.

Case presentation: we report a case of 51-year-old Chinese Tibetan male presented with 3-year low-back pain and 4-month discomfort in the right upper quadrant of the abdomen. He had been in good health. He was diagnosed with tuberculosis and was given anti-tuberculosis treatment a month prior to the visit, but the symptoms were not relieved. Abdominal computerized tomography (CT) revealed a hypodense lesion with uneven enhancement in the liver, and two ring-enhancing cystic lesions in the right abdominal wall. Lumbar spine enhanced MRI showed lesions of mixed density with uneven enhancement in the L1 vertebra and paraspinal tissue. The pathological results of the liver biopsy revealed parasitic infection and possibly echinococcosis. The metagenomic next-generation sequencing (mNGS) of the puncture fluid of abdominal cysts using Illumina X10 sequencer revealed 585 sequence reads matching *Echinococcus multilocularis*. Disseminated AE was diagnosed. Albendazole (400 mg, twice daily) was used, and the patient was in stable condition during follow-up.

Conclusions: mNGS may be a useful tool for the diagnosis of AE. The case would help clinicians to improve their diagnostic skills.

KEYWORDS

alveolar echinococcosis, next-generation sequencing, *Echinococcus multilocularis*, diagnose, albendazole (ABZ)

Background

Echinococcosis is a zoonosis, mainly including cystic echinococcosis (CE) and alveolar echinococcosis (AE), caused by *Echinococcus granulosus sensu lato* (sl) and *Echinococcus multilocularis,* respectively, with high mortality and disability rates (1). The incidence of AE is lower than that of CE, about 0.03 to 1.2 per 100,000 in endemic areas, but it has a high mortality and disability rate, and the mortality is more than 90% in untreated or inadequately treated patients within 10–15 years after diagnosis (2). The endemic areas of AE mainly include Switzerland, Alaska, Canada, eastern and central France, southern Germany, western China, and northern Japan (2–4). There are approximately 18,235 new cases of AE worldwide annually, of which about 91% cases occur in China (5). A recent epidemiological survey showed that the incidence of AE in western China was about 0.27% (4). The incidence of AE is high in the Tibetan Plateau and even higher than that of CE in several areas (6).

Clinical diagnosis of AE depends on epidemiological history, clinical presentation, radiographic findings and serology positive for AE. The diagnosis of AE is confirmed if histopathology compatible with AE or detection of *E. multilocularis* nucleic acid sequence(s) in a clinical specimen (7). However, there are false positives and false negatives in serological tests, and tissue specimens are sometimes unavailable. A study using molecular diagnosis showed that clinically diagnosed AE was misdiagnosed or unclassified in nearly 30% of cases (8). Molecular diagnosis was essential for the confirmation of AE. In recent years, due to the rapid development and substantially reduced costs of metagenomic next-generation sequencing (mNGS) technology, it has become an attractive approach for pathogen detection. mNGS also showed its advantages in the detection of parasites such as *Fasciola hepatica*, *Angiostrongylus cantonensis* and *Strongyloides stercoralis* (9–11).

Here we report a case of disseminated AE involving liver, subcutaneous tissue, and lumbar spine diagnosed by mNGS. This case highlights the challenges of diagnosing AE.

Case presentation

A 51-year-old Chinese Tibetan male presented with 3-year low-back pain and 4-month discomfort in the right upper quadrant of the abdomen. He had always been in good health without alcohol abuse and underlying diseases. He was living in a rural area and had a history of occasional contact with dogs. Magnetic resonance imaging (MRI) of the lumbar spine in a local hospital suggested bone destruction in the L1 vertebra, slight swelling and thickening of the paravertebral soft tissue, and slight swelling of the right psoas muscle. He was clinically diagnosed with tuberculosis and was given anti-tuberculosis treatment a month prior to the visit, but the symptoms of low back pain were not relieved. On examination, his vital signs were normal. He has tenderness in the right upper quadrant. The percussion test of the lumbar spine was positive. Laboratory results showed an elevated C-reactive protein (CRP) concentration (52.4 mg/L) and erythrocyte sedimentation rate (83 mm/h). Both the interferon gamma (IFN-γ) release assay (IGRA) and PPD skin test were positive. The concentration of procalcitonin was 0.04 ng/ml. The complete blood count and concentrations of aspartate aminotransferase, alanine aminotransferase, total bilirubin, alkaline phosphatase, and lactate dehydrogenase were normal. IgG antibodies to echinococcus and cysticercus were positive. Tests for human immunodeficiency virus (HIV), (1,3)-β-D-glucan (BDG) and galactomannan were negative. Antibody tests for autoimmune hepatitis were negative. Abdominal computerized tomography (CT) revealed a hypodense lesion with uneven enhancement in the right posterior lobe of the liver (6.5 × 4.6 cm) that was suggestive of an abscess or tumor (Figure 1A). There were two ring-enhancing cystic lesions in the right abdominal wall (Figure 1B), which was connected to the intrahepatic lesion. Enhanced MRI of the lumbar spine showed lesions of mixed density with uneven enhancement in the L1 vertebra and paraspinal tissue, and the lesion spread upward along the right paraspinal to the right side of the T11 vertebra (Figure 1C). A brain MRI scan was normal. Chest CT revealed chronic bronchitis, emphysema, and bullae. The pathological results of the liver biopsy showed granulomatous inflammation with necrosis, periodic acid-Schiff (PAS) staining (Figure 1D) and silver hexamine immunohistochemical staining were positive, acid fast staining and tuberculosis real-time fluorescence quantitative PCR were negative, suggesting a diagnosis of parasitic disease and possibly echinococcosis. mNGS of the puncture fluid of abdominal cysts was performed using an Illumina X10 sequencer with a unilateral read length of 75 bp. After removing human sequences, there were 585 sequence reads matching *Echinococcus multilocularis,* but no reads matched any other parasites or microorganisms. He was diagnosed with disseminated alveolar echinococcosis. After consultation with a surgeon, it was determined that this case could not be treated surgically. Albendazole (400 mg bid) was administered orally. The patient was in stable condition during follow-up. The timeline of the patient with relevant data of the episodes is presented in Figure 2.

Discussion

Western China, especially Qinghai-Tibet Plateau are the endemic regions of AE (4). Our patient came from Aba Tibetan and Qiang Autonomous Prefecture in Sichuan province, an echinococcosis epidemic area. A large epidemiological survey showed that more than 90% of AE patients here did not receive timely diagnosis and treatment due to poor

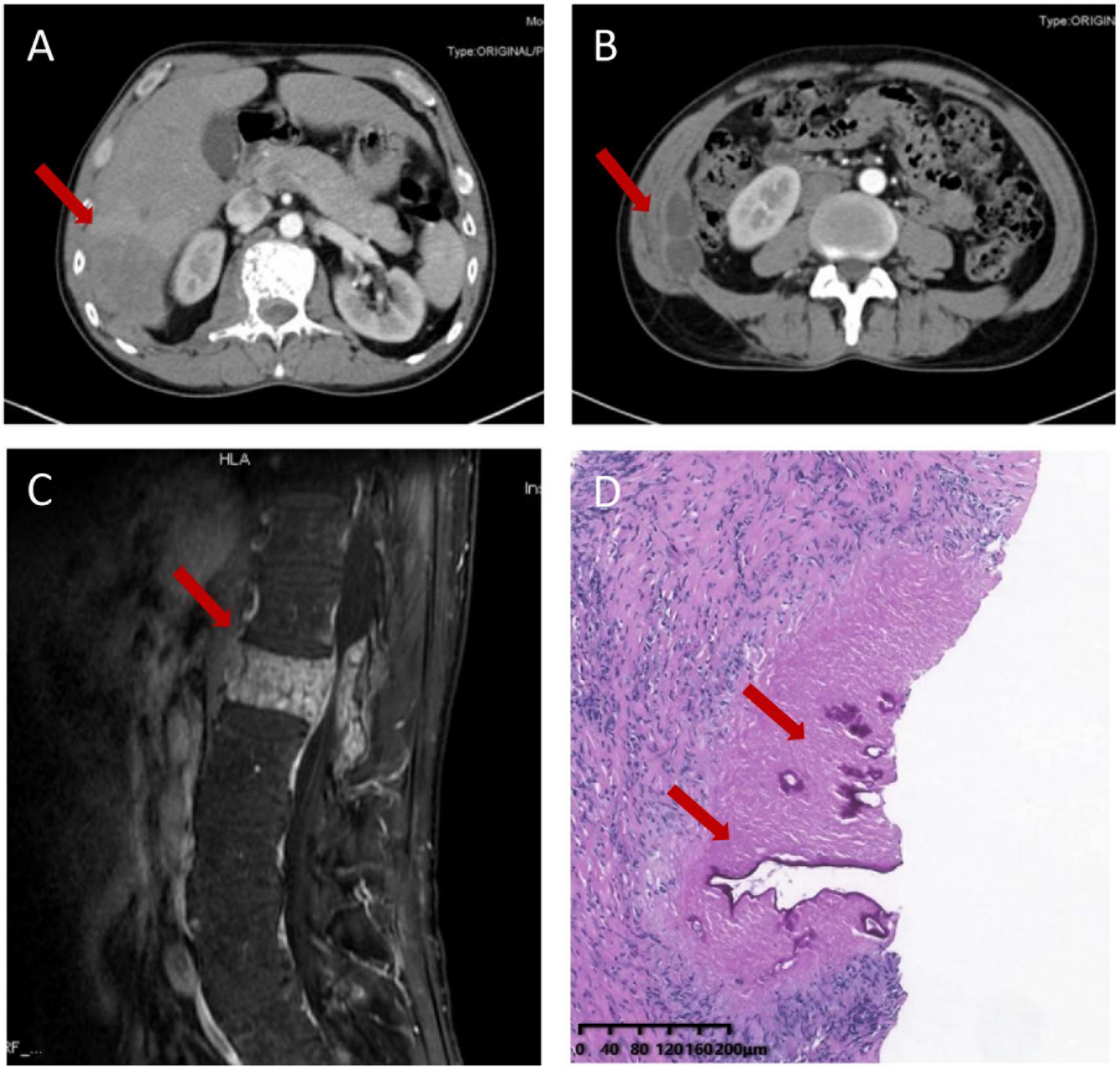

FIGURE 1
Imaging and pathological characteristics of the patient. Abdominal computerized tomography (CT) revealed a hypodense lesion with uneven enhancement in the right posterior lobe of the liver (6.5 × 4.6 cm) **(A)** and two ring-enhancing cystic lesions in the right abdominal wall **(B)**. Enhanced MRI of the thoracic and lumbar spine shows a mixed density lesion with uneven enhancement in the L1 vertebra and paraspinal tissue **(C)**. Liver biopsy sample showing granulomatous inflammation with necrosis and lamellar structure with positive periodic acid-Schiff positive staining **(D)**.

economic conditions, inconvenient transportation and poor health service facilities and diagnostic technology (4). Diverse clinical manifestations and mimicking of differential diagnoses often result in misdiagnosis or missed diagnosis of AE.

The liver is the main organ involved in more than 95% of AEs. Extrahepatic involvement is rare and mainly spreads from the liver through lymphatic or hematogenous transmission to the lung, spleen, central nervous system (CNS), bones, lymph nodes or muscle (3). Bone involvement occurs in approximately 0.02–1% of AE cases, and vertebral involvement occurs in only a few dozen cases worldwide (3, 12). Although the initial symptom of our case was low back pain, there was a large lesion in the liver, which was connected to the lesions in the abdominal wall, and the vertebral lesions may be caused by hematogenous spread from the liver or direct infiltration from nearby lesions. The most commonly involved vertebrae were lumbosacral vertebrae in CE, while in AE, the most commonly involved vertebrae were the lower thoracic spine (T7-12), paravertebral space, and upper lumbar spine (L1-3) (3, 13), as in our patient.

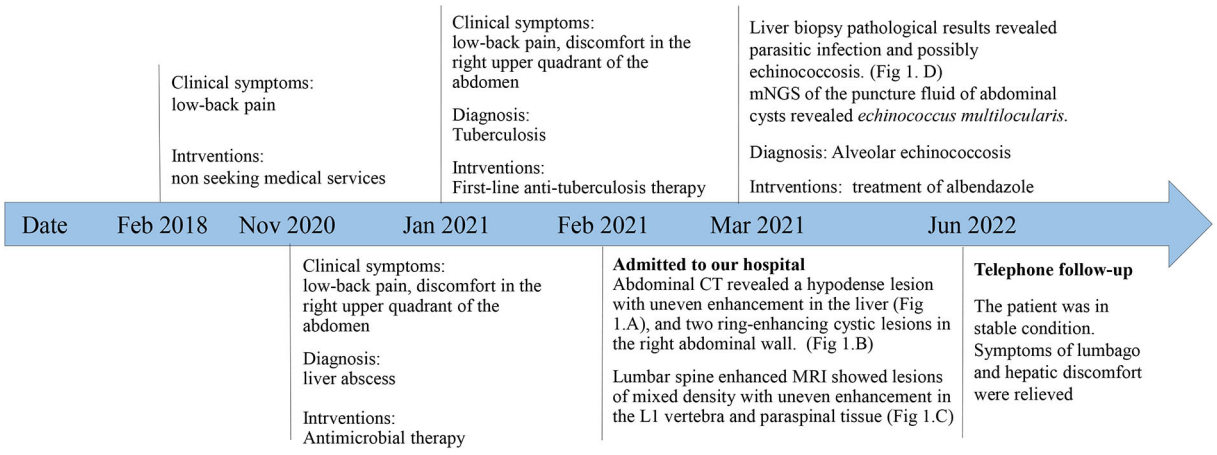

FIGURE 2
Timeline of the patient with relevant data of the past episodes and interventions.

The characteristic CT or T2-weighted MRI findings of liver AE are mainly multiple, indistinct and irregular low-density lesions (3, 14). Extrahepatic lesions have a multicystic, honeycomb appearance, with septations, and may be accompanied by calcification and/or rim enhancement (3, 15, 16). The spinal lesions presented vertebral infiltration and paravertebral abscesses. If calcifications are seen, echinococcosis is more frequently suggested. The differential diagnosis of vertebral AE includes vertebral tuberculosis, bacterial or fungal abscesses, and neoplasms. Spinal tuberculosis also occurs in the lower thoracic and lumbar vertebrae (17). The main manifestations of spinal CT or MRI are bone destruction, intervertebral disc involvement and paravertebral abscess (18). Intervertebral disc involvement is less common in spinal AE than in vertebral tuberculosis. This patient had multiple spinal bone destruction without intervertebral disc involvement, which may support the diagnosis of echinococcosis. Some new imaging techniques, such as perfusion-weighted MRI, diffusion-weighted imaging, 18F-FDG-PET-CT and 18F-FDG-PET-MRI, have also been applied in the diagnosis of AE in recent years (19–21).

AE patients with extrahepatic hematogenous metastases complicate the diagnosis. Laboratory tests are non-specific. Erythrocyte sedimentation rate (ESR) and C-reactive protein (CRP) may be elevated in patients with AE, and eosinophilia may occur in fewer patients. Our patient had normal eosinophil counts and elevated ESR and CRP. The serological methods conventionally used to distinguish AE from CE were ELISAs using purified and /or recombinant, or *in vitro*-produced *Echinococcus multilocularis* antigens (Em2/Em2+/Em18), which could identify 80–95% of cases (7). However, some studies have shown that the sensitivity of Em2-ELISA and Em18-ELISA in AE diagnosis were <50% (22). Moreover, these serological methods are not routinely available in most hospitals in China, as in our hospital. Hydatid antibody detection methods routinely obtained in Chinese hospitals cannot distinguish between *E. granulosus sl* and *E. multilocularis*. Because *Cysticercus cellulosae* and *E. multilocularis* have common antigens, serological tests for both hydatid and cysticercosis IgG may be positive, as in our patient, making differential diagnosis very difficult. An experienced pathologist can distinguish between AE and CE by histopathological examination. Histopathological findings of AE suggest Periodic-Acid-Schiff (PAS)-positive, narrower laminated layer and fibrosis, smaller cysts, with periparasitic granuloma and sparse lymphocyte inflammation (7). Pathological examination still leaves inconclusive diagnosis of AE (3). Histology-based diagnostic algorithms may be powerful in differentiating AE and CE (23).

Molecular diagnosis of AE by PCR or qPCR based on native biopsy material or formalin-fixed paraffin-embedded tissue samples is feasible and sensitive, especially in patients with atypical manifestations, extrahepatic localizations and immunosuppression (24, 25). As a rapidly developing molecular diagnostic technique, mNGS enables rapid detection and comprehensive identification of pathogens directly from clinical samples without prior presumption, with a higher sensitivity and accuracy. mNGS, in particular, has great advantages in the detection of emerging, hard-to-culture, atypical and rare pathogens, such as *Mycobacterium tuberculosis*, non-tuberculous mycobacteria, *Talaromyces marneffei*, and parasites (9, 10, 26). In one recent case report, the patient was diagnosed with AE by mNGS of CSF after multiple negative histopathological tests (27). Although our patient's histopathological findings were compatible with AE, the etiological diagnosis was ultimately dependent on mNGS. mNGS may be a useful tool to detect *E. multilocularis* in patients. mNGS may have a greater diagnostic advantage than histopathology for AE with extrahepatic involvement where tissue specimens are not readily available.

The treatment of AE should be decided by a multidisciplinary team consisting of a surgeon, radiologist, hepatologist, and infectious diseases physician. A combined surgical and medical approach is recommended for echinococcosis (7, 28, 29). The optimal treatment is a radical surgical resection with a safe margin of 2 cm. Percutaneous drainage associated with antibiotics are best adapted to the patients with central necrotic cavity complicated with bacterial/fungal infection. Perendoscopic procedures are best suited for patients with parasitic lesions that compress or block the bile ducts and are accompanied by jaundice and/or cholangitis. Palliative surgery should be avoided (30). Surgical resection is almost impossible in patients with disseminated AE, CNS involvement, or vertebral disease. Most vertebral AE patients underwent decompression to avoid paralysis, and a small number of patients underwent vertebral body resection. Puncture, aspiration, injection of hypertonic saline, and reaspiration cannot be recommended for AE (3). Albendazole is often recommended as a first choice for echinococcosis due to its high blood concentration (31). Mebendazole can also be used if albendazole is not well-tolerated. It has also been reported that in an AE patient with hematogenic subcutaneous and bone dissemination, disease progression occurred after 6 years of albendazole treatment, and the disease was stable after mebendazole treatment (32). All patients with inoperable and postoperative echinococcosis should be given long-term benzimidazoles treatment to limit the growth and metastasis of the lesion (7). *In vitro* studies of the tyrosine kinase inhibitor imatinib suggested that it may be a new treatment option for AE. However, its efficacy needs to be validated *in vivo* (33).

This study has some limitations. We did not obtain spinal histopathological or molecular biological diagnostic results, but this is more consistent with clinical practice. Our patient had evidence of AE from liver and subcutaneous masses. In addition, the lumbar spine imaging findings were similar to those of the published AE. Therefore, puncture was not performed for lumbar lesions in order to minimize trauma to the patient.

In conclusion, this case illustrates the challenges of diagnosing disseminated AE. With increasing use in some countries, such as China, mNGS may be a useful tool for the diagnosis of AE. This case may help clinicians to improve their diagnostic skills and reduce the misdiagnosis rate of AE.

Data availability statement

The datasets presented in this study can be found in the following online repository: https://www.ncbi.nlm.nih.gov/sra/PRJNA860097; PRJNA860097.

Ethics statement

The study involving human participants was reviewed and approved by the West China Hospital, Sichuan University. Written informed consent was obtained from the individual for the publication of any potentially identifiable images or data included in this article.

Author contributions

XL and JQ designed the study. JQ and HX collected and interpreted the data. JQ drafted the manuscript. XL and HX modified the manuscript and finally approved the version to be published.

Funding

This work was supported by 1●3●5 project for disciplines of excellence-clinical research incubation project, West China Hospital, Sichuan University (grant number: 2021HXFH032). The funders had no role in study design, data collection and analysis, decision to publish, or preparation of the manuscript.

Acknowledgments

We thank HX (Vision Medicals Co., Ltd.) for providing the mNGS methods and interpreting the mNGS results. We are grateful to the nursing team of Center of Infectious Disease, West China Hospital, Sichuan University for their care of the patient.

Conflict of interest

The authors declare that the research was conducted in the absence of any commercial or financial relationships that could be construed as a potential conflict of interest.

Publisher's note

References

1. Wen H, Vuitton L, Tuxun T, Li J, Vuitton DA, Zhang W, et al. Echinococcosis: advances in the 21st century. *Clin Microbiol Rev.* (2019) 32:e00075–18. doi: 10.1128/CMR.00075-18

2. McManus DP, Gray DJ, Zhang W, Yang Y. Diagnosis, treatment, and management of echinococcosis. *BMJ.* (2012) 344:e3866. doi: 10.1136/bmj.e3866

3. Meinel TR, Gottstein B, Geib V, Keel MJ, Biral R, Mohaupt M, et al. Vertebral alveolar echinococcosis-a case report, systematic analysis, and review of the literature. *Lancet Infect Dis.* (2018) 18:e87–98. doi: 10.1016/S1473-3099(17)30335-3

4. Zheng C, Xue C, Han S, Li Z, Wang H, Wang L, et al. National alveolar echinococcosis distribution - China, 2012-2016. *China CDC Wkly.* (2020) 2:1–7.

5. Torgerson PR, Keller K, Magnotta M, Ragland N. The global burden of alveolar echinococcosis. *PLoS Negl Trop Dis.* (2010) 4:e722. doi: 10.1371/journal.pntd.0000722

6. Cai H, Guan Y, Ma X, Wang L, Wang H, Su G, et al. Epidemiology of echinococcosis among school children in golog tibetan autonomous prefecture, Qinghai, China. *Am J Trop Med Hyg.* (2017) 96:674–9. doi: 10.4269/ajtmh.16-0479

7. Brunetti E, Kern P, Vuitton DA. Writing panel for the WHO-IWGE. Expert consensus for the diagnosis and treatment of cystic and alveolar echinococcosis in humans. *Acta Trop.* (2010) 114:1–16. doi: 10.1016/j.actatropica.2009.11.001

8. Shang J, Zhang G, Yu W, He W, Wang Q, Zhong B, et al. Molecular characterization of human echinococcosis in Sichuan, Western China. *Acta Trop.* (2019) 190:45–51. doi: 10.1016/j.actatropica.2018.09.019

9. Zou Y, Guan H, Wu H, Bu H, Yan L, Zhu Y, et al. Angiostrongyliasis detected by next-generation sequencing in a ELISA-negative eosinophilic meningitis: a case report. *Int J Infect Dis.* (2020) 97:177–9. doi: 10.1016/j.ijid.2020.05.108

10. Qu J,Zong Z. Strongyloidiasis in a patient diagnosed by metagenomic next-generation sequencing: a case report. *Front Med.* (2022) 9:835252. doi: 10.3389/fmed.2022.835252

11. Zhang Y, Xu H, Liu Y, Kang J, Chen H, Wang Z, et al. Case report: fascioliasis hepatica precisely diagnosed by metagenomic next-generation sequencing and treated with albendazole. *Front Med.* (2021) 8:773145 doi: 10.3389/fmed.2021.773145

12. Piarroux M, Piarroux R, Giorgi R, Knapp J, Bardonnet K, Sudre B, et al. Clinical features and evolution of alveolar echinococcosis in France from 1982 to 2007: results of a survey in 387 patients. *J Hepatol.* (2011) 55:1025–33. doi: 10.1016/j.jhep.2011.02.018

13. Neumayr A, Tamarozzi F, Goblirsch S, Blum J, Brunetti E. Spinal cystic echinococcosis–a systematic analysis and review of the literature: part 1. Epidemiology and anatomy. *PLoS Negl Trop Dis.* (2013) 7:e2450. doi: 10.1371/journal.pntd.0002450

14. Yu XK, Zhang L, Ma WJ Bi WZ, Ju SG. An overview of hepatic echinococcosis and the characteristic CT and MRI imaging manifestations. *Infect Drug Resist.* (2021) 14:4447–55. doi: 10.2147/IDR.S331957

15. Srinivas MR, Deepashri B, Lakshmeesha MT. Imaging spectrum of hydatid disease: usual and unusual locations. *Pol J Radiol.* (2016) 81:190–205. doi: 10.12659/PJR.895649

16. Polat P, Kantarci M, Alper F, Suma S, Koruyucu MB, Okur A. Hydatid disease from head to toe. *Radiographics.* (2003) 23:475-94. doi: 10.1148/rg.232025704

17. Rivas-Garcia A, Sarria-Estrada S, Torrents-Odin C, Casas-Gomila L, Franquet E. Imaging findings of Pott's disease. *Eur Spine J.* (2013) 22 Suppl 4:567–78. doi: 10.1007/s00586-012-2333-9

18. Gupta P, Prakash M, Sharma N, Kanojia R, Khandelwal N. Computed tomography detection of clinically unsuspected skeletal tuberculosis. *Clin Imaging.* (2015) 39:1056–60. doi: 10.1016/j.clinimag.2015.07.033

19. Wang F, Gao X, Rong J, Wang J, Xing H, Yang J, et al. The significance of perfusion-weighted magnetic resonance imaging in evaluating the pathological biological activity of cerebral alveolar echinococcosis. *J Comput Assist Tomogr.* (2022) 46:131–9. doi: 10.1097/RCT.0000000000001253

20. Kaltenbach TE, Graeter T, Mason RA, Kratzer W, Oeztuerk S, Haenle MM, et al. Determination of vitality of liver lesions by alveolar echinococcosis. Comparison of parametric contrast enhanced ultrasound (SonoVue®) with quantified 18F-FDG-PET-CT. *Nuklearmedizin.* (2015) 54:43–9. doi: 10.3413/Nukmed-0670-14-05

21. Eberhardt N, Peters L, Kapp-Schwoerer S, Beer M, Beer AJ, Grüner B, et al. 18F-FDG-PET/MR in alveolar echinococcosis: multiparametric imaging in a real-world setting. *Pathogens.* (2022) 11:348. doi: 10.3390/pathogens11030348

22. Gottstein B, Frey CF, Campbell-Palmer R, Pizzi R, Barlow A, Hentrich B, et al. Immunoblotting for the serodiagnosis of alveolar echinococcosis in alive and dead Eurasian beavers (Castor fiber). *Vet Parasitol.* (2014) 205:113–8. doi: 10.1016/j.vetpar.2014.06.017

23. Reinehr M, Micheloud C, Grimm F, Kronenberg PA, Grimm J, Beck A, et al. Pathology of echinococcosis: a morphologic and immunohistochemical study on 138 specimens with focus on the differential diagnosis between cystic and alveolar echinococcosis. *Am J Surg Pathol.* (2020) 44:43–54. doi: 10.1097/PAS.0000000000001374

24. Chauchet A, Grenouillet F, Knapp J, Richou C, Delabrousse E, Dentan C, et al. Increased incidence and characteristics of alveolar echinococcosis in patients with immunosuppression-associated conditions. *Clin Infect Dis.* (2014) 59:1095–104. doi: 10.1093/cid/ciu520

25. Knapp J, Lallemand S, Monnien F, Felix S, Valmary-Degano S, Courquet S, et al. Molecular diagnosis of alveolar echinococcosis in patients based on frozen and formalin-fixed paraffin-embedded tissue samples. *Parasite.* (2022) 29:4. doi: 10.1051/parasite/2022004

26. Huang H, Deng J, Qin C, Zhou J, Duan M. Disseminated Coinfection by *Mycobacterium fortuitum* and *Talaromyces marneffei* in a Non-HIV case. *Infect Drug Resist.* (2021) 14:3619–25. doi: 10.2147/IDR.S316881

27. Li K, Ma Y, Ban R, Shi Q. Case report: diagnosis of human alveolar echinococcosis via next-generation sequencing analysis. *Front Genet.* (2021) 12:666225. doi: 10.3389/fgene.2021.666225

28. Ayles HM, Corbett EL, Taylor I, Cowie AG, Bligh J, Walmsley K, et al. A combined medical and surgical approach to hydatid disease: 12 years' experience at the hospital for tropical diseases, London. *Ann R Coll Surg Engl.* (2002) 84:100–5.

29. Guidelines for treatment of cystic and alveolar echinococcosis in humans. WHO informal working group on echinococcosis. *Bull World Health Organ.* (1996) 74:231–42.

30. Vuitton DA, Azizi A, Richou C, Vuitton L, Blagosklonov O, Delabrousse E, et al. Current interventional strategy for the treatment of hepatic alveolar echinococcosis. *Expert Rev Anti Infect Ther.* (2016) 14:1179–94. doi: 10.1080/14787210.2016.1240030

31. Song XH, Ding LW, Wen H. Bone hydatid disease. *Postgrad Med J.* (2007) 83:536–42. doi: 10.1136/pgmj.2007.057166

32. Scheuring UJ, Seitz HM, Wellmann A, Hartlapp JH, Tappe D, Brehm K, et al. Long-term benzimidazole treatment of alveolar echinococcosis with hematogenic subcutaneous and bone dissemination. *Med Microbiol Immunol.* (2003) 192:193–5. doi: 10.1007/s00430-002-0171-9

33. Hemer S, Brehm K. In vitro efficacy of the anticancer drug imatinib on Echinococcus multilocularis larvae. *Int J Antimicrob Agents.* (2012) 40:458–62. doi: 10.1016/j.ijantimicag.2012.07.007

frontiers | Frontiers in Public Health

TYPE Case Report
PUBLISHED 16 September 2022
DOI 10.3389/fpubh.2022.982917

OPEN ACCESS

EDITED BY
Ana Afonso,
University of São Paulo, Brazil

REVIEWED BY
Shazia Naaz,
ESIC Medical College, India
Rakhi Gangil,
Nanaji Deshmukh Veterinary Science University, India

*CORRESPONDENCE
Yan Zeng
zengyjyh@outlook.com

†These authors share first authorship

SPECIALTY SECTION
This article was submitted to Infectious Diseases-Surveillance, Prevention and Treatment, a section of the journal Frontiers in Public Health

RECEIVED 30 June 2022
ACCEPTED 18 July 2022
PUBLISHED 16 September 2022

CITATION
Jiang Y, Li J, Qin W, Gao Y, Liao X and Zeng Y (2022) Tuberculosis with cavities? Rapid diagnosis of *Rhodococcus equi* pulmonary infection with cavities by acid-fast staining: A case report. *Front. Public Health* 10:982917. doi: 10.3389/fpubh.2022.982917

Tuberculosis with cavities? Rapid diagnosis of *Rhodococcus equi* pulmonary infection with cavities by acid-fast staining: A case report

Yuhang Jiang [1,2†], Jian Li[1,2†], Weichao Qin[1,2†], Yuan Gao[1,2], Xin Liao[3] and Yan Zeng [4*]

[1]Department of Laboratory Medicine, Chongqing University Jiangjin Hospital, Chongqing, China, [2]Department of Laboratory Medicine, Central Hospital of Jiangjin District, Chongqing, China, [3]Department of Respiratory Medicine, Chongqing University Jiangjin Hospital, Chongqing, China, [4]Department of Laboratory Medicine, Jiangjin District Maternity and Child Health Hospital, Chongqing, China

Rhodococcus equi is a conditionally pathogenic bacterium widely distributed in soil, water, and marine environments, which can cause respiratory infections, pleurisy, blood and even bone marrow infections in immunocompromised people, and particularly in patients with acquired immunodeficiency syndrome (AIDS). This case report describes a patient with initially suspicion of tuberculosis (TB) as an outpatient in a TB clinic. However, laboratory findings identified *R. equi* in his sputum sample based on a positive acid-fast stain, which was highly suggestive of a pulmonary infection caused by *R. equi*. The patient was subsequently admitted to the respiratory unit for treatment. Once the source of infection was identified, the patient was treated with a combination of antibiotics for 2 weeks and was discharged with a significant improvement in symptoms.

KEYWORDS

***Rhodococcus equi*, acid-fast staining, human immunodeficiency virus, matrix-assisted laser desorption/ionization time-of-flight mass spectrometry, pulmonary infection, case report**

Introduction

Rhodococcus equi (hereafter *R. equi*), belonging to the genus Rhodococcus of the family Nocardiaceae, is named because it causes pulmonary infection in foals (1). *Rhodococcus equi* is a Gram-positive aerobic bacteria that produce fungus-like mycelia, which detach into rods and/or spheres within a short period of time. The bacteria were previously classified as Corynebacterium (2). The appearance of rod and/or globular forms correlates with the stage of culture, the type of specimen, and the culture conditions. The clinical pathogenicity of *R. equi* has been linked to human immunodeficiency virus (HIV) infection, and reports of AIDS co-infection with *R. equi* are increasing. Nonetheless, there are few detailed reports describing laboratory identification processes. Therefore, this report provide details on the laboratory identification (including molecular biology) and morphological characteristics of *R. equi*.

Case report

The patient was a 35-year-old male, white-collar worker, with no contact with livestock. He reported cough with sputum and hemoptysis after a cold 3 months prior to consultation, but without fever, chills, hot flushes, or night sweats. As these symptoms did not attract the patient's attention, the patient did not seek medical attention at a hospital for appropriate treatment. Approximately a month prior to the patient's first visit, the patient developed recurrent fever with chills and night sweats, with a maximum temperature of 38.9°C occurring mainly at night. However, the patient still did not seek medical attention. He recently developed new symptoms, such as weakness, lack of appetite, and poor mental health, and was seen at another hospital.

Clinical findings

Physical examination of the patient on admission revealed a body temperature of 38.9°C, pulse rate of 86 beats/min, respirations of 20 breaths/min, and blood pressure of 128/78 mmHg. The patient has bilateral thickened bilateral lungs and obstructed breath sounds, coarse wet rales were heard in the right lung, and no pathological murmurs were heard at rest. The findings of a chest computed tomography (CT) (performed at another hospital) suggested possible secondary tuberculosis (TB) with cavitation in the right upper lung and middle lung lobes and thickened adhesions in the right pleura (Figures 1A,B). The patient was directed to the TB clinic to confirm the diagnosis of pulmonary TB where three sputum samples were obtained. Our laboratory performed acid-fast staining of these sputum samples and a large number of acid-fast bacteria, which could be visible under the microscope (Figures 1C,D). Nonetheless, the microscopic morphology was globular and partially colored clusters, which was not typical of that common *Mycobacterium tuberculosis*, thus the patient was suspected of infecting with *R. equi.* We then alerted the clinician about the findings, and the patient was admitted to the respiratory unit of our hospital for systematic treatment.

Laboratory examinations

The inflammatory indicators for this patient during treatment and during the follow-up review after discharge are presented in Table 1. Furthermore, the patient's HIV antibody screening test was positive and the results of the CD4+ T lymphocyte count were 31 cells/μl, the two findings that were highly suggestive of HIV infection. Furthermore, the patient's T-cell spot test was negative for TB infection, which helped to exclude pulmonary TB. More importantly, the culture of the sputum sample revealed colonies of *R. equi* (semiquantitative: 4+), which provided strong evidence of pulmonary infection with *R. equi*.

Abbreviations: WBC, white blood cell; CRP, C-reactive protein; PCT, procalcitonin; IL-6, interleukin 6; MIC, minimum inhibitory concentration.

Bacterial identification

Patient's sputum samples were spread on a Colombian blood agar plate, a Chocolate agar plate, an MacConkey agar plate, and an Sabouraud agar plate (all plates were produced in China by Zhengzhou Antu Biological Bioengineering Co.). After 24 h of incubation at 35°C and 5% CO_2, only on the Columbia blood agar plate grew a large number of mucinous colonies and we selected the mucinous colonies for pure culture, after 6 h of pure culture, colonies from the original area of the plate were selected for Gram staining, and Gram-positive rods and mycelium-like fungal bodies were visible under the microscope (Figure 2A). After 24 h of pure culture, mucinous colonies with a smooth, raised, light orange surface and ∼1 mm in size, without hemolysis, developed on the blood agar plate (Figure 2B), and the Gram staining pattern of colonies at this stage was globular in clusters under the microscope (Figure 2C). After 48 h of culture, an aerial mycelium-like material formed around the colonies (Figure 2D). The colonies were stained with a weak acid-fast stain after 48 h of pure culture, and some bacteria were observed to resist acid staining under the microscope (Figure 2E). This bacterial strain was identified with the French Mérieux VITEK-2 Compact GP identification card (complete blood count (CBC) identification cards are not routinely purchased in our laboratory) as a low-confidence *Kocuria spp*. Next, we evaluated the strain by mass spectrometry using the Zhongyuan Huiji Micro Typer MALDI-TOF and identified it as *R. equi* (Figure 2F). We extracted deoxyribonucleic acid (DNA) fragments from pure colonies and amplified 16S ribosomal ribonucleic acid (RNA) using the primers 7F and 1540R. The purified polymerase chain reaction (PCR) products were used for sequence comparison using BLAST in the National Center for Biotechnology Information database website, and a fragment of 1,433 bp in length was selected for comparison and determined to correspond to the *R. equi* strain (ATCC 6939) with a similarity of 99.86%. *The R. equi* catalase test and urease were positive and did not decompose glucose. The results of the Christie–Atkins–Munch–Peterson (CAMP) test were observed after 24 h incubation on a blood agar plate with *Staphylococcus aureus* (ATCC 25923) and *Listeria monocytogene* as controls. The results showed that *R. equi* was hemolyzed in the form of an arrowhead near *S. aureus*, while *L. monocytogene* was hemolyzed in the form of a match head near *S. aureus* (Figure 2G). Furthermore, the sputum sample was also stained with silver hexamine to determine whether the patient was infected with *Pneumocystis carinii*, but dark black *R. equi* colonies were observed by microscopy (Figure 2H), which confirmed that silver hexamine staining

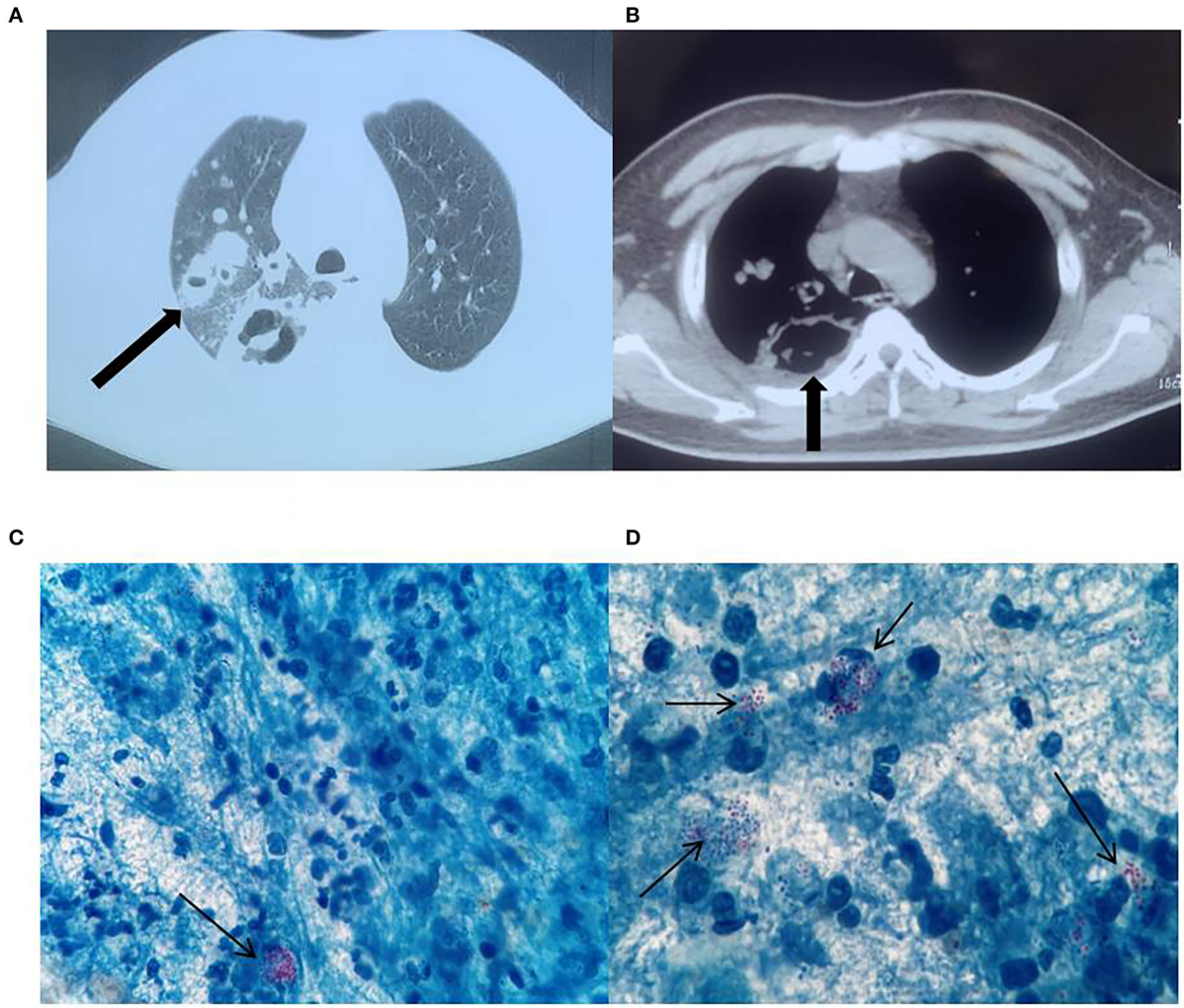

FIGURE 1
Chest computed tomography (CT) images. Right lung cavity **(A)**, thickening of and adherence to the right pleura **(B)**. Acid-fast bacteria in the microscopic field of view **(C,D)**, ×1000.

could also stain acid-resistant bacteria the same dark brown color as fungi.

Susceptibility to antibiotics

We prepared bacterial suspensions with a standard turbidity of 0.5 McFarland and tested the susceptibility of the strains to antibiotics by the *E*-test method; the results are presented in Table 2.

Clinical treatment

After the pathogen was identified, the clinician immediately treated the patient with a three-drug combination of levofloxacin combined with rifampicin and meropenem (the patient started treatment with the combination of drugs on day 3). After a week of combined treatment, the patient's symptoms and inflammatory index began to improve, and after 2 weeks the patient was discharged with a significant improvement in symptoms. The patient's condition did not deteriorate at the 2-week follow-up. The patient was asked to continue taking oral antibiotics until the $CD4^+$ T lymphoid count reached 200 cells/μl after antiviral treatment, and regular monthly follow-up of inflammatory indicators and chest CT.

Discussion

Rhodococcus equi belongs to the genus Rhodococcus. Currently, there are 57 species belonging to the genus Rhodococcus, the most common and relevant to clinical

10.3389/fpubh.2022.982917

TABLE 1 Indicator of inflammation in this patient.

	Day 1	Day 4	Day 7	Day 13	D-week 2	D-week 8
WBC count ($\times 10^9$/L)	17.60	18.09	11.59	6.00	3.30	4.21
CRP (mg/L)	>200.00	172.09	143.08	39.35	2.29	5.26
PCT (ng/mL)	0.88		1.34	<0.50		
IL-6 (pg/mL)	49.52		15.77	<7.00		

WBC, white blood cell; CRP, C-reactive protein; PCT, procalcitonin; IL-6, interleukin 6.
D-week, the number of weeks since the patient was discharged; a blank indicates that the item was not tested at that time.

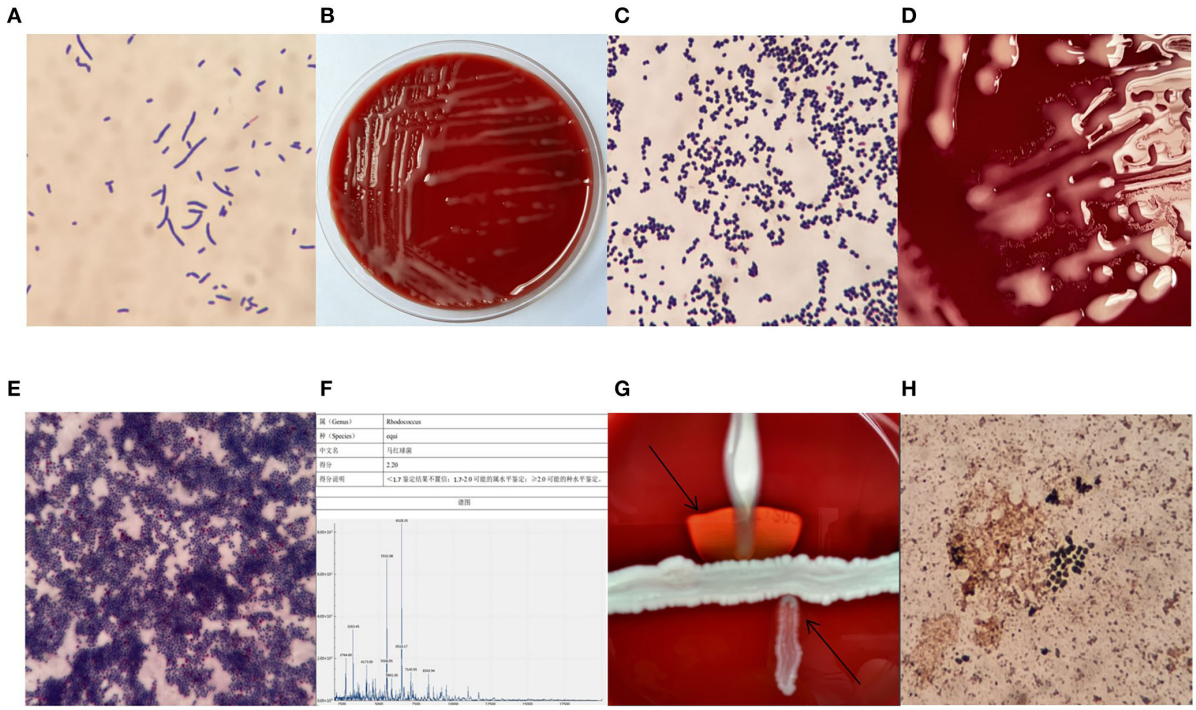

FIGURE 2
Gram stain after 6 h of pure culture **(A)** ×1,000, colony morphology after 24 h of pure culture **(B)**, Gram-stained morphology after 24 h of pure culture **(C)** ×1,000, fungal pseudomycorrhizal-like material **(D)**, the morphology of weak acid-fast stain **(E)** ×1,000, mass spectrometer identification result **(F)**, the Christie–Atkins–Munch–Peterson (CAMP) test **(G)**, the morphology of hexamine silver staining **(H)** ×1,000.

TABLE 2 Antibiotic susceptibility test for *Rhodococcus equi*.

Antibiotics	MIC (mg/L)	Antibiotics	MIC (mg/L)
Rifampin	1	Imipenem	1
Levofloxacin	1	Penicillin	8
Vancomycin	0.25	Clindamycin	4
Erythromycin	0.5	Sulfamethoxazole	2
Linezolid	1	Daptomycin	4

MIC, minimum inhibitory concentration.

medicine being *R. equi, R. roseus,* and *R. rhodochrous*. *R. equi* is widely distributed in all living environments (except Antarctica) and is a conditionally pathogenic bacterium (1). *Rhodococcus equi* is closely associated with HIV infection and approximately two-thirds of patients infected with *R. equi* are also infected with HIV (3), which should alert clinicians whether the infection with *R. equi* is accompanied by other factors that contribute to the patient's immune deficiency, such as HIV infection. Infections caused by *R. equi* are prone to misdiagnosis or underdiagnosis. One of the reasons for this is misinformation provided to clinicians by testing laboratories. The Gram staining pattern of *R. equi* is related to the stage of culture, and when a bloodstream infection occurs, Gram-positive, rod-shaped bacilli may be found in blood specimens, although the blood culture may only be positive for a short period of time. Reporting misinformation to clinicians may result in the judgment of contaminating bacteria and thus overlooking the

correct treatment plan. Tuon et al. described two deaths as a result of an outbreak of *R. equi* infections, both incorrectly identified as *Corynebacterium spp*. This misinformation led clinicians to interpret the findings as contaminating bacteria despite multiple positive blood cultures (4). Laboratories using the Mérieux VITEK-2 Compact should be aware that *R. equi* is listed in the identification catalog on the CBC identification card; whereas most laboratories using this instrument are equipped with the GP card (Gram-Positive identification card). However, neither the GP identification card nor the anaerobic and corynebacteria identification card (ANC) identification card can accurately identify *R. equi* and will give incorrect results. If laboratories provide misinformation to clinicians, this will also result in patients not receiving the correct treatment and timing. Thus, mass spectrometry is considered particularly suitable for the rapid and accurate identification of bacterial species, although specific staining techniques can also assist in the differential diagnosis of infections caused by *R. equi*, as in this case, where we initially identified a suspected infection of *R. equi* using acid-fast staining. However, the clinician's lack of experience and awareness of *R. equi* infection may also lead to misdiagnosis or underdiagnosis. As the foci of lung infection by *R. equi* are usually diffuse, pleomorphic, and associated with cavitation of the lung, they can easily be misdiagnosed as pulmonary TB with cavitation (5–7). The patient in this case had the same imaging characteristics and was also initially highly suspected of having pulmonary TB. Although both infections exhibit cavitation, the cavities in tuberculous caseous pneumonia are worm-eaten-like hollows, whereas the cavities in *R. equi* are formed when *R. equi* produces continuous lesions in the alveolar wall, and the cavities tend to have compartmentalized changes. Furthermore, pulmonary *R. equi* infections can be divided into exudative, solid, and abscess-forming stages. Early lesions are often detected by a small patch of slightly high-density shadows, but if not treated effectively, they can develop into solid lesions, forming nodular or mass-like lesions, which are remarkably similar to malignant tumors and are often combined with enlarged mediastinal lymph nodes. *Rhodococcus equi* pneumonia can show parenchymal changes in the spherical lung, some of which are well defined, but most have blurred margins and are broadly conical with the base located on the pleural side. In contrast, inflammatory lesions surrounding a lung tumor are mostly characterized by an obstructive inflammation distributed distally to the mass. The exudative inflammation surrounding *R. equi* pneumonia has no clear pattern, and there are often exudative inflammatory lesions from other lobes.

Treatment of *R. equi* infections generally recommends a combination of antibiotics (8). The Sanford Guide to Antimicrobial Therapy recommends azithromycin, levofloxacin, or rifampicin as the first choice for the anti-infective treatment of *R. equi*; vancomycin or imipenem plus levofloxacin or azithromycin or rifampicin as the second choice. Penicillin, cephalosporins, clindamycin, tetracycline, and cotrimoxazole should be avoided. It is important to note that although vancomycin may be susceptible to *R. equi in vitro*, because *R. equi* is a facultative intracellular parasitic bacterium, vancomycin cannot achieve expected intracellular concentrations, leading to reduced activity against intracellular *R. equi* and failure of treatment. Therefore, clinicians should choose antibiotics that have good cell penetration to treat the infection. The treatment period for *R. equi* infections is long and requires prolonged medication, and some patients continue to require oral medications after discharge from the hospital. The treatment period varies from a few months to a few years, while cavitary lesions should be treated for longer periods of time, as there is also a risk of recurrence (1, 8, 9). Capdevila et al. reported that only half of the 78 patients infected with *R. equi* in their hospital were cured after prolonged antibiotic treatment, it is easy to relapse after treatment, and the probability of recurrence is close to 50% (6).

Furthermore, early use of highly active antiretroviral therapy once HIV infection is diagnosed may improve the prognosis of HIV coinfection with *R. equi* and increases the chances of recovery; in untreated HIV-infected individuals, the relative risk of death from *R. equi* infection was 53 times higher than in those who received appropriate antiretroviral therapy (10). Many cases of treatment failure are due to the lack of effective antiretroviral therapy in combination with treatment for *R. equi* (11–13). For HIV patients with *R. equi* infection, it is not only necessary to monitor their inflammatory indicators [such as white blood cell (WBC) count and C-reactive protein (CRP)] at a later stage, but also the CD4+ T lymphocyte count should be monitored. Currently, there is no standard reference for the specific values of these parameters. When the CD4+ T lymphocyte count returns to more than 200 cells/μl after receiving antiretroviral therapy, this could indicate that the patient has achieved some immunity, and the treatment can be adjusted according to the patient's specific clinical condition.

It should be noted that, in this case, we initially identified a large number of acid-fast cocci in his sputum through acid-fast staining, and when combined with our experience, we correctly determined that it was *R. equi* and promptly informed the clinician and patient in advance so that they could prepare a treatment plan in advance, which saved the patient and the doctor considerable time and effort and made our findings more clinically valuable.

In conclusion, although the number of reports of *R. equi* is gradually increasing, there are still many laboratories that have difficulty in identifying the bacteria, and this is further combined with misdiagnosis and omission by the physician, which makes patients miss the correct treatment plan and timely treatment, posing a considerable challenge to both laboratory staff and clinicians. Providing accurate and prompt feedback from laboratories to clinicians will allow patients to receive the correct treatment plan as soon as possible.

Furthermore, traditional biochemical identification is slow and less accurate for rare bacteria. Mass spectrometry can quickly and accurately identify rare bacteria; therefore, microbiology laboratories should be equipped with mass spectrometers (14), which represent an inevitable trend for the future development of clinical microbiology laboratories.

Data availability statement

The original contributions presented in the study are publicly available. This data can be found here: http://www.ncbi.nlm.nih.gov/bioproject/857424 / BioProject ID: PRJNA857424.

Ethics statement

This study was approved by the Chongqing University Jiangjin Hospital institutional review board. Written informed consent was obtained from the participants for the publication of the case report.

Patient perspective

The patient agreed to our treatment plan and thanked us for the subsequent improvement in symptoms.

Author contributions

YJ wrote and revised this manuscript. YZ, WQ, and JL reviewed this manuscript. YG and XL collected the data for this manuscript. All authors contributed to the article and approved the submitted version.

Funding

This research was supported by the Key Technology Innovation Special of Key Industries of Chongqing Science and Technology Bureau Fund (cstc2020jscx-fyzxX0021).

Acknowledgments

The authors would like to acknowledge Zhongyuan Huiji Biotechnology Co. and Mr. Xiaoyue Nie for their assistance in sequencing.

Conflict of interest

The authors declare that the research was conducted in the absence of any commercial or financial relationships that could be construed as a potential conflict of interest.

Publisher's note

References

1. Lin WV, Kruse RL, Yang K, Musher DM. Diagnosis and management of pulmonary infection due to *Rhodococcus equi*. *Clin Microbiol Infect*. (2019) 25:310–5. doi: 10.1016/j.cmi.2018.04.033

2. Goodfellow M. The toxonomic status of *Rhodococcus equi*. *Vet Microbiol*. (1987) 14:205–9. doi: 10.1016/0378-1135(87)90106-4

3. Weinstock DM, Brown AE. *Rhodococcus equi*: an emerging pathogen. *Clin Infect Dis*. (2002) 34:1379–85. doi: 10.1086/340259

4. Tuon FF, Siciliano RF, Al-Musawi T, Rossi F, Capelozzi VL, Gryschek RC, et al. Rhodococcus equi bacteremia with lung abscess misdiagnosed as corynebacterium: a report of 2 cases. *Clinics*. (2007) 62:795–8. doi: 10.1590/S1807-59322007000600022

5. Gallant JE, Ko AH. Cavitary pulmonary lesions in patients infected with human immunodeficiency virus. *Clin Infect Dis*. (1996) 22:671–82. doi: 10.1093/clinids/22.4.671

6. Capdevila JA, Buján S, Gavaldá J, Ferrer A, Pahissa A. *Rhodococcus equi* pneumonia in patients infected with the human immunodefficiency virus: report of 2 cases and review of the literature. *Scand J Infect Dis*. (1997) 29:535–41. doi: 10.3109/00365549709035890

7. Savini V, Fazii P, Favaro M, Stolfi D, Polilli E, Pompilio A, et al. Tuberculosis-like pneumonias by the aerobic actinomycetes Rhodococcus, Tsukamurella and Gordonia. *Microbes Infect*. (2012) 14:401–10. doi: 10.1016/j.micinf.2011.11.014

8. Arya B, Hussian S, Hariharan S. *Rhodococcus equi* pneumonia in a renal transplant patient: a case report and review of literature. *Clin Transplant*. (2004) 18:748–52. doi: 10.1111/j.1399-0012.2004.00276.x

9. Kim R, Reboli AC. 207 - Other Coryneform Bacteria and Rhodococci. In: Bennett JE, Dolin R, Blaser MJ, editors. *Mandell, Douglas, and Bennett's Principles and Practice of Infectious Diseases (Eighth Edition)*. Philadelphia, PA: W.B. Saunders (2015). p. 2373–2382.e2374. Available online at: https://www.sciencedirect.com/science/article/pii/B9781455748013002071

10. Topino S, Galati V, Grilli E, Petrosillo N. *Rhodococcus equi* infection in HIV-infected individuals: case reports and review of the literature. *AIDS Patient Care STD*. (2010) 24:211–22. doi: 10.1089/apc.2009.0248

11. Kwa AL, Tam VH, Rybak MJ. *Rhodococcus equi* pneumonia in a patient with human immunodeficiency virus: Case report and review. *Pharmacotherapy*. (2001) 21:998–1002. doi: 10.1592/phco.21.11.998.34512

12. Lasky JA, Pulkingham N, Powers MA, Durack DT. *Rhodococcus equi* causing human pulmonary infection: review of 29 cases. *South Med J*. (1991) 84:1217–20. doi: 10.1097/00007611-199110000-00014

13. Cury JD, Harrington PT, Hosein IK. Successful medical therapy of *Rhodococcus equi* pneumonia in a patient with HIV infection. *Chest*. (1992) 102:1619–21. doi: 10.1378/chest.102.5.1619

14. Tsuchida S, Umemura H, Nakayama T. Current status of matrix-assisted laser desorption/ionization-time-of-flight mass spectrometry (MALDI-TOF MS) in clinical diagnostic microbiology. *Molecules*. (2020) 25:775. doi: 10.3390/molecules25204775

frontiers | Frontiers in Public Health

TYPE Case Report
PUBLISHED 20 September 2022
DOI 10.3389/fpubh.2022.994279

OPEN ACCESS

EDITED BY
Ana Afonso,
Universidade NOVA de Lisboa, Portugal

REVIEWED BY
Paolo Bottino,
University of Turin, Italy
Sabino Pacheco,
National Autonomous University of Mexico, Mexico
Sangeeta Deka,
Gauhati Medical College and Hospital, India
Iris Yuefan Shao,
Emory University, United States

*CORRESPONDENCE
Yan Zeng
zengyjyh@outlook.com

†These authors share first authorship

SPECIALTY SECTION
This article was submitted to Infectious Diseases-Surveillance, Prevention and Treatment, a section of the journal Frontiers in Public Health

RECEIVED 14 July 2022
ACCEPTED 23 August 2022
PUBLISHED 20 September 2022

CITATION
Jiang Y, Qin W, Li J, Gao Y and Zeng Y (2022) A case report of sepsis and death caused by *Parvimonas micra*, a rare anaerobe.
Front. Public Health 10:994279.
doi: 10.3389/fpubh.2022.994279

A case report of sepsis and death caused by *Parvimonas micra*, a rare anaerobe

Yuhang Jiang[1,2†], Weichao Qin[1,2†], Jian Li[1,2], Yuan Gao[1,2] and Yan Zeng[3*]

[1]Department of Laboratory Medicine, Chongqing University Jiangjin Hospital, Chongqing, China, [2]Department of Laboratory Medicine, Central Hospital of Jiangjin District, Chongqing, China, [3]Department of Laboratory Medicine, Jiangjin District Maternity and Child Health Hospital, Chongqing, China

Parvimonas micra is a type of Gram-positive anaerobic cocci widely distributed in the oral cavity, gastrointestinal tract, respiratory tract, and female reproductive system mucosa. It is a conditional pathogen that can cause infections in the human oral cavity, wounds, and other areas as well as sepsis. In this case report, the patient's immune system was compromised by various underlying diseases and a pulmonary infection, which led to the entry of *P. micra* infection into the bloodstream. *P. micra* is a slow-growing organism (When a bloodstream infection occurs, flagging an anaerobic bottle of blood culture as positive will usually take >48 h), which makes it hard to secure timely blood culture results. Our patient's poor physical condition eventually led to sepsis, and she died after 5 days in the hospital.

KEYWORDS

***Parvimonas micra*, bloodstream infection, blood culture, septicemia, matrix-assisted laser desorption/ionization time-of-flight mass spectrometry, molecular diagnostic technique, next-generation sequencing, diabetes mellitus**

Introduction

Parvimonas micra (hereafter *P. micra*) are Gram-positive cocci recognized as a type of oral pathogen (1). In recent years, due to the use of matrix-assisted laser desorption/ionization time-of-flight mass spectrometry and molecular diagnostic techniques, reports of infections with *P. micra* are increasing, but deaths caused by *P. micra* remain rare and, as far as we know, there are no reports in the literature containing laboratory identification details and morphological characteristics of *P. micra*. In the present paper, therefore, we offer more details about the laboratory identification process (including molecular biology techniques) and morphological characteristics of this organism. The described case was confirmed to be the first report of death in China due to sepsis and shock caused by a *P. micra* bloodstream infection that resulted in multiorgan failure of the patient. We hope this case report will encourage more clinicians and laboratory medicine staff to be aware of the potential threat represented by this bacterium.

Case report

The patient was a 53-year-old woman with rheumatoid arthritis for >20 years who was on long-term pain medication (the exact type of medication was not known) and who had a history of hypertension for >1 year (her systolic blood pressure was normally maintained at around 150 mmHg). She had high blood glucose results tested in other hospitals, but she did not undergo a confirmatory test for diabetes before she was admitted to our hospital. The patient had previously presented with lower back pain and weakness in both lower limbs with no apparent cause 1 month prior to admission to our hospital and she had been treated in another hospital for a period of time (she failed to provide the specific type of medication used for treatment). Within a few days, she had new symptoms of coughing with phlegm and black stools, and her low back pain had not improved significantly. Thus, she came to our hospital for further treatment. After additional inquiry about the patient's condition, the patient stated that she had not had any recent trauma, and had not urinated in the past 3 days. Then the patient was subsequently taken to the intensive care unit for emergency treatment. The patient finally died of multi-organ failure due to infectious shock even after 5 days of anti-infective treatment in the intensive care unit. This study was approved by the ethics committee at the Chongqing University Jiangjin Hospital, and the patient's family member provided written consent for the publication of the report.

Clinical findings

The patient was admitted with an acute painful appearance, and physical examination revealed wet rales in both lungs and significant percussion pain in the low back. Physical examination of the patient at admission revealed a body temperature of 36.2°C, pulse 136 beats/min, respiration 20 breaths/min, and blood pressure 114/70 mmHg. An emergency chest computed tomography scan revealed scattered irregular patchy and streaky shadows in both lungs and bilateral pleural effusions, fractures of the right scapula, sternum, bilateral multiple ribs and sacrum.

Laboratory examinations and clinical diagnosis

The patient's arterial blood gas analysis revealed the following values: pH, 7.41; $PaCO_2$, 27 mmHg; PaO_2, 54 mmHg; whole blood lactic acid, 3.5 mmol/L; and fasting blood glucose, 11.2 mmol/L. A complete blood count revealed the following: hemoglobin, 104 g/L; platelet count, 225 × 10^9/L; and neutrophil % count, 87.10%. The patient's biochemical parameters are shown in Table 1, and her white blood cell (WBC) count, procalcitonin concentration, and CRP level at various times during her hospital stay are shown in Table 2. Corona virus disease 2019 (COVID-19) nucleic acid test was negative. The above-mentioned tests combined with the patient's chest CT findings suggested a preliminary diagnosis of pulmonary infection, type 1 respiratory failure, and type 2 diabetes mellitus, as there was no history of trauma, the patient was considered to have a pathological fracture due to infection. The results of multiple sputum cultures were negative; a total of two sets of blood cultures were taken from the upper and lower extremities of the patient at the time of fever and sent for culturing. The anaerobic bottles were all positive, and the culture results were all *P. micra* (however, the patient had already unfortunately passed away by the time the bacterial identification results were obtained).

Bacterial identification

Both sets of blood cultures from the patient were placed in a BACT/ALERT 3D automated blood culture instrument (BioMérieux, Inc., Durham, North Carolina, USA), and one anaerobic bottle was flagged as positive by the instrument after about 107 h, while the other one was flagged as positive after >120 h of culturing. We then streaked the blood from the anaerobic bottles onto a Columbia blood agar plate, MacConkey agar plate, and non-selective chocolate agar plate (all plates sourced from Zhengzhou Antu Biological Bioengineering Co., Zhengzhou, China) to plating, then placed the plates in a 35°C and 5% CO_2 environment for culturing. Blood was then drawn again onto another Columbia blood agar plate to plating, and the plate was placed into an anaerobic environment for anaerobic culture. At the same time, a blood smear was prepared from anaerobic bottles for Gram staining microscopy. The microscopic investigation revealed that quite small Gram-positive cocci could be seen under the microscope (Figure 1A), distributed in groups or individually (Figure 1B). After 18 h of culturing, all plates in the aerobic environment were free of bacterial growth. However, tiny colonies were visible on the Columbia agar incubated in an anaerobic environment. This finding suggested that the patient had a bloodstream infection with anaerobic bacteria.

After 48 h of culturing, creamy white, round, moist colonies (there is only one type of colony) approximately 0.6 μm size were visible on the Columbia blood agar plate cultured in an anaerobic environment, with an areola-like formation around the colonies (Figures 1C,D), which was used as one of the identifying features of the bacterium. Pure colonies on the plate were then picked for Gram staining microscopy, and tiny Gram-positive cocci could be seen under the microscope, either in clusters or singly distributed (Figure 1E). Such colonies can easily be mis-stained as Gram-negative cocci, so the decolorization step of the Gram stain is vital, and the correct

TABLE 1 Biochemical parameters of this patient.

Biochemical parameters items	Results	Biochemical parameters items	Results
Blood urea nitrogen	14.4 mmol/L	interleukin-6	410.40 pg/mL
Blood uric acid	668 μmol/L	Cystatin-C	1.35 mg/L
Glycosylated hemoglobin	7.8%	Beta-2-microglobulin	7.33 mg/L
Hypersensitivity C-reactive (CRP) protein	294.05 mg/L	Prealbumin	13.7 mg/L

TABLE 2 Trends in inflammatory indicators during the patient's hospitalization.

	Day 1	Day 2	Day 3 (Antibiotic changed)	Day 4	Day 5
WBC count (×109/L)	21.19	14.77	14.17	17.94	18.36
CRP (mg/L)	>200	>200	>200	>200	>200
PCT (ng/mL)	2.93	2.55		2.55	1.63

WBC, white blood cell; CRP, C-reactive protein; PCT, procalcitonin.
A blank spot indicates that the item was not tested at that day.

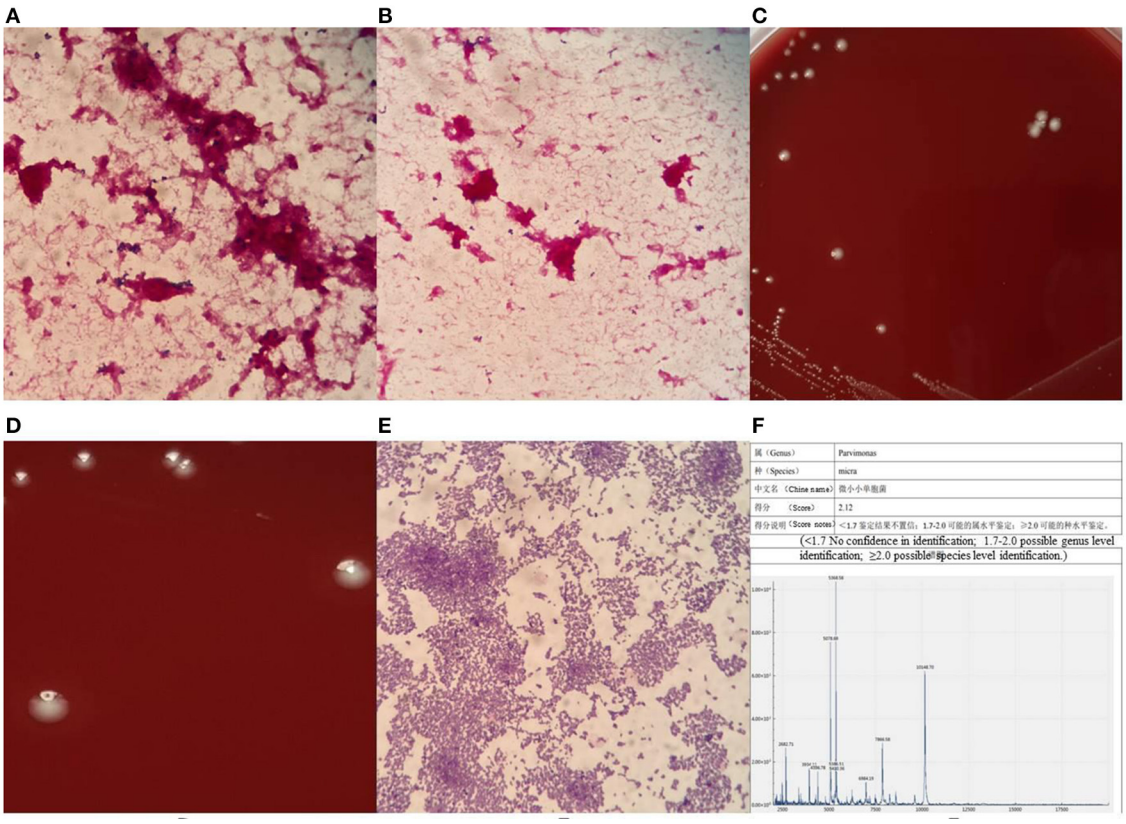

FIGURE 1
Gram stain of blood smear under microscope **(A)** × 1000, morphological distribution of *P. micra* **(B)** × 1000, morphological characteristics of colonies of *P. micra* **(C,D),** Gram-stained morphology of *P. micra* colonies **(E)** × 1000, mass spectrometer identification result **(F)**.

staining depends on the operator's experience. At this point, the strain was identified as *P. micra* using the Zhongyuan Huiji Micro Typer MALDI-TOF mass spectrometer (Chongqing Zhongyuan Huiji Biotechnology Co., Ltd., Chongqing, China) (Figure 1F). It took 1 week to finally identify the bacteria from the time the blood culture specimens were sent to the

laboratory, which was too long a time period to report the pathogen to clinicians. In order to verify whether the strain was *P. micra*, we extracted DNA fragments from pure colonies and amplified 16S ribosomal RNA using the primers "27F" and "1492R." Forward primer name 27F, 5'- AGT TTG ATC MTG GCT CAG−3', Reverse primer name 1492R, 5'- GGT TAC CTT GTT ACG ACT T−3', target fragment was about 1500 bp. Polymerase chain reaction (PCR) reaction system 50μL: PCR Mix 45μL, 2μL of each forward and reverse primer, 1μL of template DNA, dH_2O (distilled water) 22 μL.The PCR reaction conditions: pre-denaturation at 98°C for 2 min; 35 cycles of 98°C for 10s, 56°C for 10s and 72°C for 10s/kb; extension at 72 °C for 5 min; After the reaction, 2μL of amplification products and 6μL of bromophenol blue were taken and the purity of PCR products were examined by 1% agarose gel electrophoresis. The contigExpress software was used to splice the sequences and remove the inaccurate ends, and then the spliced 16s rRNA sequences wereused for sequence comparison, which was performed by using the Basic Local Alignment Search Tool on the U.S. National Center for Biotechnology Information database website, and a fragment measuring 1,400 bp in length was selected for comparison and analyzed as *P. micra* (ATCC 33270; American Type Culture Collection, Manassas, VA, USA), with a similarity of 99.64% observed.

Susceptibility to antibiotics

Because we had no resources for anaerobic bacteria *in vitro* antibiotics susceptibility testing at the time of this case, we had no way to obtain the antibiotics sensitivity results of this bacterium.

Clinical treatment and prognosis

The patient was admitted to the intensive care unit on her first day in the hospital. After consultation with our orthopedic department, the patient was advised to rest in bed and symptomatically manage other symptoms as well as eliminate the cause of the infection, taking into account his current poor physical condition. The emergency chest computed tomography images indicated infection in both lungs, and piperacillin–tazobactam was given for the first 2 days as anti-infective treatment. However, the patient's infection did not improve at all. On the day after her admission to the hospital, her blood pressure suddenly started to drop, her blood pressure needed adrenaline to maintain. At this time, her blood pressure after using adrenaline was 104/62 mmHg; her heart rate reached 131 bpm; whole blood lactate reached 4.3 mmol/L; brain natriuretic peptide (BNP) reached 297 pg/mL, and her urine output was reduced. Combining these data with the above-mentioned information and the recorded high values of inflammatory indicators, the doctor suggested that the patient had infectious shock. Norepinephrine was continued giving to raise her blood pressure, and the doctor actively gave the patient fluid replacement and used furosemide for diuretic treatment. In the meantime, the antibiotic was changed to imipenem. On the fourth day of hospitalization, the patient developed hypoxemia, and she was intubated and treated with invasive mechanical ventilation. The patient's blood pressure was maintained at 122/62 mmHg by the administration of norepinephrine combined with M-hydroxylamine, and an assessment of inflammatory indicators revealed the following values: WBC count, 17.94 $\times$ 10^9/L (percentage of neutrophils: 81.20%); procalcitonin concentration, 2.55 ng/mL; and CRP level, >200 mg/L. At this point the patient has very severe systemic inflammation. Unfortunately, the patient developed then generalized edema and on the fifth day of hospitalization and died of multiorgan failure due to septic shock. As the blood culture pathogenic results were not fed back to the clinician in a timely manner, coupled with the negative sputum culture results, the patient had to receive urgent empirical antibiotic treatment during hospitalization.

Discussion

P. micra is a species of conditionally pathogenic anaerobic bacteria that can be found in various human mucous membranes. The size of *P. micra* is tiny (0.3–0.7 μm). *P. micra* was originally classified as *Peptostreptococcus micros*, then reclassified as *Micromonas micros* in 1999 and reclassified again as *P. micra* in 2006 (2). It is recognized as an oral pathogen (1); however, *P. micra* can also cause bloodstream infections, spinal infections, septic chest, and sepsis (3, 4). In most cases of infection with *P. micra*, the first symptom is usually lower back pain, and most patients are admitted to the hospital with back pain (4, 5). The patient in this case initially sought treatment at another hospital for lower back pain. At that time, she was probably already infected with *P. micra* in her lower back but had not yet developed any symptoms of pulmonary infection; as a result, she was likely viewed as a normal lumbar spine patient and treated using pain relief and traditional Chinese medicine physiotherapy. Even when the patient had obvious signs of lung infection and a bloodstream infection, several sputum culture results were still negative, and she did not immediately receive the correct antibiotic treatment. When the patient was admitted to our hospital, her lungs might have already been infected with *P. micra*. One study reported a 49-fold increase in tumor necrosis factor α release from macrophages following the binding of *P. micra* to endotoxin with *Haemophilus actinomycetemcomitans* (6); thus, it can be proved that *P. micra* has the ability to cause severe inflammation by stimulating

macrophages to release various inflammatory factors. This may be the cause of systemic inflammation and sepsis outbreak in our patient.

In data from Tsuyoshi's study, the 30-day clinical mortality rate for bloodstream infections with *P. micra* was only about 3.7%, (4) but it is still worth drawing the attention of clinicians to this issue. The majority of patients infected with *P. micra* also have underlying medical conditions (2, 4, 7), which suggests that the prevalence of *P. micra* infection is linked to human immunity. In our case, the patient had a long history of rheumatoid arthritis and was unaware that she had diabetes. Both of these underlying conditions can cause severe disruption of and a reduction in the strength of a patient's autoimmune system, which likely led to infection of this patient's lower back with *P. micra* at first. For the treatment of *P. micra* infection, penicillin, metronidazole, and clindamycin are usually preferred (8). Our patient was initially treated with a 3-day infusion of piperacillin–tazobactam, but her infection was not controlled. The antibiotic of choice was later changed to meropenem, but the optimal timing for treatment might have passed by that point. Although both piperacillin–tazobactam and imipenem have some pharmacological effect on anaerobic bacteria, they were very ineffective in treating our patient's infection, and it is presumed that she may have also had a combination of other pathogenic infections. In a report by Yu et al., (9) a patient was treated with piperacillin–tazobactam and meropenem after lung infection with *P. micra*, but the initial outcome was unsatisfactory. The infection was finally treated with ornidazole after the pathogenic organism was identified by next-generation sequencing (NGS), and the lung infection was rapidly controlled. Thus, clinicians should consider the use of narrow-spectrum anti-anaerobic drugs in cases where conventional antibiotic therapy has failed.

In some reports of infections with *P. micra*, the final diagnosis is made by reference to the NGS results (9). NGS is the process of randomly fragmenting and splicing DNA, preparing sequencing libraries, and ultimately obtaining sequence information by performing extension reactions on the tens of thousands of clones in the library and detecting the corresponding signals (the core principle is sequencing while synthesizing). NGS can quickly provide results in as little as 24 h and is capable of detecting pathogens, including viruses, rickettsiae, and other pathogens, that cannot be detected by conventional culture methods. However, there were some shortcomings in our study and we regret that the doctors did not send the patients' blood specimens and respiratory specimens for NGS analysis in time to rule out mixed infections. Conventional anaerobic culture has a very low positive rate and takes a very long time, so new diagnostic techniques such as NGS should be considered when the source of infection is not clear and the infection is severe, as this approach can greatly reduce the time taken to find the causative agent, save time for the patient, and provide the clinician with the right treatment ideas.

Data availability statement

The original contribution of this manuscript is available from (http://www.ncbi.nlm.nih.gov/bioproject/PRJNA859504).

Author contributions

YJ wrote the manuscript. YZ reviewed the manuscript. YG, JL, and WQ collected the data for the manuscript. YJ and YZ share first authorship. All authors contributed to the article and approved the submitted version.

Funding

This research was supported by the key technology innovation special of key industries of 246 Chongqing Science and Technology Bureau Fund (cstc2020jscx-fyzxX0021).

Acknowledgments

The authors like to acknowledge Zhongyuan Huiji Biotechnology Co., and Mr. Xiaoyue Nie for providing sequencing assistance.

Conflict of interest

The authors declare that the research was conducted in the absence of any commercial or financial relationships that could be construed as a potential conflict of interest.

Publisher's note

References

1. van Duijvenbode DC, Kuiper JWP, Holewijn RM, Stadhouder A. Parvimonas micra spondylodiscitis: a case report and systematic review of the literature. *J Orthop Case Rep*. (2018) 8:67–71. doi: 10.13107/jocr.2250-0685.1216

2. Miyazaki M, Asaka T, Takemoto M, Nakano T. Severe sepsis caused by Parvimonas micra identified using 16S ribosomal RNA gene sequencing following patient death. *IDCases*. (2020) 19:e00687. doi: 10.1016/j.idcr.2019.e00687

3. Gorospe L, Bermudez-Coronel-Prats I, Gomez-Barbosa CF, Olmedo-Garcia ME, Ruedas-Lopez A, Gomez del Olmo V, et al. Parvimonas micra chest wall abscess following transthoracic lung needle biopsy. *Korean J Intern Med*. (2014) 29:834–7. doi: 10.3904/kjim.2014.29.6.834

4. Watanabe T, Hara Y, Yoshimi Y, Fujita Y, Yokoe M, Noguchi Y. Clinical characteristics of bloodstream infection by Parvimonas micra: retrospective case series and literature review. *BMC Infect Dis*. (2020) 20:578. doi: 10.1186/s12879-020-05305-y

5. Uemura H, Hayakawa K, Shimada K, Tojo M, Nagamatsu M, Miyoshi-Akiyama T, et al. Parvimonas micra as a causative organism of spondylodiscitis: a report of two cases and a literature review. *Int J Infect Dis*. (2014) 23:53–5. doi: 10.1016/j.ijid.2014.02.007

6. Yoshioka M, Grenier D, Mayrand D. Binding of Actinobacillus actinomycetemcomitans lipopolysaccharides to Peptostreptococcus micros stimulates tumor necrosis factor alpha production by macrophage-like cells. *Oral Microbiol Immunol*. (2005) 20:118–21. doi: 10.1111/j.1399-302X.2004.00204.x

7. Cobo F, Rodríguez-Granger J, Sampedro A, Aliaga-Martínez L, Navarro-Marí JM. Pleural effusion due to Parvimonas micra. A case report and a literature review of 30 cases. *Rev Esp Quimioter*. (2017) 30:285–92. Available online at: https://pubmed.ncbi.nlm.nih.gov/28537064

8. Rams TE, Sautter JD, van Winkelhoff AJ. Antibiotic resistance of human periodontal pathogen Parvimonas micra over 10 years. *Antibiotics*. (2020) 9:709. doi: 10.3390/antibiotics9100709

9. Yu Q, Sun L, Xu Z, Fan L, Du Y. Severe pneumonia caused by Parvimonas micra: a case report. *BMC Infect Dis*. (2021) 21:364. doi: 10.1186/s12879-021-06058-y

frontiers | Frontiers in Medicine

TYPE Case Report
PUBLISHED 23 September 2022
DOI 10.3389/fmed.2022.1003103

OPEN ACCESS

EDITED BY
Francesco Paolo Bianchi,
University of Bari Aldo Moro, Italy

REVIEWED BY
Matthew Durstenfeld,
University of California, San Francisco, United States
Julie Boucau,
Ragon Institute, United States

*CORRESPONDENCE
Lavanya Visvabharathy
lavanya.visvabharathy@northwestern.edu
Igor J. Koralnik
igor.koralnik@northwestern.edu

SPECIALTY SECTION
This article was submitted to Infectious Diseases – Surveillance, Prevention and Treatment, a section of the journal Frontiers in Medicine

RECEIVED 25 July 2022
ACCEPTED 01 September 2022
PUBLISHED 23 September 2022

CITATION
Visvabharathy L, Orban ZS and Koralnik IJ (2022) Case report: Treatment of long COVID with a SARS-CoV-2 antiviral and IL-6 blockade in a patient with rheumatoid arthritis and SARS-CoV-2 antigen persistence.
Front. Med. 9:1003103.
doi: 10.3389/fmed.2022.1003103

Case report: Treatment of long COVID with a SARS-CoV-2 antiviral and IL-6 blockade in a patient with rheumatoid arthritis and SARS-CoV-2 antigen persistence

Lavanya Visvabharathy*, Zachary S. Orban and Igor J. Koralnik*

Ken and Ruth Davee Department of Neurology, Feinberg School of Medicine, Northwestern University, Chicago, IL, United States

Introduction: Long COVID, or post-acute sequelae of SARS-CoV-2 infection (PASC) in ∼30% of all infected individuals. Here, we present a case of PASC in a patient with rheumatoid arthritis characterized by viral persistence in the nasopharynx for 6 months after acute infection. We demonstrate transient disappearance of antigen persistence and decreased antiviral and autoimmune T cell responses after nirmatrelvir/ritonavir and tocilizumab treatment.

Case presentation: A 37-year-old female with a 7-year history of rheumatoid arthritis enrolled in a COVID-19 research study was found to continuously test SARS-CoV-2 antigen positive in the nasopharynx for 6 months after acute infection. She simultaneously presented with new-onset PASC symptoms including chronic occipital headache and periods of intense fatigue 8 weeks after acute infection. The patient was prescribed nirmatrelvir/ritonavir to treat SARS-CoV-2 persistence at 3.5 months post-acute infection and observed a reduction in PASC symptoms 3 weeks after completing antiviral treatment. After resurgence of PASC symptoms, she stopped treatment with tocilizumab for rheumatoid arthritis to attempt complete SARS-CoV-2 viral clearance. The severity of the patient's PASC symptoms subsequently increased, and she developed new-onset brain fog in addition to previous symptoms, which resolved after resumption of tocilizumab treatment. Assessment of adaptive immune responses demonstrated that nirmatrelvir/ritonavir and tocilizumab treatment decreased antiviral and autoreactive T cell activation. After resuming tocilizumab treatment, the patient's PASC symptoms were significantly reduced, but nasopharyngeal antigen positivity remained.

Conclusion: These data suggest that nirmatrelvir/ritonavir should be considered in the treatment of PASC in patients who have SARS-CoV-2

antigen persistence, though care must be taken to monitor the patient for symptom resurgence or viral reactivation. In addition, the IL-6 inhibitor tocilizumab may ameliorate PASC symptoms in patients with persistent headache, fatigue, and brain fog.

KEYWORDS

long COVID, nirmatrelvir/ritonavir, tocilizumab, autoimmunity, case report

Introduction

SARS-CoV-2 is a (+)-strand RNA β-coronavirus first identified in December, 2019 and is the causative agent of COVID-19. There have been more than 560 million cases and 6.3 million deaths globally attributable to the COVID-19 pandemic (1). Although highly effective vaccines are now used to prevent severe disease and death from SARS-CoV-2, long-term sequelae after infection have become an urgent medical concern (2, 3). The rapid emergence of variants with enhanced virulence profiles and increased ability to evade vaccine-elicited immunity make it crucial to find alternative treatment options for COVID-related sequelae (4).

Post-acute sequelae of SARS-CoV-2 infection (PASC), or "long COVID," includes symptoms persisting for more than 4 weeks after acute infection and affects an estimated 30% of people infected with SARS-CoV-2 (5). Neuro-PASC is clinically defined as new neurologic or neurocognitive symptoms persisting for more than 4 weeks after disease onset and is often not concomitant with diagnosis of acute infection (6, 7). Currently, there are only symptomatic treatment options for Neuro-PASC (8), demonstrating the urgent need for new therapeutic approaches that address the underlying cause(s).

We describe a unique case of Neuro-PASC in a patient with a 7-year history of rheumatoid arthritis (RA). The patient tested continuously positive by SARS-CoV-2 by FlowFlex rapid antigen test for more than 6 months after acute infection. Treatment with nirmatrelvir/ritonavir and modifying treatment with tocilizumab decreased or eliminated PASC symptoms as well as antiviral and autoreactive T cell responses.

Case presentation

A 37-year-old South Asian woman on bi-weekly 162 mg/ml tocilizumab injections for RA was enrolled in a Neuro-PASC research study at Northwestern University in Chicago (demographics in **Figure 1A**; study design in **Figure 1B**). She was acutely symptomatic with new onset severe fatigue, occipital headache, and loss of appetite. She tested SARS-CoV-2^{+} by nasopharyngeal rapid antigen test in December, 2021. She experienced persistent headache and fatigue for >6 weeks after infection. The patient tested RT-PCR^{-} for SARS-CoV-2 at 14 days post-infection and multiple times thereafter but continued to test intermittently antigen^{+} for 14 weeks post-infection despite no overt exposure to SARS-CoV-2 infected individuals. The patient lived alone, did not leave her residence without a surgical-grade N95 mask, and never removed the mask in public. She was subsequently prescribed a 5-day course of nirmeltravir/ritonavir 300/100 mg twice daily, a SARS-CoV-2-specific antiviral, on the basis of her continued positive antigen tests. Patient was in compliance with all prescribed treatment courses. Initially, all PASC symptoms resolved, and the patient tested antigen^{-} 3 weeks after completion of nirmeltravir/ritonavir, but PASC symptoms and antigen positivity subsequently reappeared at 4 weeks (**Figures 1B,C**). The patient halted tocilizumab therapy for RA upon her rheumatologist's recommendation for 10 days in an attempt to fully clear the virus, during which time she developed more severe PASC symptoms and the appearance of new-onset cognitive impairment (brain fog). She resumed tocilizumab and within 3 weeks, her fatigue and brain fog had resolved while the occipital headache decreased in severity (**Figure 1C**).

Analysis of antiviral T cell responses by IFN-γ ELISPOT showed that Spike-specific T cell activation was induced by vaccination and infection, as expected after receiving Spike protein-based vaccines. However, the patient's non-Spike responses (to Nucleocapsid) were enhanced as well after receiving the Moderna vaccine booster dose. Nirmatrelvir/ritonavir treatment resulted in the retention of Spike- but not Nucleocapsid-specific T cell responses, while halting tocilizumab correlated with elevated T cell responses against both proteins. Resumption of tocilizumab subsequently decreased T cell responses to both viral antigens (**Figure 2A**). Antibody titers against Spike receptor-binding domain (RBD) followed similar kinetics (**Figure 2B**, top), while the patient never mounted an antibody response against Nucleocapsid (**Figure 2B**, bottom).

Flow cytometric analysis of (antibodies used in **Supplementary Table 1**) CD4^{+} T follicular helper cells (Tfh; involved in T cell help for antibody production) showed that antiviral T cell activation was highest at V3 (post-infection, post-boost) and V5 (post-infection, -boost, -nirmatrelvir/ritonavir,

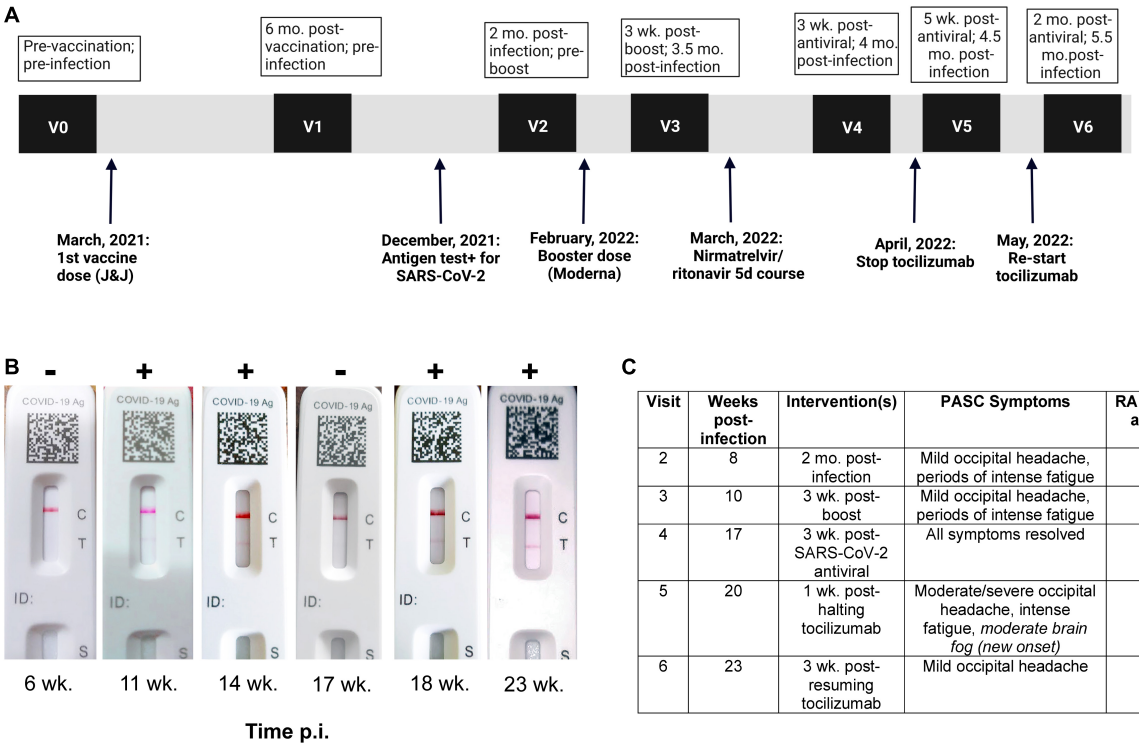

C

Visit	Weeks post-infection	Intervention(s)	PASC Symptoms	RA disease activity
2	8	2 mo. post-infection	Mild occipital headache, periods of intense fatigue	+/-
3	10	3 wk. post-boost	Mild occipital headache, periods of intense fatigue	+/-
4	17	3 wk. post-SARS-CoV-2 antiviral	All symptoms resolved	+
5	20	1 wk. post-halting tocilizumab	Moderate/severe occipital headache, intense fatigue, *moderate brain fog (new onset)*	++
6	23	3 wk. post-resuming tocilizumab	Mild occipital headache	+/-

FIGURE 1
Post-acute sequelae of SARS-CoV-2 infection (PASC) patient exhibits persistent SARS-CoV-2 antigen positivity in nasopharynx. **(A)** Study visit timeline, including vaccination, infection, and intervention dates. **(B)** FlowFlex™ SARS-CoV-2 antigen test results over time. Time p.i., weeks post-infection. **(C)** PASC symptoms vs. rheumatoid arthritis symptoms.

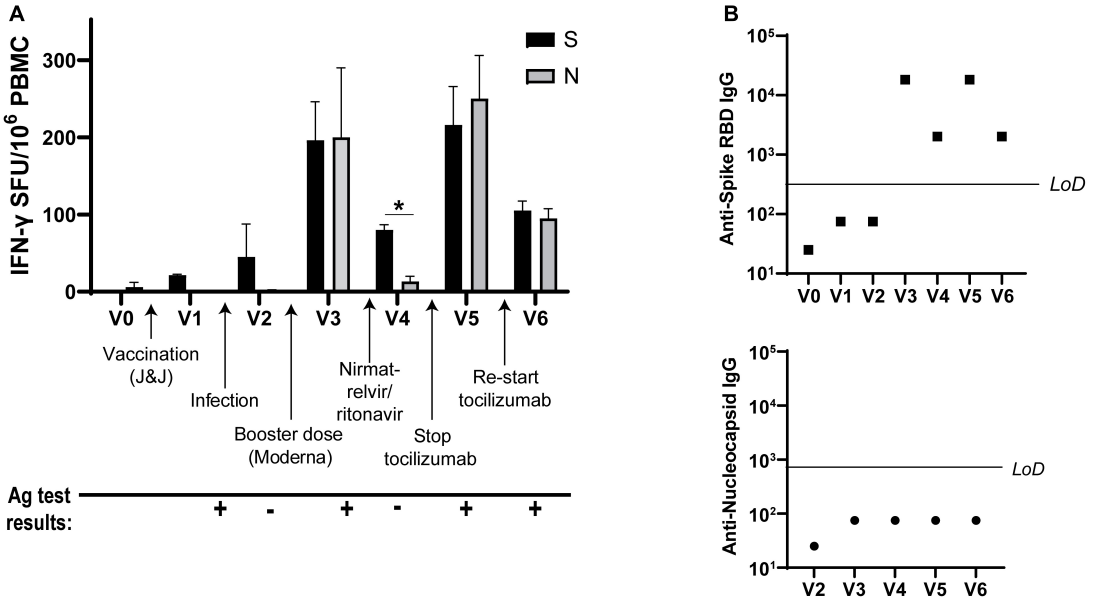

FIGURE 2
IFN-γ T cell responses to SARS-CoV-2 vary over time. **(A)** IFN-γ production from SARS-CoV-2 Spike- and Nucleocapsid-specific T cells at each visit as determined by ELISPOT. **(B)** Spike receptor-binding domain (RBD)-specific IgG titers (top) and Nucleocapsid-specific IgG (bottom) at each visit. LoD, limit of detection. All ELISPOT data in panel **(A)** from duplicate wells. Data representative of 2 individual experiments, $*p < 0.05$ by Student's *t*-test.

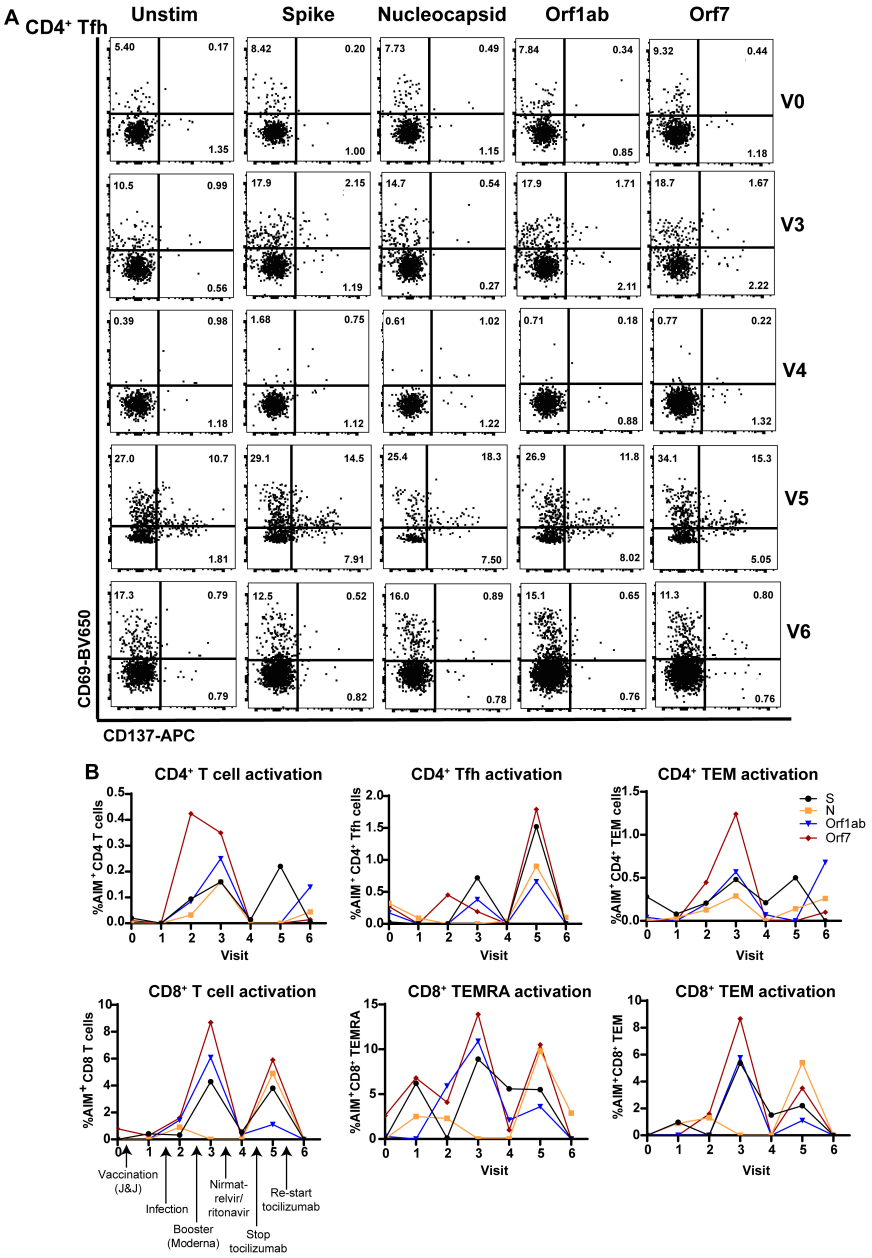

FIGURE 3
Virus-specific CD4$^+$ and CD8$^+$ T cell subset activation correlates with antiviral and tocilizumab treatment. **(A)** Flow cytometry showing elevated virus-specific CD4$^+$ T helper cell (Tfh) cell activation after vaccine booster dose (V3; 2nd row) and stopping tocilizumab treatment (V5; 4th row). **(B)** Total CD4$^+$ T cells (left), CD4$^+$ T helper cells (Tfh, middle), and CD4$^+$ memory T cells (TEM, right) have enhanced reactivity to SARS-CoV-2 structural (S, N) and non-structural (Orf1ab, Orf7) peptides after vaccine booster (V3) and stopping tocilizumab (V5), but low reactivity after nirmatrelvir/ritonavir treatment (V4) and resuming tocilizumab therapy (V6). **(B)** Total CD8$^+$ T cells (right) and CD8$^+$ memory T cell subsets (CD8$^+$ TEMRA, TEM; middle, right) show increased activation after vaccine boost (V3) and stopping tocilizumab (V5), but low reactivity after nirmatrelvir/ritonavir treatment (V4) and resuming tocilizumab (V5). Data combined from 3 independent experiments.

and halting tocilizumab treatment). Tfh activation determined by the activation-induced marker assay (AIM) (9) was lowest 3 weeks after nirmatrelvir/ritonavir treatment and resumption of tocilizumab (Figure 3A). Similarly, total CD4$^+$ and CD8$^+$ T cells, CD4$^+$ and CD8$^+$ T effector memory (TEM) cells, and CD8$^+$ TEM cells re-expressing CD45RA (CD8$^+$ TEMRA; terminally differentiated and highly cytotoxic T cells) exhibited maximal SARS-CoV-2-specific activation to Spike, Nucleocapsid, Orf1ab, and Orf7 antigens at V3 and V5, with limited activation at V4 and V6 (Figure 3B).

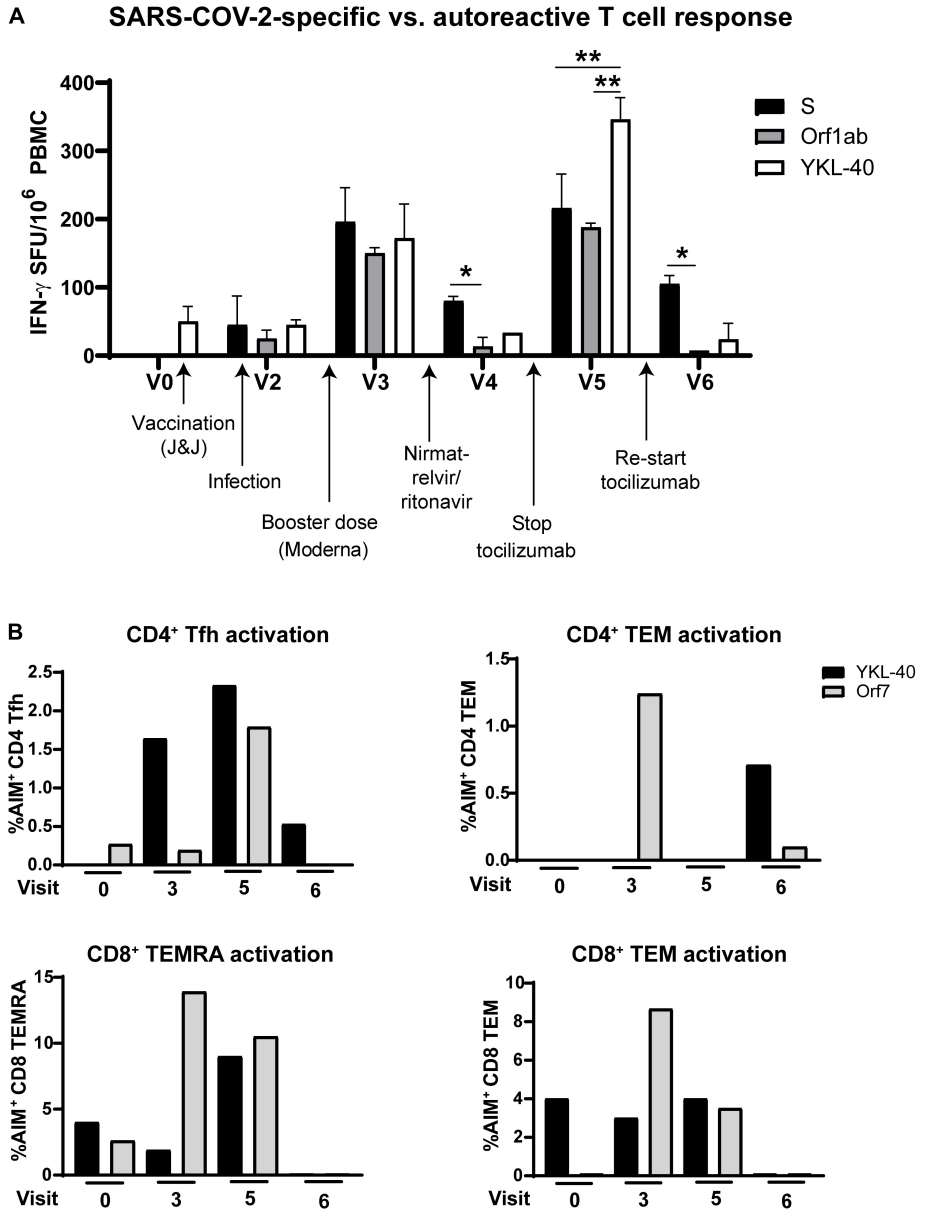

FIGURE 4
Autoreactive T cell responses oscillate in coordination with SARS-CoV-2-specific responses after infection. **(A)** T cell production of IFN-γ after stimulation with rheumatoid arthritis-associated cartilage autoantigen YKL-40 compared with Spike- and Orf1ab-specific activation. **(B)** Activation of T cell subsets over the course of the study after stimulation with the rheumatoid arthritis-associated antigen YKL-40 or SARS-CoV-2 Orf7 peptides. Stopping tocilizumab resulted in increased virus-specific and autoreactive T cell reactivity, while resuming tocilizumab suppressed autoreactivity in most T cell subsets. Data representative of 2 individual experiments, $*p < 0.05$, $**p < 0.01$ by one-way ANOVA with Tukey's post-test.

Antiviral and autoreactive T cell responses demonstrated a parallel oscillation over time. Comparison of IFN-γ production from T cells in response to Spike and Orf1ab vs. the RA-associated cartilage antigen YKL-40 showed the highest activation at V3 and V5, and the lowest activation at V4 after nirmatrelvir/ritonavir and V6 after resuming tocilizumab treatment (Figure 4A). Flow cytometry revealed similar activation patterns in T cell memory and Tfh cell subsets (Figure 4B). No other clinical diagnostic testing was performed on the patient.

Discussion and conclusion

COVID-19 is increasingly being recognized as a multi-organ disease with long-term sequelae associated with neurological

dysfunction. PASC has been reported in up to 30% of those with mild disease who do not require hospitalization (10, 11). Long-term sequelae after coronavirus infections can persist for years (12); therefore, individual case reports can inform us on how PASC symptoms may be impacted by available treatment options.

This case study described a Neuro-PASC patient presenting with long-term nasopharyngeal viral shedding as determined by SARS-CoV-2 antigen tests. Persistent viral colonization has been described previously both in the nasopharynx and extra-respiratory sites (13, 14) and is associated with being immunocompromised (15), though it is unknown whether viral persistence is more common in PASC patients than in healthy COVID convalescents. In this case, the patient was on immunosuppressive therapy with tocilizumab for pre-existing RA when she contracted SARS-CoV-2, which may have contributed to viral persistence over 6 months. However, tocilizumab may also decrease the severity of acute SARS-CoV-2 infection in hospitalized patients (16). The patient's mild acute symptoms combined with an escalation in Neuro-PASC symptom severity after stopping tocilizumab, as well as their resolution after resuming treatment suggests that IL-6 blockade should be studied further as a potential therapeutic intervention for Neuro-PASC.

Nirmatrelvir/ritonavir (Paxlovid) treatment is indicated within the first 72 h of a confirmed SARS-CoV-2 infection diagnosis to limit disease progression and decrease symptom severity (17). Though not indicated for the treatment of PASC, the treating physician felt that her prolonged nasopharyngeal antigen positivity warranted the treatment. Indeed, the patient's PASC symptoms fully resolved 3 weeks after completing antiviral treatment, which was corroborated by testing antigen$^-$ (**Figure 1C**) and having decreased non-Spike adaptive immune responses (**Figures 2**, **3**). Her symptoms and antigen positivity resumed 4 weeks post-nirmatrelvir/ritonavir treatment along with enhanced T cell and antibody responses to SARS-CoV-2 (**Figures 2**, **3**), suggestive of viral reactivation after antiviral treatment. SARS-CoV-2 viral rebound has been reported after a 5-day course of nirmatrelvir/ritonavir during acute infection (18, 19). A similar mechanism could be at play in the case of Neuro-PASC given evidence of a persistent SARS-CoV-2 infection.

Increased IL-6 has been associated with PASC in multiple studies. Elevated serum IL-6 was found in the majority of PASC patients compared with asymptomatic convalescent controls 8 months post-infection (20). There is speculation that IL-6 dysfunction may underlie persistent neuropsychiatric symptoms of PASC (21), and IL-6-producing B effector cells were elevated relative to IL-10-producing B regulatory cells in severe COVID-19 patients (22). Finally, a large cohort study of PASC patients assessed at 5 months post-infection found increased plasma IL-6 levels in patients with severe or moderate symptoms with cognitive impairment (23). Our own group has shown that Neuro-PASC patients have increased CD8$^+$ T cell production of IL-6 following stimulation with SARS-CoV-2 antigens compared with healthy COVID convalescents (24). Combined with the data in this case report, these studies provide a compelling argument for investigating the efficacy of IL-6 blockade with tocilizumab in treatment of PASC.

A confounding factor in characterizing the current patient's PASC symptoms and accompanying immune responses was her pre-existing RA. RA has been associated with an increased susceptibility to infections even in the absence of immunosuppressive therapy (25). There are also significant positive correlations between susceptibility to PASC and pre-existing autoimmune disease diagnoses (2). In this case, the patient's autoreactive T cell response to the RA-associated cartilage antigen YKL-40 (26) fluctuated depending on PASC symptom severity and RA disease activity (**Figure 1C**) as well as tocilizumab treatment (**Figure 4**). This suggests that tocilizumab may be used for management of rheumatic disease as well as Neuro-PASC symptoms. This case report highlights the need for further research into the contribution of autoimmunity to Neuro-PASC in addition to exploring the use of tocilizumab in Neuro-PASC treatment.

Currently, there are only symptomatic treatments for Neuro-PASC (8). We present the first case of a Neuro-PASC patient whose symptoms and antiviral adaptive immune responses were reduced by a 5-day course of nirmatrelvir-ritonavir. Additionally, we raise the possibility that tocilizumab should be further studied as a therapeutic intervention for Neuro-PASC. PASC impacts millions of people worldwide, and its incidence is only modestly diminished by vaccination (27, 28). Urgent research is needed to study the role of existing treatments to ameliorate the devastating impacts of PASC.

Limitations

The first author performed all experiments and analyses, and thus the study could not be blinded. We also note that this is one patient's experience and thus should not be used to generalize to larger patient populations without further clinical trials.

Author disclosure

The first author is the patient described in the study and gave full consent to use the data in this manuscript.

Data availability statement

The raw data supporting the conclusions of this article will be made available by the authors upon request, without undue reservation.

Ethics statement

The studies involving human participants were reviewed and approved by Northwestern University Institutional Review Board. The patients/participants provided their written informed consent to participate in this study. IRB study number STU00212583. Written informed consent was obtained from the individual(s) for the publication of any potentially identifiable images or data included in this article.

Author contributions

LV: conceptualization. LV and ZO: investigation and formal analysis. LV and IK: resources, data curation, supervision, project administration, and funding acquisition. LV: writing with feedback from all authors. All authors contributed to the article and approved the submitted version.

Conflict of interest

The authors declare that the research was conducted in the absence of any commercial or financial relationships that could be construed as a potential conflict of interest.

Publisher's note

All claims expressed in this article are solely those of the authors and do not necessarily represent those of their affiliated organizations, or those of the publisher, the editors and the reviewers. Any product that may be evaluated in this article, or claim that may be made by its manufacturer, is not guaranteed or endorsed by the publisher.

Supplementary material

The Supplementary Material for this article can be found online at: https://www.frontiersin.org/articles/10.3389/fmed.2022.1003103/full#supplementary-material

References

1. Johns Hopkins Coronavirus Resource Center. *Cumulative Worldwide Covid-19 Cases*. Baltimore, MD: Johns Hopkins University of Medicine (2021).

2. Graham EL, Clark JR, Orban ZS, Lim PH, Szymanski AL, Taylor C, et al. Persistent neurologic symptoms and cognitive dysfunction in non-hospitalized Covid-19 "long haulers". *Ann Clin Transl Neurol.* (2021) 8:1073–85. doi: 10.1002/acn3.51350

3. Higgins, V, Sohaei D, Diamandis EP, Prassas I. COVID-19: From an acute to chronic disease? Potential long-term health consequences. *Crit Rev Clin Lab Sci.* (2020). 58, 297–310. doi: 10.1080/10408363.2020.1860895

4. Newman J, Thakur N, Peacock TP, Bialy D, Elrefaey AME, Bogaardt C, et al. Neutralizing antibody activity against 21 SARS-CoV-2 variants in older adults vaccinated with BNT162b2. *Nat Microbiol.* (2022) 7:1180–8. doi: 10.1038/s41564-022-01163-3

5. Ladds E, Rushforth A, Wieringa S, Taylor S, Rayner C, Husain L, et al. Persistent symptoms after Covid-19: qualitative study of 114 "long Covid" patients and draft quality principles for services. *BMC Health Serv Res.* (2020) 20:1144. doi: 10.1186/s12913-020-06001-y

6. Moghimi N, Di Napoli M, Biller J, Siegler JE, Shekhar R, McCullough LD, et al. The Neurological manifestations of post-acute sequelae of SARS-CoV-2 infection. *Curr Neurol Neurosci Rep.* (2021) 21:44. doi: 10.1007/s11910-021-01130-1

7. Nalbandian A, Sehgal K, Gupta A, Madhavan MV, McGroder C, Stevens JS, et al. Post-acute COVID-19 syndrome. *Nat Med.* (2021) 27:601–15. doi: 10.1038/s41591-021-01283-z

8. Graham EL, Koralnik IJ, Liotta EM. Therapeutic Approaches to the Neurologic Manifestations of COVID-19. *Neurotherapeutics.* (2022) [Epub ahead of print]. doi: 10.1007/s13311-022-01267-y

9. Havenar-Daughton C, Reiss SM, Carnathan DG, Wu JE, Kendric K, Torrents de la Pena A, et al. Cytokine-independent detection of antigen-specific germinal center t follicular helper cells in immunized nonhuman primates using a live cell activation-induced marker technique. *J Immunol.* (2016) 197:994–1002. doi: 10.4049/jimmunol.1600320

10. Hirschtick JL, Titus AR, Slocum E, Power LE, Hirschtick RE, Elliott MR, et al. Population-based estimates of post-acute sequelae of SARS-CoV-2 infection (PASC) prevalence and characteristics. *Clin Infect Dis.* (2021) 73:2055–64. doi: 10.1093/cid/ciab408

11. Havervall S, Rosell A, Phillipson M, Mangsbo SM, Nilsson P, Hober S, et al. Symptoms and functional impairment assessed 8 months after mild COVID-19 among health care workers. *JAMA.* (2021) 325:2015–6. doi: 10.1001/jama.2021.5612

12. Ahmed H, Patel K, Greenwood DC, Halpin S, Lewthwaite P, Salawu A, et al. Long-term clinical outcomes in survivors of severe acute respiratory syndrome and middle east respiratory syndrome coronavirus outbreaks after hospitalisation or ICU admission: a systematic review and meta-analysis. *J Rehabil Med.* (2020) 52:jrm00063.

13. Ferrari A, Trevenzoli M, Sasset L, Di Liso E, Tavian T, Rossi L, et al. Prolonged SARS-CoV-2-RNA detection from nasopharyngeal swabs in an oncologic patient: What impact on cancer treatment? *Curr Oncol.* (2021) 28:847–52. doi: 10.3390/curroncol28010083

14. Natarajan A, Zlitni S, Brooks EF, Vance SE, Dahlen A, Hedlin H, et al. Gastrointestinal symptoms and fecal shedding of SARS-CoV-2 RNA suggest prolonged gastrointestinal infection. *Med.* (2022) 3:371–387.e9. doi: 10.1016/j.medj.2022.04.001

15. Thornton CS, Huntley K, Berenger BM, Bristow M, Evans DH, Fonseca K, et al. Prolonged SARS-CoV-2 infection following rituximab treatment: clinical course and response to therapeutic interventions correlated with quantitative viral cultures and cycle threshold values. *Antimicrob Resist Infect Control.* (2022) 11:28. doi: 10.1186/s13756-022-01067-1

16. Snow TAC, Saleem N, Ambler G, Nastouli E, Singer M, Arulkumaran N. Tocilizumab in COVID-19: a meta-analysis, trial sequential analysis, and meta-regression of randomized-controlled trials. *Intensive Care Med.* (2021) 47:641–52. doi: 10.1007/s00134-021-06416-z

17. Wen W, Chen C, Tang J, Wang C, Zhou M, Cheng Y, et al. Efficacy and safety of three new oral antiviral treatment (molnupiravir, fluvoxamine and Paxlovid) for

COVID-19a meta-analysis. *Ann Med.* (2022) 54:516–23. doi: 10.1080/07853890.2022.2034936

18. Boucau J, Uddin R, Marino C, Regan J, Flynn JP, Choudhary MC, et al. Characterization of virologic rebound following nirmatrelvir-ritonavir treatment for COVID-19. *Clin Infect Dis.* (2022) [Epub ahead of print]. doi: 10.1093/cid/ciac512

19. Wang L, Berger NA, Davis PB, Kaelber DC, Volkow ND, Xu R. COVID-19 rebound after Paxlovid and Molnupiravir during January-June 2022. *medRxiv* [Preprint]. (2022) doi: 10.1101/2022.06.21.22276724

20. Phetsouphanh C, Darley DR, Wilson DB, Howe A, Munier CML, Patel SK, et al. Immunological dysfunction persists for 8 months following initial mild-to-moderate SARS-CoV-2 infection. *Nat Immunol.* (2022) 23:210–6. doi: 10.1038/s41590-021-01113-x

21. Kappelmann N, Dantzer R, Khandaker GM. Interleukin-6 as potential mediator of long-term neuropsychiatric symptoms of COVID-19. *Psychoneuroendocrinology.* (2021) 131:105295. doi: 10.1016/j.psyneuen.2021.105295

22. Shuwa HA, Shaw TN, Knight SB, Wemyss K, McClure FA, Pearmain L, et al. Alterations in T and B cell function persist in convalescent COVID-19 patients. *Med.* (2021) 2:720–735.e4. doi: 10.1016/j.medj.2021.03.013

23. Evans RA, McAuley H, Harrison EM, Shikotra A, Singapuri A, Sereno M. Clinical characteristics with inflammation profiling of long COVID and association with 1-year recovery following hospitalisation in the UK: a prospective observational study. *Lancet Respir Med.* (2022) 10:761–75. doi: 10.1016/S2213-2600(22)00127-8

24. Visvabharathy L, Hanson B, Orban Z, Lim PH, Palacio NM, Jain R, et al. Neuro-COVID long-haulers exhibit broad dysfunction in T cell memory generation and responses to vaccination. *medRxiv* [Preprint]. (2021) doi: 10.1101/2021.08.08.21261763

25. Listing J, Gerhold K, Zink A. The risk of infections associated with rheumatoid arthritis, with its comorbidity and treatment. *Rheumatology.* (2013) 52:53–61. doi: 10.1093/rheumatology/kes305

26. Sekine T, Masuko-Hongo K, Matsui T, Asahara H, Takigawa M, Nishioka K, et al. Recognition of YKL-39, a human cartilage related protein, as a target antigen in patients with rheumatoid arthritis. *Ann Rheum Dis.* (2001) 60:49–54. doi: 10.1136/ard.60.1.49

27. Al-Aly Z, Bowe B, Xie Y. Long COVID after breakthrough SARS-CoV-2 infection. *Nat Med.* (2022) 28:1461–7. doi: 10.1038/s41591-022-01840-0

28. Azzolini E, Levi R, Sarti R, Pozzi C, Mollura M, Mantovani A, et al. Association between BNT162b2 vaccination and long COVID after infections not requiring hospitalization in health care workers. *JAMA.* (2022) 328:676. doi: 10.1001/jama.2022.11691

frontiers | Frontiers in Medicine

TYPE Original Research
PUBLISHED 20 October 2022
DOI 10.3389/fmed.2022.1028171

OPEN ACCESS

EDITED BY
Francesco Paolo Bianchi,
University of Bari Aldo Moro, Italy

REVIEWED BY
Yijun Zheng,
Lanzhou University Second Hospital, China
Soobin Jang,
Daegu Haany University, South Korea

*CORRESPONDENCE
Jia Wu
wuyinameng@sina.com

SPECIALTY SECTION
This article was submitted to Infectious Diseases - Surveillance, Prevention and Treatment, a section of the journal Frontiers in Medicine

RECEIVED 25 August 2022
ACCEPTED 21 September 2022
PUBLISHED 20 October 2022

CITATION
Wu J, Tang F, Zhang X-Q, Fu Z-L and Fu S (2022) Application of Jiawei Maxing Shigan Tang in the treatment of COVID-19: An observational study. *Front. Med.* 9:1028171. doi: 10.3389/fmed.2022.1028171

Application of Jiawei Maxing Shigan Tang in the treatment of COVID-19: An observational study

Jia Wu[1]*, Feng Tang[2], Xiao-Qiang Zhang[3], Zai-Lin Fu[1] and Shui Fu[4]

[1]Department of Pharmacy, Linping Campus, The Second Affiliated Hospital of Zhejiang University School of Medicine, Hangzhou, China, [2]Department of Traditional Chinese Medicine, Linping Campus, The Second Affiliated Hospital of Zhejiang University School of Medicine, Hangzhou, China, [3]Department of Infection, Linping Campus, The Second Affiliated Hospital of Zhejiang University School of Medicine, Hangzhou, China, [4]Department of Clinical Laboratory, Linping Campus, The Second Affiliated Hospital of Zhejiang University School of Medicine, Hangzhou, China

Objective: To explore the clinical efficacy and adverse reactions of Jiawei Maxing Shigan Tang (JMST; a modified decoction of ephedra, apricot kernel, gypsum, and licorice) combined with western medicine in the symptomatic treatment of COVID-19.

Methods: In this study, we retrospectively collected the basic data of 48 patients with COVID-19 who were discharged from our hospital between January 20 and February 28, 2020. Besides, the blood routines, biochemical indexes, nucleic acid detection results, clinical symptoms, lung imaging improvements, adverse reactions, and other clinical data of these patients before and after treatment were recorded. Finally, we drew comparisons between the outcomes and adverse reactions of patients in the combined treatment group (therapeutic regimen recommended by authoritative guidelines and supplemented by JMST) and the conventional treatment group (therapeutic regimen recommended by authoritative guidelines).

Results: There were no significant differences in age, gender, clinical classification, and underlying medical conditions between the combined treatment group (28 cases) and the conventional treatment group (20 cases). However, the combined treatment group presented superior results to the conventional treatment group in several key areas. For instance, patients produced negative nasal/throat swab-based nucleic acid detection results in a shorter time, clinical symptoms were more effectively alleviated, and the absorption time of lung exudation was shorter ($P < 0.05$). Furthermore, the combined treatment group had a shorter length of stay (LOS) and faster lymphocyte recovery duration than the conventional treatment group, although the differences were not statistically significant. Moreover, there were no significant differences concerning gastrointestinal reaction, hepatic injury, renal impairment, myocardial injury, and other adverse reactions between the two groups.

10.3389/fmed.2022.1028171

Conclusion: The results of this study indicate that JMST combined with the recommended therapeutic regimen enhances the recovery of COVID-19 patients without increasing the risk of adverse reactions. Therefore, this therapy promotes positive outcomes for COVID-19 patients.

KEYWORDS

Jiawei Maxing Shigan Tang, COVID-19, efficacy comparison, adverse reactions, lung imaging, lymphocyte

Introduction

The coronavirus disease (COVID-19), caused by severe acute respiratory syndrome coronavirus 2(SARS-CoV-2), a highly pathogenic novel coronavirus, has started a worldwide pandemic since December 2019. COVID-19 has received a great deal of attention from all sectors of society due to its threat to the lives and health of people, economic development, and social stability worldwide (1, 2). As a result, several versions of the *Diagnosis and Treatment Protocol for COVID-19* have been published in China (3–5). According to the World Health Organization (WHO), COVID-19 has been designated "2019-nCoV acute respiratory disease". The treatment of patients diagnosed with COVID-19 is an important component of epidemic prevention and control and it is also the primary measure to protect people's lives. To date, there are no specific drugs for treating this disease in clinical applications, but the efficacy of traditional Chinese medicine (TCM) in the treatment of severe acute respiratory syndrome (SARS) has been verified (6, 7). Because novel coronavirus and SARS-COV exhibit high homology in gene sequencing (8), it can be inferred that Chinese herbal medicine also has certain effects in the treatment of COVID-19. Thus, combined therapies that integrate TCM and western medicine may be promising treatment methods. Our hospital is designated to receive patients with COVID-19 and is a National General Hospital Traditional Chinese Medicine Work Demonstration Unit. The TCM experts in our hospital extracted the essence from ancient recipes and applied them to the diagnosis and treatment protocols for COVID-19. They rapidly formulated a TCM therapeutic regimen for COVID-19 patients by actively implementing the latest national diagnosis and treatment protocols for COVID-19 in combination with their experience in clinical diagnosis and treatment. Based on these efforts, patients with COVID-19 were treated promptly with TCM. In this study, 48 COVID-19 patients were treated with Jiawei Maxing Shigan Tang (JMST), a modified decoction of ephedra, apricot kernel, gypsum, and licorice, and an established prescription of our hospital. Their treatment was continuously optimized in clinical practice to assist experts in western medicine. We established that a combination of TCM and western medicine contributed to realizing a superposition effect. Furthermore, TCM promoted the recovery of patients at the convalescent stage, thereby achieving favorable clinical outcomes. Exploring the effectiveness of combined therapies integrating TCM and western medicine is expected to provide a valuable reference for clinicians who are engaged in the fight against the COVID-19 pandemic.

Data and methods

Participants

In this study, we retrospectively collected the data from a total of 48 patients with common COVID-19 who were discharged from our hospital between January 20 and February 28, 2020. The cohort included 26 males and 22 females with an average age of 47.54 ± 13.29 years, ranging from 29 to 70 years old. The diagnosis, classification, and medication of all participants were performed based on the *Diagnosis and Treatment Protocol for COVID-19 (Trial Version 5)* (5) and the *Recommended Scheme for Prevention and Treatment of COVID-19 by Traditional Chinese Medicine (Trial Version 4) in Zhejiang Province* (9). All participants included in the study received treatment based on the therapeutic regimen for at least 1 week. The inclusion criteria included: (1) patients with positive nucleic acid detection results in blood/respiratory tract samples by real-time PCR (RT-PCR); (2) patients with signs of viral pneumonia, such as ground glass opacity (GGO) and mixed ground glass opacity (mGGO), in a spiral CT scan of the chest; (3) patients who had signed informed consent. The exclusion criteria were: (1) pregnant patients; (2) pediatric patients; (3) patients with ongoing immunosuppressive therapy; (4) patients with acquired immunodeficiency syndrome (AIDS); (5) patients who recovered within 48 h. The criteria for release from isolation and discharge were: (1) patients whose clinical symptoms (high body temperature, cough, expectoration, physical strength, and other related symptoms) were alleviated or had disappeared; (2) patients with more than two negative nucleic acid detection results from respiratory tract samples, with sampling performed over at least 2 days; (3) patients with negative nucleic acid detection results of fecal samples. Those who met all of the above three criteria were considered cured and were discharged from the hospital.

Treatment methods and groupings

The patients were divided into the conventional treatment group and the combined treatment group, which involved combining JMST and conventional treatment. The routine treatment group was administered: lopinavir/ritonavir (200 mg/50 mg per tablet), two tablets/time, twice a day; arbidol, 200 mg/time, three times a day; aerosol inhalation of interferon-α, 5 million U/time, twice a day. The JMST prescription consisted of 30 g gypsum (decocted later), 10 g Rhizoma atractylodis, 10 g notopterygium root, 10 g Agastache rugosa, 9 g apricot kernel, 9 g betel nut, 9 g dried tangerine peel, 6 g ephedra, 6 g licorice, and 6 g amomum tsao-ko. Among the cohort, there were 20 patients in the conventional treatment group, including 12 males and 8 females, with an age of 47.66 ± 13.56 years, ranging from 30 to 70 years old. The combined treatment group consisted of 28 subjects, including 16 males and 12 females, with an average age of 47.45 ± 13.21 years, ranging from 29 to 69 years old.

Data collection

General data

General data included gender, age, duration from onset of symptoms to treatment, and underlying medical conditions. The patients were subjected to scientific clinical classification according to the *Diagnosis and Treatment Protocol for COVID-19 (Trial Version 5)*, based on their symptoms, signs, lung imaging features, laboratory examination results, and treatment information at the time of admission.

Clinical efficacy

(1) Length of stay (LOS): The LOS was calculated from the date of confirmed diagnosis based on positive nucleic acid detection results to the date of discharge based on the discharge standard. (2) Remission duration of the main symptoms: This was determined as the time from the date of onset and appearance of symptoms to the date the clinical symptoms disappeared, according to medical records. Clinical symptoms included higher body temperature, cough, expectoration, and respiratory symptoms.

Imaging improvement

(1) Duration for the initial absorption of lung infection lesions: calculated as the time from the date of the first chest CT scan to that of initial improvement in acute exudative lesions. (2) Duration for the complete absorption of lung lesions: the number of days between the first chest CT scan and the complete elimination of acute exudative lesions.

Duration for nasal/throat swab-based nucleic acid detection results to become negative

This was calculated as the time from initially obtaining positive nucleic acid detection results to the date of obtaining negative nucleic acid detection results in the respiratory tract and fecal samples more than twice with a sampling interval of 1 day.

Lymphocyte recovery duration

According to the national treatment standard, we tested the levels of white blood cells, lymphocytes, ALT, and calcitonin. We discovered that only the lymphocyte count decreased in all patients enrolled in clinical laboratory index detection. Hence, the lymphocyte count was selected as the observation index. The lymphocyte recovery duration was expressed as the number of days from obtaining positive nucleic acid detection results to when the lymphocyte count returned to within the normal reference levels.

Adverse reactions

(1) Gastrointestinal symptoms: If at least one gastrointestinal symptom, such as abdominal distension, abdominal pain, nausea, vomiting, eructation, hiccupping, eating obstruction, or pain occurred in patients, the patients were diagnosed with gastrointestinal reactions; (2) Liver dysfunction: If the levels of one or more indexes, including serum alanine aminotransferase (ALT), aspartate aminotransferase (AST), total bilirubin (TBIL), or γ-glutamyltranspeptidase (γ-GT), significantly increased in patients, they were diagnosed with liver dysfunction; (3) Renal impairment: If one or more indexes, such as serum blood urea nitrogen (BUN), creatinine (Cr), and uric acid (UA) exhibited substantially increased levels in patients, they were diagnosed with renal impairment; (4) Myocardial injury: If any of the following indexes: serum creatine kinase isoenzyme-MB (CK-MB), lactate dehydrogenase (LDH), orcardiac troponin I (TnI) had significantly increased levels, the patients were diagnosed with myocardial injury.

Statistical methods

In this study, SPSS 26.0 was utilized to process the data and the Shapiro-Wilk test was conducted to analyze data distribution. The data with normal distribution were expressed by $\bar{x} \pm s$. The independent sample *t*-test was performed to make comparisons between groups, and the chi-square (χ^2) test was employed to compare the rates, Additionally, the enumeration data were analyzed using the Wilcoxon-Mann-Whitney rank sum test. Values of $P < 0.05$ indicated that there was a statistically significant difference.

Results

Basic data comparison of patients in both groups

In this study, we collected the basic data of 48 patients in two groups. As Table 1 indicates, there were no significant differences in gender distribution, age distribution, duration from onset of symptoms to treatment, clinical classification and underlying medical conditions between the groups ($P > 0.05$).

LOS and remission duration of main symptoms

There was no significant difference in average LOS between the two groups. However, the time for clinical symptoms to disappear in the combined treatment group was much shorter than in the conventional treatment group, and the difference was statistically significant (Table 2).

Imaging improvement

The duration of initial and complete absorption/obvious absorption of lung exudation lesions in the combined treatment group was considerably shorter than in the conventional treatment group, with a statistically significant difference. However, the complete absorption rate in the combined treatment group was higher than that in the conventional treatment group, but the difference was not statistically significant (Table 3).

Main laboratory indexes

The duration required for the nasal/throat swab-based nucleic acid detection result to become negative was substantially shorter in the combined treatment group than in the conventional treatment group, and the difference was statistically significant. However, there was no significant difference in the lymphocyte recovery duration between the two groups (Figure 1).

Adverse reactions

Gastrointestinal reaction, hepatic injury, renal impairment, and myocardial injury were slightly higher in the combined treatment group than in the conventional treatment group, but the difference was not statistically significant (Table 4).

TABLE 1 General data analysis of patients in both groups.

Group	Cases	Gender (cases/%)		Age (years, $\bar{x} \pm s$)	Clinical classification (case/%)				Duration from onset of symptoms to treatment (days, $\bar{x} \pm s$)	Basic diseases (cases/%)				
		Male	Female		Mild	Moderate	Severe	Critical		Diabetes mellitus	Hypertension	Lung disease	Tumor	No underlying medical conditions
Conventional treatment group	20	12/60	8/40	47.66 ± 13.56	1/5	17/85	2/10	0/0	3.14 ± 0.76	1/5	5/25	3/15	2/10	9/45
Combined treatment group	28	16/57.14	12/42.86	47.45 ± 13.21	2/7.14	23/82.15	3/10.71	0/0	3.25 ± 0.81	2/7.14	9/32.14	6/21.43	3/10.71	8/28.58
Statistical value	—	$\chi 2 = 0.039$		t = 0.678			Z = −0.571		t = 0.932			Z = −1.056		
P value	—	0.843		0.532			0.568		0.216			0.291		

Discussion

In recent years, there have been an increasing number of new viral infectious diseases. However, effective treatment methods have not been implemented for several of these illnesses, and acute outbreaks often cause panic and become major social problems. The effectiveness of several drugs in TCM and western medicine for the treatment of COVID-19 remains unclear. However, from the perspective of TCM, the regular forms of the body under the attack of foreign pathogens can be determined, even though COVID-19 is a new disease. TCM had a vital role in the treatment of SARS in 2003, so we can presume that TCM can also play a crucial part in the prophylaxis and treatment of COVID-19 (10, 11).

Hangzhou is located to the south of the Yangtze River, and the latitude of Hangzhou is approximately 30° N, which is the same as Wuhan. In the winter of 2019, the weather was abnormally cold and damp. Besides, rainy weather dominated from January to mid-February, and Wang et al. (10) also proposed the "wet" evil in their report. Additionally, Zhang et al. (12) proposed that the distribution of urban residents in Hangzhou with a moderate or biased constitution had similar proportions (52.6 vs. 47.4%).The 48 patients in this study had a history of living in Hubei Province or had come into contact with COVID-19 patients in Hubei Province or Hangzhou within 14 days of disease onset, with a specific etiology, location, and symptoms. According to *Wenyi Lun*, compiled by Wu Youke in the Qing Dynasty, "In years with a strong or weak abnormal climate, those who have a slight decline in healthy energy will get sick when they touch it"; "disease occurs either in the city or in the village, anywhere with a crowd"; "individuals from all families are equal when encountering disease". In TCM, the term "plague" refers to a kind of disease with strong infectivity and the potential to cause epidemics. Therefore, COVID-19 belongs to a disease category within TCM that is caused by cold-damp epidemic pathogenic factors. Tong (13) also defined the TCM name of novel coronavirus pneumonia as "cold-damp disease". COVID-19 is caused by damp-heat epidemic pathogenic factors. Hence, its core pathogenesis lies in dampness and toxins, combined with cold and heat. After the pathogenic factors affect the ying blood, the yang qi or yin fluids are damaged to varying degrees. The lungs and spleen are mainly involved, while the heart, liver, kidneys, and other organs are affected in severe cases.

According to *Su Wen – CifaLun* (14), five infectious diseases are prone to becoming pandemic, and there are similar symptoms among the different severity levels. Based on the *Diagnosis and Treatment Protocol for COVID-19* issued by the National Health Commission and National Administration of Traditional Chinese Medicine, our hospital focuses on treatments based on disease differentiation, according to epidemic features and similar symptoms. JMST is also widely adopted as a general treatment. "If the evil is not eliminated, the disease will not be cured; it will be aggravated due to delayed treatment over a long period." The principle of JMST treatment is to dispel cold, remove dampness, avoid filth, and convert turbidity. As the main component of JMST, the recipe for Maxing Shigan Tang (MST) is derived from the traditional medical text *Shanghan Lun*. The original prescription is mainly used to treat taiyang diseases and is a basic treatment for asthma and cough with unsolved exogenous pathogens and evil heat constraints in the lung pattern. Combined with betel nut, amomum tsao-ko, and other herbs, which are the main components of the classic prescription Dayuan-Yin from *Wenyi Lun*, MST can be modified according to the appearance of the patient's tongue and other concurrent syndromes. In the decoction, ephedra spreads lung qi, relieves asthma, and

TABLE 2 Comparison of length of stay and time for clinical symptoms to disappear between the groups.

Group	Cases	Length of stay (days, $\bar{x} \pm s$)	Time for clinical symptoms to disappear (days, $\bar{x} \pm s$)
Conventional treatment group	20	23.78 ± 4.48	18.25 ± 2.44
Combined treatment group	28	22.60 ± 3.56	12.14 ± 1.76
t value	—	0.328	2.387
P value	—	0.747	0.049

TABLE 3 Comparison of the initial and complete absorption duration of lung infection lesions between the groups.

Group	Cases	Initial absorption duration (days, $\bar{x} \pm s$)	Obvious or complete absorption duration (days, $\bar{x} \pm s$)	Complete absorption cases (cases/%)
Conventional treatment group	20	9.23 ± 1.21	22.78 ± 4.31	8/40
Combined treatment group	28	7.56 ± 1.02	13.09 ± 2.31	15/53.57
Statistical value	—	t = 1.956	t = 2.243	$\chi 2 = 0.861$
P	—	0.042	0.040	0.353

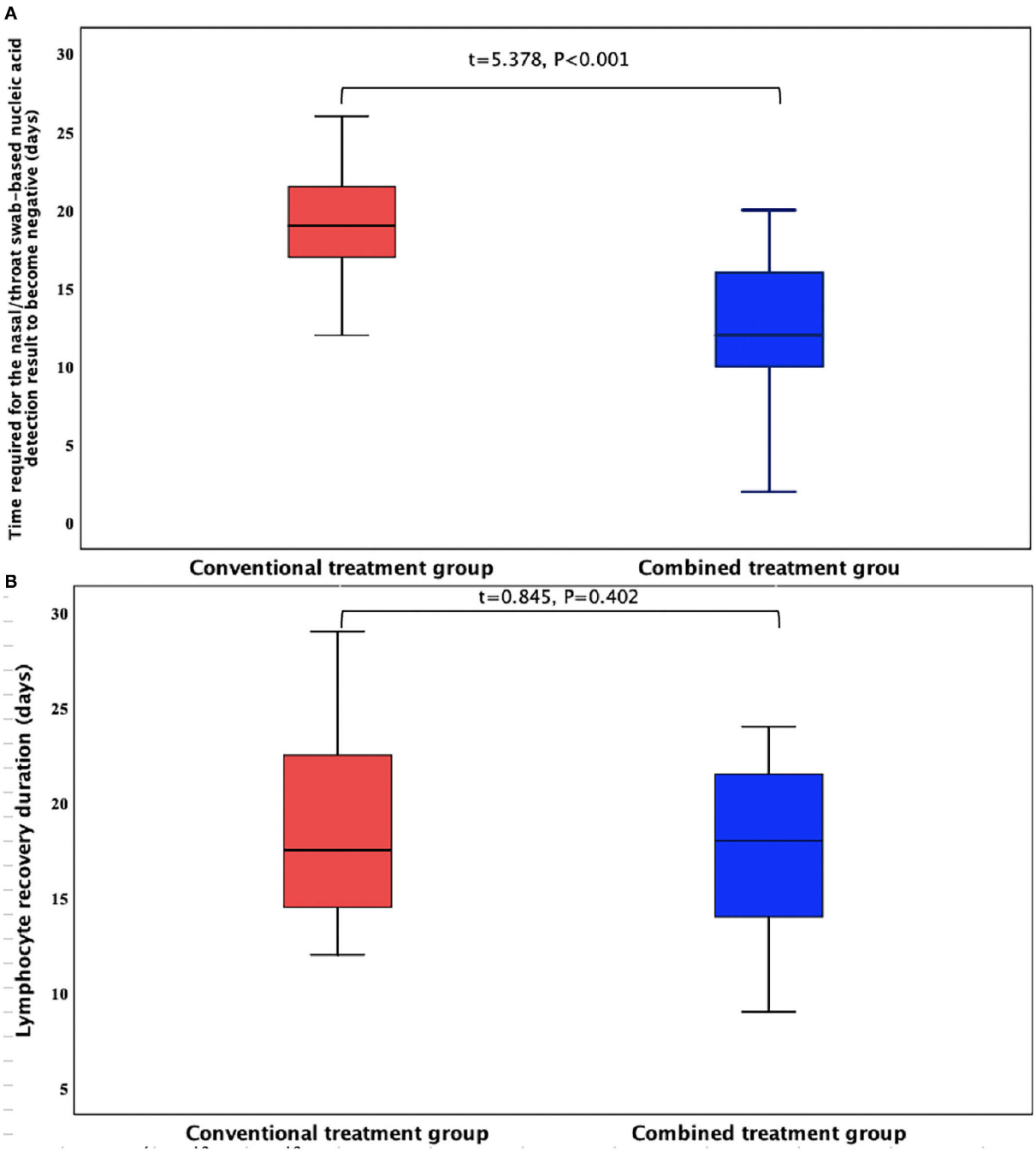

FIGURE 1
Comparison of the main experimental indexes of the two patient groups. **(A)** Time required for the nasal/throat swab-based nucleic acid detection result to become negative (days); **(B)** Lymphocyte recovery duration (days).

disperses evil; apricot kernel lowers lung qi; gypsum relieves lung heat; amomum tsao-ko features a pungent flavor and suppresses evil, eliminates filth, and prevents vomiting; betel nut disperses damp evil, eliminates phlegm, breaks constraints, and eliminates evil; Rhizoma atractylodis eliminates dampness, invigorates the spleen, expels wind, and removes cold; notopterygium root generates warmth, dispels cold, expels wind, and eliminates dampness; Agastache rugosa features a fragrant flavor and eliminates dampness, regulates qi, harmonizes the body, and relieves external symptoms; dried tangerine peel promotes the circulation of qi, calms negative energy, and dissipates phlegm; licorice regulates all the herbal components. As an ancient

TABLE 4 Incidence of adverse reactions in both groups (cases/%).

Group	Cases	Gastrointestinal reaction	Hepatic injury	Renal impairment	Myocardial injury
Conventional treatment group	20	7/35	5/25	3/15	1/5
Combined treatment group	28	13/46.43	9/32.14	7/25	2/7.15
χ^2 value	—	0.627	0.288	0.231	0.091
P value	—	0.428	0.591	0.631	0.762

TCM prescription, JMST possesses antitussive, expectorant, spasmolytic, antiallergic, and anti-inflammatory effects. This prescription is used for treating cough and asthma caused by lung heat. Furthermore, it dispels evil using flavorful ingredients with cooling properties, removes lung heat, and relieves asthma. JMST is widely used for treating pneumonia induced by various factors and has achieved favorable curative effects (15–17), and it is also commonly known as "Pneumonia Mixture II" (18). Therefore, JMST is an appropriate remedy for COVID-19 since it is especially effective for pathogenic heat accumulation in the lungs.

According to the climate characteristics and the physique of the local population in Hangzhou, our hospital formulated an "epidemic prevention TCM prescription" for the general adult population. The prescription consisted of 15 g astragalus, 12 g stir-fried ovate atractylodes root, 12 g Poria cocos, 10 g Perillae folium, 9 g wrinkled giant hyssop herb, 9 g honeysuckle flower, 6 g dried tangerine peel, 6 g Saposhnikovia divaricata root, and 3 g licorice. In the concoction, the astragalus features sweet and warm flavors and contributes to the qi of the spleen and the lungs to consolidate superficial defense; stir-fried ovate atractylodes root strengthens the spleen, replenishes qi, and disperses evil; honeysuckle flower features cool and light properties, clears away heat and toxic materials, and dispels wind and heat; Perillae folium relieves external symptoms, dispels cold, and regulates qi; Poria cocos invigorates the spleen and dispels dampness; Agastache rugosa is a fragrant herb that eliminates dampness and regulates qi; dried tangerine peel invigorates the spleen and regulates qi and dryness (19, 20). The first-line clinical patients in our hospital mainly presented phlegmatic hygrosis, so the combined administration of three prescriptions eliminated dampness and filth in patients with the cold-damp constraint or damp-heat accumulation in their lungs. Licorice benefits the throat by clearing away heat and toxic materials, and it also regulates the other herbal components. This prescription tonifies qi, strengthens the exterior, prevents evil spirits, and eliminates turbidity. It also boosts the immunity of the body and prevents infection. At the critical moment of epidemic prevention and control, symptomatic treatments combining TCM and western medicine and the policy of isolation and flow control can achieve satisfactory results (21, 22), confirming the effectiveness of TCM.

During the design of this study, we adopted a therapeutic regimen for the control group according to recommendations from authoritative departments. Additionally, an integrated therapy combining the recommended regimen and JMST was applied in the comprehensive treatment group. Due to the potential risks of COVID-19, we did not create a JMST-only treatment group, which may have led to some deficiencies in the study design. However, results suggested that the combined treatment group achieved better outcomes than the conventional treatment group in terms of the time to obtain a negative test result for nasal/throat swab-based nucleic acid detection, alleviation of clinical symptoms, and absorption time of lung exudation. This indicated that JMST alleviates symptoms, promotes rehabilitation, and reduces sequelae. Therefore, it is necessary to provide a thorough summary and conduct further investigations. The LOS and lymphocyte recovery times in the combined treatment group were also shorter than in the conventional treatment group, but the difference was not statistically significant. This may be related to the exaggerated effect of statistical false negatives due to the small sample size. Besides, there were no significant differences in gastrointestinal reaction, hepatic injury, renal impairment, myocardial injury, and other adverse reactions between the two groups. This indicates that JMST does not aggravate side effects during treatment, which is consistent with the low level of side effects that TCM generally causes. In the treatment of COVID-19 patients, the combined therapy, which integrated authoritative diagnosis and treatment with JMST, alleviated COVID-19 symptoms and promoted the recovery of patients without causing any significant adverse reactions. Thus, JMST achieves favorable therapeutic effects as adjuvant therapy in the treatment of patients with ordinary COVID-19.

It is worth noting that in the third nucleic acid detection sampling, one patient's respiratory tract specimen was single gene positive. This was probably due to the sampling method, conduct of the sampling personnel, or sensitivity of the test reagent. The nucleic acid test result of this patient was negative in the fourth detection test. Moreover, the fifth nucleic acid test returned a negative result and the fecal sample also tested negative. As a result, this patient was confirmed to have a negative nucleic acid test result and was

subsequently discharged from the hospital. Few COVID-19 patients were admitted to our hospital during the pandemic in Hangzhou, and the observation durations were relatively short. Also, to avoid further infection, only some patients received the tongue diagnosis and pulse diagnosis. Therefore, in subsequent studies, it is necessary to determine a more suitable population and endpoint index. Furthermore, we must fully consider the feasibility of the sample size and other aspects of the test. Since this study was performed in a single center with a small sample size, there may be some limitations to our results. Therefore, it is necessary to comprehensively explore the effects of JMST on COVID-19 based on a larger sample size. Additionally, the dose of JMST proposed in the *Recommended Scheme for Prevention and Treatment of COVID-19 by Traditional Chinese Medicine (Trial Version 4)* was adopted in this study, and related cytokines were not detected. For that reason, the JMST dosage was not adjusted after patients suffered cytokine storms. Further investigations from this perspective are required to address this limitation of the study.

Conclusion

In summary, we explored the efficacy of JMST in the treatment of COVID-19 patients based on authoritative diagnosis and treatment schemes after strict statistical analysis. The combined treatment accelerates the alleviation of primary symptoms, promotes the absorption of lung infection lesions, and shortens the time required to obtain a negative nasal/throat swab-based nucleic acid detection result. However, it is still necessary to further investigate shorter LOS and lymphocyte recovery duration based on larger sample sizes. Furthermore, since JMST does not increase the occurrence of adverse reactions, this treatment approach significantly enhances the rehabilitation of COVID-19 patients.

Data availability statement

The original contributions presented in the study are included in the article/supplementary material, further inquiries can be directed to the corresponding author/s.

Ethics statement

The studies involving human participants were reviewed and approved by Linping Campus, The Second Affiliated Hospital of Zhejiang University School of Medicine (No. 2019001). Written informed consent for participation was not required for this study in accordance with the national legislation and the institutional requirements. Written informed consent was not obtained from the individual(s) for the publication of any potentially identifiable images or data included in this article.

Author contributions

JW and X-QZ: conceptualization and research design. FT: data acquisition. SF: data analysis and interpretation. JW and Z-LF: writing of the manuscript. JW and SF: critical revision of the manuscript for intellectual content. All authors have read and approved the final draft.

Acknowledgments

We would like to acknowledge the hard and dedicated work of all the staff that implemented the intervention and evaluation components of the study.

Conflict of interest

The authors declare that the research was conducted in the absence of any commercial or financial relationships that could be construed as a potential conflict of interest.

Publisher's note

All claims expressed in this article are solely those of the authors and do not necessarily represent those of their affiliated organizations, or those of the publisher, the editors and the reviewers. Any product that may be evaluated in this article, or claim that may be made by its manufacturer, is not guaranteed or endorsed by the publisher.

References

1. Pollard CA, Morran MP, Nestor-Kalinoski AL. The COVID-19 pandemic: a global health crisis. *Physiol Genomics*. (2020) 52:549–57. doi: 10.1152/physiolgenomics.00089.2020

2. Singhal T., A review of coronavirus disease-2019 (COVID-19). *Indian J Pediatr*. (2020) 87:281–6. doi: 10.1007/s12098-020-03263-6

3. Notice on Printing and Distributing the *Diagnosis and Treatment Protocol for COVID-19* (Trial Version 3) (GWBYH [2020] No. 66). [EB/OL]. National Administration of Traditional Chinese Medicine, National Health Commission of the People's Republic of China. Available online at: http://www.gov.cn/zhengce/zhengceku/2020-01/23/content_5471832.htm (accessed January 22, 2020).

4. Notice on Printing and Distributing the *Diagnosis and Treatment Protocol for COVID-19* (Trial Version 4) (GWBYH [2020] No. 77). [EB/OL]. National Administration of Traditional Chinese Medicine, National Health Commission of

the People's Republic of China. Available online at: http://www.gov.cn/zhengce/zhengceku/2020-01/28/content_5472673.htm (accessed January 27, 2020).

5. Notice on Printing and Distributing the *Diagnosis and Treatment Protocol for COVID-19* (Trial Version 5) (GWBYH [2020] No. 103). [EB/OL]. National Administration of Traditional Chinese Medicine, National Health Commission of the People's Republic of China. Available online at: http://www.nhc.gov.cn/yzygj/s7653p/202002/3b09b894ac9b4204a79db5b8912d4440.shtml (accessed February 4, 2020).

6. Gao Z, Xu Y, Sun C, Wang X, Guo Y, Qiu S, et al. systematic review of asymptomatic infections with COVID-19. *J Microbiol Immunol Infect.* (2021) 54:12–6. doi: 10.1016/j.jmii.2020.05.001

7. Liu CX. Pay attention to situation of SARS-CoV-2 and TCM advantages in treatment of novel coronavirus infection. *Chin Herb Med.* (2020) 12:97–103. doi: 10.1016/j.chmed.2020.03.004

8. Dao TL, Hoang VT, Gautret P. Recurrence of SARS-CoV-2 viral RNA in recovered COVID-19 patients: a narrative review. *Eur J Clin Microbiol Infect Dis.* (2021) 40:13–25. doi: 10.1007/s10096-020-04088-z

9. Yang JC, Wang Z, Cai WR, Ge LY, Xu ZY, Chen Y, et al. Interpretation of Recommended Scheme for Prevention and Treatment of COVID-19 by Traditional Chinese Medicine (Trial Version 4) in Zhejiang Province. *J Zhejiang Chin Med Univ.* (2020) 3:223–5. doi: 10.16466/j.issn1005-5509.2020.03.003

10. Wang YG Qi WS, Ma JJ, Ruan LG, Lu YR Li XC, et al. Clinical features and syndrome differentiation of novel coronavirus pneumonia in traditional chinese medicine. *J Tradit Chin Med.* (2020) 61:281–5. doi: 10.13288/j.11-2166/r.2020.04.002

11. Zeng C, Yuan Z, Pan X, Zhang J, Zhu J, Zhou F, et al. Efficacy of Traditional Chinese Medicine, Maxingshigan-Weijing in the management of COVID-19 patients with severe acute respiratory syndrome: A structured summary of a study protocol for a randomized controlled trial. *Trials.* (2020) 21:1029. doi: 10.1186/s13063-020-04970-3

12. Zhang XL, Yong Y, Xu H, Liu QS, Fei YJ. The correlation investigation research of distribution characteristics of health status and TCM physical type in Hangzhou Zhejiang. *J Tradit Chin Med.* (2011) 5:358–319. Available online at: https://chkdx.cnki.net/kcms/detail/detail.aspx?QueryID=93&CurRec=1&dbcode=CHKJ&dbname=CHKJ0911&filename=ZJZZ201105006&urlid=&yx=&uid=WEEvREcwSlJHSldTTEYySCtSOEd0WXZ6MU91RjQrZFBxTWtFQnE3T2tLQT0=$9A4hF_YAuvQ5obgVAqNKPCYcEjKensW4IQMovwHtwkF4VYPoHbKxJw!!&v=MzIxNTlPUHlmUmRMRzRIOURNcW85RllvUjhlWDFMdXhZUzdEaDFUM3FUcldNMUZyQ1VSN2lmYnVScEZDdmxXcjc=

13. Tong XL, Li XY, Zhao LH, Li Q, Yang Y, Lin Y, et al. Discussion on Traditional Chinese Medicine Prevention and Treatment Strategies of New Coronavirus Pneumonia (COVID-19) from the Perspective of "Cold and Wet Epidemic" [J/OL]. *J Tradit Chin Med*. (2020) 1–6.

14. Gu ZS. Reassessment of the Writings from Huang Di Nei Jing Su Wen. *J Tradit Chin Med.* (2004) 11:868–9. doi: 10.13288/j.11-2166/r.2004.11.042

15. Zhu CC. Clinical Study on the Treatment of Chronic Obstructive Pulmonary Disease Combined with Pulmonary Infection with JMST. *Modern Traditional Chinese Medicine.* (2021) 41:86–90. doi: 10.13424/j.cnki.mtcm.2021.04.020

16. Zhong S. Clinical Efficacy of JMST in the Treatment of Wind-warm Disease with Syndrome of Pathogenic Heat Congesting Lung in Community-acquired Pneumonia. *Inner Mongolia J Tradit Chin Med.* (2021) 40:53–4. doi: 10.16040/j.cnki.cn15-1101.2021.09.032

17. Wang W, Tang B, Li X. Treating 157 Cases of Infantile Pneumonia of Phlegm-heat Stagnating Lung Patternwith Modified Maxing Shigan Decoction. *Western J Tradit Chin Med.* (2019) 32:82–4. Available online at: https://chkdx.cnki.net/kcms/detail/detail.aspx?QueryID=84&CurRec=1&dbcode=CHKJ&dbname=CHKJ1519&filename=GSZY201908024&urlid=&yx=&uid=WEEvREcwSlJHSldTTEYySCtSOEd0WXZ6MU91RjQrZFBxTWtFQnE3T2tLQT0=$9A4hF_YAuvQ5obgVAqNKPCYcEjKensW4IQMovwHtwkF4VYPoHbKxJw!!&v=MTI1MTVUcldNMUZyQ1VSN2lmYnVScEZDdmxVTHZBSWo3UmQ3RzRIOWpNcDQ5SFlJUjhlWDFMdXhZUzdEaDFUM3E=cldNMUZyQ1VSN2lmYnVScEZDdmxVTHZBSWo3UmQ3RzRIOWpNcDQ5SFlJUjhlWDFMdXhZUzdEaDFUM3E=

18. Liu HR, Lin ZB. A pharmacological study of pneumonia mixture II (JMST). *J Peking Univ.* (1979) 01:69–70. Available online at: https://chkdx.cnki.net/kcms/detail/detail.aspx?QueryID=102&CurRec=1&dbcode=CHKJ&dbname=CHKJ7993&filename=BYDB1979010023&urlid=&yx=&uid=WEEvREcwSlJHSldTTEYySCtSOEd0WXZ6MU91RjQrZFBxTWtFQnE3T2tLQT0=$9A4hF_YAuvQ5obgVAqNKPCYcEjKensW4IQMovwHtwkF4VYPoHbKxJw!!&v=MTM3NjFYMUx1eFlTN0RoMVQzcVRyV00xRnJDVVI3aWZidVJwRkN2bFc3ektKelRQYkxLeEdkak1ybzlIWjRSOGU=

19. Ye YY, Xuan ZH, Luo XF. Clinical Observation on 35 Cases of Ventilator-associated Pneumonia Prevented by Modified Shenling Baizhu Powder. *Zhejiang J Tradit Chin Med.* (2019) 54:328. doi: 10.13633/j.cnki.zjtcm.2019.05.013

20. Shi Y, Zhang ZR, Cai DL, Wang LC. Observation on 30 Cases of Ventilator-associated Pneumonia in Ventilator-dependent Patients Prevented by Shenling Baizhu Powder. *Zhejiang J Tradit Chin Med.* (2018) 53:335. doi: 10.13633/j.cnki.zjtcm.2018.05.014

21. Deng SQ, Peng HJ. Characteristics of and Public Health Responses to the Coronavirus Disease 2019 Outbreak in China. *J Clin Med.* (2020) 9:575. doi: 10.3390/jcm9020575

22. Lai CC, Shih TP, Ko WC, Tang HJ, Hsueh PR. Severe acute respiratory syndrome coronavirus 2 (SARS-CoV-2) and coronavirus disease-2019 (COVID-19): The epidemic and the challenges. *Int J Antimicrob Agents.* (2020) 55:105924. doi: 10.1016/j.ijantimicag.2020.105924

frontiers | Frontiers in Medicine

TYPE Case Report
PUBLISHED 03 November 2022
DOI 10.3389/fmed.2022.1055465

OPEN ACCESS

EDITED BY
Francesco Paolo Bianchi,
University of Bari Aldo Moro, Italy

REVIEWED BY
Katarina Westling,
Karolinska Institutet (KI), Sweden
Lurdes Santos,
Centro Hospitalar Universitário de São João (CHUSJ), Portugal

*CORRESPONDENCE
Mai Sasaki Aanensen Fraz
mai.sasaki.aanensen@gmail.com

SPECIALTY SECTION
This article was submitted to Infectious Diseases – Surveillance, Prevention and Treatment, a section of the journal Frontiers in Medicine

RECEIVED 27 September 2022
ACCEPTED 14 October 2022
PUBLISHED 03 November 2022

CITATION
Fraz MSA, Dahle G, Skaug KM, Jarraud S, Frye S, Bjørnholt JV and Nordøy I (2022) Case report: A prosthetic valve endocarditis caused by *Legionella bozemanae* in an immunocompetent patient. *Front. Med.* 9:1055465. doi: 10.3389/fmed.2022.1055465

Case report: A prosthetic valve endocarditis caused by *Legionella bozemanae* in an immunocompetent patient

Mai Sasaki Aanensen Fraz[1,2,3]*, Gry Dahle[4], Kirsten Margrete Skaug[1], Sophie Jarraud[5], Stephan Frye[1], Jørgen Vildershøj Bjørnholt[1,6] and Ingvild Nordøy[7,8]

[1]Department of Microbiology, Oslo University Hospital, Oslo, Norway, [2]Centre for Rare Disorders, Oslo University Hospital, Oslo, Norway, [3]Department of Medicine, Lovisenberg Diaconal Hospital, Oslo, Norway, [4]Department of Cardiothoracic Surgery, Oslo University Hospital, Oslo, Norway, [5]National Reference Centre for Legionella, Institute of Infectious Agents, Hospices Civils de Lyon, Lyon, France, [6]Faculty of Medicine, Institute of Clinical Medicine, University of Oslo, Oslo, Norway, [7]Section for Clinical Immunology and Infectious Diseases, Oslo University Hospital, Oslo, Norway, [8]Research Institute of Internal Medicine, Oslo University Hospital, Oslo, Norway

Extrapulmonary infections with *Legionella species* are rare, but important to acknowledge. We report a case of infective endocarditis (IE) with *Legionella bozemanae* in a 66-year-old immunocompetent man with an aortic homograft. The diagnosis was made by direct 16S rRNA gene amplification from valve material, confirmed by a targeted *Legionella*-PCR in serum and the detection of *L. bozemanae* specific antibodies. To our knowledge, this is the first confirmed case of IE with *L. bozemanae* as causative pathogen. The infected aortic prosthesis was replaced by a homograft, and the patient was successfully treated with levofloxacin and azithromycin for 6 weeks.

KEYWORDS

endocarditis, prosthetic valve endocarditis (PVE), molecular diagnostic techniques, blood culture negative endocarditis, *Legionella bozemanae*, *Legionella bozemanii*

Introduction

The *Legionellaceae* are widespread in water and soil environment, and can colonize manmade water sources. This is also true for *Legionella bozemanae*, which has also been found in commercial potting soils (1–4). *L. bozemanae* is uncommonly a pathogen, but it has been reported to be able to cause severe and necrotizing pneumonia in immunocompromised patients (5, 6). Extrapulmonary infections with *L. bozemanae* are even rarer, however cases of arthritis and soft tissue infections are described (7–9). There are 18 previous reports of infective endocarditis (IE) caused by *Legionella species* in the English literature, and in only two of these, the affected valve was native (10–20). The presentation of *Legionella* endocarditis tends to be subacute, with weight loss, low-grade fever and anemia, and without peripheral manifestations as embolic events or immune complex depositions (21). Exceptions from this are two reports of bacterial seeding to the central nervous system and one case of digital microembolisms (15, 19, 20).

In the previous reports of *Legionella* endocarditis, the majority of IE patients had no preceding or concurrent airway infection, with only four of 18 cases reporting clinical or radiological findings consistent with pneumonia. In one case series, the *Legionella* endocarditis cases were believed to be part of hospital outbreaks of *Legionella* (10). Another feature of the reported *Legionella* IEs in the literature is that although small valvular vegetations are often visible at surgery, they are frequently undetectable by echocardiograms (10, 17). Accordingly, as the patients also often display only moderate signs of inflammation, the diagnosis of IE can be delayed.

Case description

A 66-year-old immunocompetent man with an increasingly symptomatic aortic stenosis and bicuspid aortic valve underwent aortic valve replacement in April 2021 at Oslo University Hospital, Rikshospitalet. He was otherwise healthy, besides an occasional migraine. The inserted prosthetic aortic valve was a biological 23 mm Perimount prosthesis (Edwards Lifesciences, Irvine, CA, United States), and an aorta Intergard woven graft 30 mm (Getinge, Göteborg, Sweden) was also inserted (Day 0). The surgical procedure was uneventful, and per operative echocardiogram and postoperative chest x-ray were normal. The further disease course, diagnostics and treatment in this case is illustrated in the timeline of **Figure 1**.

The patient was transferred to his local hospital for postoperative care on Day 3 after surgery. Physical examination at the day of transfer revealed no heart murmur or pulmonary crepitations. During the first postoperative week he developed fever and CRP increased to a maximum of 329 mg/L on Day 8. Antibiotic treatment with cefotaxime was started. There were no visible valvular vegetations by transthoracic echocardiogram on Day 14. As his condition failed to improve, a chest CT was performed on Day 15 displaying a possible infected aortic root hematoma. CT also demonstrated pleural- and pericardial fluid, but no lung parenchymal infiltrations. In this period, the patient complained of a non-productive troublesome cough. CRP levels did not fall significantly, and the antibiotic treatment was switched to meropenem. Pleural fluid was drained. Subsequently, CRP decreased to 34 mg/L and the patient's condition somewhat improved. The patient was discharged to his home with a 10 days course of oral clindamycin.

However, he continued to have nightly fever and weight loss after the discharge. He also had a short self-limiting episode of pain, rubor and swelling in his left knee. On Day 41 he was readmitted to his local hospital with increasing fever, and CRP had increased to 84 mg/L. There were normal findings by physical examination of his knee joint. Chest CT was repeated on Day 42 with unchanged findings around the aortic root, and still no lung parenchymal infiltrations. The patient was observed without starting any antibiotic treatment, with the aim of catching a pathogen by repeated blood culturing. He stayed afebrile the following 2 days, and was again discharged without any blood culture findings. However, the patient did not improve clinically, and CRP was continuously moderately elevated. Therefore, chest CT was again repeated on Day 83, this time revealing some reduction of fluid accumulation around the aortic root and ascendens graft. Finally, transesophageal echocardiogram was performed Day 86, showing pendulating material at the ventricular side of the aortic valve cusps, consistent with endocarditis (**Figure 2**). The patient had at this time developed a second degree atrioventricular block, and a temporary pacemaker was inserted.

As blood cultures remained negative, the patient was treated empirically with ceftriaxone and vancomycin from Day 86. The patient's condition deteriorated despite this treatment, and he was decided to undergo redo surgery. The Perimount prosthesis and the ascendens graft were excised and replaced by a Homograft 22 mm (Cell and Tissue laboratory, Sahlgrenska, Sweden) on Day 96. Microscopy of acridin stained excised valve material demonstrated scarcely distributed rods (**Figure 3**), but culture of the explant on standard bacterial and fungal media did not yield growth. However, direct 16S rRNA gene amplification of valve material yielded sequences of 720 base pairs matching 100% with *L. bozemanae* in the National Center for Biotechnology Information (NCBI) Blast database and EzBioCloud (22). The valve tissue DNA extraction and 16S rRNA gene amplification were performed twice with same result. Seeding of the explanted valve material was also done on buffered charcoal-yeast extract (BCYE) media for *Legionella*, but we were not able to grow *L. bozemanae*. The patient was finally treated with levofloxacin and azithromycin for 6 weeks. The atrioventricular block progressed to a total block after the redo, and a permanent pacemaker was implanted after 4 weeks. Transthoracal echocardiogram was performed by the end of the antibiotic treatment, displaying an aortic graft in satisfactory position, without leakage. Post treatment CT arteriography showed significant decline of fluid around the aortic root. The patient is now physically fit and is doing well, a year after completed therapy.

An environmental search was performed to detect *Legionella spp.* in water sources at the local hospital, at the university hospital where the surgery was performed and at the patient's home. *L. bozemanae* was not detected in any of these locations.

The diagnosis of *L. bozemanae* was confirmed retrospectively by a hybridization probe-based dual-color LightCycler real-time PCR with primers that amplify a 378-bp product within the 16S rRNA gene of *Legionella spp.* of the patient's serum (23). The serum was sampled and stored frozen from 6 days (Day 90) before the reoperation. Subsequent melting point analysis corresponded with *L. bozemanae*. Additionally, an assay to detect *L. bozemanae* specific antibodies was performed by the French National Reference Center for Legionella (Lyon, France). Serum from 2 days before the primary operation (Day-2), was negative (<1:16) for

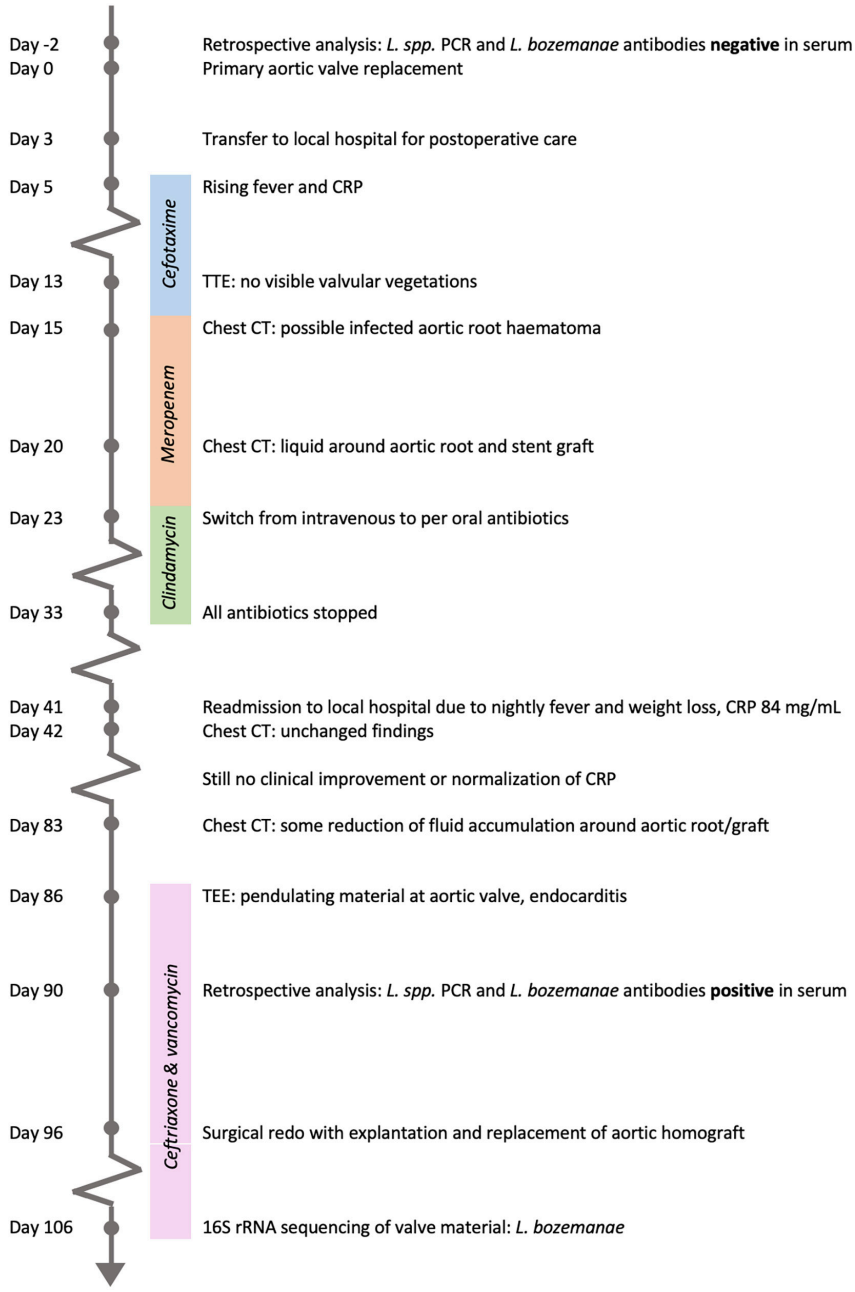

FIGURE 1
Timeline from admission for the primary aortic valve replacement until microbial diagnosis by 16S rRNA sequencing of valve material.

L. bozemanae antibodies, while in serum from Day 90 the titer was positive (>1:2048).

Finally, although the diagnosis was certain, we performed 16S Nanopore sequencing on both cardiac valve material and serum from Day 90 to see if this method would detect *L. bozemanae*. DNA was extracted by SelectNAplus from Molzym (Bremen, Germany) and prepared for Nanopore sequencing using a 16S Barcoding Kit (SQK-RAB204, Oxford Nanopore Technologies, Oxford, UK). Sequencing was performed on a MinION flowcell (FLO-MIN106D, Oxford Nanopore Technologies, Oxford, UK) for 43 h. Sequences were filtered by size and quality using ProwlerTrimmer and blasted against the NCBI 16S rRNA refseq database, which was complemented with a full-length sequence of the 16S rRNA gene of *L. bozemanae*, extracted from the whole genome assembly GCF_900640135.1. While the serum sample from Day 90 yielded 36,673 reads before filtering and 10,678 after, the valve sample only gave 153 reads with 90 reads left

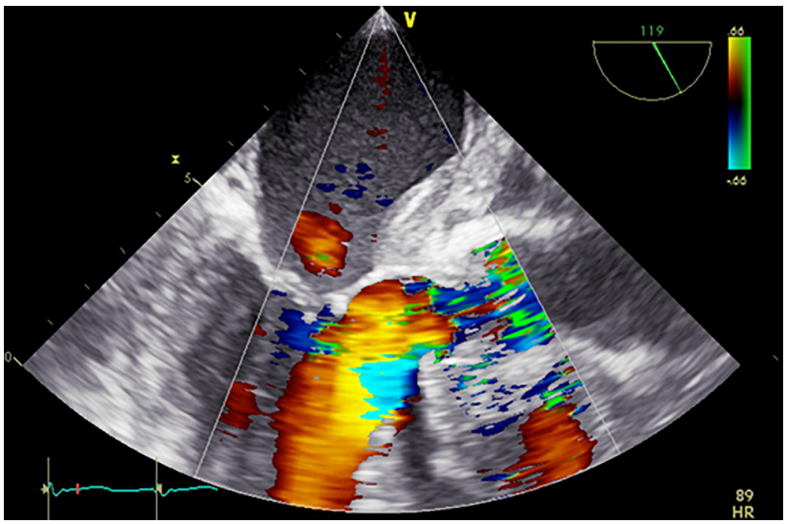

FIGURE 2
Pre-operative transesophageal echocardiogram. Severe aortic regurgitation and thickened aortic wall.

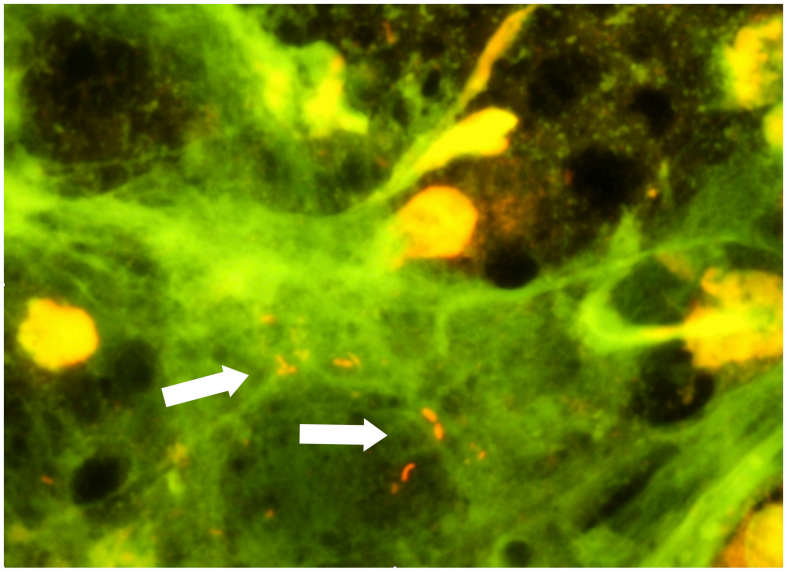

FIGURE 3
Excised valve material, acridin stain. Rods marked by white arrows.

after filtering. No *Legionella* specific sequences were found in the serum-derived reads. On the other hand, 89 of the 90 (98%) reads from the valve sample were identified as *L. bozemanae* specific.

Discussion

Infective endocarditis has a high mortality rate, and early identification of the causative microbe is important to target antibiotic therapy and improve outcome. *Legionella spp.* are not routinely recoverable from blood cultures and will not be covered by standard empiric antibiotic treatment for endocarditis. A subacute disease course without typical IE findings adds to making the diagnosis of this infection challenging. This case report has several take-away lessons: Most important, although *Legionella spp.* are infrequent causes of infectious endocarditis in general, they should be considered in culture negative cases of post-surgery prosthetic valve endocarditis (PVE) (24). This case also demonstrates that PVE

caused by *L. bozemanae* is possible in an otherwise healthy and immunocompetent host.

Furthermore, this and most other similar cases show that the *Legionella* bacteria's way of entrance to cause endocarditis often remains unknown. Although *Legionella* is often associated with airway infection, the literature shows that airway symptoms are often not present in *Legionella* PVE. Our patient experienced a protracted disease course after the primary surgery, with fluctuating fever and CRP. Repeated chest CT showed no pulmonary infiltrations, and *Legionella* was not detected by *Legionella* PCR in bronchial lavage fluid after the reoperation. The patient experienced some dry cough, but this could as well be attributed to pleural irritation by pleural fluid present. *L. bozemanae* was neither detected in the water systems of the operating hospital, the local hospital nor the patient's house.

When it comes to treatment, there are no randomized trials involving legionellosis with non-pneumophila species. For long, antimicrobial susceptibility testing (AST) for *Legionella* has been challenging and not standardized, until the European Society of Clinical Microbiology and Infectious Diseases (ESCMID) Study Group for Legionella Infections recently issued a recommendation (25). In this case, AST was impossible due to lack of a positive culture. The literature regarding antibiotic susceptibility for *Legionella species* other than pneumophila is scarce, but AST studies performed by broth microdilution and in a human monocyte cell line demonstrate higher activity of quinolones than erythromycin against *L. bozemanae* (26). However, fluoroqinolone resistance may be induced during antibiotic treatment (27). Based on this knowledge and the gravity of the infection in this case, our patient was given a combination of levofloxacin and azithromycin. However, long QT interval should always be considered and monitored when combining these drugs (28).

We identified the microbial cause of endocarditis by broad-range 16S rRNA gene amplification of the excised specimen. This is common practice in blood culture negative endocarditis (BCNE) when explanted valve material is available, and can identify a microbial cause in about two thirds of cases (29). In cases of IE where surgery has not been performed, a reliable molecular method to detect relevant microbial genetic material in blood, serum or plasma would be an ideal diagnostic tool. Unfortunately, as of today no such method has shown satisfactory performance. Metagenomic next-generation sequencing of plasma is suggested as a promising aid in systemic infections, although both false positive and false negative results, as well as the noise of polymicrobial identification can make interpretation of results challenging (30–32). Our 16S Nanopore sequencing of the patient's serum were not able to detect any *Legionella*.

In this case, targeted *Legionella* PCR was positive in serum from 6 days before the redo. The European Society of Cardiology guidelines recommend the use of targeted PCR of EDTA-blood when IE with *Bartonella spp*., *Tropheryma whipplei* or fungi are suspected (33). The guidelines also recommend systematic serological testing for *Legionella pneumophila* in BCNE according to local epidemiology. However, most serological assays for *Legionella* only detect *L. pneumophila*, which leaves a diagnostic gap for other *Legionella* spp. that may be underdiagnosed. Serological assays for *Legionella species* other than pneumophila are not avaliable in Norway, and is in general not widely performed as there are no commercial tests. International laboratory collaboration partners or networks can be helpful in cases like ours. Targeted *Legionella* PCR is on the other hand more commonly performed, and is mostly used in airway specimens. The sensitivity of targeted *Legionella* PCR in sera of patients with *Legionella* pneumonia has previously been reported to be 30–63% depending on the target gene, and the specificity to be 100% (34–36).

In conclusion, *Legionella* endocarditis is difficult to diagnose due to both indistinct clinical findings and the fact that microbiological identification depends on the clinicians' suspicion. Targeted *Legionella* PCR of serum should be considered in cases of culture negative PVE, and *Legionella* spp. as a cause of BCNE are likely underdiagnosed.

Data availability statement

The genomic sequences presented in this case report are included in the **Supplementary material**. Further inquiries can be directed to the corresponding author.

Ethics statement

Written informed consent was obtained from the individual(s) for the publication of any potentially identifiable images or data included in this article.

Author contributions

MF collected the data and drafted the manuscript. KS, SF, SJ, and JB analyzed and interpreted the data. GD and IN provided clinical care for the patient. All authors reviewed, edited, and approved the final manuscript.

Acknowledgments

We acknowledge all healthcare and laboratory workers involved in the diagnosis and treatment of the patient. We especially thank Bente Cecilie Borgen and the other infection prevention workers who performed the environmental search.

Conflict of interest

The authors declare that the research was conducted in the absence of any commercial or financial relationships that could be construed as a potential conflict of interest.

Publisher's note

All claims expressed in this article are solely those of the authors and do not necessarily represent those of their affiliated organizations, or those of the publisher, the editors and the reviewers. Any product that may be evaluated in this article, or claim that may be made by its manufacturer, is not guaranteed or endorsed by the publisher.

Supplementary material

The Supplementary Material for this article can be found online at: https://www.frontiersin.org/articles/10.3389/fmed.2022.1055465/full#supplementary-material

References

1. Casati S, Gioria-Martinoni A, Gaia V. Commercial potting soils as an alternative infection source of *Legionella pneumophila* and other Legionella species in Switzerland. *Clin Microbiol Infect.* (2009) 15:571–5. doi: 10.1111/j.1469-0691.2009.02742.x

2. Koide M, Arakaki N, Saito A. Distribution of Legionella longbeachae and other legionellae in Japanese potting soils. *J Infect Chemother.* (2001) 7:224–7. doi: 10.1007/s101560170017

3. Patterson WJ, Hay J, Seal DV, McLuckie JC. Colonization of transplant unit water supplies with *Legionella* and protozoa: precautions required to reduce the risk of legionellosis. *J Hosp Infect.* (1997) 37:7–17. doi: 10.1016/s0195-6701(97)90068-2

4. Lee HK, Shim JI, Kim HE, Yu JY, Kang YH. Distribution of Legionella species from environmental water sources of public facilities and genetic diversity of L. pneumophila serogroup 1 in South Korea. *Appl Environ Microbiol.* (2010) 76:6547–54. doi: 10.1128/AEM.00422-10

5. Harris A, Lally M, Albrecht M. Legionella bozemanii pneumonia in three patients with AIDS. *Clin Infect Dis.* (1998) 27:97–9. doi: 10.1086/514618

6. Miller ML, Hayden R, Gaur A. Legionella bozemanii pulmonary abscess in a pediatric allogeneic stem cell transplant recipient. *Pediatr Infect Dis J.* (2007) 26:760–2. doi: 10.1097/INF.0b013e318054e338

7. Just SA, Knudsen JB, Uldum SA, Holt HM. Detection of *Legionella bozemanae*, a new cause of septic arthritis, by PCR followed by specific culture. *J Clin Microbiol.* (2012) 50:4180–2. doi: 10.1128/JCM.01899-12

8. Ibranosyan M, Beraud L, Lemaire H, Ranc AG, Ginevra C, Jarraud S, et al. The clinical presentation of *Legionella* arthritis reveals the mode of infection and the bacterial species: case report and literature review. *BMC Infect Dis.* (2019) 19:864. doi: 10.1186/s12879-019-4488-z

9. Neiderud CJ, Vidh AL, Salaneck E. Soft tissue infection caused by Legionella bozemanii in a patient with ongoing immunosuppressive treatment. *Infect Ecol Epidemiol.* (2013) 3:10.3402/iee.v3i0.20739. doi: 10.3402/iee.v3i0.20739

10. Tompkins LS, Roessler BJ, Redd SC, Markowitz LE, Cohen ML. Legionella prosthetic-valve endocarditis. *N Engl J Med.* (1988) 318:530–5.

11. Park D, Pugliese A, Cunha BA. Legionella micdadei prosthetic valve endocarditis. *Infection.* (1994) 22:213–5.

12. Chen TT, Schapiro JM, Loutit J. Prosthetic valve endocarditis due to *Legionella pneumophila*. *J Cardiovasc Surg.* (1996) 37:631–3.

13. McCabe RE, Baldwin JC, McGregor CA, Miller DC, Vosti KL. Prosthetic valve endocarditis caused by *Legionella pneumophila*. *Ann Intern Med.* (1984) 100:525–7.

14. Patel MC, Levi MH, Mahadevi P, Nana M, Merav AD, Robbins N. L. micdadei PVE successfully treated with levofloxacin/valve replacement: case report and review of the literature. *J Infect.* (2005) 51:e265–8. doi: 10.1016/j.jinf.2005.03.011

15. Young JS, Farber BF, Pupovac SS, Graver LM. Prosthetic valve legionella endocarditis. *Ann Thorac Surg.* (2019) 108:e271–2.

16. Pearce MM, Theodoropoulos N, Mandel MJ, Brown E, Reed KD, Cianciotto NP. Legionella cardiaca sp. nov., isolated from a case of native valve endocarditis in a human heart. *Int J Syst Evol Microbiol.* (2012) 62(Pt. 12):2946–54. doi: 10.1099/ijs.0.039248-0

17. Leggieri N, Gouriet F, Thuny F, Habib G, Raoult D, Casalta JP. Legionella longbeachae and endocarditis. *Emerg Infect Dis.* (2012) 18:95–7.

18. Compain F, Bruneval P, Jarraud S, Perrot S, Aubert S, Napoly V, et al. Chronic endocarditis due to Legionella anisa: a first case difficult to diagnose. *New Microbes New Infect.* (2015) 8:113–5. doi: 10.1016/j.nmni.2015.10.003

19. Fukuta Y, Yildiz-Aktas IZ, William Pasculle A, Veldkamp PJ. Legionella micdadei prosthetic valve endocarditis complicated by brain abscess: case report and review of the literature. *Scand J Infect Dis.* (2012) 44:414–8. doi: 10.3109/00365548.2011.645506

20. Massey R, Kumar P, Pepper JR. Innocent victim of a localised outbreak: legionella endocarditis. *Heart.* (2003) 89:e16. doi: 10.1136/heart.89.5.e16

21. Brusch JL. Legionnaire's disease: cardiac manifestations. *Infect Dis Clin North Am.* (2017) 31:69–80.

22. Yoon SH, Ha SM, Kwon S, Lim J, Kim Y, Seo H, et al. Introducing EzBioCloud: a taxonomically united database of 16S rRNA gene sequences and whole-genome assemblies. *Int J Syst Evol Microbiol.* (2017) 67:1613–7. doi: 10.1099/ijsem.0.001755

23. Reischl U, Linde HJ, Lehn N, Landt O, Barratt K, Wellinghausen N. Direct detection and differentiation of Legionella spp. and *Legionella pneumophila* in clinical specimens by dual-color real-time PCR and melting curve analysis. *J Clin Microbiol.* (2002) 40:3814–7. doi: 10.1128/JCM.40.10.3814-3817.2002

24. Brouqui P, Raoult D. Endocarditis due to rare and fastidious bacteria. *Clin Microbiol Rev.* (2001) 14:177–207.

25. Portal E, Descours G, Ginevra C, Mentasti M, Afshar B, Chand M, et al. Legionella antibiotic susceptibility testing: is it time for international standardization and evidence-based guidance? *J Antimicrob Chemother.* (2021) 76:1113–6. doi: 10.1093/jac/dkab027

26. Stout JE, Arnold B, Yu VL. Comparative activity of ciprofloxacin, ofloxacin, levofloxacin, and erythromycin against *Legionella* species by broth microdilution and intracellular susceptibility testing in HL-60 cells. *Diagn Microbiol Infect Dis.* (1998) 30:37–43. doi: 10.1016/s0732-8893(97)00174-0

27. Hennebique A, Bidart M, Jarraud S, Beraud L, Schwebel C, Maurin M, et al. Digital PCR for detection and quantification of fluoroquinolone resistance in *Legionella pneumophila*. *Antimicrob Agents Chemother.* (2017) 61:e00628–617. doi: 10.1128/AAC.00628-17

28. Wang JY, Li X, Chen JY, Tong B. Epileptic seizure after use of moxifloxacin in man with legionella longbeachae pneumonia. *Emerg Infect Dis.* (2020) 26:2725–7. doi: 10.3201/eid2611.191815

29. Fournier PE, Thuny F, Richet H, Lepidi H, Casalta JP, Arzouni JP, et al. Comprehensive diagnostic strategy for blood culture-negative endocarditis: a prospective study of 819 new cases. *Clin Infect Dis.* (2010) 51:131–40. doi: 10.1086/653675

30. Ramchandar N, Burns J, Coufal NG, Pennock A, Briggs B, Stinnett R, et al. Use of metagenomic next-generation sequencing to identify pathogens in pediatric osteoarticular infections. *Open Forum Infect Dis.* (2021) 8:ofab346.

31. Chan WS, Au CH, Leung HC, Ho DN, Li D, Chan TL, et al. Potential utility of metagenomic sequencing for improving etiologic diagnosis of infective endocarditis. *Fut. Cardiol.* (2019) 15:411–24. doi: 10.2217/fca-2018-0088

32. Lee RA, Al Dhaheri F, Pollock NR, Sharma TS. Assessment of the clinical utility of plasma metagenomic next-generation sequencing in a pediatric hospital population. *J Clin Microbiol.* (2020) 58:e00419–20. doi: 10.1128/JCM.00419-20

33. Habib G, Lancellotti P, Antunes MJ, Bongiorni MG, Casalta JP, Del Zotti F, et al. 2015 ESC Guidelines for the management of infective endocarditis: the task force for the management of infective endocarditis of the European society of cardiology (ESC). Endorsed by: European association for cardio-thoracic surgery (EACTS), the European association of nuclear medicine (EANM). *Eur Heart J.* (2015) 36:3075–128. doi: 10.1093/eurheartj/ehv319

34. Diederen BMW, de Jong CMA, Marmouk F, Kluytmans J, Peeters MF, Van der Zee A. Evaluation of real-time PCR for the early detection of *Legionella pneumophila* DNA in serum samples. *J Med Microbiol.* (2007) 56(Pt. 1):94–101. doi: 10.1099/jmm.0.46714-0

35. Murdoch DR, Walford EJ, Jennings LC, Light GJ, Schousboe MI, Chereshsky AY, et al. Use of the polymerase chain reaction to detect Legionella DNA in urine and serum samples from patients with pneumonia. *Clin Infect Dis.* (1996) 23:475–80.

36. Lindsay DSJ, Abraham WH, Findlay W, Christie P, Johnston F, Edwards GFS. Laboratory diagnosis of Legionnaires' disease due to *Legionella pneumophila* serogroup 1: comparison of phenotypic and genotypic methods. *J Med Microbiol.* (2004) 53(Pt. 3):183–7. doi: 10.1099/jmm.0.05464-0

frontiers | Frontiers in Medicine

TYPE Case Report
PUBLISHED 04 November 2022
DOI 10.3389/fmed.2022.1009557

OPEN ACCESS

EDITED BY
Francesco Paolo Bianchi,
University of Bari Aldo Moro, Italy

REVIEWED BY
Ilnaz Rahimmanesh,
Isfahan University of Medical Sciences, Iran
Paolo Bottino,
University of Turin, Italy

*CORRESPONDENCE
Shih-Ming Tsao
tsmhwy@ms24.hinet.net

SPECIALTY SECTION
This article was submitted to Infectious Diseases – Surveillance, Prevention and Treatment, a section of the journal Frontiers in Medicine

RECEIVED 02 August 2022
ACCEPTED 03 October 2022
PUBLISHED 04 November 2022

CITATION
Wang W-Y, Lee Y-T, Wang Y-T, Chen J-Z, Lee S-Y and Tsao S-M (2022) A case series report on successful management of patients with COVID-19-associated lymphopenia and potential application of PG2. *Front. Med.* 9:1009557. doi: 10.3389/fmed.2022.1009557

A case series report on successful management of patients with COVID-19-associated lymphopenia and potential application of PG2

Wei-Yao Wang[1], Yuan-Ti Lee[1], Yao-Tung Wang[2], Ji-Zhen Chen[3], Su-Yin Lee[4] and Shih-Ming Tsao[2]*

[1]Division of Infectious Disease, School of Medicine, Chung Shan Medical University Hospital, Chung Shan Medical University, Taichung, Taiwan, [2]Division of Chest Medicine, School of Medicine, Chung Shan Medical University Hospital, Chung Shan Medical University, Taichung, Taiwan, [3]Department of Internal Medicine, Chung Shan Medical University Hospital, Taichung, Taiwan, [4]Infection Control Center, Chung Shan Medical University Hospital, Taichung, Taiwan

Background: Lymphopenia and the resultant high neutrophil-to-lymphocyte ratio (NLR) are hallmark signs of severe COVID-19, and effective treatment remains unavailable. We retrospectively reviewed the outcomes of COVID-19 in a cohort of 26 patients admitted to Chung Shan Medical University Hospital (Taichung City, Taiwan). Twenty-five of the 26 patients recovered, including 9 patients with mild/moderate illness and 16 patients with severe/critical illness recovered. One patient died after refusing treatment.

Case presentation: We report the cases of four patients with high NLRs and marked lymphopenia, despite receiving standard care. A novel injectable botanical drug, PG2, containing *Astragalus* polysaccharides, was administered to them as an immune modulator. The decrease in the NLR in these four patients was faster than that of other patients in the cohort (0.80 vs. 0.34 per day).

Conclusion: All patients recovered from severe COVID-19 showed decreased NLR and normalized lymphocyte counts before discharge. Administration of PG2 may be of benefit to patients with moderate to severe COVID-19 and lymphopenia.

KEYWORDS

COVID-19, lymphopenia, *Astragalus* polysaccharides, PG2, neutrophil-to-lymphocyte ratio

Introduction

Lymphopenia accompanying inflammatory cytokine storms is frequently reported (35–83%) in patients who with SARS-CoV-2 infection (1–4). A decreased absolute lymphocyte count (ALC) and an increased neutrophil-to-lymphocyte ratio (NLR) is indicative of severe COVID-19 and are associated with a poor prognosis (5, 6). There is no medical treatment currently available to reverse lymphopenia and prevent disease progression (7). In this context, we report our experience of the effectiveness of PG2 in the management of such patients; PG2® lyophilized injection is an approved botanical drug containing bioactive polysaccharides of dried *Astragalus membranaceus* (Chinese: Huang-Chi) roots and was originally used for treatment of cancer-related fatigue. According to the approved label information and previous publications (8), PG2 or *Astragalus* polysaccharides can elicit a broad spectrum of therapeutic effects, including modulation of the immune system. More specifically, PG2 has been shown to induce differentiation of splenic dendritic cells (DCs), expand the $CD11c^{high}CD45RB^{low}$ DC pool, increase the Th1/Th2 ratio, and enhance the T cell-mediated immunity *in vitro* (9). Previous clinical studies suggest that PG2 also modulates the inflammatory cascade *via* suppression of pro-inflammatory cytokines (10).

The Taiwanese government has employed strict boarder control and no community-acquired cases of COVID-19 were observed until the COVID-19 epidemic in May 2021, in which a total of 16,278 confirmed cases were reported, with 851 deaths. A total of 26 patients (11 males and 16 females), with COVID-19, were admitted to Chung Shan Medical University Hospital (CSMUH) in central Taiwan between May 19, 2021 and June 10, 2021. Taiwan. **Table 1** shows the demographic and clinical characteristics and the outcomes of these patients. Nine patients were categorized as mild or moderate severity, and the other 16 patients were categorized as severe or critical, according to the World Health Organization (WHO) criteria (11). We also evaluated the clinical severity, on admission and during the hospitalization period of the 26 patients, using a widely accepted 7-point ordinal scale (12). Patient with severe disease were older in age, with more comorbidities including diabetes, cardiovascular (CV) risk factors and histories of malignancies when compared to those with mild to moderate disease on admission. Only one of our 26 patients died after refusing treatment. The other 25 patients, including 9 with mild/moderate illness and 16 with severe/critical illness, recovered with adequate therapy. A cycle threshold (Ct) of SARS-CoV-2 RT-PCR greater than 30 indicated viral negative and/or non-contagious for discharge.

Four patients in this cohort had marked lymphopenia, despite standard care. We treated them with PG2 injections, after receiving emergency authorization from the hospital's institutional review board. Written informed consent was obtained from the patients or their legal guardian, prior to initiation of this treatment. The dosage of PG2 was as follows: 500 mg dissolved in 500 mL normal saline *via* intravenous infusion for 2.5–3.5 h, once every other day (QOD). Summaries of the clinical characteristics, outcomes and laboratory and radiologic findings are shown in **Table 2** and **Supplementary Table 1**, respectively.

Case descriptions

Case I

A 46-year-old woman without comorbidities, was transferred from a government quarantine facility to our hospital; she had marked oxygen desaturation on admission. Dexamethasone 6 mg once per day (QD) was given for 7 days on admission. On the second day, a standard 5-day course of remdesivir (200 mg on day 1, followed by 100 mg from days 2 to 5) was initiated; in addition, a single dose of tocilizumab 8 mg/kg was also administered to manage the patient's high C-reactive protein (CRP) level (9.6 mg/dL), in accordance with the standard guidelines of the Taiwan Center for Disease Control (Taiwan CDC) (13). However, on day 3, laboratory data showed a higher NLR (4.9) than on admission and the patient's Chest X-ray (CXR) showed persistent bilateral infiltrates. She was treated with a PG2 infusion (500 mg in 500 mL 0.9% saline) QOD for five doses. No adverse reactions were noted. Her clinical condition improved and a CXR also showed improvement. Laboratory tests showed an increase in the lymphocyte count, and lactate dehydrogenase (LDH) and CRP levels within the normal range. The patient's NLR decreased to 1.9 on day 5 of hospitalization and remained stable (1.3–2.2) below the cut-off value of 3.5 throughout the remaining hospitalization period. She was discharged 10 days after admission with a Ct value: 38 for SARS-CoV-2 PCR.

Case II

A 50-year-old man was admitted to the respiratory intensive care unit (ICU) on account of dyspnea, hypoxia (SpO_2 90% on oxygen 3 L/min *via* nasal cannula) and fever (>38°C). He was administered standard therapy including remdesivir (200 mg on day 1, followed by 100 mg from day 2 to day 5), dexamethasone 8 mg QD, and a single dose of tocilizumab 640 mg. However, his clinical condition deteriorated with progressive dyspnea and hypoxia on day 3. The oxygen treatment was switched to high flow nasal cannula (HFNC) with a positive end-expiratory pressure (PEEP) of 8 cm H_2O. PG2 500 mg QOD was then initiated since day 4. His condition improved and the oxygen support was switched from a HFNC to a nasal cannula on day 5. He was discharged on day 11 after his condition

TABLE 1 Clinico-demographic data and outcome profiles of 26 patients with laboratory-confirmed COVID-19.

Characteristic of cases	Total cases (%) (26 cases, 100%)	Severity (%)		
		Mild to moderate (9 cases, 34.6%)	Severe without PG2 treatment (13 cases, 50.0%)	Severe with PG2 treatment (4 cases, 15.4%)
Age (years) (±SD)	49.8	30.7	59.5	54.5
Male sex	11 (42.3)	4 (44.4)	5 (38.5)	2 (50)
Comorbidities[a]	13 (50.0)	3 (33.3)	9 (69.2)	1 (25.0)
Diabetes mellitus	4 (15.4)	0 (0)	4 (30.8)	0 (0)
CV risk factor	8 (30.8)	1 (11.1)	6 (46.2)	1 (25.0)
Malignancy	3 (11.5)	0 (0)	3 (23.0)[b]	0 (0)
Day from illness onset to dyspnea (±SD)	5.5 ± 3.1	3.9 ± 2.8	6.2 ± 2.6	7.0 ± 4.5
Systolic blood pressure on admission, mmHg (±SD)	131.1 ± 16.6	123.6 ± 15.9	134.1 ± 15.1	138.3 ± 20.8
Respiratory rate > 24 breaths/min on admission	7 (26.9)	0 (0)	5 (38.5)	2 (50)
Disease severity on admission (1–7 points) (±SD)	4.7 ± 1.5	2.9 ± 0.6	5.8 ± 0.4	5.3 ± 1.5
Highest disease severity (1–7 points) (±SD)	4.8 ± 1.5	2.9 ± 0.6	5.8 ± 0.4	5.8 ± 0.5
Oxygen therapy on admission	12 (46.2)	0 (0)	9 (69.2)	3 (75.0)
Mechanic ventilation	5 (19.2)	0 (0)	4 (30.8)	1 (25.0)
Death	1 (3.8)[c]	0 (0)	1 (7.7)	0 (0)

[a]No patient with comorbidity of chronic obstructive pulmonary disease (COPD), chronic kidney disease (CKD), chronic liver disease (CLD), and current smoking.
[b]Endometrial carcinoma, breast cancer, and prostatic cancer for each one patient.
[c]The patient died after refusing treatment and issuing a "do not resuscitate" order.

TABLE 2 Clinico-demographic data, treatment modalities, and outcomes of four patients with severe/critical COVID-19 infection who received PG2 treatment.

Characteristic	Case I	Case II	Case III	Case IV
Age (years)	46	50	47	75
Sex	F	M	M	F
Comorbidities	None	Hypertension, hyperlipidemia, stroke	None	None
Days from onset of illness to dyspnea	4	7	4	8
Systolic pressure on admission (mmHg)	122	126	137	168
Respiratory rate > 24 breaths/min	No	Yes	No	Yes
SpO_2 (%), room air	88	90	96	82
Disease severity on admission (1–7 points)	6	6	3	6
Highest disease severity during hospitalization (1–7 points)	6	6	5	6
Antibiotic treatment	Yes	Yes	Yes	Yes
Corticosteroid treatment	Yes	Yes	Yes	Yes
Remdesivir treatment	Yes	Yes	Yes	Yes
Tocilizumab treatment	Yes	Yes	No	Yes
Oxygen therapy on admission	HFNC (15 L/min)	HFNC (15 L/min)	O_2 nasal cannula (3 L/min)	No
Mechanic ventilation	No	No	No	Yes
Lymphopenia prior to PG2 treatment *	Gr. 2	Gr. 3	Gr. 2	Gr. 3
Outcome	Recovered	Recovered	Recovered	Recovered

*Grading according to CTCAE v5.0 with the adverse event term "lymphocyte count decreased."

stabilized and his polymerase chain reaction (PCR) test showed a negative result. On admission, his NLR and ALC were 10.5 and 381 cells/μL, respectively. On day 9 after administration of PG2, his NLR decreased to 5.26 and his ALC increased to 1,608 cells/μL. On day 13, PCR showed negative result of viral RNA. A total of 6 vials of PG2 was given in 10 days and the patient was discharged after 18 days of hospitalization. He had follow-up chest computed tomography (CT) scans 1 and 3 months after discharge. The CT revealed lung consolidation and gradual resolution of the fibrosis, without any residual lesion (**Figure 1**).

Case III

A 47-year-old man, without comorbidities, was transferred from a government quarantine facility to our hospital. Initially, his O_2 saturation remained above 94%, after insertion of a O_2 nasal cannula. However, his NLR increased to 5.8 and his ALC decreased to 611 cells/μL. His CRP level increased from 2.951 to 6.421 mg/dL 10 days post admission, despite the administration of standard therapy (remdesivir, corticosteroids, and antibiotics). PG2 treatment (500 mg QOD) was initiated on day 10 of hospitalization. His NLR decreased to 4.1 and his ALC increased to 1,118 cells/μL 3 days after starting PG2 treatment. His laboratory test results showed a decrease in LDH and CRP levels. On day 11, his Ct value was 35 for SARS-CoV-2 PCR. The patient was discharged from the hospital on day 17.

Case IV

A 75-year-old woman, without comorbidities, was transferred to our hospital 8 days after the onset of COVID-19 symptoms, which included intermittent fever. Her oxygen saturation decreased progressively while receiving oxygen *via* a non-rebreathing mask and she showed clinical signs of respiratory distress, so she was intubated and admitted to the ICU. A standard course of remdesivir (200 mg on day 1, followed by 100 mg from day 2 to day 5), and one dose of tocilizumab 8 mg/kg were administered. Within the first 4 weeks of hospitalization, she contracted multiple nosocomial and secondary infections, including fungal infection, herpes zoster, and a urinary tract infection. Furthermore, she developed acute kidney failure and hemodialysis was initiated. Repeated attempts were made to wean her from the ventilator and regular hemodialysis was continued. On day 30 of hospitalization, laboratory tests showed a high NLR (40.65) and an ALC of 303 cells/μL; CXR revealed increasing infiltrations bilaterally in addition to a left-sided pleural effusion. She was administered a PG2 infusion 500 mg QOD for five doses until her clinical condition stabilized. Her CXR improved after the PG2

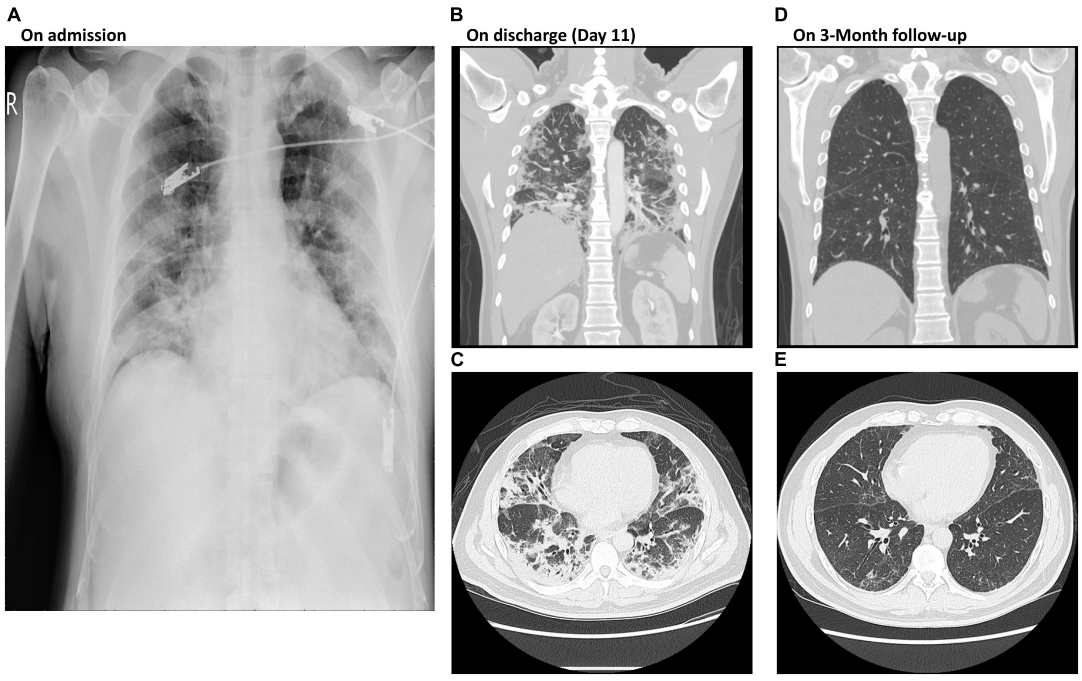

FIGURE 1
Chest X-rays of Case II on admission and at 3-month follow-up post discharge. **(A)** Diffuse bilateral lung infiltration shown by chest X-ray on admission. **(B,C)** Patchy shadows of high density in lobule were detected by CT images on discharge at day 11. **(D,E)** Clear CT images show both lobules without patchy shadows at 3-month follow up post discharge. CT, computer tomography; PCR, polymerase chain reaction.

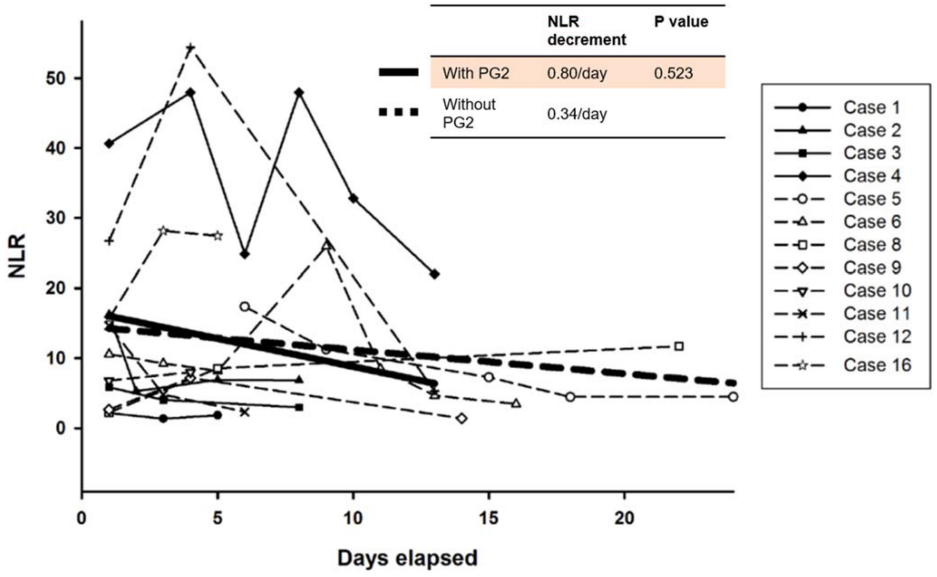

FIGURE 2
Time course changes of neutrophil-to-lymphocyte (NLR) ratio in patients with severe COVID-19. The bold straight line indicates estimates of the NLR decrease per day by linear mixed model in patients treated with PG2, whereas the dotted straight line indicates integrated trend in the NLR in patients who were not treated with PG2.

treatment. Prior to initiation of PG2 therapy, her NLR was 11.8 on admission and increased progressively, reaching 50 on day 24. Her NLR did not improve after administration of antibiotics and steroid treatment. After completion of the PG2 therapy, laboratory tests showed improvement in the NLR (21.98) and ALC (576 cells/μL). Her SARS-CoV-2 PCR result showed Ct: 28 on day 15 and Ct: 38 on day 38. She was hospitalized for a further 2.5 months due to continuous lung infiltration. She experienced recurrent infections but her clinical condition gradually improved and she was weaned from the ventilator and hemodialysis was discontinued prior to discharge. She was discharged from the hospital after 132 days of admission, and was provided with home care with low flow supplemental oxygen *via* a nasal cannula.

Discussion

The 25 patients admitted to with COVID-19 received standard care guided by the protocol adopted from guidelines of Taiwan CDC including the use of supplemental oxygen, prone positioning, and systemic sequential treatment with corticosteroids, remdesivir, and tocilizumab, as well as anticoagulation agents as needed (13). However, there is no specific clinical guideline for patients with persistent respiratory distress, lymphopenia, and a high NLR. Among the 25 patients, 16 were considered to have severe disease based on an SpO_2 of <93% breathing room air and requiring high flow supplemental oxygen or ventilator support. Twelve of the 16 patients with severe disease had an ALC < 1,000 cells/μL during their hospitalization. Four patients received PG2 in addition to standard care, and 8 patients who received only standard care served as control group for comparison. Four patients did not experience a decrease in their ALC to <1,000 cells/μL. The NLR of these patients remained relatively low and their clinical condition did not deteriorate during their hospitalization. Patients who received PG2 showed faster decrease in the NLR than those who did not receive PG2. A linear mixed model was used to compare the tendency of time course change in the NLR among patients with an ALC < 1,000 cells/μL. Patients who received PG2 had an average NLR decrease of 0.80 per day, compared to those who did not receive PG2 had an average NLR decrease of 0.34 per day overtime (**Figure 2**). Although the comparison was not statistically significant (P = 0.523), the tendency for ALC to increase and NLR to decrease after administration of PG2 warrants further investigation and clinical development on its immune modulatory effects.

There is a need for novel therapies for treating patients with COVID-19 and lymphopenia as currently there is no treatment available for treating lymphopenia and T-cell depletion in routine clinical practice (7, 14). A similar situation also arises in patients with other infectious diseases and during cancer therapy (15). A previous study revealed a similar pattern, and showed that patients with severe COVID had significantly higher neutrophil counts, lower lymphocyte counts, higher NLRs, and lower percentages of monocytes, eosinophils and basophils (16). In addition to a significant reduction in both CD4 + and CD8 + lymphocyte subsets has been observed in patients with severe COVID-19, including lower CD8 + lymphocyte count, and an increase

in the CD8 + lymphocyte count was associated with clinical improvement (17). In a previous study, we demonstrated the immunomodulatory effect of PG2 for treating lung cancer patients with moderate to severe fatigue while receiving immune checkpoint inhibitors (18). Compared with patients without PG2, those who received PG2 were more likely to experience a lowering of their NLR to $\leq$ 3.5, which was probably attributable to the rapid increase in lymphocytes during their treatment. Furthermore, a previous study showed that *Astragalus* polysaccharides suppress pro-inflammatory cytokines, including interleukin 6 and tumor necrosis factor alpha (19), which have both been found to play a role in the cytokine storm of acute respiratory distress syndrome, a major cause of COVID-19-associated death. Further studies reveal that PG2 promoted the polarization of THP-1-derived macrophages into an anti-inflammatory phenotype, and inhibited LPS-induced cytokine release. This suggests that PG2 could potentially prevent viral infection of host cells and prevent the development of severe COVID-19 *via* regulation of macrophage activity, similar to previously reported effects with *Astragalus* polysaccharides (19). We believe that PG2 may also restore functionality to exhausted lymphocytes and restore immune homeostasis after severe COVID-19. However, randomized controlled trials are required to confirm the beneficial effects of PG2.

There are several limitations to the present study. Only four patients were treated with PG2 due to the limited number of patients with severe COVID-19 admitted to our hospital. The results were obtained retrospectively. The possibility of selection bias cannot be ruled out.

In conclusion, PG2 demonstrated potential benefit in promoting recovery of lymphocytes in patients with severe COVID-19 and COVID-19-associated lymphopenia. No drug related adverse reactions were observed. Randomized controlled trials are needed to investigate the role of PG2 in controlling lymphopenia in patients with COVID-19.

Data availability statement

The original contributions presented in this study are included in the article/**Supplementary material**, further inquiries can be directed to the corresponding author.

Author contributions

S-MT led the care of COVID-19 patients and obtained emergency authorization from the institutional review board for use of novel therapeutic agents. W-YW, Y-TL, and Y-TW took care of the patients. J-ZC and S-YL collected data. All authors reviewed, edited, and approved the final manuscript.

Acknowledgments

The authors thank PhytoHealth Corporation (Taipei, Taiwan) for their kind provision of the marketed products, PG2® injection, free of charge for the treated patients.

Conflict of interest

The authors declare that the research was conducted in the absence of any commercial or financial relationships that could be construed as a potential conflict of interest.

Publisher's note

Supplementary material

The Supplementary Material for this article can be found online at: https://www.frontiersin.org/articles/10.3389/fmed.2022.1009557/full#supplementary-material

References

1. Guan WJ, Ni ZY, Hu Y, Liang WH, Ou CQ, He JX, et al. Clinical characteristics of coronavirus disease 2019 in China. *N Engl J Med.* (2020) 382:1708–20. doi: 10.1056/NEJMoa2002032

2. Chen N, Zhou M, Dong X, Qu J, Gong F, Han Y, et al. Epidemiological and clinical characteristics of 99 cases of 2019 novel coronavirus pneumonia in Wuhan, China: a descriptive study. *Lancet.* (2020) 395:507–13. doi: 10.1016/S0140-6736(20)30211-7

3. Fan BE, Chong VCL, Chan SSW, Lim GH, Lim KGE, Tan GB, et al. Hematologic parameters in patients with COVID-19 infection. *Am J Hematol.* (2020) 95:E131–4. doi: 10.1002/ajh.25774

4. Tan L, Wang Q, Zhang D, Ding J, Huang Q, Tang YQ, et al. Lymphopenia predicts disease severity of COVID-19: a descriptive and predictive study. *Sig Transduct Target Ther.* (2020) 5:33. doi: 10.1038/s41392-020-0159-1

5. Bhatraju PK, Ghassemieh BJ, Nichols M, Kim R, Jerome KR, Nalla AK, et al. Covid-19 in critically ill patients in the Seattle region – Case series. *N Engl J Med.* (2020) 382:2012–22. doi: 10.1056/NEJMoa2004500

6. Huang C, Wang Y, Li X, Ren L, Zhao J, Hu Y, et al. Clinical features of patients infected with 2019 novel coronavirus in Wuhan, China. *Lancet.* (2020) 395:497–506. doi: 10.1016/S0140-6736(20)30183-5

7. Fathi N, Rezaei N. Lymphopenia in COVID-19: therapeutic opportunities. *Cell Biol Int.* (2020) 44:1792–7. doi: 10.1002/cbin.11403

8. Zheng Y, Ren W, Zhang L, Zhang Y, Liu D, Liu Y. A review of the pharmacological action of astragalus polysaccharide. *Front Pharmacol.* (2020) 11:349. doi: 10.3389/fphar.2020.00349

9. Liu QY, Yao YM, Zhang SW, Sheng ZY. Astragalus polysaccharides regulate T cell-mediated immunity via CD11c(high)CD45RB(low) DCs in vitro. *J Ethnopharmacol.* (2011) 136:457–64. doi: 10.1016/j.jep.2010.06.041

10. Huang WC, Kuo KT, Bamodu OA, Lin YK, Wang CH, Lee KY, et al. Astragalus polysaccharide (PG2) ameliorates cancer symptom clusters, as well as improves quality of life in patients with metastatic disease, through modulation of the inflammatory cascade. *Cancers.* (2019) 11:1054. doi: 10.3390/cancers11081054

11. US National Institutes of Health. *Clinical Spectrum of SARS-CoV-2 Infection (COVID-19 Treatment Guidelines).* (2021). Available online at: https://www.covid19treatmentguidelines.nih.gov/overview/clinical-spectrum/ (accessed March 31, 2022).

12. Ader F, Bouscambert-Duchamp M, Hites M, Peiffer-Smadja N, Poissy J, Belhadi D, et al. Remdesivir plus standard of care versus standard of care alone for the treatment of patients admitted to hospital with COVID-19 (DisCoVeRy): a phase 3, randomised, controlled, open-label trial. *Lancet Infect Dis.* (2022) 22:209–21. doi: 10.1016/S1473-3099(21)00485-0

13. Taiwan Center for Disease Control. *Interim Guidelines for Clinical Management of SARS-CoV-2 Infection (5th Edition).* (2020). Available online at: https://www.cdc.gov.tw/Uploads/e05d4feb-faf5-4636-86b8-3cf21598b4ce.pdf (accessed March 30, 2022).

14. Song JW, Zhang C, Fan X, Meng FP, Xu Z, Xia P, et al. Immunological and inflammatory profiles in mild and severe cases of COVID-19. *Nat Commun.* (2020) 11:3410. doi: 10.1038/s41467-020-17240-2

15. Wherry EJ. T cell exhaustion. *Nat Immunol.* (2011) 12:492–9. doi: 10.1038/ni.2035

16. Qin C, Zhou L, Hu Z, Zhang S, Yang S, Tao Y, et al. Dysregulation of immune response in patients with coronavirus 2019 (COVID-19) in Wuhan, China. *Clin Infect Dis.* (2020) 71:762–8. doi: 10.1093/cid/ciaa248

17. Wang F, Nie J, Wang H, Zhao Q, Xiong Y, Deng L, et al. Characteristics of peripheral lymphocyte subset alteration in COVID-19 pneumonia. *J Infect Dis.* (2020) 221:1762–9. doi: 10.1093/infdis/jiaa150

18. Tsao SM, Wu TC, Chen J, Chang F, Tsao T. Astragalus polysaccharide injection (PG2) normalizes the neutrophil-to-lymphocyte ratio in patients with advanced lung cancer receiving immunotherapy. *Integr Cancer Ther.* (2021) 20:153473542199525. doi: 10.1177/1534735421995256

19. Yeh YC, Doan LH, Huang ZY, Chu LW, Shi TH, Lee YR, et al. Honeysuckle (*Lonicera japonica*) and Huangqi (*Astragalus membranaceus*) suppress SARS-CoV-2 entry and COVID-19 related cytokine storm in vitro. *Front Pharmacol.* (2022) 12:765553. doi: 10.3389/fphar.2021.765553

frontiers | Frontiers in Public Health

TYPE Original Research
PUBLISHED 15 November 2022
DOI 10.3389/fpubh.2022.1048108

OPEN ACCESS

EDITED BY
Francesco Paolo Bianchi,
University of Bari Aldo Moro, Italy

REVIEWED BY
Lubna Pinky,
Eastern Virginia Medical School, United States
Pengyue Zhao,
The First Center of Chinese PLA General Hospital, China

*CORRESPONDENCE
Jian Cai
jcai@cdc.zj.cn
Yin Chen
yinch@cdc.zj.cn
Enfu Chen
enfchen@cdc.zj.cn

†These authors have contributed equally to this work

SPECIALTY SECTION
This article was submitted to Infectious Diseases - Surveillance, Prevention and Treatment, a section of the journal Frontiers in Public Health

RECEIVED 19 September 2022
ACCEPTED 25 October 2022
PUBLISHED 15 November 2022

CITATION
Liu S, Zhu A, Pan J, Ying L, Sun W, Wu H, Zhu H, Lou H, Wang L, Qin S, Yu Z, Cai J, Chen Y and Chen E (2022) The clinical and virological features of two children's coinfections with human adenovirus type 7 and human coronavirus-229E virus. *Front. Public Health* 10:1048108. doi: 10.3389/fpubh.2022.1048108

The clinical and virological features of two children's coinfections with human adenovirus type 7 and human coronavirus-229E virus

Shelan Liu[1†], An Zhu[2†], Jinren Pan[1†], Lihong Ying[3], Wanwan Sun[1], Hanting Wu[4], Haiying Zhu[2], Haiyan Lou[5], Lan Wang[6], Shuwen Qin[1], Zhao Yu[1], Jian Cai[1]*, Yin Chen[7]* and Enfu Chen[1]*

[1]Department of Infectious Diseases, Zhejiang Provincial Center for Disease Control and Prevention, Hangzhou, China, [2]Department of Pediatrics, Second People's Hospital of Jinyun County, Lishui, China, [3]Department of Infectious Diseases, Jinyun District Center for Disease Control and Prevention, Lishui, China, [4]School of Public Health, Zhejiang Chinese Medical University, Hangzhou, China, [5]Department of Radiology, First Affiliated Hospital, Zhejiang University School of Medicine, Hangzhou, China, [6]Department of Geriatrics, First Affiliated Hospital, Zhejiang University School of Medicine, Hangzhou, China, [7]Department of Microbiology, Zhejiang Provincial Center for Disease Control and Prevention, Hangzhou, China

Objective: Human adenovirus (HAdV) coinfection with other respiratory viruses is common, but adenovirus infection combined with human coronavirus-229E (HCoV-229E) is very rare.

Study design and setting: Clinical manifestations, laboratory examinations, and disease severity were compared between three groups: one coinfected with HAdV-Ad7 and HCoV-229E, one infected only with adenovirus (mono-adenovirus), and one infected only with HCoV-229E (mono-HCoV-229E).

Results: From July to August 2019, there were 24 hospitalized children: two were coinfected with HAdV-Ad7 and HCoV-229E, and 21 were infected with a single adenovirus infection. Finally, one 14-year-old boy presented with a high fever, but tested negative for HAdV-Ad7 and HCoV-229E. Additionally, three adult asymptotic cases with HCoV-229E were screened. No significant difference in age was found in the coinfection and mono-adenovirus groups (11 vs. 8 years, $p = 0.332$). Both groups had the same incubation period (2.5 vs. 3 days, $p = 0.8302$), fever duration (2.5 vs. 2.9 days, $p = 0.5062$), and length of hospital stay (7 vs. 6.76 days, $p = 0.640$). No obvious differences were found in viral loads between the coinfection and mono-adenovirus groups (25.4 vs. 23.7, $p = 0.570$), or in the coinfection and mono-HCoV-229E groups (32.9 vs. 30.06, $p = 0.067$). All cases recovered and were discharged from the hospital.

Conclusion: HAdV-Ad7 and HCoV-229E coinfection in healthy children may not increase the clinical severity or prolong the clinical course. The specific interaction mechanism between the viruses requires further study.

KEYWORDS

HAdV-Ad7, respiratory tract infections, coinfections, case-control study, children, human coronavirus-229E(HCoV-229E)

What is new?

This preliminary study is the first to investigate the differences between groups coinfected with HAdV-Ad7 and HCoV-229E versus a single adenovirus infection. This research for the extremely small sample size found that coinfection with HAdV-Ad7 and HCoV-229E in healthy children may not increase the clinical severity or prolong the clinical course.

Introduction

Human adenoviruses (HAdVs) are non-enveloped, double-stranded DNA viruses in the *adenoviridae* family (1). Since the first isolation of the adenovirus in 1953, seven species (A–G) have been recognized, including 113 known genotypes or serotypes of HAdV (2–6). More than 60 genotypes are known to cause human infection (7). Adenoviruses can cause illness in people of all ages at any time of the year (8). Most children have had at least one adenovirus infection by age 10 (9). Globally, 5–7% of respiratory tract infections in pediatric patients are ascribed to HAdV (10, 11).

Human coronaviruses (HCoVs) are enveloped, single-stranded RNA viruses (12, 13).

HCoV-229E is one of seven HCoVs: HCoV-229E, HCoV-NL63, HCoV-OC43, HCoV-HKU1, severe acute respiratory syndrome coronavirus (SARS-CoV), Middle East respiratory syndrome coronavirus (MERS-CoV), and severe acute respiratory syndrome coronavirus 2 (SARS-CoV-2) (14–16). HCoV-229E usually causes mild to moderate upper-respiratory tract illness, similar to the common cold (17). People generally become infected with HCoV-229E in the fall and winter, but infection can occur at any time of the year (17).

Human adenovirus (HAdV) is commonly associated with acute respiratory illnesses (ARI) in children and is also frequently co-detected with other viral pathogens (18). HAdV co-detection with other respiratory viruses was associated with greater disease severity among children with ARI compared to HAdV detection alone (18). However, coinfection with HCoV is very rare and unusual. For example, national data from China indicate a rate of 7.2% for coinfection in hospitalized acute lower respiratory infections (ALRIs), with the most common pairs being adenovirus + respiratory syncytial virus (9.71%), followed by human parainfluenza viruses + adenovirus (3.86%); and influenza + adenovirus (3.45%) (19). Pathogen coinfection occurred only two times between adenovirus and hCoV (0.94%) (19). Additional research from Beijing indicated that, among 90 HAdV-positive children, 61.11% (55/90) were coinfected with other respiratory viruses, the most common of which were human respiratory syncytial virus (34.5%) and human rhinovirus (10.9%). The fewest cases of coinfection occurred with adenovirus and HCoV (only 1.8%) (20). To date, there are no documented adenovirus coinfections with HCoV-229E, so the clinical outcome of this pair of coinfections remains unknown.

An adenovirus outbreak was recognized in 2019 in Lihui city, Zhejiang Province, China. This outbreak involved 97 cases, including 24 admitted cases in the pediatric ward, with two confirmed coinfections of adenovirus and HCoV-229E. In order to compare clinical presentation and outcomes, and virological features in young children with HAdV detected alone vs co-detected with HCoV-229E, we explored a rare phenomenon in this study.

Materials and methods

Study design and participants

China's national surveillance system for influenza-like illness (ILI), severe acute respiratory illness, and pneumonia of unexplained origin indicated an outbreak of 97 adenovirus infections during July and August of 2019. Twenty-four children were hospitalized in the pediatric ward of the Second Hospital of JinYun. Two cases were confirmed to be HCoV-229E and adenovirus coinfections, and these children were admitted to different rooms (Rooms 830, 845) in the same pediatric ward. Twenty-one cases were identified as mono-adenovirus. One case involved a 14-year boy with a high fever who tested negative for Ad7 and HCoV-229E; this case was not included in our research.

Through extensive symptom surveillance, we found an additional three people (the parents of one of the coinfections and one doctor) who were confirmed as HCoV-229E positive. HAdV patients coinfected with HCoV-229E were categorized into the research group. For each patient in the research group, we matched three cases with a single HCoV-229E infection and 21 with a single adenovirus infection as controls.

The diagnosis of adenovirus and HCoV-229E followed the Protocol for Adenovirus Pneumonia Diagnosis and Treatment issued by the National Health Commission of the People's Republic of China in 2018.

Clinical information collection

The patients' clinical manifestations, laboratory examinations, imaging characteristics, disease severity, and clinical progress were collected from electronic medical records in the Second Hospital of JinYun's hospital information system (HIS). Radiologic abnormalities were determined according to descriptions in the clinical charts. All variables were compared between the three groups, including coinfections with adenovirus, mono-adenovirus, and HCoV-229E respectively.

Three methods were used to evaluate the severity and clinical progress of the disease. First, according to the national guidelines for pediatric CAP (community-acquired pneumonia)

in China, we divided cases of pneumonia into mild and severe (10). Second, the extrapulmonary manifestations involved in our study included kidney manifestations, myocardial damage, liver damage, and coagulation function. Third, we observed the number of days with fever, the highest degree of fever, and the median days from illness onset to discharge.

Laboratory testing

We collected specimens from the upper respiratory tract using pharyngeal swabs. All of the patients were laboratory confirmed using real-time reverse transcriptase polymerase chain reaction (RT-PCR) or PCR assays. Laboratory confirmation was also performed on other common respiratory pathogens, including influenza-A virus (H1N1, H3N2), influenza B virus, respiratory syncytial virus (RSV), parainfluenza virus, adenovirus, SARS-associated coronavirus (SARS-CoV), and human coronavirus HCoV-229E. Any coinfections were included from this study. Genetic sequences of viruses were obtained directly from positive clinical specimens or from virus isolates using an MiSeq desktop sequencer (Illumina, Inc., San Diego, CA, USA), as described (21).

Statistical analysis

Quantitative measurements were presented as medians; qualitative measurements were presented as counts and percentages. Abnormally high or low levels of laboratory findings were defined using age-specific or otherwise universal reference ranges. The differences between groups were analyzed using the Wilcoxon signed-ranks test (for continuous data) or McNemar's chi-square test (for binary data), with a p-value of less than 0.05 considered statistically significant. All analyses were conducted with R (version 3.4.6; The R Foundation for Statistical Computing, Vienna, Austria).

Results

Demographic characteristics and exposure history

We collected a total of two cases of coinfection with adenovirus and HCoV-229E, three cases with single HCoV-229E infection, and 21 cases with single adenovirus infection. None of the patients had underlying diseases. Patients' median ages were 11, 38, and eight years in the coinfection group with adenovirus and HCoV-229E, the mono-infection group with HCoV-229E, and the mono-infection group with adenovirus, respectively ($p = 0.332$) (Table 1). The male to female ratio was 0:2 in the coinfection group, 1:2 in the mono-infection with HCoV-229E group, and 2.5:1 in the mono-infection with adenovirus group ($p = 0.111$) (Table 1). All of the children with coinfections and adenovirus mono-infection had been to a swimming pool and had been exposed to someone with a fever. However, the three individuals with mono-infections of HCoV-229E had provided bedside and medical care for the two children with coinfections, as shown in Table 1.

Comparison of clinical characteristics

Coinfection-case 1

The first coinfection patient was a 13-year-old girl (a student from Jinyun) who had no underlying diseases. She had taken swimming classes at a swimming center on July 25, 2019, where an adenovirus outbreak was identified, as seen in Figure 1. She was admitted to room 830 of the pediatric ward on July 30 (see Figure 2), presenting with a dry cough, a continual fever for two days with an initial temperature of 38.6°C and a high temperature of 40.2°C. She had no gastrointestinal symptoms. On physical examination, she had a body mass index of 23.5 kg/m^2, and her vital signs were as follows: a heart rate of 120 beats per minute, 28 breaths per minute, an oxygen saturation of 95% at ambiance, and pharyngeal congestion oozing. Further examination revealed a decreased neutrophil absolute count and percentage, but normal liver, heart, and kidney functions and C-reactive protein (CRP) levels, as seen in Table 2. Chest radiography, performed on August 2 following disease onset, indicated slight thickening of the wall of the anterior and posterior segments of the right upper lobe, with the lumen slightly narrowed and the lower right lung slightly inflamed (Figure 3). Symptomatic treatment was started on the day of illness onset, without any oxygen or glucocorticoid therapy. The fever and cough resolved by August 1 and August 4, respectively (Figure 1). A throat swab sample collected on August 2 was positive for adenovirus (ct value: 28.8) and HCoV-229E (ct value: 32.5), as seen in Table 1. On August 5, the patient was discharged and recovered completely (Table 1). The period from illness onset to discharge was eight days (see Table 1 and Figure 1).

Coinfection-case 2

The second co-case patient was a healthy nine-year-old girl who had visited the same swimming center as the first patient on July 28, 2019. She was admitted to room 845 of the pediatric ward on August 1 because of a history of high fever, 38.6°C for one day (Figures 1, 2). The fever continued for four days, reaching a high of 39.5°C. Upon physical examination, the patient had pharyngeal congestion oozing. The lab test indicated that the patient had a normal

TABLE 1 Comparison of the characteristics of two children coinfected with HCoV-229E and adenovirus admitted to different rooms of the same pediatric ward and mono-infections with HCoV-229E and Adenovirus in Lishui, Zhejiang Province, July–August 2019.

Characteristic	Coinfection withHCoV-229E and adenovirus ($n = 2$)		Mono-infection with HCoV-229E ($n = 3$)			Mono-infection with adenovirus ($n = 21$)	*p*-value
	Co-case 1	Co-case 2	Case 1	Case 2	Case 3		
Demographics							
Age (in years)	13	9	54	59	43	8 (2–14)	0.332
Gender	Female	Female	Female	Male	Female	Male/female = 2.5:1.0	0.111
Occupation	Student	Student	Farmer	Farmer	Doctor	Preschool children or students	/
Basic situation							
History of alcohol use	No	No	No	No	No	No	/
History of smoking	No	No	No	Yes	No	No	/
Underlying conditions	No	No	No	No	No	No	/
Exposure history							
Visit to the swimming center	Yes	Yes	No	No	No	100%	/
Exposure to a febrile person	Yes	Yes	Yes	Yes	Yes	100%	/
Provided bedside care	No	No	Yes	Yes	No	No	/
Medical care services	No	No	No	No	Yes	No	/
Laboratory results							
Specimen collection date	August 2	August 2	August 2	August 2	August 2	August 2	/
Specimen collection type	Throat swab	Throat swab	Throat swab	Throat swab	Throat swab	Throat swab	/
Diagnostic method	rRT-PCR and sequencing	rRT-PCR and sequencing	rRT-PCR and sequencing	rRT-PCR and sequencing	rRT-PCR and sequencing	rRT-PCR and sequencing	/
Date of confirmation	August 5	August 5	August 7	August 7	August 7	August 5	/
viral load (ct value)	Adenovirus (28.8)	Adenovirus (22)	Adenovirus (Negative)	Adenovirus (Negative)	Adenovirus (Negative)	Adenovirus (Average: 23.78)	0.570
	HCoV-229E (32.5)	HCoV-229E (33.3)	HCoV-229E (28.4)	HCoV-229E (30.5)	HCoV-229E (31.3)	HCoV-229E (Negative)	0.067
Clinical features							
Max temperature (°C)	40.2	39.8	/	/	/	39.3	0.1431
Fever duration (days)	3	2	/	/	/	2.90	0.5062
Exposure to onset (days)	2	3	No symptoms	No symptoms	No symptoms	3 (0–7)	0.8302
Onset to admission (days)	2	1	/	/	/	2.9 (0–6)	0.332
Hospital stays (days)	6	8	/	/	/	6.76 (3–13)	0.640
Days from onset to be discharged (days)	8	9	/	/	/	9.67 (3–17)	0.285

CT, cycle threshold. In this table, all of the statistical analyses were performed using the statistical package for the social sciences (SPSS; version 26.0). Categorical variables were compared using Fisher's exact test. The Mann–Whitney test was used to compare continuous variables. All statistical tests were two-sided, and a *p*-value of 0.05 was considered statistically significant. The symbol / indicates that data are not available.
P-value notes the comparison of the coinfection group and the mono-adenovirus group.

10.3389/fpubh.2022.1048108

FIGURE 1
Symptoms and results of rtPCR testing and antigen rapid test for the two children coinfected with HCoV-229E and adenovirus; they were admitted to different rooms in the same pediatric ward in Lishui, Zhejiang Province, July–August 2019. rtPCR = real-time PCR. ADV = adenovirus. The red cross indicates that the pathogens (adenovirus or 229E) were detected by PCR or rapid antigen detection. The gray – indicates an HCoV-229E negative test.

blood count, liver function, and kidney function, but slightly increased lactate dehydrogenase (Table 2). A throat swab sample collected on August 2 was positive for adenovirus (ct value: 22) and HCoV-229E (ct value: 33.3), as shown in Table 1. Symptomatic treatment and support therapy was started, without any glucocorticoid therapy. The patient was discharged eight days after admission (see Table 1 and Figure 1).

Mono-infection with HCoV-229E

The parents of coinfection-case 1 (mother: 54 years old, father: 59 years old, both farmers) undertook bedside care and remained asymptomatic (Table 1). A 43-year-old female doctor without any symptoms was in charge of the two co-cases. Three throat samples collected on August 6 showed that the parents (ct values: 30.5, 28.4, respectively) and doctor had HCoV-229E (ct value: 31.3) (Table 1).

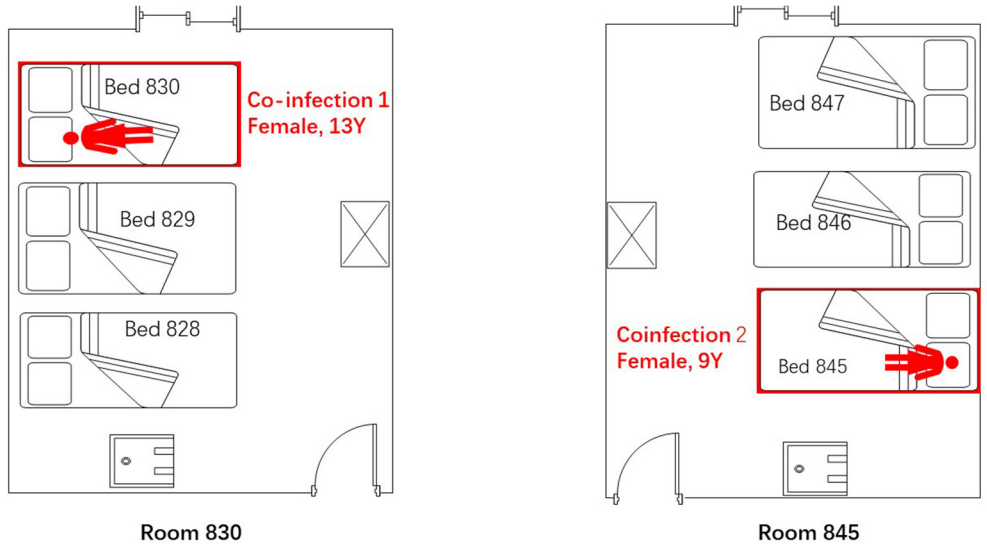

FIGURE 2
Spatial distribution of the two admitted children who were coinfected with adenovirus and HCoV-229E in the pediatric ward of Lishui, Zhejiang Province, July–August 2019.

TABLE 2 Hematological and blood biochemical measurements of two children coinfected with HCoV-229E and adenovirus admitted to different rooms of the same pediatric ward and mono-infections with adenovirus in Lishui, Zhejiang Province, July–August 2019.

Variables	Coinfection-case 1	Coinfection-case 2	Mono-infections with adenovirus ($n = 21$)	Normal range	*p*-value
Blood routine					
WBC ($\times 10^9$ per L)	2.1	4.7	5.66	4.0–10.0	0.347
Lymphocyte absolute count ($\times 10^9$ per L)	1.22	1.02	2.61	0.8–4	0.06
Neutrophil absolute count ($\times 10^9$ per L)	0.63	3.17	2.11	2–7.7	0.764
Lymphocyte percentage (%)	59.54	21.90	50.57	20–40	0.648
Neutrophil percentage (%)	30.74	68.00	42.10	50–70	0.876
Platelet count ($\times 10^9$ per L)	210	201	234.91	100–300	0.465
Hemoglobin (g/L)	115	127	119.32	110–150	0.917
Blood biochemistry					
Albumin (g/L)	39.7	36.5	39.48	35.0–55.0	0.958
ALT (U/L)	7	13	15.64	0–40	0.295
AST (U/L)	24	28	26.77	0–40	0.793
Urea (mmol/l)	3.60	3.14	3.84	2.50–7.20	0.497
Creatinine(μmol/L)	50	38	42.41	44–132	0.754
C reactive protein (mg/dl)	3.0	0.5	5.61	0–10	0.825
Lactate dehydrogenase (UI/liter)	186	229	240.82	65–220	0.230

AST, alanine aminotransferase; *ALT*, aspartate aminotransferase.

Mono-infection with adenovirus

All patients infected with a single adenovirus showed mild illness, with no serious illness found (Table 3). The most common clinical symptoms or signs were fever (100%, 22/22), fatigue (40.91%, 9/22), sore throat (40.91%, 9/22), and vomiting (36.36%, 8/22) (Supplementary Figure 1). The highest fever temperature (40 vs. 39.3°C, $p = 0.1431$) and fever duration (2.5 vs. 2.9 days, $p = 0.5062$) were the same between the coinfection

FIGURE 3
Chest X-ray and CT scan taken for a 13-year-old girl with HCoV-229E and adenovirus coinfection-induced fever on July 27, 2019. Chest CT scan and chest X-ray indicated slight thickening of the wall of the anterior and posterior segments of the right upper lobe, a slightly narrower lumen, and slight inflammation of the lower right lung. The bilateral hilum was normal, and no pleural effusion was observed. No obvious swollen lymph node shadow was found in the mediastinum. **(A)** Left, Chest X-ray taken on July 30, 2019. **(B)** Right, Chest CT scan taken on August 2, 2019.

TABLE 3 Treatment and disease severity of two children coinfected with HCoV-229E and adenovirus admitted to different rooms of the same pediatric ward and mono-infections with adenovirus in Lishui, Zhejiang Province, July–August 2019.

Variables	Co-case 1	Co-case 2	Mono-infections with adenovirus ($n = 21$)	p-value
Mild CAP	Yes	No	One case	Not available
Severe CAP	No	No	No	Not available
Extremely severe pneumonia	No	No	No	Not available
PICU admission	No	No	No	Not available
Immune global protein	No	No	No	Not available
Glucocorticoids therapy	No	No	One two-year-old child	Not available
NCPAP	No	No	No	Not available
Invasive mechanical ventilation	No	No	No	Not available
Oxygen therapy	No	No	No	Not available
Clinical outcome	Survival	Survival	Survival	Not available

CAP, community-acquired pneumonia; *NCPAP*, nasal continuous positive airway pressure; *PICU*, the pediatric intensive care unit.

and mono-infection with adenovirus groups (Table 1). We compared the clinical progress among the 21 mono-adenovirus infections with the HAdV-7 group and two coinfections with HAdV-7. Between the coinfection group and mono-HAdV-7 group, the results indicated no differences in average days from exposure to onset (2.5 vs. 3 days, $p = 0.8302$), onset to admission (1.50 vs. 2.90 days, $p = 0.332$), hospital stay (7 vs. 6.76 days, $p = 0.640$), or onset to discharge (8.50 vs. 9.67 days, $p = 0.285$) (see Table 1).

One coinfection with adenovirus mycoplasma pneumoniae

The case patient was a healthy two-year-old boy who had visited a JinYun swimming center on July 27, 2019. On July 31, he developed a constant high fever of 40.2°C and a cough, leading to admission to room 840 of the pediatric ward on August 4 (Figure 4). The lab test indicated that the patient had an elevated white blood cell count, an increased lymphocyte percentage, a decreased neutrophil percentage, and a low level of hemoglobin (113 g/L). A chest X-ray was taken on August 4, 2019, depicting exudation and small patchy shadows in the upper lobe of the right lung. In addition, the right hilum shadow was slightly enlarged (Figure 5A). A chest CT (Computed Tomography) scan on August 5 showed signs of an air bronchogram in the consolidation tissue, accompanied by segmental consolidation in the dorsal segment of the right lower lobe (see Figure 5B). On August 5, the mycoplasma DNA loads by rt-PCR were 3.60×10^4 copies/ml (normal level: <400) (Figure 4). A throat swab sample collected on August 2 was positive for adenovirus (ct value: 21.4) (Figure 4). A chest CT plain scan taken on August 11 indicated that the upper lobe of the right lung was redilated (Figure 5C). The patient was discharged on August 17 after the use of glucocorticoids (Figure 4 and Table 3). None of the above patients were treated with invasive mechanical ventilation, transferred to the

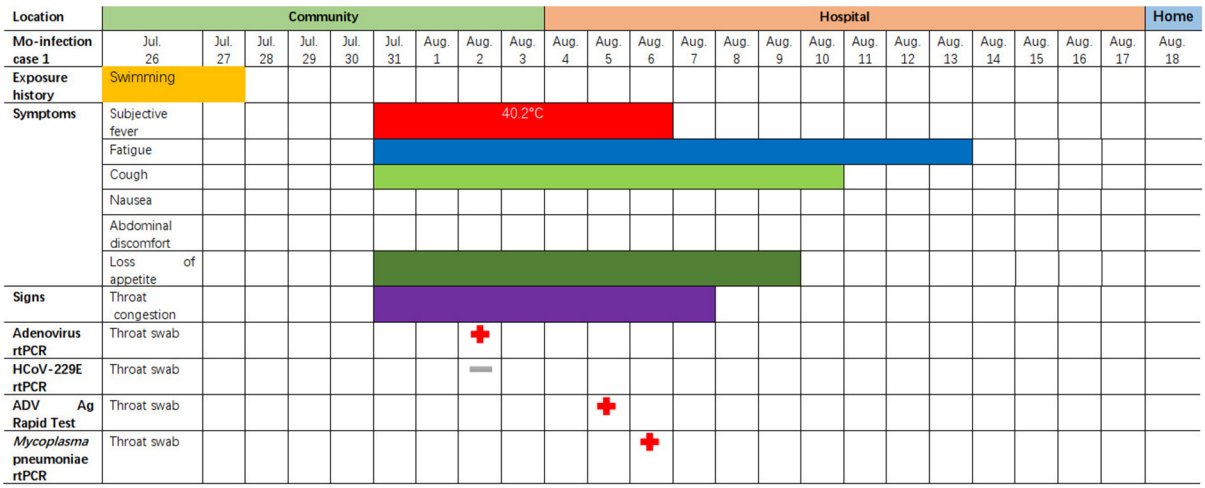

FIGURE 4
Symptoms and results of rtPCR testing and antigen rapid test for a two-year-old child coinfected with adenovirus and *single M. pneumoniae* who was admitted to the pediatric ward in Lishui, Zhejiang Province, August 4–17, 2019. rtPCR = real-time PCR. ADV = adenovirus. The red cross indicates that the pathogen (adenovirus or single *M. pneumoniae*) was detected by PCR or rapid antigen detection. The gray—indicates an HCoV-229E negative result.

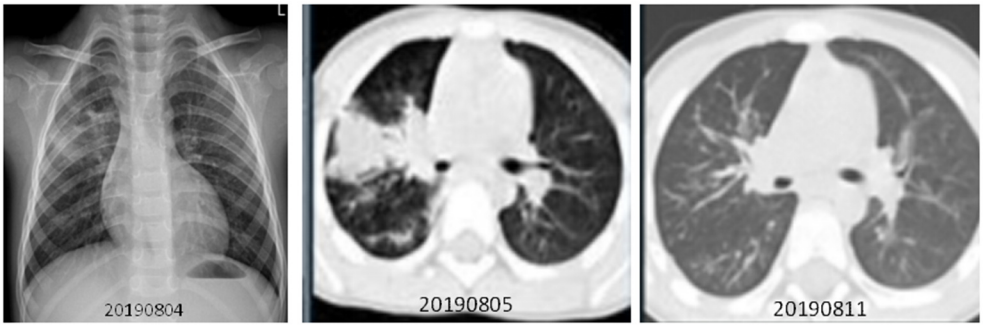

FIGURE 5
Chest X-ray and CT scan were taken for a two-year-old boy with adenovirus and *mycoplasma pneumoniae* coinfection-induced fever on July 31, 2019. (1) **(A)** Left, Chest X-ray taken on August 4, 2019. Exudation and small patchy shadows in the upper lobe of the right lung. The right hilum shadow was slightly enlarged, and the left hilum was normal. No bilateral pleural effusion was observed. (2) **(B)** Middle, Chest CT plain scan was taken on August 5, 2019. Incomplete, segmental lung consolidation and exudation lesions were observed. Signs of air bronchogram were seen in the consolidation tissue, accompanied by segmental consolidation in the dorsal segment of the right lower lobe. The right hilar shadow was enlarged, and the left hilar was normal. There was no bilateral pleural effusion and no obvious enlarged lymph nodes in the mediastinum. **(C)** Right, Chest CT plain scan taken on August 11. The upper lobe of the right lung was redilated, showing upper, middle, and lower lobe bronchial wall thickening in the right lung as well as a weak patchy shadow distributed along the airway. There was no thickening of the lobular septum or pleura, and no pleural effusion was observed. The hilar had a normal morphology, and there was no significantly enlarged lymph node shadow in the mediastinum. Compared with the CT scans from the week prior, the right lung lesion had been significantly absorbed.

PICU (Pediatric Intensive Care Unit), or given oxygen therapy (Table 3).

Comparison of viral loads and genetic identity

The average viral ct was 25.4 and 23.7 in the coinfection and single adenovirus groups ($p = 0.570$), while the average viral ct was 32.9 and 30.06 in the coinfection and single HCoV-229E groups ($p = 0.067$), respectively (Table 1). The difference in viral loads was not statistically significant between the two groups (Table 1).

Regarding the alignment of the penton, fiber, and hexon of the adenovirus isolated from the coinfection group ($n = 2$) and single adenovirus group ($n = 21$), these adenovirus sequences shared 99.5 and 100% of the nucleic acid sequence identity. The HCoV-229E S1 gene segments for the coinfection group ($n = 2$) and single HCoV-229E group ($n = 3$) were 97.5–99.9% identical.

Discussion

We report on the rare phenomenon of HAdV-Ad-7 and adenoviral HCoV-229E coinfection in children. Compared with HAdV-Ad-7 mono-infection, there was no increase in clinical severity for children coinfected with HCoV-229E. There were also no differences in terms of incubation, fever duration, high temperature, length of hospital stays, or viral load between the two groups. The three adults infected with HCoV-229E did not develop any symptoms. No patients with coinfections or mono-infections of HAdV-Ad-7 or HCoV-229E had severe complications; they fully recovered after early and adequate supportive and symptomatic treatment.

Several studies have reported on HAdV-Ad-7 coinfections with other pathogens (19). One study indicated that 4% of pediatric pneumonia admissions were associated with endemic HCoVs, with a high proportion of cases co-occurring with another respiratory virus (22, 23). However, coinfection with HCoV-229E and adenovirus has not been documented in the literature. In this study, our joint investigation team continuously sampled the outbreak cases (symptomatic and asymptomatic patients) and used a more sensitive method (Multiplex PCR method for simultaneous tests of 14 different pathogens). Finally, two co-infections were isolated from the 24 admitted cases of human adenovirus genotype 7, accounting for 8.33% (2/24) of the total number of cases. This number was far lower than adenovirus coinfected with other pathogens, such as respiratory syncytial virus (19/37, 34.5%) and influenza virus (6/37, 10.9%] (20). The exact reasons for the coinfections remain unclear, but several factors may have played a role. Most importantly, the children infected with adenovirus were weakened and susceptible to other pathogens after the persistent high fever. Secondly, there are no vaccines against adenovirus or HCoV-229E virus in China. Meanwhile, HCoV-229E has a low prevalence in this area. As a result, most of population has no immunity to these two viruses (24). Thirdly, adenoviruses are non-enveloped viruses that are unusually resistant to physical and chemical agents, which gives them prolonged survival capacity in various environments (25).The incubation period for mono- or coinfection was 2–3 days, which aligns with previous estimates of adenovirus incubation periods (26). However, mono-adenovirus infection, mono-HCoV-229E infection, and coinfection with HAdV-Ad-7 and HCoV-229E involve non-specific signs and symptoms. This lack of specific symptoms contributes to delayed diagnosis and treatment (27–29).

Furthermore, the present study showed that both groups had similar clinical signs and laboratory test results, such as white blood cell (WBC), AST and ALT, lactate dehydrogenase (LDH), and C-reaction protein (CRP) counts. Therefore, it is difficult to distinguish whether or not patients have a mono-infection with adenovirus or coinfection with two viruses based on clinical signs and routine blood tests. Although coinfection is not common, in cases where the disease is not explained by a single pathogen, additional studies, such as a nested PCR for multi-respiratory panel pathogens, are required to detect potentially treatable pathogens, such as COVID-19 mycoplasma, influenza virus, and 229E (30, 31).

Fever is a manifestation of the body's resistance to inflammation, often used to judge the progress or outcomes of a disease (32). In this study, both groups developed acute illness, characterized by a constant high fever; they also had similar fever durations (3–5 days), which was not consistent with previous reports (33). Chen et al., for instance, indicated that 6/103 of the children in their study had HAdV coinfected with *mycoplasma pneumoniae,* and the proportion of fever duration >10 days (40.8%) in the mixed infection group was significantly higher than in the mono-infection group (24.5%, $p = 0.014$) (34). The present study found no significant difference in patient age and sex between the mono- and coinfection groups. The median duration of hospital stay in the two groups was generally shorter than eight days, which aligns with information on single adenovirus infections reported from Beijing (20). This limited data suggest that coinfection with two viruses does not prolong the clearance time of the pathogen, aggravate the host immune response, lead to organ damage, or show more internal and exogenous pyrogen.

Regarding the severity of disease, some research has indicated that HAdV has strong virulence that can cause high mortality in children (32). HAdV-7 in particular may cause severe infection (35, 36). One study indicates that HAdV coinfection with another pathogen aggravates the severity of pneumonia in children (10). Studying the risk factors of severe atypical pneumonia using multivariate logistic regression analysis, Huong et al. found that coinfection with a respiratory virus was a risk factor for severe atypical community-acquired pneumonia in children (OR = 4.36, $p = 0.008$) (37). Previous studies indicated that HAdV coinfection with another pathogen aggravates the severity of pneumonia in children (10). For example, Juan et al. reported that adenovirus and SARS-CoV-2 mixed infections are associated with adverse clinical outcomes, such as shock, lymphopenia, and thrombocytopenia. Patients with these mixed infections are also more likely to require ventilatory support and admission to intensive care units (38). However, these studies are not consistent with our findings, indicating that both mono- and coinfections typically resulted in mild upper respiratory tract infections. Furthermore, the cases in this study also did not show any liver damage, which differed from other studies that found the adenovirus 41 genotype to lead to hepatitis of unknown origin (39–44). Only one 13-year-old girl, coinfected with adenovirus and HCoV-229E, and one two-year-old boy with adenovirus and mycoplasma, developed mild pneumonia, without any severe

complications. Both patients were cured and discharged after the use of symptomatic support therapy and glucocorticoids. The severity of HAdV infection is affected by many factors, including the patient's age, immune status, diagnosis, viral load, and socioeconomic status (20). In this study, all cases presented mild illness regardless of whether they had a single infection (adenovirus or HCoV-229E) or coinfection with two viruses. Several factors may have contributed to this outcome. First, all coinfections and mono-infections were in young children who had no underlying diseases or need for regular medicine administration. By contrast, adenovirus has been recognized as a cause of severe illness among immunocompromised children (45). Second, diagnosis and therapy was provided early and in a timely fashion for these cases. Third, the viral loads in the two groups were at the low to middle level, without any mutations associated with viral reproduction. However, the acute mechanism of severity following HAdV-7 and HCoV-229E co-infections should be further investigated in the future.

In summary, this study explored the unusual phenomenon of HAdV-7 and HCoV-229E coinfection in healthy children. Compared with single adenovirus infections, coinfection with HAdV-Ad7 and HCoV-229E virus did not contribute to disease severity, a finding that may be attributed to the children's good underlying health and low viral loads. Other factors in these positive outcomes include early identification of a potential adenovirus coinfection and successful treatment. However, larger and better-designed prospective analytical studies are required to examine further risk factors as well as the interaction between adenoviruses and other respiratory pathogen coinfections.

This study has some shortcomings. First, as a retrospective study, data are inevitably missing; for example, the serum antibody counts against the adenovirus and HAdV or HCoV-229E and the systemic inflammatory cytokines were not available for the mono-infections or coinfections. Second, the number of ADV+ HAdV-229E coinfections was relatively small. The interpretation and extrapolation of these results should be conducted with caution. A multicenter prospective study with a larger sample is needed. Third, the epidemiology level of adenovirus coinfection with other pathogens in the general population was unclear in this research area.

The world is at a new stage of the COVID-19 pandemic. With non-pharmaceutical interventions (NPIs) having been released, HAdV and HCoVs, including SARS-CoV-2, are circulating endemically in human populations. The early signs and symptoms of infection with adenovirus and HCoV-229E are similar to those of COVID-19 (27). In the future, physicians and public health doctors should be alert to the possibility of HAdV coinfection during the COVID-19 pandemic.

Data availability statement

The original contributions presented in the study are included in the Supplementary material for this article. All sequences from mono-infections with adenovirus and the HCoV 229E, and coinfections with adenovirus and the HCoV-229E were submitted to the NIH genetic sequence database (GenBank, https://www.ncbi.nlm.nih.gov/genbank/). The number of the sequence GenBank are seen in Supplementary Table 1. Further inquiries can be directed to the corresponding author/s.

Ethics statement

The studies involving human participants were reviewed and approved by the study was approved by the Medical Ethics Committee of the Zhejiang Province Center for Disease Control and Prevention (No. 2019013). Written consent was obtained from all patients or their family. Written informed consent to participate in this study was provided by the participants' legal guardian/next of kin.

Author contributions

SL drafted the first version of the manuscript and obtained funding for the study. AZ, JP, LY, WS, and HW collected clinical data for the study. HZ and HL verified and analyzed data for the study. LW, SQ, ZY, JC, and EC conducted the investigation. YC analyzed all samples. All of the authors contributed data to the study and participated in data interpretation and critical review of the manuscript. All of the authors approved the final manuscript for submission.

Funding

This work was supported by the Zhejiang Provincial Program for The Cultivation of High-Level Innovative Health Talents.

Acknowledgments

We would like to thank the local Diseases Centers for Prevention and Control and local hospital workers who helped us conduct the field investigation. We would also like to express our appreciation to Dr. King Wun Lau from Shanghai High School, International Division of China, who aided us in searching for published articles and inputting raw data.

Conflict of interest

The authors declare that the research was conducted in the absence of any commercial or financial relationships that could be construed as a potential conflict of interest.

Publisher's note

All claims expressed in this article are solely those of the authors and do not necessarily represent those of their affiliated organizations, or those of the publisher, the editors and the reviewers. Any product that may be evaluated in this article, or claim that may be made by its manufacturer, is not guaranteed or endorsed by the publisher.

Supplementary material

The Supplementary Material for this article can be found online at: https://www.frontiersin.org/articles/10.3389/fpubh.2022.1048108/full#supplementary-material

References

1. Charman M, Herrmann C, Weitzman MD. Viral and cellular interactions during adenovirus DNA replication. *FEBS Lett.* (2019) 593:3531–50. doi: 10.1002/1873-3468.13695

2. Hage E, Dhingra A, Liebert UG, Bergs S, Ganzenmueller T, Heim A. Three novel, multiple recombinant types of species of human mastadenovirus D(HAdV-D 73, 74, and 75) isolated from diarrhoeal faeces of immunocompromised patients. *J Gen Virol.* (2017) 98:3037–45. doi: 10.1099/jgv.0.000968

3. Li J, Lu X, Sun Y, Lin C, Li F, Yang Y, et al. swimming pool-associated outbreak of pharyngoconjunctival fever caused by human adenovirus type 4 in Beijing, China. *Int J Infect Dis.* (2018) 75:89–91. doi: 10.1016/j.ijid.2018.08.009

4. Vassilara F, Spyridaki A, Pothitos G, Deliveliotou A, Papadopoulos A. A rare case of human coronavirus 229E associated with acute respiratory distress syndrome in a healthy adult. *Case Rep Infect Dis.* (2018) 2018:6796839. doi: 10.1155/2018/6796839

5. Kajon AE, Lamson DM, Bair CR, Lu X, Landry ML, Menegus M, et al. Adenovirus type 4 respiratory infections among civilian adults, northeastern United States, 2011-2015(1). *Emerg Infect Dis.* (2018) 24:201–9. doi: 10.3201/eid2402.171407

6. Lynch BL, Dean J, Brady D, De Gascun C. Adenovirus type 4 respiratory infections among civilian adults, northeastern United States, 2011-2015. *Emerg Infect Dis.* (2018) 24:1392–3. doi: 10.3201/eid2407.180137

7. Binder AM, Biggs HM, Haynes AK, Chommanard C, Lu X, Erdman DD, et al. Human adenovirus surveillance—United States, 2003–2016. *MMWR Morb Mortal Wkly Rep.* (2017) 66:1039–42. doi: 10.15585/mmwr.mm6639a2

8. CDC. *Adenovirus.* (2019). Available online at: https://www.cdc.gov/adenovirus/adenovirus-factsheet-508.pdf (accessed August 28, 2019)

9. Shieh WJ. Human adenovirus infections in pediatric population—an update on clinico-pathologic correlation. *Biomed J.* (2022) 45:38–49. doi: 10.1016/j.bj.2021.08.009

10. Gao J, Xu L, Xu B, Xie Z, Shen K. Human adenovirus Coinfection aggravates the severity of *Mycoplasma* pneumoniae pneumonia in children. *BMC Infect Dis.* (2020) 20:420. doi: 10.1186/s12879-020-05152-x

11. Ghebremedhin B. Human adenovirus: viral pathogen with increasing importance. *Eur J Microbiol Immunol.* (2014) 4:26–33. doi: 10.1556/EuJMI.4.2014.1.2

12. Xu Z, Shi L, Wang Y, Zhang J, Huang L, Zhang C, et al. Pathological findings of COVID-19 associated with acute respiratory distress syndrome. *Lancet Respir Med.* (2020) 8:420–2. doi: 10.1016/S2213-2600(20)30076-X

13. Mulabbi EN, Tweyongyere R, Byarugaba DK. The history of the emergence and transmission of human coronaviruses. *Onderstepoort J Vet Res.* (2021) 88:e1–8. doi: 10.4102/ojvr.v88i1.1872

14. Kesheh MM, Hosseini P, Soltani S, Zandi M. An overview on the seven pathogenic human coronaviruses. *Rev Med Virol.* (2022) 32:e2282. doi: 10.1002/rmv.2282

15. Aleebrahim-Dehkordi E, Soveyzi F, Deravi N, Rabbani Z, Saghazadeh A, Rezaei N. Human coronaviruses SARS-CoV, MERS-CoV, and SARS-CoV-2 in children. *J Pediatr Nurs.* (2021) 56:70–9. doi: 10.1016/j.pedn.2020.10.020

16. Ma Z, Li P, Ji Y, Ikram A, Pan Q. Cross-reactivity towards SARS-CoV-2: the potential role of low-pathogenic human coronaviruses. *Lancet Microbe.* (2020) 1:e151. doi: 10.1016/S2666-5247(20)30098-7

17. CDC. *Human Coronavirus Types*. (2020). Available online a: https://www.cdc.gov/coronavirus/types.html (accessed February 15, 2020).

18. Probst V, Spieker AJ, Stopczynski T, Stewart LS, Haddadin Z, Selvarangan R, et al. Clinical presentation and severity of adenovirus detection alone vs adenovirus co-detection with other respiratory viruses in US children with acute respiratory illness from 2016 to 2018. *J Pediatric Infect Dis Soc.* (2022) 11:430–9. doi: 10.1093/jpids/piac066

19. Feng L, Li Z, Zhao S, Nair H, Lai S, Xu W, et al. Viral etiologies of hospitalized acute lower respiratory infection patients in China, 2009–2013. *PLoS ONE.* (2014) 9:e99419. doi: 10.1371/journal.pone.0099419

20. Huang Y, Wang C, Ma F, Guo Q, Yao L, Chen A, et al. Human adenoviruses in paediatric patients with respiratory tract infections in Beijing, China. *Virol J.* (2021) 18:191. doi: 10.1186/s12985-021-01661-6

21. Ravi RK, Walton K, Khosroheidari M. MiSeq: a next generation sequencing platform for genomic analysis. *Methods Mol Biol.* (2018) 1706:223–32. doi: 10.1007/978-1-4939-7471-9_12

22. Biere B, Oh DY, Wolff T, Durrwald R. Surveillance of endemic human Coronaviruses in Germany, 2019/2020. *Lancet Reg Health Eur.* (2021) 11:1–4. doi: 10.1016/j.lanepe.2021.100262

23. Otieno GP, Murunga N, Agoti CN, Gallagher KE, Awori JO, Nokes DJ. Surveillance of endemic human coronaviruses(HCoV-NL63, OC43 and 229E) associated with childhood pneumonia in Kilifi, Kenya. *Wellcome Open Res.* (2020) 5:150. doi: 10.12688/wellcomeopenres.16037.2

24. Shi Y, Shi J, Sun L, Tan Y, Wang G, Guo F, et al. Insight into vaccine development for Alpha-coronaviruses based on structural and immunological analyses of spike proteins. *J Virol.* (2021). doi: 10.1128/JVI.02284-20

25. Liu S, Cai J, Li Y, Ying L, Li H, et al. Outbreak of acute respiratory disease caused by human adenovirus type 7 and human coronavirus-229E in Zhejiang Province, China. *J Med Virol.* (2022) 28. doi: 10.1002/jmv.28101

26. Lessler J, Reich NG, Brookmeyer R, Perl TM, Nelson KE, Cummings DA. Incubation periods of acute respiratory viral infections: a systematic review. *Lancet Infect Dis.* (2009) 9:291–300. doi: 10.1016/S1473-3099(09)70069-6

27. Imran M, Yasmeen R. SARS-CoV2 Outbreak: Emergence, transmission and clinical features of human coronaviruses. *J Ayub Med Coll Abbottabad.* (2020) 32:S710–3.

28. Li SW, Lin CW. Human coronaviruses: Clinical features and phylogenetic analysis. *Biomedicine.* (2013) 3:43–50. doi: 10.1016/j.biomed.2012.12.007

29. Varghese L, Zachariah P, Vargas C, LaRussa P, Demmer RT, Furuya YE, et al. Epidemiology and clinical features of human coronaviruses in the pediatric population. *J Pediatric Infect Dis Soc.* (2018) 7:151–8. doi: 10.1093/jpids/pix027

30. Lai S, Ruktanonchai NW, Zhou L, Prosper O, Luo W, Floyd JR, et al. Effect of non-pharmaceutical interventions to contain COVID-19 in China. *Nature.* (2020) 585:410–3. doi: 10.1038/s41586-020-2293-x

31. Shou MH, Wang ZX, Lou WQ. Effect evaluation of non-pharmaceutical interventions taken in China to contain the COVID-19 epidemic based on the

susceptible-exposed-infected-recovered model. *Technol Forecast Soc Chang.* (2021) 171:120987. doi: 10.1016/j.techfore.2021.120987

32. Wei J, Wu S, Jin X, Zhang J, Pan S. Association of Mycoplasma pneumoniae coinfection with adenovirus pneumonia severity in children. *Allergol Immunopathol.* (2022) 50:31–6. doi: 10.15586/aei.v50i1.476

33. Wu PQ, Zeng SQ, Yin GQ, Huang JJ, Xie ZW, Lu G, et al. Clinical manifestations and risk factors of adenovirus respiratory infection in hospitalized children in Guangzhou, China during the 2011-2014 period. *Medicine.* (2020) 99:e18584. doi: 10.1097/MD.0000000000018584

34. Chen LL, Cheng YG, Chen ZM Li SX, Li XJ, Wang YS. Mixed infections in children with *Mycoplasma* pneumoniae pneumonia. *Zhonghua Er Ke Za Zhi.* (2012) 50:211–5.

35. Cai R, Mao N, Dai J, Xiang X, Xu J, Ma Y, et al. Correction: genetic variability of human adenovirus type 7 circulating in mainland China. *PLoS ONE.* (2020) 15:e0234681. doi: 10.1371/journal.pone.0234681

36. Cai R, Mao N, Dai J, Xiang X, Xu J, Ma Y, et al. Genetic variability of human adenovirus type 7 circulating in mainland China. *PLoS ONE.* (2020) 15:e0232092. doi: 10.1371/journal.pone.0232092

37. Huong Ple T, Hien PT, Lan NT, Binh TQ, Tuan DM, Anh DD. First report on prevalence and risk factors of severe atypical pneumonia in Vietnamese children aged 1-15 years. *BMC Public Health.* (2014) 14:1304. doi: 10.1186/1471-2458-14-1304

38. Motta JC, Gomez CC. Adenovirus and novel coronavirus(SARS-Cov2) coinfection: a case report. *IDCases.* (2020) 22:e00936. doi: 10.1016/j.idcr.2020.e00936

39. Baker JM, Buchfellner M, Britt W, Sanchez V, Potter JL, Ingram LA, et al. Acute hepatitis and adenovirus infection among children—Alabama, October 2021–February 2022. *MMWR Morb Mortal Wkly Rep.* (2022) 71:638–40. doi: 10.15585/mmwr.mm7118e1

40. Baker JM, Buchfellner M, Britt W, Sanchez V, Potter JL, Ingram LA, et al. Acute hepatitis and adenovirus infection among children—Alabama, October 2021–February 2022. *Am J Transpl.* (2022) 22:1919–21. doi: 10.1111/ajt.16665

41. Gutierrez Sanchez LH, Shiau H, Baker JM, Saaybi S, Buchfellner M, Britt W, et al. A case series of children with acute hepatitis and human adenovirus infection. *N Engl J Med.* (2022) 387:620–30. doi: 10.1056/NEJMoa2206294

42. Hakim MS. The recent outbreak of acute and severe hepatitis of unknown etiology in children: a possible role of human adenovirus infection? *J Med Virol.* (2022) 94:4065–8. doi: 10.1002/jmv.27856

43. Paraskevis D, Papathedoridis G, Sypsa V, Sfikakis P, Tsiodras S, Zaoutis T. Alpha proposed etiology for an aberrant response to enteric adenovirus infection in previously SARS-CoV-2-infected children with acute hepatitis. *J Pediatric Infect Dis Soc.* (2022). doi: 10.1093/jpids/piac053

44. Shan S, Jia JD. The relationship between adenovirus infection and severe acute hepatitis of unknown etiology. *Zhonghua Gan Zang Bing Za Zhi.* (2022) 30:470–2. doi: 10.3760/cma.j.cn501113-20220429

45. van Tol MJ, Kroes AC, Schinkel J, Dinkelaar W, Claas EC. Jol-van der Zijde CM, et al. Adenovirus infection in paediatric stem cell transplant recipients: increased risk in young children with a delayed immune recovery. *Bone Marrow Transpl.* (2005) 36:39–50. doi: 10.1038/sj.bmt.1705003

frontiers | Frontiers in Medicine

TYPE Case Report
PUBLISHED 07 December 2022
DOI 10.3389/fmed.2022.1013294

OPEN ACCESS

EDITED BY
Francesco Paolo Bianchi,
University of Bari Aldo Moro, Italy

REVIEWED BY
Maryam Dadar,
Razi Vaccine and Serum Research Institute, Iran
Steven Olsen,
Agricultural Research Service (USDA), United States

*CORRESPONDENCE
Naibin Yang
yangnb01@163.com
Jinguo Chu
chujg@126.com

SPECIALTY SECTION
This article was submitted to Infectious Diseases: Pathogenesis and Therapy, a section of the journal Frontiers in Medicine

RECEIVED 06 August 2022
ACCEPTED 08 November 2022
PUBLISHED 07 December 2022

CITATION
Huang K, Yu X, Yu Y, Cen Y, Shu J, Yang N and Chu J (2022) Relative bradycardia presented as a clinical feature of *Brucella melitensis* infection: A case report. *Front. Med.* 9:1013294. doi: 10.3389/fmed.2022.1013294

Relative bradycardia presented as a clinical feature of *Brucella melitensis* infection: A case report

Kai Huang, Xuxia Yu, Yushan Yu, Yin Cen, Jie Shu, Naibin Yang* and Jinguo Chu*

Ningbo First Hospital, Ningbo, China

Brucellosis, caused by *Brucella* species, is an infectious disease transmitted through contact with infected animals or their secretions. The clinical disease is characterized by fever and headache. Relative bradycardia is an inappropriate response of heart rate to body temperature, in which the heart rate does not increase proportionally despite a high fever. In this report, we document one case of *Brucella melitensis* infection demonstrating relative bradycardia. To our knowledge, this is the first report of relative bradycardia in a patient with brucellosis.

KEYWORDS

brucellosis, *Brucella melitensis*, relative bradycardia, clinical feature, heart rate and body temperature relationship

Introduction

Brucellosis is a zoonotic disease that causes more than 500,000 new infections per year across the world. The disease is usually transmitted from animals to humans through contact with infected animals or by consuming contaminated animal products. Common symptoms of brucellosis include headache, fever, fatigue, sweating, joint pain, and weakness (1, 2). Brucellosis is still very common and often considered a neglected disease (3). Relative bradycardia is an important diagnostic clue in a variety of infectious and non-infectious diseases (4, 5). Previous studies found that relative bradycardia was not associated with brucellosis (4, 5). In this study, we report a case of *Brucella melitensis* infection exhibiting relative bradycardia. To the best of our knowledge, no similar cases have previously been reported in the literature.

Case presentation

On 24 May 2021, a 51-year-old woman was admitted to our hospital with a 1-week history of fever. She developed a fever of 39.5°C with chills that lasted for about 20–30 min as well as cough, headaches, sweating, and fatigue. The patient was evaluated in an emergency department 5 days previous to the presentation. On examination, blood analysis demonstrated normal white blood

cell counts (4.25×10^9/L) and neutrophil percentage (63.7%), and elevated C-reactive protein (CRP, 8.66 mg/L) with chest computed tomography (CT) within normal limits. The patient was treated with ceftriaxone (2g qd ivgtt) for 2 days but body temperatures remained elevated (>39–40°C) and other clinical symptoms also persisted. The patient was admitted for hospitalization.

The patient's history indicated that she was a farmer and worked with sheep. The patient reported no previous history of symptoms and was not on medication that could cause symptoms. Other family members did not report similar symptoms. Physical examination was within normal limits. Laboratory results indicated significant elevations of CRP and serum amyloid protein A (SAA) and moderate to minor elevations of D-dimer, alanine aminotransferase, aspartate aminotransferase, adenosine deaminase, creatinine, procalcitonin (PCT), and hepatitis B surface antibody (Table 1).

At admission, electrocardiograms (ECGs) showed a heart rate (HR) of only 74 beats per minute (bpm) with sinus rhythm despite a body temperature of 39.1°C. The ECG demonstrated no arrhythmia, shortening of the PR segment, ST elevation or depression, conduction block, or T wave changes (Figure 1). Throughout the clinical course, the echocardiogram demonstrated normal left ventricular function and intracardiac structure, without asynergy. While hospitalization with a high fever sometimes exceeded 40°C, the HR remained between 70 and 100 bpm with a sinus rhythm (Figure 2). The patient was not receiving beta-blocker therapy. In accordance with Cunha's criteria (5), the patient was diagnosed with relative bradycardia.

On day 6, blood culture was positive for the recovery of *B. melitensis* identified by mass spectrometry (MALDI-TOF MS), and the patient was diagnosed with brucellosis. The patient resided in a part of China (Zhejiang Province) that is not considered endemic for brucellosis.

After being diagnosed with brucellosis, the patient was treated with rifampicin (450 mg qd po) and doxycycline (100 mg bid po) for 6 weeks in accordance with Chinese guidelines (6). The patient responded to antibiotic treatment without any adverse clinical effects. After treatment, the patient's body temperature returned to normal limits on day 9 and she was discharged from the hospital in stable condition on day 13. At the latest follow-up 3 months after discharge, the patient did not report any symptoms. The whole process was concluded (Figure 3).

TABLE 1 Laboratory examination results of the case at admission.

Items	Values	Reference range
White blood cell count ($\times10^9$ /L)	3.62	3.50–9.50
Neutrophil count ($\times10^9$ /L)	2.4	1.8–6.3
Lymphocyte count ($\times10^9$ /L)	0.9	1.1–3.2
Monocyte count ($\times10^9$ /L)	0.4	0.1–0.6
Red blood cell count ($\times10^{12}$ /L)	4.32	3.8–5.1
Hemoglobin (g/L)	115	115.0–150.0
Platelet count ($\times10^9$ /L)	134	125.0–350.0
High sensitivity C-reactive protein(mg/l)	48.13	0–5.0
D-dimer(ng/ml)	1,406	0–243
Erythrocyte sedimentation rate (mm/h)	29	<38
Glycated-hemoglobin(%)	5.8	4.0–6.0
Alanine aminotransferase (U/L)	42	7–40
Aspartate aminotransferase (U/L)	55	13–35
γ-Glutamyl transpeptidase (U/L)	27	7–45
Alkaline phosphatase (U/L)	80	50–135
Total bilirubin (μmol/L)	4.4	3.4–20.5
Direct bilirubin (μmol/L)	2.1	0.0–6.84
Indirect bilirubin (μmol/L)	2.3	1.7–13.7
Adenosine deaminase (U/L)	42.3	4.0–22.0
Urea nitrogen (mmol/l)	4.4	2.6–7.5
Creatinine (umol/l)	74	41–73
Creatine kinase isoenzyme (ng/ml)	1.54	0–5.0
Procalcitonin(ng/ml)	0.37	0–0.05
Serum Amyloid Protein A(mg/l)	368.7	0–10.0
EBVDNA	$<5.0\times10^3$	$<5.0\times10^3$
CMVDNA	$<2.0\times10^3$	$<2.0\times10^3$
Blood plasmodium	Negative	Negative
Widal test	Negative	Negative
Hepatitis B surface antigen (IU/ml)	0.01	0.00–0.05
Hepatitis B surface antibody (mIU/ml)	18.46	0.00–10.00
Hepatitis C virus antibody	Negative	Negative
Human immunodeficiency virus antibody	Negative	Negative
Treponema pallidum antibody	Negative	Negative
Blood culture	*Brucella melitensis*	Negative

Discussion

Brucella melitensis is the most virulent and the most prevalent worldwide among *Brucella* species. The hosts of *B. melitensis* are sheep and goats. *B. melitensis* is commonly infected by exposure to animals or animal products (1, 2). The incubation period is usually between 5 and 60 days (7). Based on clinical symptoms, epidemiological history, and positive blood culture, our case was diagnosed with brucellosis. The indications of occupational exposure had regulatory importance as the patient was from an area considered to be non-endemic for brucellosis. In the current case of *B. melitensis* infection, we observed elevated inflammatory biomarkers (CRP, PCT, and SAA) and also noted indications of damage to liver function consistent with other reports (8, 9).

Cardiac involvement (such as endocarditis, myocarditis, and pericarditis) occurs in <2% of patients with brucellosis, but in endemic regions, this rate can increase between 7 and 10% and is the most common cause of death (10). The most

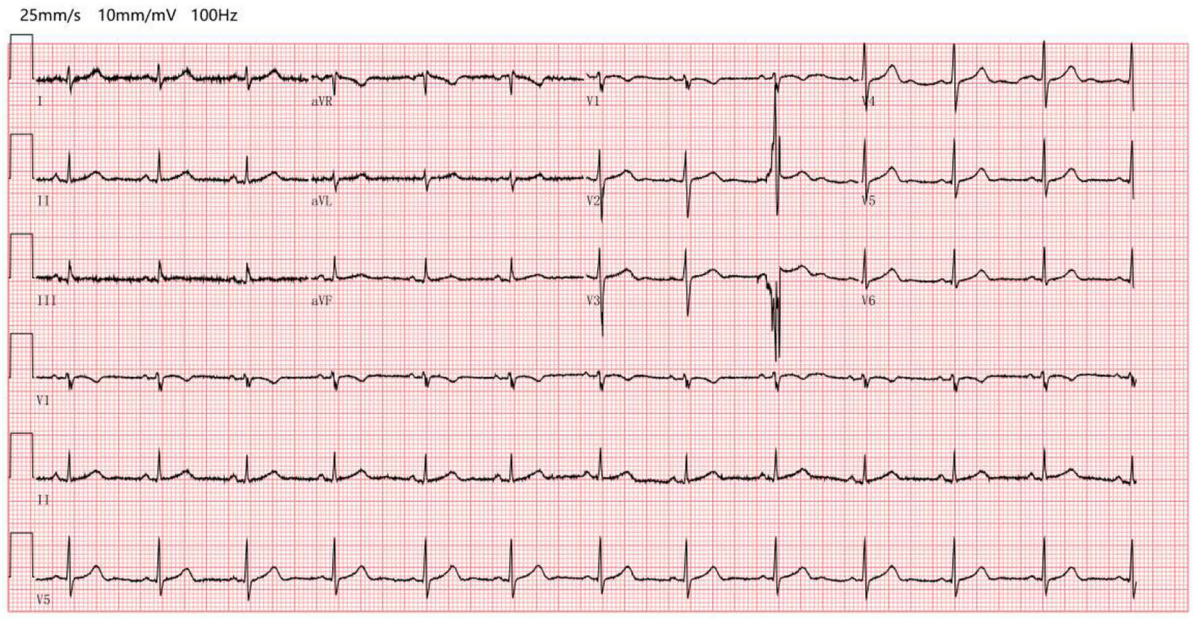

FIGURE 1
Electrocardiograms at admission (electrocardiograms showed a heart rate of only 74 beats per minute with sinus rhythm despite a body temperature of 39.1°C, without arrhythmia, no shortening of the PR segment, ST elevation or depression, and conduction block or T wave change).

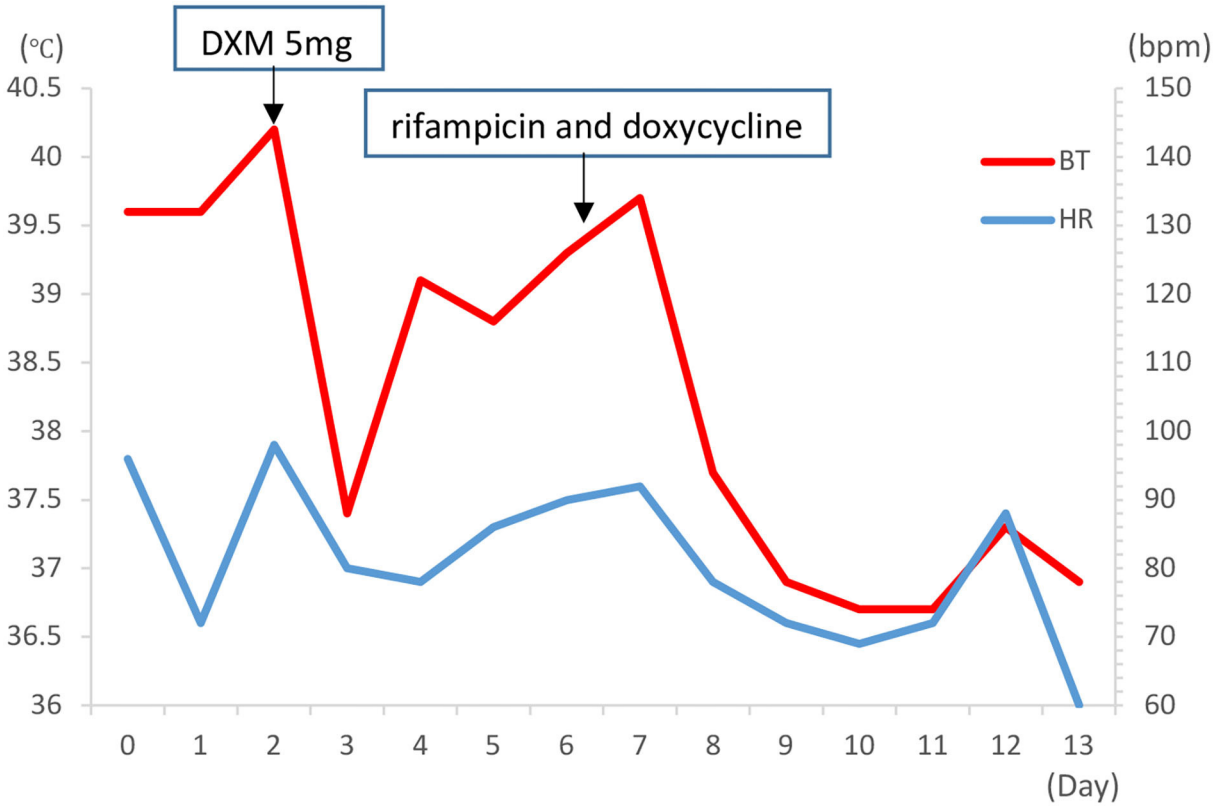

FIGURE 2
The time course of heart rate, fever, and treatment in the case (during the first week of hospitalization, persistently high fever with highest temperature >40°C, the HR remained within 70–100 bpm with sinus rhythm. bpm, beats per minute; BT, body temperature; HR, heart rate; DMX, dexamethasone).

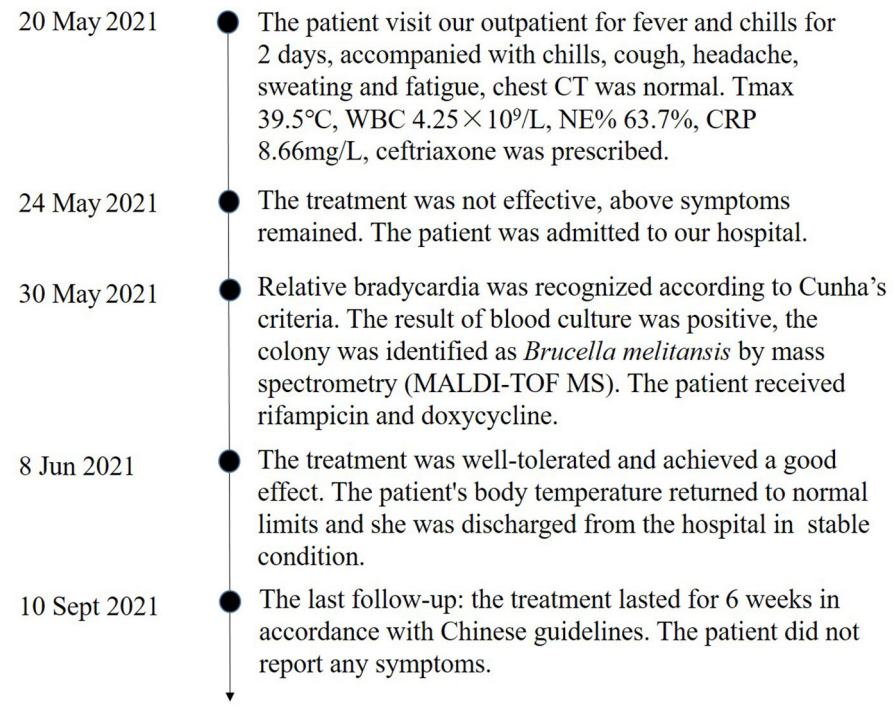

FIGURE 3
Timeline of the case.

common and most important complication is endocarditis (11). *Brucella* endocarditis has a predominance of aortic involvement and is prone to left ventricular failure (12). Cetin M et al. demonstrated that the parameters of ECG including Pmax, Pdis, QTmax, QTdis, QTcdis, Tp-edis interval, Tp-emax/QTmax, and Tp-emax/QTcmax ratios were significantly longer among children with brucellosis compared with healthy children, which indicates that the cardiac conduction pathways are affected (13).

Relative bradycardia is a clinical phenomenon demonstrating an insufficient increase in the heart rate despite the high fever, which may occur in some infectious diseases (including COVID-19) (14, 15). Bradycardia occurrence may correlate with the severity of the disease, as these cases were more likely to develop relative bradycardia (14), and HR tends to be lower, sometimes <60 bpm among patients with COVID-19 (15). In the current case, HR varied from 60 to 100 bpm, and there was no evidence that relative bradycardia was associated with the severity of brucellosis.

Although mechanisms causing relative bradycardia remain unknown, inflammatory cytokines (such as interleukin 6), direct pathogenic effects on the heart (such as the sinoatrial node), increased vagal tone, and/or induction of electrolyte abnormalities have been proposed (4, 16). In the current case, cardiac biomarkers, ECG, and echocardiogram were all within normal limits and no evidence of myocardial damage was detected. The elevations in CRP, PCT and SAA suggest a role for inflammation. We considered that relative bradycardia of *B. melitensis* infection might be caused by inflammatory cytokines.

We have described and considered the potential mechanisms of a case of brucellosis with relative bradycardia. Relative bradycardia could be used as a clinical tool for the diagnosis of various disease etiologies, especially infectious diseases (4, 13). Our case demonstrates that relative bradycardia could be associated with *B. melitensis* infection, an observation that has not been previously reported. Clinicians should consider brucellosis in patients with high fever exhibiting relative bradycardia.

Some limitations were discovered in this case study. First, IL-6 was not measured, so the relation between IL-6 and relative bradycardia is not evaluated. Second, because the follow-up time was short, the long-term effect of the treatment of rifampicin and doxycycline should be assessed in future studies.

Data availability statement

The original contributions presented in the study are included in the article/supplementary material, further inquiries can be directed to the corresponding author/s.

Ethics statement

The study involving human participant was reviewed and approved by the Medical Ethical Committees of Ningbo First Hospital (approval number: 2022RS125). Written informed consent from the [patients/ participants OR patients/participants legal guardian/next of kin] was not required to participate in this study in accordance with the national legislation and the institutional requirements.

Author contributions

KH and XY analyzed and interpreted the clinical data. KH, XY, YY, YC, and JS drafted the manuscript. NY and JC revised the manuscript. All authors have read and approved the manuscript.

Conflict of interest

The authors declare that the research was conducted in the absence of any commercial or financial relationships that could be construed as a potential conflict of interest.

Publisher's note

All claims expressed in this article are solely those of the authors and do not necessarily represent those of their affiliated organizations, or those of the publisher, the editors and the reviewers. Any product that may be evaluated in this article, or claim that may be made by its manufacturer, is not guaranteed or endorsed by the publisher.

References

1. Hayoun MA, Muco E, Shorman M. Brucellosis. In: *StatPearls*. (2022). Treasure Island (FL): StatPearls Publishing. Available from: https://www.ncbi.nlm.nih.gov/books/NBK441831/ (accessed on May 9, 2022).

2. Deng Y, Liu X, Duan K, Peng Q. Research progress on brucellosis. *Curr Med Chem.* (2019) 26:5598–608. doi: 10.2174/0929867325666180510125009

3. Franco MP, Mulder M, Gilman RH, Smits HL. Human brucellosis. *Lancet Infect Dis.* (2007) 7:775–86. doi: 10.1016/S1473-3099(07)70286-4

4. Ye F, Hatahet M, Youniss MA, Toklu HZ, Mazza JJ, Yale S. The clinical significance of relative bradycardia. WMJ.2018; 117:73-78.

5. Cunha BA. The diagnostic significance of relative bradycardia in infectious disease. *Clin Microbiol Infect.* (2000) 6:633–4. doi: 10.1046/j.1469-0691.2000.0194f.x

6. National Health Commission of the People's Republic of China. *Guidelines for diagnosis and treatment of brucellosis.* Available online at: http://www.nhc.gov.cn/cms-search/xxgk/getManuscriptXxgk.htm?id=56110 (accessed on October 22, 2012; June 8, 2022).

7. Marr JS, Cathey JT. A Century in the Life of the Control of Communicable Diseases Manual: 1917 to 2017. *J Public Health Manag Pract*. (2016) 22:597–602. doi: 10.1097/PHH.0000000000000435

8. Liu J, Zhao X. Clinical features and serum profile of inflammatory biomarkers in patients with brucellosis. *J Infect Dev Ctries.* (2017) 11:840–6. doi: 10.3855/jidc.8872

9. Okan DH, Gökmen Z, Seyit B, Yuksel K, Cevdet Z, Deniz A. Mean platelet volume in brucellosis: correlation between brucella standard serum agglutination test results, platelet count, and C-reactive protein. *Afr Health Sci.* (2014) 14:797–801. doi: 10.4314/ahs.v14i4.4

10. Okan DH, Gökmen Z, Seyit B, Yuksel K, Cevdet Z, Deniz A. Brucella endocarditis: clinical, diagnostic, and therapeutic approach. *Eur J Clin Microbiol Infect Dis.* (2003) 22:647–50. doi: 10.1007/s10096-003-1026-z

11. Abid L, Frikha Z, Kallel S, Chokri Z, Ismahen B, Amin B, et al. Brucella myocarditis: a rare and life-threatening cardiac complication of brucellosis. *Intern Med.* (2012) 51:901–4. doi: 10.2169/internalmedicine.51.6379

12. Luo L, Zhou BT, Wang HL, Dou HT, Li TS. A clinical analysis of six patients with Brucella endocarditis and literature review. *Zhonghua Nei Ke Za Zhi*. (2017) 56:734–7. Chinese.

13. Çetin M, Turfan N, Karaman K, Yaşar AS, Güven B, Tunçdemir P. The Pattern of Tpeak-Tend Interval and QTdis, and Pdis in Children with Brucellosis. *J Trop Pediatr*. (2019) 65:474–80. doi: 10.1093/tropej/fmy078

14. Yoshizane T, Ishihara A, Mori T, Tsuzuku A, Suzuki J, Noda T. Relative bradycardia in patients with moderate-to-severe COVID-19: a retrospective cohort study. *SN Compr Clin Med.* (2022) 4:65. doi: 10.1007/s42399-022-01146-9

15. Hiraiwa H, Goto Y, Nakamura G, Yasuda Y, Sakai Y, Kasugai D, et al. Relative bradycardia as a clinical feature in patients with coronavirus disease 2019 (COVID-19): A report of two cases. *J Cardiol Cases.* (2020) 22:260–4. doi: 10.1016/j.jccase.2020.07.015

16. Ye F, Winchester D, Stalvey C, Jansen M, Lee A, Khuddus M, et al. Proposed mechanisms of relative bradycardia. *Med Hypotheses.* (2018) 119:63–7. doi: 10.1016/j.mehy.2018.07.014

frontiers | Frontiers in Public Health

TYPE Case Report
PUBLISHED 19 December 2022
DOI 10.3389/fpubh.2022.1028989

OPEN ACCESS

EDITED BY
Francesco Paolo Bianchi,
University of Bari Aldo Moro, Italy

REVIEWED BY
Valentina A. Feodorova,
Federal Research Center for Virology and Microbiology, Branch in Saratov, Russia
Lili Chen,
University of South China, China

*CORRESPONDENCE
Yanfei Yang
✉ yyfshare@163.com

SPECIALTY SECTION
This article was submitted to Infectious Diseases: Epidemiology and Prevention, a section of the journal Frontiers in Public Health

RECEIVED 26 August 2022
ACCEPTED 30 November 2022
PUBLISHED 19 December 2022

CITATION
Wang J, Zhu Y, Mo Q and Yang Y (2022) Case Report: A *Chlamydia psittaci* pulmonary infection presenting with migratory infiltrates. *Front. Public Health* 10:1028989. doi: 10.3389/fpubh.2022.1028989

Case Report: A *Chlamydia psittaci* pulmonary infection presenting with migratory infiltrates

Jundi Wang [1], Yurou Zhu [2], Qiongya Mo [2] and Yanfei Yang [2*]

[1]Department of Rheumatology, Affiliated Hangzhou First People's Hospital, Zhejiang University School of Medicine, Hangzhou, Zhejiang, China, [2]Department of Respiratory Diseases, Hangzhou TCM Hospital Affiliated to Zhejiang Chinese Medical University, Hangzhou, Zhejiang, China

Community-acquired pneumonia is a public health problem in all countries in the world, with a broad range of causative agents and *Chlamydia psittaci* infection tends to be overlooked. Pulmonary migratory infiltrates are commonly seen in eosinophilic pneumonia, cryptogenic organizing pneumonia, etc. However, the association of *Chlamydia psittaci* and pulmonary migratory infiltrates has been seldom described in literatures before. We reviewed a 64-year-old man referred to our hospital for treatment against *Chlamydia psittaci* pneumonia which was diagnosed by metagenomics next generation sequencing (mNGS). During the treatment period, chest imaging showed migratory infiltrates, which has been rarely described before.

KEYWORDS

***Chlamydia psittaci*, migratory infiltrates, CT, mNGS, pneumonia**

Introduction

The first report of the human-to-human transmission of *Chlamydia psittaci* was documented by Zhenjie Zhang in China in 2020 (1). Pulmonary migratory infiltrates are commonly seen in eosinophilic granulomatosis with polyangiitis (EGPA), cryptogenic organizing pneumonia and so on Tiralongo et al. (2), the imaging manifestations are intrapulmonary infiltrative lesions, no fixed lung segment or lobe distribution, and intrapulmonary migratory shadow. However, the association of *Chlamydia psittaci* pulmonary infection and migratory infiltrates has been never described in literatures before.

Patients suffering from severe *Chlamydia psittaci* infection are prone to sepsis and multiple organ failure. The difficulty in identifying psittacosis with traditional detection methods usually leads to misdiagnosis of this condition in clinical practice (3), because before metagenomic next-generation sequencing (mNGS), the main method for scientists to diagnose *Chlamydia psittaci* infection was to notice an elevation of chlamydia-specific IgG antibodies in serological assays, and its convalescent serum increased four-fold (4). It's an approach of retrospective as we all know. Within the global scope, mNGS develops so fast with the unprecedented speed as to improve the speed and accuracy of clinic diagnosis (5). We herein describe a patient with *Chlamydia psittaci* pulmonary infection diagnosed by bronchoalveolar lavage fluid mNGS who presented with migratory infiltrates, and be cured after antimicrobial therapy.

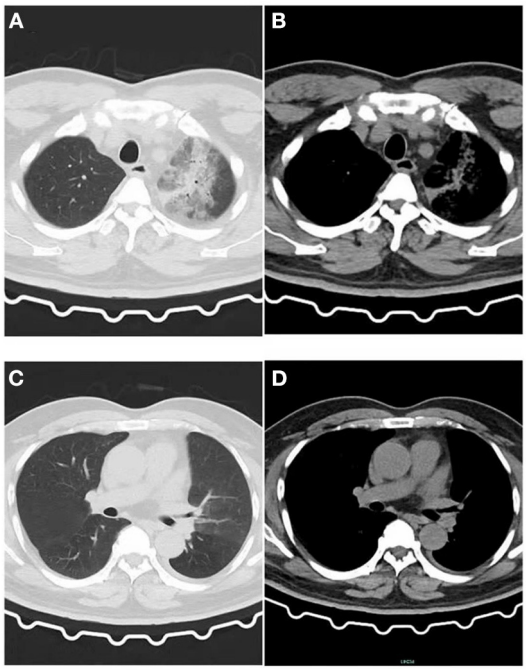

FIGURE 1
Image of the patient's first CT inspection on June 5, 2021. **(A)** Lung window: Patchy high-density shadow in the upper lobe of the left lung with blurred edges. **(B)** Mediastinal window: Patchy exudative lesions in the upper lobe of the left lung. **(C)** Lung window: No obvious exudative lesions in the left lower lobe, and a small amount of pleural effusion on the left. **(D)** Mediastinal window: No obvious exudative lesions.

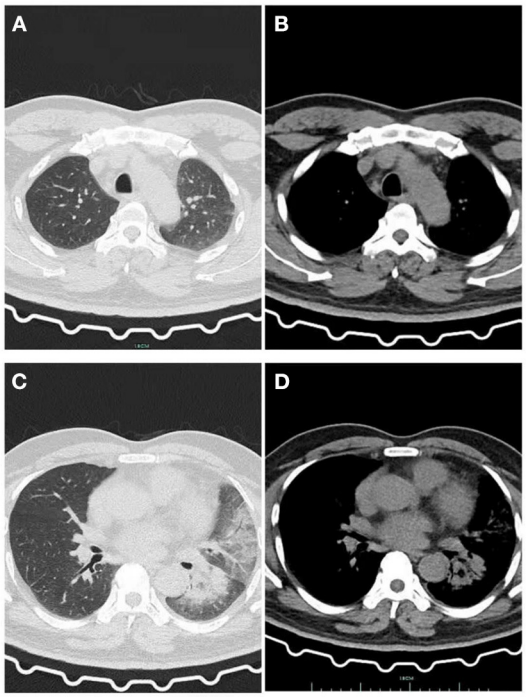

FIGURE 2
After he was given Latamoxef Sodium as empirical treatment for 6 days. **(A)** Lung window: The patchy high-density shadow in the upper lobe of the left lung is obviously absorbed. **(B)** Mediastinal window: Exudative lesions in the upper lobe of the left lung were obviously absorbed. **(C)** Lung window: New patchy high-density shadow in the lower lobe of the left lung with i blurred edges, pleural effusion was absorbed more than before. **(D)** Mediastinal window: Newly emerging exudative lesions in the left lower lobe.

Case presentation

A 64-year-old male patient was admitted to our hospital on June 5, 2021. He was a 64-year-old retired public health worker. Following his retirement, He owned a non-commercial chicken-farms. He presented to our hospital with the chief complaint of fever and cough. Initially, he was diagnosed with bacterial pneumonia with 3 weeks of low-grade fever. CT revealed exudative lesions on the left upper lung field at the onset of disease (Figure 1). Latamoxef Sodium—a broad-spectrum cephalosporin—was given intravenously as empirical treatment in this patient for the treatment as the patient had been misdiagnosed as bacterial pneumonia at first. During treatment, the patient complained of intermittent cough and chest congestion. Before transferred to our department, he was evaluated by computed tomography (CT) scan again, which indicated a new lesion of consolidation in the left lower lobe (Figure 2). During the period following his referral, he had a continuous cough and a high fever of 39.5°C (Figure 3). Chest imaging showed migratory infiltrates. During detailed medical history taking, we noticed that the patient had exposure to chicken manure. Thus, we highly suspect that there could potentially be infected by atypical infections included cryptococcal infection or *Chlamydia psittaci*. To fight against atypical pathogens (mostly the Chlamydia spp), the patient was empirically treated with Moxifloxacin (400 mg/d) intravenously which resulted in an improvement of clinical symptoms. In parallel, we performed bronchoscopy for this patient whose bronchoalveolar lavage fluid were collected for mNGS. Although his serum was negative for anti- *Chlamydia psittaci* antibody, mNGS of his bronchoalveolar lavage fluid (BALF) showed only the presence of *Chlamydia psittaci* pneumophila(The mNGS data indicated 16 sequences aligning to *Chlamydia psittaci)*, and eosinophils and white blood cell counts in routine blood tests were normal. So the treatment with Doxycycline(100 mg q12 h)was instituted for him. Assuredly, the treatment improved his cough and sputum, as well as his pulmonary lesions (Figure 4).

Abbreviations: mNGS, metagenomic next-generation sequencing; BALF, Bronchoalveolar lavagefluid; PMI, Pulmonary migratory infiltrates; CEP, Chronic eosinophilic pneumonia; Mp, Mycoplasma pneumonia; CT, Computed tomography.

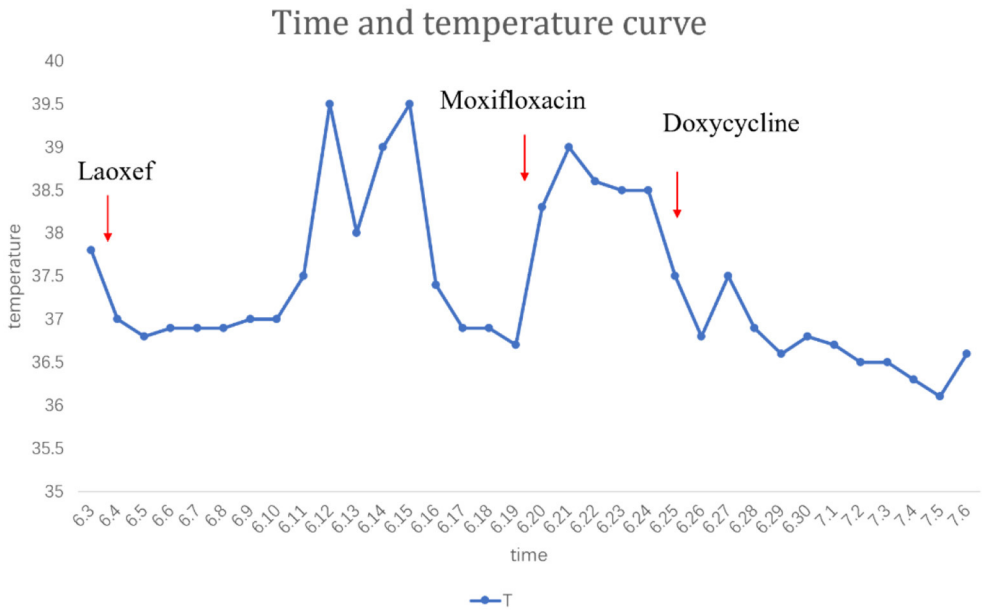

FIGURE 3
The temperature during his treatment.

However, we are still confused about the CT imaging results which was characterized by fleeting infiltrates.

Discussion and conclusions

In our case, the patient had a clear contact history of chicken manure. We suspect that his exposure to *Chlamydia psittaci* might be derived from the chicken manure because he had a big chicken farm. Notwithstanding, there were no features of the spread of *Chlamydia psittaci* pneumonia among his family. Although it has previously been reported that Chlamydia has the potential for human-to-human transmission (1, 6). This can partly be explained by the known epidemiology of *Chlamydia psittaci* in humans in that most human cases are a result of animal-to-human transmission, rather than human-to-human transmission. Since there are 10 genotypes of *Chlamydia psittaci* (7), with varying preference for host species, further study is necessary to determine the genetic diversity of *Chlamydia psittaci*.

Normally, *Chlamydia psittaci* pneumonia shows certain characteristics, including high fever, cough, fatigue, etc. CT imaging often shows different degrees of exudation and patchy consolidation, unilateral involvement is more common, and the white blood cell count can be normal (8). Molecular diagnostic methods such as mNGS could lead to rapid diagnosis and treatment which can shorten the course of hospitalization and thus improve prognosis (9). In our case, mNGS provides basis for the accurate diagnosis of *Chlamydia psittaci* (The mNGS data indicated 16 sequences aligning to *Chlamydia psittaci)*. Doxycycline-based therapy is effective in severe *Chlamydia psittaci* pneumonia. Failure to diagnose the disease or identify the pathogen in time, with delayed use of effective antibiotics can cause high mortality in severe cases (10).

Chlamydia psittaci infection tends to be overlooked due to relatively low awareness by physicians. The current case series indicated that mNGS could be used to diagnose *Chlamydia psittaci* infection (7). Considering the high cost of mNGS test, we recommend the early use of mNGS testing in failure cases of empirical treatment and severe cases. In our case, the patient had a history of direct exposure to chicken manure. When the patient had persistent fever even after the use of empiric antibiotic therapy, the patient received mNGS analysis of bronchoalveolar lavage fluid (BALF) and mNGS clearly and unambiguously detected 16 sequences for *Chlamydia psittaci* in BALF. In accordance with previous results by mNGS, *Chlamydia psittaci* pulmonary infection was determined. The patient received doxycycline and moxifloxacin with a successful therapeutic response. However, until now, rarely literature has described the association of pulmonary migratory infiltrates with *Chlamydia psittaci* pulmonary infection. The migratory characteristic of these infiltrates can be seen in chronic eosinophilic pneumonia (CEP) (11), ANCA-associated vasculitis, including granulomatosis with polyangiitis, eosinophilic granulomatosis with polyangiitis, and microscopic polyangiitis (12). Previous studies revealed that a case of pulmonary migratory infiltrates

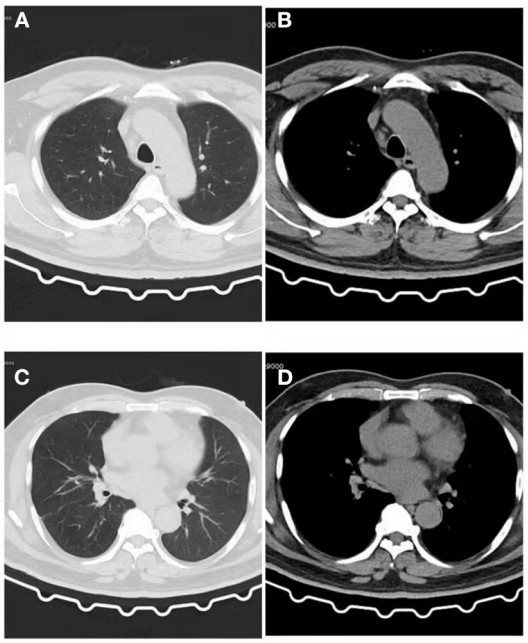

FIGURE 4
CT of the patient after recovery. **(A)** Lung window: The patchy high-density shadow in the upper lobe of the left lung have been completely absorbed, and a few cord-like shadows can be seen with clear edges. **(B)** Mediastinal window: No obvious exudative lesions in the left upper lobe. **(C)** Lung window: The patchy high-density shadow and pleural effusion in the lower lobe of the left lung have been completely absorbed, and a few cord-like shadows can be seen with clear edges. **(D)** Mediastinal window: No obvious exudative lesions in the left lower lobe.

(PMI) attributed to *mycoplasma pneumonia (Mp)* infection (4). In our case, The imaging manifestations of pulmonary migratory infiltrates attributed to *Chlamydia psittaci* infection can be rare. To our knowledge, there are rare reports of such cases. It has already been reported that organizing pneumonia was also appeared in some cases of atypical organisms' infection (13). These findings can be seen as non-specific reactions to injury and also occur in association with some infections. We suspect that infectious agents such as *Chlamydia psittaci* may have caused some cases of COP and some of them may have shown migratory pulmonary infiltrates (and some of them recovered without steroid therapy) (14). We suspect that similar circumstance was in our case. However, we have never used steroids, the lesion has completely disappeared. Of course, it could also be a combined bacterial infection, but mNGS did not provide a basis of bacterial infection.

In conclusion, the present study described an extremely rare case of *Chlamydia psittaci* pulmonary infection, which was initially misdiagnosed as bacterial pneumonia. Patients described overall satisfaction with the treatment, after all, we have reduced invasive examination on patient such as Lung puncture and so on. If the patient does not respond to treatment, an alternative diagnosis should be considered and invasive procedures should be performed to provide an accurate diagnosis. We call for mNGS examination for patients with migratory pulmonary infiltrates, not just a lung puncture in those patients (previously, migratory pneumonia was mainly considered as non-infectious organized pneumonia). More than anything, CT of the chest may show migratory infiltrates in *Chlamydia psittaci* infection.

Data availability statement

The original contributions presented in the study are included in the article/supplementary material, further inquiries can be directed to the corresponding author.

Ethics statement

Written informed consent was obtained from the individual(s) for the publication of any potentially identifiable images or data included in this article.

Author contributions

Conception, design, collection, and assembly of data: YY. Data analysis and interpretation: YZ and QM. Manuscript writing: JW and YY. Final approval of manuscript: All authors.

Conflict of interest

The authors declare that the research was conducted in the absence of any commercial or financial relationships that could be construed as a potential conflict of interest.

Publisher's note

All claims expressed in this article are solely those of the authors and do not necessarily represent those of their affiliated organizations, or those of the publisher, the editors and the reviewers. Any product that may be evaluated in this article, or claim that may be made by its manufacturer, is not guaranteed or endorsed by the publisher.

References

1. Zhang Z, Zhou H, Cao H, Ji J, Zhang R, Li W, et al. Human-to-human transmission of *Chlamydia psittaci* in China, 2020: an epidemiological and aetiological investigation. *Lancet Microbe*. (2022) 3:e512–e20. doi: 10.1016/S2666-5247(22)00064-7

2. Tiralongo F, Palermo M, Distefano G, Vancheri A, Sambataro G, Torrisi SE, et al. Cryptogenic organizing pneumonia: evolution of morphological patterns assessed by HRCT. *Diagnostics (Basel, Switzerland)*. (2020) 10:262. doi: 10.3390/diagnostics10050262

3. Yuan Y, Zhang X, Gui C. Detection of *Chlamydia psittaci* in both blood and bronchoalveolar lavage fluid using metagenomic next-generation sequencing: a case report. *Medicine*. (2021) 100:e26514. doi: 10.1097/MD.0000000000026514

4. You W, Chen B, Li J, Shou J, Xue S, Liu X, et al. Pulmonary migratory infiltrates due to mycoplasma infection: case report and review of the literature. *J Thorac Dis*. (2016) 8:E393–8. doi: 10.21037/jtd.2016.03.85

5. Wang K, Liu X, Liu H, Li P, Lin Y, Yin D, et al. Metagenomic diagnosis of severe psittacosis using multiple sequencing platforms. *BMC Genomics*. (2021) 22:406. doi: 10.1186/s12864-021-07725-9

6. Zhao W, He L, Xie XZ, Liao X, Tong DJ, Wu SJ, et al. Clustering cases of *Chlamydia psittaci* pneumonia mimicking COVID-19 pneumonia. *World J Clin Cases*. (2021) 9:11237–47. doi: 10.12998/wjcc.v9.i36.11237

7. Gu L, Liu W, Ru M, Lin J, Yu G, Ye J, et al. The application of metagenomic next-generation sequencing in diagnosing *Chlamydia psittaci* pneumonia: a report of five cases. *BMC Pulm Med*. (2020) 20:65. doi: 10.1186/s12890-020-1098-x

8. Ravichandran K, Anbazhagan S, Karthik K, Angappan M, Dhayananth B. A comprehensive review on avian chlamydiosis: a neglected zoonotic disease. *Trop Anim Health Prod*. (2021) 53:414. doi: 10.1007/s11250-021-02859-0

9. De Luigi G, Meoli M, Zgraggen L, Kottanattu L, Simonetti GD, Terrani I, et al. Mucosal respiratory syndrome: A systematic literature review. *Dermatology*. (2022) 238:53–9. doi: 10.1159/000514815

10. Shi Y, Chen J, Shi X, Hu J, Li H, Li X, et al. A case of *chlamydia psittaci* caused severe pneumonia and meningitis diagnosed by metagenome next-generation sequencing and clinical analysis: a case report and literature review. *BMC Infect Dis*. (2021) 21:621. doi: 10.1186/s12879-021-06205-5

11. Katz U, Shoenfeld Y. Pulmonary eosinophilia. *Clin Rev Allergy Immunol*. (2008) 34:367–71. doi: 10.1007/s12016-007-8053-y

12. Nasser M, Cottin V. The respiratory system in autoimmune vascular diseases. *Respiration*. (2018) 96:12–28. doi: 10.1159/000486899

13. Coultas DB, Samet JM, Butler C. Bronchiolitis obliterans due to Mycoplasma pneumoniae. *West J Med*. (1986) 144:471–4.

14. Imokawa S, Yasuda K, Uchiyama H, Sagisaka S, Harada M, Mori K, et al. Chlamydial infection showing migratory pulmonary infiltrates. *Intern Med*. (2007) 46:1735–8. doi: 10.2169/internalmedicine.46.0180

frontiers | Frontiers in Public Health

TYPE Original Research
PUBLISHED 05 January 2023
DOI 10.3389/fpubh.2022.1078719

OPEN ACCESS

EDITED BY
Ana Afonso,
Universidade NOVA de Lisboa, Portugal

REVIEWED BY
Boudewijn Catry,
Centrum voor Onderzoek in Diergeneeskunde en Agrochemie, Belgium
Nicholas Adam Young,
Private Health Management, United States
Giovanni Battista Orsi,
Sapienza University of Rome, Italy

*CORRESPONDENCE
Federica Mele
✉ fedemele1987@gmail.com

SPECIALTY SECTION
This article was submitted to Infectious Diseases: Epidemiology and Prevention, a section of the journal Frontiers in Public Health

RECEIVED 24 October 2022
ACCEPTED 14 December 2022
PUBLISHED 05 January 2023

CITATION
Marrone M, Caricato P, Mele F, Leonardelli M, Duma S, Gorini E, Stellacci A, Bavaro DF, Diella L, Saracino A, Dell'Erba A and Tafuri S (2023) Analysis of Italian requests for compensation in cases of responsibility for healthcare-related infections: A retrospective study. *Front. Public Health* 10:1078719. doi: 10.3389/fpubh.2022.1078719

Analysis of Italian requests for compensation in cases of responsibility for healthcare-related infections: A retrospective study

Maricla Marrone[1], Pierluigi Caricato[1], Federica Mele[1]*, Mirko Leonardelli[1], Stefano Duma[1], Ettore Gorini[2], Alessandra Stellacci[1], Davide Fiore Bavaro[3], Lucia Diella[3], Annalisa Saracino[3], Alessandro Dell'Erba[1] and Silvio Tafuri[4]

[1]Section of Legal Medicine, Department of Interdisciplinary Medicine, Aldo Moro University of Bari, Bari, Italy, [2]Attorney of Supreme Court, Department of Economics and Finance, Aldo Moro University of Bari, Bari, Italy, [3]Department of Precision and Regenerative Medicine and Ionian Area, Clinic of Infectious Diseases, Aldo Moro University of Bari, Bari, Italy, [4]Section of Public Health, Department of Interdisciplinary Medicine, Aldo Moro University of Bari, Bari, Italy

Introduction: The aim of this study was to examine the type of compensation claims for alleged medical malpractice in the field of healthcare-related infections in Italy.

Methods: It was analyzed which was the most frequent clinical context, the characteristics of the disputes established, which were the alleged damages most often complained of, which were the possibly censurable behaviors of the health professionals, and which were the reasons for acceptance or rejection of the request for compensation.

Results: In 90.2%, the issue questioned regarded surgical site infections. The most common pathogens involved were coagulase-negative Staphylococci (34.1%) and *Staphylococcus aureus* (24.4%). The lack or non-adherence to protocols of prophylaxis and/or prevention of healthcare-related infections was the most reported cause of acceptance of the request of compensation.

Discussion: According to our data, a stronger effort should be made in terms of risk management perspective in order to ensure the develop and application of protocols for prevention of Gram-positive healthcare-related infections and strengthen infection control and antimicrobial stewardship programs.

KEYWORDS

healthcare-related infections, surgical site infection, health malpractice, risk management, health responsibility

Introduction

Hospital or nosocomial infections, also called healthcare-related infections (HAIs) are defined as infections acquired during the hospitalization, not incubating during the hospital admission, and occurring at least 48 h after admission. Infections arising after discharge but resulting from hospitalization are also considered HAIs (1).

Surgical site infection (SSI) represents the most frequent type of HAIs in post-surgical hospitalizations and is burdened by high mortality rates, lengthened hospitalization times, need for intensive treatments, and need of hospital readmission (2). However, the incidence of SSIs has gradually decreased over time thanks to the prevention activities that have been implemented in healthcare facilities (3–5).

Hospital infection prevention and containment activities are part of the quality improvement actions and are essential to ensure patient safety (6). Healthcare facilities adopt infection prevention protocols by applying risk reduction interventions related to exposure to healthcare (7). The results of the Study of the Efficacy of Nosocomial Infection Control highlighted that the application of surveillance models can lead to a significant decrease in nosocomial or healthcare-related infections (8).

In recent years, the increase attention to the prevention of healthcare-related infection has allowed the creation of official protocols, supervised by doctors and/or trained health personnel. The management by accreditation teams, the increase of internal hospital protocols, the impact on hospital reimbursements, and the transparency of the dissemination of infection-related outcomes have allowed infection prevention protocols to become a cornerstone of healthcare in all areas.

Furthermore, the implementation models have increasingly focused on the prevention of infection rather than on its monitoring, with the progressive creation of working groups focused on the exclusive prevention of "healthcare-related" infection. At the same time, since healthcare has gradually decentralized from the hospital environment to the community, the concept of health epidemiology was born in order to define the multiple preventative actions that can be implemented in different healthcare realities.

Despite the diverse types of organizations found in the various Countries, the members of the infection prevention group have the task of implementing initiatives aimed at improving quality and ensuring patient safety, led by a team leader in direct contact with the hospital management (9).

In Italy, in order to ensure territorial uniformity in the management of nosocomial infections, the Circular of the Ministry of Health 52/1985 "Fight against hospital infections" was issued. It set up a technical commission responsible for the fight against HAIs with different tasks and purposes (define the strategy, verify the effective application of surveillance and control programs and their effectiveness, and take care of the cultural and technical training of the hospital staff).

According to this Circular, the committee must be made up of personnel specialized in microbiology, infectious diseases and hygiene, whose actions are managed by the Medical Director (10).

The subsequent Circular of the Ministry of Health 8/1988 underlines how passive surveillance, i.e., based on notification systems, does not represent an effective method for HAIs surveillance. Active surveillance must therefore be implemented: this could be proposed in different forms, depending on the type of healthcare facility.

Dell'Erba et al. (11) assess that the specialist in forensic medicine should be part of the technical commission for the fight against hospital infections. In fact, due to the growing judicial litigation in the field of health responsibility and hospital infections, it seems clear that forensic, due to specific training, is the most suitable figure to direct the complex clinical risk management process. In fact, no other figure has the responsibility of the complex ethical and deontological implications of the problem, including those related to informed consent and to the patient's information about the risk of acquiring a nosocomial infection (12).

In the following years, because of the importance that HAIs play in Public Health, the issue was the subject of specific documents such as the Compendium of measures for the control of HAIs and the Recommendations for the control the nosocomial spread of methicillin-resistant *Staphylococcus aureus* (MRSA). In addition, the National Prevention Plan 2014–2018 and the National Antimicrobial Resistance Contrast Plan 2017–2020 reports its importance (13).

On this basis, this study aims to examine the type of compensation claims for alleged medical malpractice in the field of hospital infections in Italy. Moreover, in order to confirm or deny the results, authors have expanded, the case history of a recent work concerning claims for compensation for hospital infections (10).

On the basis of the dataset, it was analyzed which was the most frequent clinical context, the characteristics of the disputes established, which were the alleged damages most often complained of, which were the possibly censurable behaviors of the health professionals, and, above all, which were the reasons for acceptance or rejection of the request for compensation. We have also interpreted these results according to the preventive logic inherent in the management of clinical risk.

Materials and methods

We conducted a retrospective study using the Portal of Telematic Services of the Ministry of Justice. This is a search engine that allows the search of sentences.

We randomly selected 41 judgments issued from 2020 to 2021 in Italy and concerning claims for healthcare-related infections. Keywords for the sentences' selections were: "hospital infection," "nosocomial infection" and "health responsibility." The content of the sentences was therefore examined in detail.

Abbreviations: ICAs, healthcare-related infections; SA, *Staphylococcus aureus*; SSI, surgical-site infection; MRSA, methicillin-resistant *Staphylococcus aureus*; MSSA, methicillin-susceptible *Staphylococcus aureus*; MDR-GNB, multidrug resistant Gram-negative bacteria; ND, not determined.

TABLE 1 Request for compensation 2020–2021 in Italy.

Court	Gender-age range of the applicant	Types of infection	Further specifications	Type of intervention / treatment	Outcome judgment	Reason for judgment
Court of Bologna - 2021	M – N.D.	Prosthesis infection	*Staphylococcus epidermidis*	Knee arthroplasty	Acceptance of the application	Lack or non-adherence to protocols of prophylaxis and/or prevention of nosocomial infection
Court of L'Aquila - 2020	M – N.D.	Post-surgical infection	*Klebsiella pneumoniae*	Placement of ventricular drainages	Rejection of the application	No recognition of the cause link
Court of Rome - 2020	F – 75–80	Post-surgical infection	*Staphylococcus* (not specificied)	Excision of neoplasm	Rejection of the application	No recognition of the cause link
Court of Vicenza - 2020	F – 50–55	Post-surgical infection	*Staphylococcus con methicillin-resistant*	Arthrodesis	Acceptance of the application	Delay in diagnosis
Court of Salerno - 2020	F – N.D.	Post-surgical infection	*Pseudomonas aeruginosa + tafilococcus aureus*	Leg osteosynthesis	Acceptance of the application	Lack or non-adherence to protocols of prophylaxis and/or prevention of nosocomial infection
Court of Salerno - 2021	F – N.D.	Prosthesis infection	*Staphylococcus epidermidis + Aspergillus flavus + Acinetobacter baumannii*	Knee arthroplasty	Acceptance of the application	Lack or non-adherence to protocols of prophylaxis and/or prevention of nosocomial infection
Court of Ravenna - 2020	M – 65–70	Prosthesis infection	*Staphylococcus hemoliticus*	Knee arthroplasty	Acceptance of the application	Lack or non-adherence to protocols of prophylaxis and/or prevention of nosocomial infection
Court of Locri - 2020	F – N.D.	Post-surgical infection	*Candida* (not specificied)	Heart valve replacement	Acceptance of the application	Delay in diagnosis
Court of Firenze – 2021	M – N.D	Post-surgical infection	*Staphylococcus aureus*	Knee arthroplasty	Acceptance of the application	Lack or non-adherence to protocols of prophylaxis and/or prevention of nosocomial infection
Court of l'aquila - 2021	M– N.D.	Post-surgical infection	*Staphylococcus aureus*	Leg osteosynthesis	Rejection of the application	No recognition of the cause link
Court of Savona - 2021	F – N.D	Post-surgical infection	*Staphylococcus epidermidis*	Breast implant replacement	Rejection of the application	No recognition of the cause link
Court of Rome - 2020	M– 60-65	Other nosocomial infection	*Staphylococcus* (not specificied) *klebsiella*	Post traumatic bed rest	Rejection of the application	No recognition of the cause link
Court of Milan - 2021	M - N.D	Post-surgical infection	N.D.	Crystalline substitution	Acceptance of the application.	Lack or non-adherence to protocols of prophylaxis and/or prevention of nosocomial infection
Court of Rome - 2020	M - N.D	Post-surgical infection	*Staphylococcus aureus*	Rectal polyp removal	Acceptance of the application	Lack or non-adherence to protocols of prophylaxis and/or prevention of nosocomial infection

(Continued)

10.3389/fpubh.2022.1078719

TABLE 1 (Continued)

Court	Gender-age range of the applicant	Types of infection	Further specifications	Type of intervention / treatment	Outcome judgment	Reason for judgment
Court of Rome - 2020	M – N.D.	Post-surgical infection	*Acinetobacter emoliticus; Escherichia coli; Haemolyticus*	Hemicolectomy	Rejection of the application	No recognition of the cause link
Court of Torino - 2021	F – N.D	Post-surgical infection	*Klebsiella* (not specificied); *Enterobacter aerogens*	Cerebral vascular malforation excision	Acceptance of the application	Lack or non-adherence to protocols of prophylaxis and/or prevention of nosocomial infection
Court of Genova – 2020	M- N.D	Post-surgical infection	*Klebsiella pneumoniae*	Ureteroscopy	Acceptance of the application.	Lack or non-adherence to protocols of prophylaxis and/or prevention of nosocomial infection
Court of Viterbo - 2021	M - 0	Other nosocomial infection	*Escherichia coli*	Acute meningitis	Acceptance of the application.	Lack or non-adherence to protocols of prophylaxis and/or prevention of nosocomial infection
Court of Perugia - 2021	M – 55–60	Post-surgical infection	*Staphylococcus aureus*	Meniscectomy	Acceptance of the application.	Lack or non-adherence to protocols of prophylaxis and/or prevention of nosocomial infection
Court of Perugia - 2020	F – N.D	Post-surgical infection	N.D.	Knee arthroplasty	Acceptance of the application.	Lack or non-adherence to protocols of prophylaxis and/or prevention of nosocomial infection
Court of Rome - 2021	M – 80–85	Post-surgical infection	*Acinetobacter; Klebsiella pneumoniae; Staphylococcus aureus*	Excision of brain tumor	Acceptance of the application.	Lack or non-adherence to protocols of prophylaxis and/or prevention of nosocomial infection
Court of Ravenna - 2021	M – N.D	Post-surgical infection	*Staphylococcus epidermidis; Escherichia coli; Klebsiella pneumoniae*	Heart valve replacement	Rejection of the application	No recognition of the cause link
Court of Firenze - 2021	M – N.D	Post-surgical infection	*Staphylococcus saprofiticus*	Knee arthroplasty	Acceptance of the application.	Lack or non-adherence to protocols of prophylaxis and/or prevention of nosocomial infection
Court of Rome - 2020	F – 75-80	Post-surgical infection	N.D.	Vertebral decompression	Rejection of the application	No recognition of the cause link
Court Of Perugia - 2020	F – 55–60	Post-Surgical Infection	*Staphylococcus aureus Mrsa*	Treatment Of Hallux Valgus	Acceptance Of The Application.	Lack or non-adherence to protocols of prophylaxis and/or prevention of nosocomial infection
Court of Catania - 2020	F – 15–20	Prosthesis infection	*Staphylococcus* (not specificied)	Breast lift	Acceptance of the application.	Lack or non-adherence to protocols of prophylaxis and/or prevention of nosocomial infection – inadequate therapy

(Continued)

10.3389/fpubh.2022.1078719

TABLE 1 (Continued)

Court	Gender-age range of the applicant	Types of infection	Further specifications	Type of intervention / treatment	Outcome judgment	Reason for judgment
Court of Palermo - 2020	F – 70–75	Prosthesis infection	N.D.	Knee arthroplasty	Acceptance of the application.	Lack or non-adherence to protocols of prophylaxis and/or prevention of nosocomial infection
Court of Latina - 2020	F - N.D.	Post-surgical infection	*Staphylococcus epidermidis*	Knee arthroplasty	Acceptance of the application.	Lack or non-adherence to protocols of prophylaxis and/or prevention of nosocomial infection
Court of Milano - 2020	F - N.D.	N.D.	*Pseudomonas aeruginosa*	N.D.	Acceptance of the application.	Lack or non-adherence to protocols of prophylaxis and/or prevention of nosocomial infection
Court of Brindisi - 2020	M - N.D.	Other nosocomial infection	*Klebsiella pneumoniaea*	Intestinal excision	Rejection of the application	No recognition of the cause link
Court of Milano - 2020	M – 35–40	Prosthesis infection	*Escherichia coli*	Gluteoplastic	Acceptance of the application.	Lack or non-adherence to protocols of prophylaxis and/or prevention of nosocomial infection
Court of Pistoia - 2020	F – 55–60	Post-surgical infection	*Pseudomonas aeruginosa*	Cerebral malformation excision	Acceptance of the application.	Lack or non-adherence to protocols of prophylaxis and/or prevention of nosocomial infection
Court of Catania - 2020	F – 35–40	Post-surgical infection	N.D.	Foreign body removal	Acceptance of the application.	Lack or non-adherence to protocols of prophylaxis and/or prevention of nosocomial infection – inadequate therapy
Court of Torino - 2020	F – 80–85	Post-surgical infection	*Citrobacter freundii*	Crystalline substitution	Acceptance of the application.	Lack or non-adherence to protocols of prophylaxis and/or prevention of nosocomial infection
Court of Vicenza – 2021	F – 55–60	Post-surgical infection	*Serratia marcescens*	Brain tumor excision	Acceptance of the application.	Lack or non-adherence to protocols of prophylaxis and/or prevention of nosocomial infection
Court of Lecce - 2021	M - N.D.	Post-surgical infection	*Acinetobacter baumanii*	Cholecystectomy	Acceptance of the application.	Lack or non-adherence to protocols of prophylaxis and/or prevention of nosocomial infection
Court of Milano - 2021	F - N.D.	Prosthesis infection	*Staphylococcus aureus*	Knee arthroplasty	Acceptance of the application.	Lack or non-adherence to protocols of prophylaxis and/or prevention of nosocomial infection
Court of Palermo - 2021	F – 60–65	Post-surgical infection	*Staphylococcus aureus*	Arm osteosynthesis	Acceptance of the application.	Inadequate therapy
Court of Rieti - 2021	F – 60–65	Prosthesis infection	*Staphylococcus epidermidis*	Femoral osteosynthesis	Rejection of the application	No recognition of the cause link

(Continued)

10.3389/fpubh.2022.1078719

10.3389/fpubh.2022.1078719

TABLE 1 (Continued)

Court	Gender-age range of the applicant	Types of infection	Further specifications	Type of intervention / treatment	Outcome judgment	Reason for judgment
Court of Firenze - 2021	M - N.D.	Prosthesis infection	*Staphylococcus aureus*	Pacemaker implant	Acceptance of the application.	Delay in diagnosis
Court of Bologna - 2021	F - N.D.	Post-surgical infection	*Staphylococcus* (not specificied)	Knee arthroplasty	Acceptance of the application.	Lack or non-adherence to protocols of prophylaxis and/or prevention of nosocomial infection

ND, not determined.
The content of judgement and judge's decisions.

The most important characteristics of each sentence were considered, in addition to the competent Court and the date of the sentence, the sex and age of the plaintiff/appellant, the type of hospital infection, the pathogenic microorganism responsible for the infection, the type of intervention/treatment suffered by the patient, the outcome of the dispute and the reason for the sentence. These data are shown in Table 1.

Due to the severity of the Italian legislation on privacy and protection of personal data, it was not possible, in some cases, to infer some data, such as the registry data (e.g., age), of little relevance for the purpose of our discussion. However, in all the sentences, the motivation of the Judge's decision was exhaustively reported.

Data analysis

Statistical analysis was conducted using Microsoft Excel 2013 software (Microsoft Corporation Redmond, WA, USA) and IBM SPSS Statistic version 25 for Windows (IBM Corporation, Armonk, NY, USA). The categories examined were represented in percentage terms.

Results

We examined forty-one judgments issued by the relevant jurisprudence in Italy from 2020 to 2021 and relating to cases alleged health malpractice in the context of infections contracted in a hospital setting. Of all cases, 19 were brought by males (46.3%), while 22 by females (53.7%).

For 37 cases out of 41 (90.2%) the judgement regarded surgical site infections. By assessing surgical interventions, 18 (41%) were orthopedic, 6 (15%) neurosurgical, 5 (10%) general surgery, 3 (7%) plastic surgery, 3 (7%) cardiac surgery, 2 (5%) ophthalmological (Figure 1).

The most common pathogens involved were Gram positive bacteria belonging to *Staphylococcus* spp., 14 coagulase-negative Staphylococci (34.1%) and 10 *Staphylococcus aureus* (24.4%). The remaining were Gram negative bacteria, including multidrug resistant pathogens—6 (14.6%) *Klebsiella pneumoniae*, 3 (7.3%) *Pseudomonas aeruginosa* and 4 (9.8%) *Acinetobacter baumannii* -; 6 (14.6%) infections were caused by *Escherichia coli*, 1 (2.4%) *Citrobacter freundii*, 1 (2.4%) *Serratia marcescens*. In addition, 3 (7.3%) were caused by *Candida* spp. The pathogen was not isolated in 5 cases (12.2%). Polymicrobial infections were diagnosed in 6 cases (14.6%) (Table 2, Figure 2).

The judgments examined resulted in the claim of the plaintiff being accepted in 31 cases (75.6%) and in the rejection of the claim in 10 cases (24.4%) (Figure 3).

Analyzing the group of 24 infections caused by Gram-positive pathogens (3 polymicrobial), 17 (71%) were accepted: in 14 cases (82.4%) the reason for acceptance was the lack or

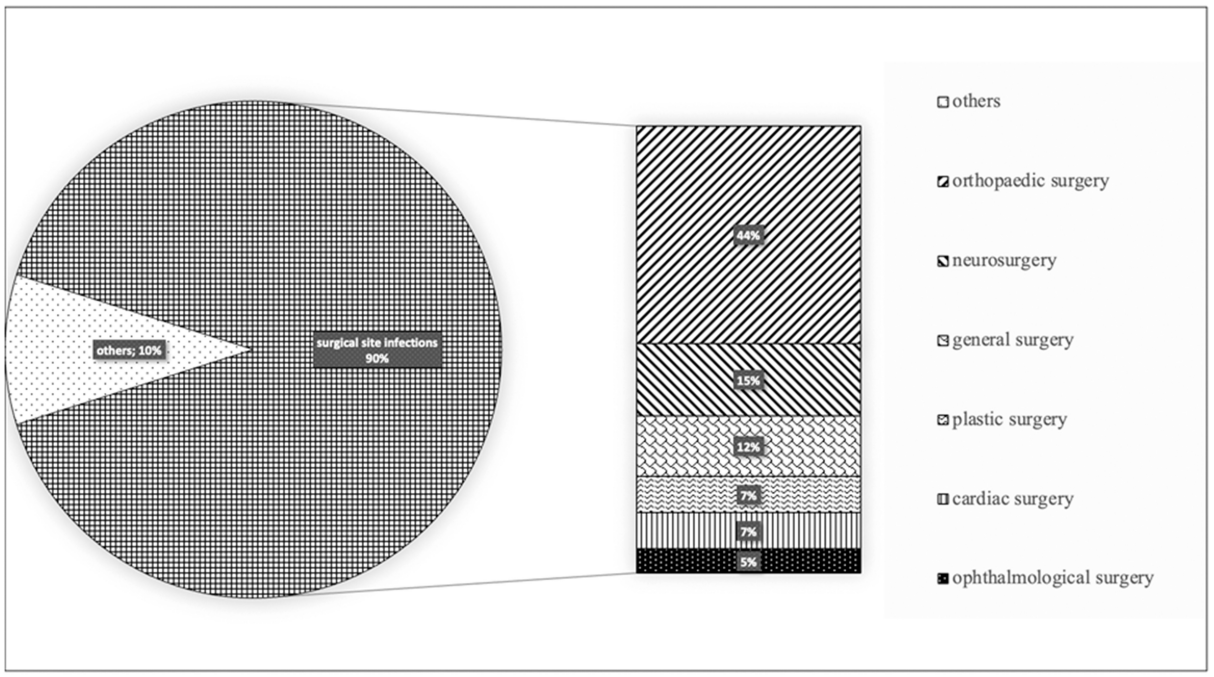

FIGURE 1
Types of nosocomial infections divided by hospital wards.

TABLE 2 Request for compensation 2020–2021 in Italy.

Pathogens	*N*	%
Coagulase – negative Staphylococci	14	34.1
Staphylococcus aureus	10	24.4
Klebsiella pneumoniae	6	14.6
Pseudomonas aeruginosa	3	7.3
Acinetobacter baumanii	4	9.8
Escherichia coli	6	14.6
Citobacter freundii	1	2.4
Serratia marcescens	1	2.4
Candida spp	3	7.3
Polymicrobial infections	6	14.6
N.d.	5	12.2

Nd, not determined.
Types of pathogens.

non-adherence to protocols of prophylaxis and/or prevention of nosocomial infection; in 2 cases (11.8%) and 1 case (5.9%) due to delay in diagnosis or inadequate therapy, respectively.

Among the 13 cases of infections caused by multidrug resistant organism, 9 (69.2%) were accepted due to the lack or non-adherence to protocols of prevention of nosocomial infection.

Finally, among the remaining, 9 were accepted: 8 (88.9%) due to lack or non-compliance to protocols and 1 (11.1%) due to diagnostic delay (Table 3).

Discussion

This works revised a series of sentences by various Italian Courts regarding surgical site/hospital acquired infection, in order to identify the major causes of acceptance of claims. In general, the lack or non-adherence to protocols of prophylaxis and/or prevention of nosocomial infection was the predominant cause of acceptance, while diagnostic delay or inadequate therapy caused a residual part of acceptance.

This case series is in line with previous studies showing that the majority of surgical site infections are caused by *Staphylococcus* spp, in particular by Staphylococcus aureus (14), both methicillin-susceptible (MSSA) and methicillin-resistant *Staphylococcus aureus* (MRSA), that are burdened by high rate of mortality and healthcare costs (15).

Consequently, bundles for prevention of *Staphylococcus aureus*-SSI (SA-SSI) for patients undergoing major clean surgery, including cardiothoracic and orthopedic devices implantation have been studied and implemented in several facilities (16, 17).

These preventive strategies are based on the following points: identification of SA carriers by nasal swab and

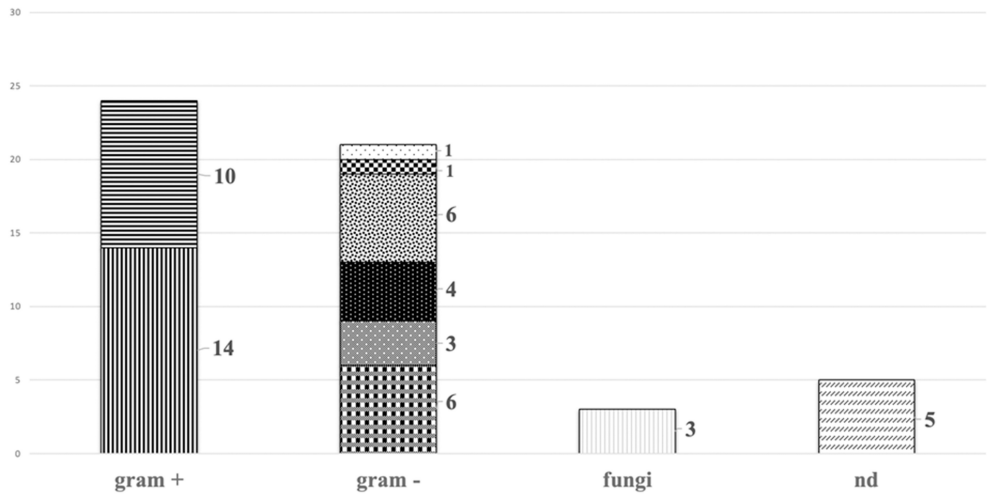

FIGURE 2
Types of pathogens.

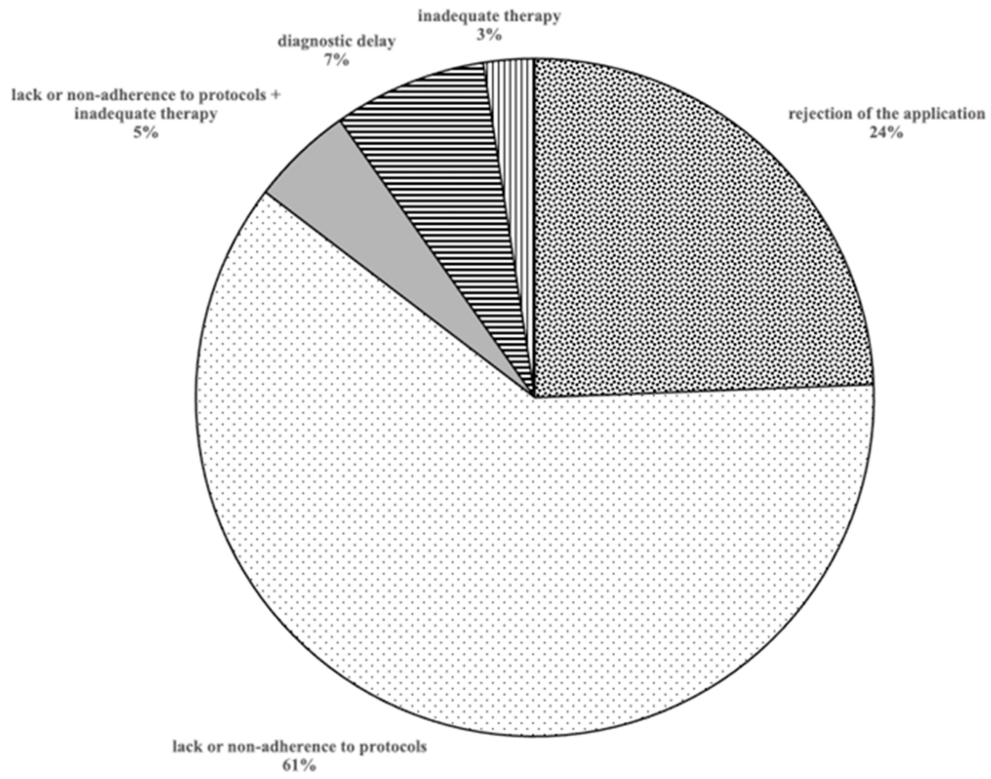

FIGURE 3
Reasons of acceptance or rejection of the requests of compensations.

de-colonization of carriers with mupirocin (intranasal) and chlorhexidine (for skin and hair) (18, 19); pre-operative prophylaxis including vancomycin for patients colonized by MRSA (20); education of healthcare personnel on hand hygiene and contact isolation for colonized patients.

Hence, given the strengthened of evidence about the efficacy of preventive measure for reduction of risk for SA-SSI, the

10.3389/fpubh.2022.1078719

TABLE 3 Request for compensation 2020–2021 in Italy.

	Gram positive pathogens (%)	Multidrug resistant pathogens (%)	Others pathogens (%)
Lack or non-compliance to protocols	14 (82.4%)	9 (69.2%)	8 (88.9%)
Diagnostic delay	2 (11.8%)	/	1 (11.1%)
Inadequate therapy	1 (5.9%)	/	/

Acceptance of the requests divided by pathogens.

neglect in adoption of protocol exposes the clinicians to sentences of responsibility for nosocomial infection. However, if a SA-SSI occurs, despite the proper implementation of strategies for infection prevention and control, health practitioners are exempted from responsibility; indeed, it should be considered that up to 55–70% of hospital acquired infection are potentially preventable (21).

Despite Gram positive bacteria are the mainly involved pathogens, even Gram-negative bacteria including *Enterobacterales* and non-fermentative rods may cause surgical site infections in cardiac surgery (22) and orthopedic surgery (23).

In particular, the diffusion of multidrug resistant Gram-negative bacteria (MDR-GNB) pose a high risk of SSI, increasing mortality rate, length of hospital stays, legal disputes and, in turn, costs. Indeed, standard antibiotic prophylaxis may be ineffective against Gram negative pathogens, especially in case of MDR-GNB. Still, protocols for prevention of GNB SSI are lacking, especially in Italy.

For instance, in the field of colorectal surgery, a carbapenem-based prophylaxis for carriers of extended spectrum Beta-Lactamase producing Enterobacteriaceae, usually unresponsive to common prophylaxis, showed to be effective in reducing incidence of SSI, if compared with standard protocols (24). However, the benefit of this approach in other setting is unknown, and standard prophylaxis with cephalosporins in non-colorectal surgery in patients with rectal colonization by ESBL could be considered appropriate. Beyond the choice of an appropriate antibiotic, the route of administration of antibiotic drug plays an important role in the effectiveness of prophylaxis. According to current literature, the antibiotic should be administered intravenously within 60–120' before skin incision, in order to achieve adequate blood and tissue concentration during surgical procedure, considering half-life of molecules (25). In this regard, antibiotic redosing during surgical intervention lasting more than 2 times the half-life of drug is effective in lowering risk of SSI (26). In addition, the combination of oral and intravenous antibiotic prophylaxis has shown to be a viable approach in reducing rate of SSI in colorectal elective surgery (27). Still, antibiotic prophylaxis should be discontinued within 24–48 h after surgical procedure, because longer duration is not associated with a lower rate of SSI, but rather with increase of adverse events and increased risk of nosocomial infections (28). Nevertheless, despite the scarcity of protocols for prevention of GNB-SSI in major clean surgery, the clinicians are not free from responsibility in case of MDR infection, if measurements of stewardship and infection control are not properly applied.

Furthermore, if on the one hand the protocols for the prevention of nosocomial infections need to be implemented and continuously updated, also in relation to the biological variability of the microorganisms involved, on the other hand Health Facilities were often condemned as they were not able to provide documentary evidence of the use of these protocols. This occurred regardless of whether the doctors had actually taken steps to prevent the onset of hospital infection. In Italy the legal rules for sharing the burden of proof are stringent. The legal principles governing the responsibility of healthcare workers and the health facilities are linked to the "hospitalization contract." In the case of non-compliance, the provisions of art. 1,218 "liability of the debtor" and art. 1,228 "liability for acts auxiliaries" of the Civil Code were applied. On the basis of these dictates, Healthcare Facility must demonstrate that it has fulfilled all the specific obligations (disinfection, sterilization, hand washing, environmental monitoring) or, alternatively, the absence of the causal link between the alleged breach and damage (i.e., between the conduct and the occurrence of the infection). This principle constitutes an application of the art. 1,218 of the Italian Civil Code which divides the burden of proof in the contractual context to which governs civil litigation in the field of health liability.

However, due to the complexity of all the procedures, it is challenging for the structure to demonstrate that it has actually carried out the proper conduct.

Although infections might not be attributable to the hospital, once it is demonstrated that a patient has contracted a nosocomial infection, the hospital must prove the adoption of all the necessary measures for the correct sanitation, to avoid contamination of patients by nosocomial pathogens.

This aspect justifies the divergence between our cases and the results of civil trials for medical liability in Italy. Data extracted from Consulcesi, an Italian company operating in the field of legal health assistance and health professionals, report that about 66% of civil trials in the field of health responsibility in Italy are rejected (29). In our case series, however, only 24.4% of the cases examined resulted in a non-acceptance of the plaintiff's request.

10.3389/fpubh.2022.1078719

TABLE 4 Incidence of surgical site infections per major types of surgical procedures in Italy and European countries.

Type of surgical procedure	Incidence in Italy	State with lowest incidence in EU/EAA	State with higher incidence in EU/EAA	Incidence in EU/EAA	Difference (Italy vs. EU/EAA)
In-hospital incidence per 1,000 post-operative days (N/1,000)					
Coronary artery bypass graft	1.3	Norway = 0.7	Lithuania = 3.2	1.2	0.1
Cholecystectomy	0.9	Lithuania = 0.5	England = 7.6	1.4	−0.5
Colon surgery	3.1	Lithuania = 2.7	Portugal = 10.2	4.9	−1.8
Cesarean section	0.1	Italy = 0.1	Estonia = 1.7	0.6	−0.5
Hip prosthesis	0.3	Finland = 0.2	Hungary = 0.9	0.3	0.0
Knee prosthesis	0.2	France = 0.1	Portugal = 0.4	0.1	0.1
Laminectomy	0.3	Germany = 0.2	Hungary = 2.2	0.4	−0.1
Incidence of SSI per 100 operations					
Coronary artery bypass graft	2.4	England = 2.2	Lithuania = 5.5	2.7	−0.3
Cholecystectomy	1.0	Lithuania = 0.4	England = 4.0	1.5	−0.5
Colon surgery	5.0	Lithuania = 3.9	Portugal = 16.2	8.5	−3.5
Cesarean section	0.5	Italy = 0.5	England = 5.3	1.9	−1.4
Hip prosthesis	0.8	Ireland = 0.4	Norway = 2.2	1.0	−0.2
Knee prosthesis	0.6	England = 0.2	Hungary = 2.7	0.5	0.1
Laminectomy	1.0	Ireland = 0.2	Hungary = 2.7	0.7	0.3

EU/EAA = European Union/ European Economic Area.

According to ECDC surveillance atlas of infectious diseases of 2017, SSI occur after 2.4% of surgical intervention in Italy, while European incidence is 2.7 % (30). The rate of SSI may be further reduced throughout the implementation of national surveillance programs, with the aim to identify the appropriate intervention to reach the objective (31).

According to these considerations and our data, a stronger effort should be made in terms of risk management perspective in order to: ensure the application of documented protocols for prevention of SSI by Gram positive; develop protocols to prevent GNB-SSI, based on local and regional epidemiology and risk assessment; strengthen infection control and antimicrobial stewardship programs. The application of SSI prevention bundle, including pre-operative procedures (skin decolonization with mupirocin and chlorhexidine for SA carriers, appropriate administration of antibiotic prophylaxis, proper washing of healthcare personnel and surgical room), intraoperative procedures (adequate blood oxygenation, glycaemia, normothermia) is associated with lower risk of SSI. The implementation of educational programs for healthcare personnel, along with periodic performance monitoring and multidisciplinary audit could represent some applicable strategy to promote the application of good clinical practice for prevention of SSI (32, 33).

In this scenario, the involvement of patients in informative programs is of great relevance. Healthcare professionals should educate patients about infectious risk and foster correct behavior for its decrease, including preoperative shower, *S. aureus* decolonization, stop smoking, and correct wound care after surgery (34).

Additionally, other important strategies should be implemented at hospital-level to reduce the risk of hospital acquired infections: (i) infection control and preventions protocols in all wards (35); (ii) controlled prescription of antimicrobial therapies, especially those with high selective pressure (36); (iii) dedicated microbiological alert in case of severe infections, including bloodstream infections and/or detection of multidrug resistant pathogens (37).

Interestingly, by comparing data of incidence of surgical site infections (Table 4), based on European Center for Disease Prevention and Control (eCDC) surveillance data of the year 2017 (38), the incidence of infective complications after surgery may significantly differ between different Countries and different types of surgical procedures. This support the need of tailoring specific preventing strategies, in addition to aforementioned ones, according to local epidemiology.

If this proactive approach is fundamental in public health, it would be equally useful to raise the awareness of healthcare personnel toward medico-legal issues. Furthermore, the Italian Law requires to demonstrate what has been done by the hospital

and this consequently means that hospital must keep the complete documentation of the preventive activities.

Finally, to encourage a correct reactive approach to the nosocomial infection, the contribution of an infectious disease specialist in order to avoid that any infection could be simplistically charged to a health responsibility.

Data availability statement

The original contributions presented in the study are included in the article/supplementary material, further inquiries can be directed to the corresponding authors.

Author contributions

ASa, AD, ST, and MM contributed to conception and design of the study. PC and ML organized the database. SD performed the statistical analysis. FM, EG, ASt, DB, and LD wrote sections of the manuscript. All authors contributed to manuscript revision, read, and approved the submitted version.

Funding

This research was funded by Puglia Regional Observatory for Epidemiology.

Conflict of interest

The authors declare that the research was conducted in the absence of any commercial or financial relationships that could be construed as a potential conflict of interest.

Publisher's note

All claims expressed in this article are solely those of the authors and do not necessarily represent those of their affiliated organizations, or those of the publisher, the editors and the reviewers. Any product that may be evaluated in this article, or claim that may be made by its manufacturer, is not guaranteed or endorsed by the publisher.

References

1. Moroni M, Esposito R, Antinori S. *Infectious diseases, 8th Edn.* Milan: Edra editions (2010). p. 947–55.

2. Kirkland KB, Briggs JP, Trivette SL, Wilkinson WE, Sexton DJ. The impact of surgical-site infections in the 1990s: attributable mortality, excess length of hospitalization, and extra costs. *Infect Control Hosp Epidemiol.* (1999) 20:725–30. doi: 10.1086/501572

3. Hoang SC, Klipfel AA, Roth LA, Vrees M, Schechter S, Shah N. Colon and rectal surgery surgical site infection reduction bundle: to improve is to change. *Am J Surg.* (2019) 217:40–5. doi: 10.1016/j.amjsurg.2018.07.008

4. Brunner S, Liesenberg J, Fourie L, Metzger J, Scheiwiller A, Zschokke I, et al. Implementation of a bundle of care in colorectal surgery to reduce surgical site infections successfully at cantonal hospital lucerne: study protocol for a prospective observational study. *Int J Surg Protoc.* (2021) 25:220–6. doi: 10.29337/ijsp.150

5. Agency for Healthcare Research and Quality. *AHRQ National Scorecard on Hospital-Acquired Conditions*. Available online at: http://www.ahrq.gov/sites/default/files/wysiwyg/professionals/quality-patient-safety/pfp/natlhacratereport-rebaselining2014-2016_0.pdf (accessed September 02, 2022).

6. Centers for Disease Control and Prevention. *Guidelines for Environmental Infection Control in Health-Care Facilities: Recommendations of CDC and the Healthcare Infection Control Practices Advisory Committee (HICPAC)*. Available online at: http://www.cdc.gov/hicpac/pdf/guidelines/eic_in_hcf_03.pdf (accessed September 02, 2022).

7. Rutala WA, Weber DJ, the Healthcare Infection Control Practices Advisory Committee (HICPAC). *Guideline for Disinfection and Sterilization in Healthcare Facilities.* (2008). Available online at: http://www.cdc.gov/hicpac/pdf/guidelines/disinfection_nov_2008.pdf (accessed September 02, 2022).

8. Haley RW, Quade D, Freeman HE, Bennett JV, The SENIC Project. Study on the efficacy of nosocomial infection control (SENIC Project) Summary of study design. *Am J Epidemiol.* (1980) 111:472–85. doi: 10.1093/oxfordjournals.aje.a112928

9. Siegel JD, Rhinehart E, Jackson M, Chiarello L. *The Healthcare Infection Control Practices Advisory Committee, 2007 Guideline for Isolation Precautions: Preventing Transmission of Infectious Agents in Healthcare Settings*. Available online at: http://www.cdc.gov/infectioncontrol/guidelines/isolation/index.html (accessed September 02, 2022).

10. Marrone M, Stellacci A, Caricato P, Leonardelli M, De Luca BP, Buongiorno L, et al. Nosocomial infection. *J Leg Ethical Regul Issues.* (2021) 24:1–10.

11. Dell'Erba A, Quaranta R, Di Nunno N, Vimercati F. The role of the forensic doctor in clinical risk management. *Med Law Rev.* (2003) 2:351–64.

12. Cucci M, Casali MB. Le infezioni nosocomiali: il contributo del medico legale. *Riv It Med Leg.* (2009) 1:17–37.

13. Ministry of Health. *How to Reduce the Impact of ICAs.* (2019). Available online at: https://www.salute.gov.it/portale/malattieInfettive/dettaglioContenutiMalattieInfettive.jsp?lingua=italiano&id=4807&area=Malattie%20infettive&menu=vuoto (accessed September 05, 2022).

14. Jenks PJ, Laurent M, McQuarry S, Watkins R. Clinical and economic burden of surgical site infection (SSI) and predicted financial consequences of elimination of SSI from an English hospital. *J Hosp Infect.* (2014) 86:24e33. doi: 10.1016/j.jhin.2013.09.012

15. Weigelt JA, Lipsky BA, Tabak YP, Derby KG, Kim M, Gupta V. Surgical site infections: causative pathogens and associated outcomes. *Am J Infect Control.* (2010) 38:112–20. doi: 10.1016/j.ajic.2009.06.010

16. Awad SS, Palacio CH, Subramanian A, Byers PA, Abraham P, Lewis DA, et al. Implementation of a methicillin-resistant Staphylococcus aureus (MRSA) prevention bundle results in decreased MRSA surgical site infections. *Am J Surg.* (2009) 198:607–10. doi: 10.1016/j.amjsurg.2009.07.010

17. Kawamura H, Matsumoto K, Shigemi A, Orita M, Nakagawa A, Nozima S, et al. A bundle that includes active surveillance, contact precaution for carriers, and cefazolin-based antimicrobial prophylaxis prevents methicillin-resistant Staphylococcus aureus infections in clean orthopedic surgery. *Am J Infect Control.* (2016) 44:210–4. doi: 10.1016/j.ajic.2015.09.014

18. Humphreys H, Becker K, Dohmen PM, Petrosillo N, Spencer M, van Rijen M, et al. Staphylococcus aureus and surgical site infections: benefits of screening and decolonization before surgery. *J Hosp Infect.* (2016) 94:295–304. doi: 10.1016/j.jhin.2016.06.011

19. Bode LG, Kluytmans JA, Wertheim HF, Bogaers D, Vandenbroucke-Grauls CMJE, Roosendaal R, et al. Preventing surgical-site infections in nasal carriers of *Staphylococcus aureus*. *N Engl J Med.* (2010) 362:9–17. doi: 10.1056/NEJMoa0808939

20. Bull AL, Worth LJ, Richards MJ. Impact of vancomycin surgical antibiotic prophylaxis on the development of methicillin-sensitive Staphylococcus aureus surgical site infections: report from Australian Surveillance Data (VICNISS). *Ann Surg.* (2012) 256:1089–92. doi: 10.1097/SLA.0b013e31825fa398

21. Bearman G, Doll M, Cooper K, Stevens MP. Hospital infection prevention: how much can we prevent and how hard should we try? *Curr Infect Dis Rep.* (2019) 21:2. doi: 10.1007/s11908-019-0660-2

22. Berríos-Torres SI Yi SH, Bratzler DW, Ma A, Mu Y, Zhu L, et al. Activity of commonly used antimicrobial prophylaxis regimens against pathogens causing coronary artery bypass graft and arthroplasty surgical site infections in the United States, 2006–2009. *Infect Control Hosp Epidemiol.* (2014) 35:231–9. doi: 10.1086/675289

23. Norton TD, Skeete F, Dubrovskaya Y, Philips MS. Bosco JD, Mehta SA. Orthopedic surgical site infections: analysis of causative bacteria and implications for antibiotic stewardship. *Am J Orthop.* (2014) 43:E89–92.

24. Nutman A, Temkin E, Harbarth S, Carevic B, Ris F, Fankhauser-Rodriguez C, et al. Personalized ertapenem prophylaxis for carriers of extended-spectrum β-lactamase-producing enterobacteriaceae undergoing colorectal surgery. *Clin Infect Dis.* (2020) 70:1891–7. doi: 10.1093/cid/ciz524

25. de Jonge SW, Boldingh QJJ, Koch AH, Daniels L, de Vries EN, Spijkerman IJB, et al. Timing of preoperative antibiotic prophylaxis and surgical site infection: TAPAS, an observational cohort study. *Ann Surg.* (2021) 274:e308–14. doi: 10.1097/SLA.0000000000003634

26. Wolfhagen N, Boldingh, QJJ, de Lange M, Boermeester MA, de Jonge SW. Intraoperative redosing of surgical antibiotic prophylaxis in addition to preoperative prophylaxis versus single-dose prophylaxis for the prevention of surgical site infection: a meta-analysis and GRADE recommendation. *Ann Surgery*. (2022) 275:1050–7. doi: 10.1097/SLA.0000000000005436

27. Sangiorgio G, Vacante M, Basile F, Biondi A. Oral and Parenteral vs. parenteral antibiotic prophylaxis for patients undergoing laparoscopic colorectal resection: an intervention review with meta-analysis. *Antibiotics.* (2021) 11:21. doi: 10.3390/antibiotics11010021

28. Nagata K, Yamada K, Shinozaki T, Miyazaki T, Tokimura F, Tajiri Y, et al. Effect of antimicrobial prophylaxis duration on health care-associated infections after clean orthopedic surgery: a cluster randomized trial. *JAMA Netw Open.* (2022) 5:e226095. doi: 10.1001/jamanetworkopen.2022.6095

29. Consulcesi data. *The Numbers of the Doctor-Patient Legal Dispute.* (2019). Available online at: https://www.consulcesi.it/blog/tutele_diritti_medico/i-numeri-del-contenzioso-legale-medici-pazienti (accessed September 10, 2022).

30. ECDC. *Surveillance Atlas of Infectious Disease.* (2017). Available online at: https://atlas.ecdc.europa.eu/public/index.aspx?Dataset=27&HealthTopic=77 (accessed December 10, 2022).

31. Marchi M, Pan A, Gagliotti C, Morsillo F, Parenti M, Resi D, et al. The Italian national surgical site infection surveillance programme and its positive impact, 2009 to 2011. *Euro Surveill.* (2014) 19:20815. doi: 10.2807/1560-7917.ES2014.19.21.20815

32. Koek MBG, Hopmans TEM, Soetens LC, Wille JC, Geerlings SE, Vos MC, et al. Adhering to a national surgical care bundle reduces the risk of surgical site infections. *PLoS ONE.* (2017) 12:e0184200. doi: 10.1371/journal.pone.0184200

33. Tomsic I, Heinze NR, Chaberny IF, Krauth C, Schock B, von Lengerke T. Implementation interventions in preventing surgical site infections in abdominal surgery: a systematic review. *BMC Health Serv Res.* (2020) 20:236. doi: 10.1186/s12913-020-4995-z

34. Tartari E, Weterings V, Gastmeier P, Rodríguez Baño J, Widmer A, Kluytmans J, et al. Patient engagement with surgical site infection prevention: an expert panel perspective. *Antimicrob Resist Infect Control.* (2017) 6:45. doi: 10.1186/s13756-017-0202-3

35. Ariyo P, Zayed B, Riese V, Anton B, Latif A, Kilpatrick C, et al. Implementation strategies to reduce surgical site infections: a systematic review. *Infect Control Hosp Epidemiol.* (2019) 40:287–300. doi: 10.1017/ice.2018.355

36. Al-Omari A, Al Mutair A, Alhumaid S, Salih S, Alanazi A, Albarsan H, et al. The impact of antimicrobial stewardship program implementation at four tertiary private hospitals: results of a five-years pre-post analysis. *Antimicrob Resist Infect Control.* (2020) 9:95. doi: 10.1186/s13756-020-00751-4

37. Morency-Potvin P, Schwartz DN, Weinstein RA. Antimicrobial stewardship: how the microbiology laboratory can right the ship. *Clin Microbiol Rev.* (2016) 30:381–407. doi: 10.1128/CMR.00066-16

38. *European Centre for Disease Prevention and Control, Surveillance Data – Year.* (2017). Available online at: https://www.ecdc.europa.eu/en/surgical-site-infections/surveillance-and-disease-data (accessed December 09, 2022).

frontiers | Frontiers in Public Health

TYPE Case Report
PUBLISHED 06 January 2023
DOI 10.3389/fpubh.2022.1073893

OPEN ACCESS

EDITED BY
Ana Afonso,
Universidade NOVA de Lisboa, Portugal

REVIEWED BY
Nomonde Mvelase,
University of KwaZulu-Natal, South Africa
Gulsen Ozkaya Sahin,
Consultant, Lund, Sweden

*CORRESPONDENCE
Zheng-Xiang Gao
✉ GAOZX84@163.com

†These authors have contributed equally to this work

SPECIALTY SECTION
This article was submitted to Infectious Diseases: Epidemiology and Prevention, a section of the journal Frontiers in Public Health

RECEIVED 19 October 2022
ACCEPTED 15 December 2022
PUBLISHED 06 January 2023

CITATION
Peng L-W, Gao Y-J, Cui Y-l, Xu H and Gao Z-X (2023) Missed opportunities for screening congenital syphilis early during pregnancy: A case report and brief literature review.
Front. Public Health 10:1073893.
doi: 10.3389/fpubh.2022.1073893

Missed opportunities for screening congenital syphilis early during pregnancy: A case report and brief literature review

Lei-Wen Peng[1,2†], Yu-Jie Gao[3†], Ya-li Cui[1,2,3], Huang Xu[3] and Zheng-Xiang Gao[1,2*]

[1]Department of Laboratory Medicine, West China Second University Hospital, Sichuan University, Chengdu, China, [2]Key Laboratory of Birth Defects and Related Diseases of Women and Children, Sichuan University, Ministry of Education, Chengdu, Sichuan, China, [3]Department of Laboratory Medicine, Meishan Women and Children's Hospital, Alliance Hospital of West China Second University Hospital, Sichuan University, Meishan, China

Congenital syphilis is a significant public health problem. Pregnant women infected with Treponema pallidum present with various clinical manifestations, mainly including skin or visceral manifestations. The extensive clinical manifestations of *T. pallidum* infection mimic those of many other diseases during pregnancy, which may lead to delayed diagnosis and serious consequences. We report a case of fetal *T. pallidum* infection and premature delivery in a woman whose syphilis screening was negative at 16 weeks of gestation. Despite presenting to the dermatologist at 24 weeks of gestation with maculopapular rash which is usually associated with secondary syphilis, the diagnosis of syphilis was not considered. This case shows that even if early syphilis screening of pregnant women is negative, they may still get infected with *T. pallidum* later on in pregnancy. Therefore, in patients presenting with a rash without an obvious cause, *T. pallidum* infection should be excluded. The health status of patients' spouses should be assessed during pregnancy. Additionally, perinatal health education is necessary for women and their spouses during pregnancy. The abovementioned factors could reduce the probability of *T. pallidum* infection in pregnant women and their infants.

KEYWORDS

awareness, congenital syphilis, pregnancy, prevention, *Treponema pallidum*, prenatal screening

Introduction

Syphilis is a chronic infectious disease caused by *Treponema pallidum*. In recent years, the incidence of syphilis has increased annually (1). Congenital syphilis is caused by *T. pallidum* infection and is generally transmitted vertically. If a pregnant woman with active syphilis is not effectively treated, *T. pallidum* can cross the placenta and infect the fetus *in utero*. Mother-to-child transmission of syphilis imposes heavy economic and medical burdens worldwide. The direct medical cost of mother-to-child transmission of syphilis is 309 million dollars per year (2). *T. pallidum* can infect women and be

transmitted to the fetus at any stage of pregnancy, causing lesions in multiple organs and resulting in stillbirth, abortion, neonatal death, premature birth, low birth weight and other adverse pregnancy outcomes (3). Compared with uninfected pregnant women, pregnant women with syphilis are 12 times more likely to experience adverse pregnancy outcomes; those who receive treatment still have a 2.5 times higher risk than seronegative women (4). Among all global infectious diseases associated with stillbirth, fetal syphilis accounts for a large proportion of stillbirths (5). Therefore, early screening and treatment of pregnant women could significantly reduce the incidence of congenital syphilis. In this case study, we report a case of premature delivery and fetal congenital syphilis in a pregnant woman whose syphilis screening was negative in early pregnancy. It is important to recognize that congenital syphilis may still occur in countries with high prenatal screening rates, and women might be infected with *T. pallidum* between the time of testing during pregnancy and childbirth. Here, we review the literature on the epidemiology, transmission, clinical manifestations, diagnosis and prevention of *T. pallidum* infection and subsequently discuss the key information of this case.

Case presentation

A premature baby boy was born at 34 weeks 1/7 days of pregnancy to a G2P2, 29-year-old mother. The infant had Apgar scale scores of 10, 10, and 10 at 1, 5, and 10 min, respectively. The birth weight was 2,200 g. The pregnant woman went to the hospital for prenatal care at 16 weeks 1/7 days of pregnancy, and serological tests for hepatitis B, hepatitis C, human immunodeficiency virus (HIV) and syphilis by chemiluminescent immunoassay (CLIA) were negative. The oral glucose tolerance testing (OGTT) results were as follows: fasting: 5.8 mmol/L, 1 h after meal: 11.7 mmol/L, and 2 h after meal: 11.8 mmol/L. A diagnosis of gestational diabetes was made, and diet control was recommended. At 24 weeks of gestation, the woman developed a generalized body maculopapular rash that was non-itchy. She went to the dermatology department of the local hospital, and the dermatologist confirmed that the HIV, hepatitis B and syphilis screening results were negative at 3 months of pregnancy. The maculopapular rash was considered to be related to pregnancy, and it subsided without treatment. The pregnant woman went to the hospital for prenatal care at 32 weeks 4/7 days of pregnancy, and the treponemal serological test (CLIA) was positive. The toluidine red unheated serum test (TRUST) titer was 1:16. Subsequently, her husband was screened for syphilis. The treponemal serological test (CLIA) was positive, and the TRUST titer was 1:32. The woman reported that she had unprotected sexual behaviors with her husband during pregnancy. Both individuals were treated with 2.4 million U of benzathine penicillin by intramuscular injection every 7 days for a total of three cycles.

At 34 weeks 1/7 days of pregnancy, the pregnant woman presented with abnormal vaginal bleeding. She was diagnosed with threatened premature labor and placental abruption was suspected; subsequently, the newborn was delivered by cesarean section. After birth, the newborn was transferred to the Neonatology Department for further care and treatment. Physical examination revealed the following: temperature of 36.3 C, pulse of 132 beats/min, respiration rate of 45 breaths/min, strong cry, and no petechiae or ecchymosis on his skin. Physical examination of the lungs, heart and abdomen was normal. The muscle tension of his extremities was normal. The four main primitive reflexes, namely, the sucking reflex, grasp reflex, rooting reflex and Moro reflex, could be drawn out completely. The laboratory test results are shown in Table 1. Skull ultrasound showed no abnormalities. The infant had no clinical manifestations of neurosyphilis, a nervous system physical examination showed no abnormalities. The results of CSF white blood cell and total protein tests were normal. Therefore, CSF testing for syphilis was not performed. After admission, the infant received an intravenous penicillin G solution (50,000 units/kg per 6 h) for 10 days and was then re-examined for syphilis. The treponemal serological test (CLIA) was positive, the TRUST titer was 1:16, and he was discharged home with his parents. When the infant was 6 months old, his parents brought him to the hospital for follow-up. His growth and development indicators were similar to those of normal children. The treponemal serological test was positive, and the TRUST was negative. The clinical manifestations and syphilis detection timeline of the mother and the patient are shown in Figure 1. We obtained informed consent from the infant's parents for the publication of this case report.

Review and discussion

Epidemiology

The World Health Organization (WHO) estimates that ~2 million pregnant women are infected with syphilis each year and that the incidence of congenital syphilis is ~700,000–1.5 million. Syphilis in pregnancy kills an estimated 650,000 fetuses and newborns in developing countries annually (6). In 2016, the global prevalence of maternal syphilis was 0.7%, with a total of 661,000 congenital syphilis cases worldwide, resulting in 355,000 adverse pregnancy outcomes. Among these adverse pregnancy outcomes, 203,000 (57%) occurred in pregnant women who received antenatal care but did not undergo syphilis screening, 55,000 (16%) occurred in women who underwent syphilis screening but did not receive treatment, and 23,000 (6%) occurred in women who underwent screening and received treatment (7).

10.3389/fpubh.2022.1073893

TABLE 1 Laboratory test results.

Laboratory test	Value	Reference
Complete blood count		
White blood cells (×109/L)	12.36	5.30–12.00
Neutrophil percentage (%)	38.00	9.4–30.4
Lymphocyte percentage (%)	56.70	55.6–82.6
Red blood cells (×1,012/L)	3.89	5.10–5.20
Hemoglobin (g/L)	155.00	129–151
Platelets (×109/L)	136.00	100–300
Blood biochemistry		
Total bilirubin (μmol/L)	68.90	2.00–210.00
Direct bilirubin (μmol/L)	22.50	<10.00
Indirect bilirubin (μmol/L)	46.40	<193.00
Alanine aminotransferase (U/L)	9.00	<49.00
Aspartate aminotransferase (U/L)	38.00	<40.00
Total protein (g/L)	46.00	46.00–70.00
Albumin (g/L)	29.70	28.00–44.00
Globulin (g/L)	16.30	18.00–26.00
Alkaline phosphatase (U/L)	123.00	108.00–212.00
Cholinesterase (U/L)	5,991.00	4,000.00–12,600.00
C-reactive protein (mg/L)	<5.00	0.00–10.00
Glucose (mmol/L)	6.24	3.90–11.10
K+ (mmol/L)	5.27	3.50–5.50
Na+ (mmol/L)	140.40	132.00–146.00
Cl- (mmol/L)	97.20	99.00–110.00
Ca2+ (mmol/L)	1.61	1.10–2.67
Urea nitrogen (mmol/L)	4.22	3.20–8.20
Creatinine (μmol/L)	56.00	17.30–57.60
Uric acid (μmol/L)	547.00	137.00–488.00
Cystatin C (mg/L)	1.2	<1.02
Cerebrospinal fluid test		
Total cell count (×106/L)	5.00	0.00–30.00
White blood cells (×106/L)	5.00	0.00–30.00
Red blood cells (×106/L)	0.00	0.00–0.00
Glucose (mmol/L)	1.97	2.50–4.40
Cl- (mmol/L)	114.10	120.00–130.00
Total protein (g/L)	0.42	0.15–0.45
Cerebrospinal fluid culture	Negative	Negative
Blood culture	Negative	Negative
Treponemal serological test	Positive	Negative
Toluidine red unheated serum test (TRUST)	1:64	Negative

According to the latest statistics released by the Centers for Disease Control and Prevention (CDC) in 2021, the incidence of congenital syphilis in the United States has increased dramatically since 2012. A total of 1,870 cases of congenital syphilis were reported in 2019. The rate of congenital syphilis infection in 2019 was 41% higher than that in 2018 and 477% higher than that in 2012. From 2015 to 2019, the incidence of congenital syphilis increased by 291.1%. Most cases were due to delayed or a lack of screening in pregnant women and delayed or inadequate treatment (8). In most European Union (EU)/European Economic Area (EEA) countries, the incidence and number of congenital syphilis infections have remained low due to effective national antenatal screening programs and control of syphilis transmission in heterosexual populations. In 2019, only 13 EU countries reported 72 confirmed cases of congenital syphilis, which was an increase of 6 from 2018 (9). In China, the number of congenital syphilis cases ranged from 2.6 cases per 100,000 live births in 2000 to 69.9 in 2013 (10). The incidence of syphilis in China has increased annually, from 30.9 cases per 100,000 in 2014 to 38.4 in 2019, with an average annual growth of 4.4%. China's National Health Commission has strengthened and improved prevention strategies targeting mother-to-child transmission of syphilis, and the incidence of congenital syphilis decreased significantly from 54.1 cases per 100,000 live births in 2014 to 11.9 in 2019 (11).

Developed countries, such as EU/EEA countries, and developing countries, such as China, have reduced mother-to-child syphilis transmission, as evidenced by the low incidence of congenital syphilis, through high coverage of prenatal screening and treatment of infected pregnant women (12). This indicates that appropriate antenatal screening programs and congenital syphilis case reporting systems are very effective and necessary in eliminating mother-to-child syphilis transmission and reducing the rate of congenital syphilis.

Mother-to-child transmission

T. pallidum can enter the fetal blood circulation through the placenta and cause congenital syphilis. The risk of syphilis transmission to the fetus through the placenta is 60–80%, and the risk increases in the second half of pregnancy. Neonatal exposure to secretions, blood or genital lesions of women with syphilis during delivery could also result in *T. pallidum* infection. Congenital syphilis most commonly occurs in infants of infected women who have not received adequate treatment or any treatment. Mother-to-child transmission can occur at any time during pregnancy, and the risk of transmission is related to the maternal stage of infection, which is relatively high at 60% to 90% in untreated women with primary or secondary syphilis, 40% in women with early latent syphilis, and <10% in women

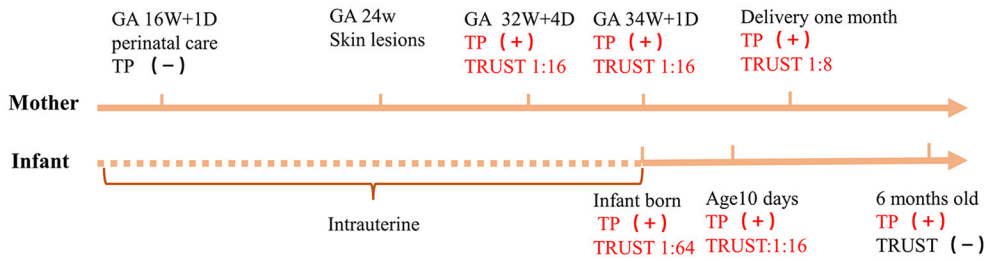

FIGURE 1
Timeline of the newborn and his mother. +, indicates a positive result; −, indicates a negative result; TP, treponemal serological test; GA, gestational age; 16W + 1D = 16 weeks 1/7 days, 32W + 4D = 32 weeks 4/7 days, 34W + 1D = 34 weeks 1/7 days.

with late latent syphilis (13). Pregnancy syphilis can be divided into primary syphilis, secondary syphilis, tertiary syphilis and latent syphilis. A chancre often develops in primary syphilis. The most common symptom of secondary syphilis is a rash that is widely distributed on the skin and mucosa. The most common rash types are maculopapular (50–70%), papular (12%), macular (10%) and annular papular (6–14%). The rash typically appears on the palms and soles of the feet (14, 15). Tertiary syphilis mainly manifests as severe damage to the bone, skin, mucous membranes or other organs.

In this case, the mother had no syphilis-related clinical features before pregnancy, she denied a history of *T. pallidum* infection or other sexually transmitted diseases, and she had unprotected sexual behaviors with her husband during pregnancy. The pregnant woman went to the medical institution for prenatal care in early pregnancy and was screened for sexually transmitted diseases, including syphilis, and no abnormalities were found. At ∼24 weeks of gestation, the pregnant woman presented with a non-itchy maculopapule with no obvious cause. She went to the dermatology department of the local hospital, and syphilis infection was not considered in the diagnosis. Although skin abnormalities may be one of the clinical manifestations of syphilis infection, the lesions of syphilis (which are known to be great imitators) are often mistaken for those of other infections, and early diagnosis may be hampered.

The clinical features of syphilis in pregnant women are the same as those in non-pregnant people. However, latent syphilis is most frequently reported in pregnancy, and ∼70% of *T. pallidum*-infected pregnant women have latent syphilis (16). Therefore, it is difficult to identify and diagnose the disease depending only on the pregnant woman's medical history and clinical symptoms. In some countries, syphilis in pregnancy can be diagnosed and effectively treated in a timely manner through syphilis screening, which can prevent congenital syphilis. In this case, the pregnant woman did not visit a medical institution for antenatal care and syphilis screening at 28 weeks of pregnancy; thus, the opportunity to diagnose and treat the infection earlier was likely missed and increased the incidence of *T. pallidum* infection of the fetus and premature delivery. *T. pallidum* is easily transmitted to the fetus, leading to adverse pregnancy outcomes. This case illustrates that owing to the low rate of *T. pallidum* infection, syphilis may not be considered in the differential diagnosis when the patient has non-specific symptoms, such as rash. More importantly, for pregnant women with negative syphilis screening results in early pregnancy, it is less likely that *T. pallidum* infection is considered when they have non-specific symptoms (such as maculopapular rash) in the second and third trimesters. Therefore, clinicians should be aware that pregnant women may still be infected with *T. pallidum* after prenatal screening.

Clinical manifestations of and diagnostic tests for congenital syphilis

Congenital syphilis is generally divided into early congenital syphilis, late congenital syphilis and latent congenital syphilis (17). Early congenital syphilis can present at any time within 2 years after birth; it usually presents in the neonatal period and rarely later than 3–4 months after birth. Most affected infants are asymptomatic at birth, and two-thirds of infants develop clinical symptoms at 3–8 weeks after birth. Neonates are often born prematurely, and infant symptoms include stunting, underweight, low-grade fever, anemia, thrombocytopenia, osteochondritis, nasal congestion, maculopapular rash, and iritis. Late congenital syphilis results in a variety of skeletal and dental defects as well as neural deafness and interstitial keratitis, which usually develops at 2 years of age (18). Latent congenital syphilis generally causes no symptoms and is diagnosed by only a positive serological test; moreover, the examination of cerebrospinal fluid is often normal. Because the clinical manifestations of congenital syphilis are diverse and often non-specific, even absent, the diagnosis is often missed.

The detection methods for congenital syphilis mainly include direct detection and serological detection. Direct detection includes dark field microscopy and *T. pallidum*

fluorescence immunostaining methods. The advantages of these two methods are that they are simple and rapid, but they require high-quality clinical specimens, and a negative test cannot rule out *T. pallidum* infection. Currently, the abovementioned methods have been largely replaced by more sensitive nucleic acid amplification tests (NAATs). Placental tissue, amniotic fluid, neonatal mucus, cerebrospinal fluid and blood may be suitable sample types for NAATs (19). Compared to that of culture, sensitivity using Tpp47 targets was 75–100% in amniotic fluid, 60–75% in neonatal cerebrospinal fluid, and 67–94% in neonatal whole blood or serum (20). Although the detection of *T. pallidum* by NAATs is feasible, this method is expensive, and its sensitivity and specificity vary depending on the tested tissue and target gene; therefore, it is not widely performed in hospitals.

Serological testing is still the main laboratory method for the diagnosis of congenital syphilis. There are two types of tests: treponemal serological tests and non-treponemal serological tests. The specificity for treponemal serological tests is higher than that of non-treponemal serological tests. However, a positive test cannot be used to diagnose congenital syphilis because it cannot be determined whether IgG antibodies are of maternal origin or from neonates (21). When the fetus is infected by *T. pallidum*, B lymphocytes will generally produce anti-*T. pallidum* IgM antibodies after ∼2 weeks, which are not able to cross the placental barrier due to their high molecular weight. With the development of antibody preparation technology, anti-*T. pallidum* IgM antibody tests have been gradually applied for laboratory diagnosis. The current detection methods include the 19S-IgM-fluorescent treponemal antibody absorption test, *T. pallidum* immunity blot assay and *T. pallidum*-IgM-enzyme-linked immunosorbent assay (22). If detected in neonatal blood or cerebrospinal fluid, congenital infection is considered, but a negative test does not exclude the diagnosis. Moreover, due to limitations of reagents, instruments and operating procedures, the above three tests have not been widely applied in hospitals. Non-treponemal serological tests mainly include the rapid plasma response (RPR) test, TRUST, and the venereal disease research laboratory (VDRL) test. To establish a diagnosis of congenital syphilis, the neonatal titer should be at least 4 times higher than the maternal titer on the non-treponemal serological test (21).

Congenital syphilis diagnosis requires a combination of maternal serological findings and treatment, comparison of maternal and neonatal non-treponemal serological titres, and clinical evaluation of the neonate. Different countries have different definitions and diagnostic criteria for congenital syphilis. In China, the diagnostic criteria for congenital syphilis are any of the following in children born to syphilis-infected mothers: 1. *T. pallidum* detection in skin/mucosal lesions and tissues in infants with early congenital syphilis by dark-field microscopy or silver staining or a positive *T. pallidum* nucleic acid test; 2. *T. pallidum* IgM antibody serological test positivity; 3. a positive non-treponemal serological test at birth, a $\geq$ 4-fold higher titer than the maternal titer, and treponemal serological test positivity; 4. non-treponemal serological test negativity at birth or a titer<4-fold higher than the maternal titer, and a change in the test from negative to positive at the subsequent follow-up; alternatively, the titer increased with clinical symptoms, and the treponemal serological test was positive; and 5. treponemal serological tests remained positive throughout the first 18 months after birth (23). According to the 2021 sexually transmitted disease (STD) Prevention and Control Guidelines in the United States, congenital syphilis can be diagnosed by meeting criterion 1 or 3. A treponemal serological test is not recommended because passively transferred maternal antibodies can persist for as long as 18 months (8).

A commonality between the above two diagnostic criteria is a neonatal titer for the non-treponemal serological test that is 4-fold higher than the maternal titer. In addition to pathogen detection, this is a key indicator of congenital syphilis diagnosis. The newborn with early congenital syphilis had no typical symptoms after birth in this case. The diagnosis was mainly based on the mother's history of syphilis infection and serological testing. The treponemal serological test(CLIA) was positive, and the TRUST titer was 1:64, i.e., 4-fold higher than the mother's titer (1:16). Related studies have shown that neonatal non-treponemal serological test titres 4-fold higher than those of the mother are rare, with sensitivities ranging from 4 to 13% (21). Considering the abovementioned results, this newborn was diagnosed with early congenital syphilis.

Prevention

No effective vaccine has been developed to prevent syphilis infection (24), but congenital syphilis is preventable through syphilis screening and treatment in early pregnancy. The WHO recommends that all women be tested at their first antenatal visit and again in the third trimester. If the result is positive, it is recommended that their partner also undergo syphilis screening and treatment. The United States CDC recommends that all pregnant women should be screened for syphilis at the first prenatal visit. If there are risk factors for syphilis infection (living in a community with high syphilis morbidity or behaviors conducive to syphilis acquisition during pregnancy) during pregnancy, syphilis screening should be performed again at 28 weeks of pregnancy and at delivery (25). The European CDC recommends that pregnant women should be screened for syphilis within the first 3 months of pregnancy. Retesting is recommended in late pregnancy (before 32 weeks of gestation) to allow sufficient time for effective treatment. If syphilis screening is not performed during pregnancy, it

should be done at the time of delivery. An analysis of 25 published studies evaluating the effectiveness of infection screening and infection management interventions during pregnancy found that syphilis-focused interventions resulted in a significant 80% reduction in stillbirth rates compared to strategies to treat, detect and/or prevent other infections in pregnancy (26).

In China, a management system has been established to standardize maternal health care, which provides strong support for the prevention of syphilis in pregnancy and the control of congenital syphilis. Since 2015, China's National Health Commission has comprehensively carried out prevention strategies targeting mother-to-child transmission of HIV, syphilis and hepatitis B and provided free screening for HIV, syphilis and hepatitis B for pregnant women and intervention services for infected pregnant women and their children. It is recommended that the first prenatal care visit and syphilis screening be completed within the first 3 months of pregnancy. Pregnant women with high-risk factors for *T. pallidum* infection in late pregnancy (28 weeks) and at the time of delivery should undergo syphilis screening again; this process could prevent *T. pallidum* infection in the fetus in the second and third trimesters of pregnancy. A study showed that 500,000 pregnant women from Shenzhen (China) underwent syphilis screening and that the mother-to-child transmission rate of syphilis decreased significantly from 54/100,000 to 22/100,000 (27). Another study in China analyzed 23,879 pregnant women from 2009 to 2018 and found that the prevalence of syphilis among pregnant women decreased from 1.5 to 0.3% after the implementation of prenatal screening (28). The above two studies indicate that regular prenatal syphilis screening can greatly reduce the incidence of congenital syphilis.

In this case, the pregnant woman did not seek timely prenatal care and syphilis screening at 28 weeks of gestation after the first negative prenatal test. Syphilis screening was performed at 32 weeks 4/7 days of gestation, and the treponemal serological test (CLIA) was positive, with a TRUST titer of 1:16. Before the end of treatment, the fetus was delivered because of threatened premature delivery at 34 weeks 1/7 days of gestation, and congenital syphilis was found by laboratory testing. Studies have shown that missing the optimal window for diagnosing syphilis is mainly due to pregnant women having negative screening results at their first prenatal visit and not being rescreened at delivery (29) or because routine syphilis screening is not offered to pregnant women in some countries (30). If a pregnant woman lacks prenatal care awareness, even though the initial syphilis screening is negative, she may be infected with *T. pallidum* in the second half of pregnancy and may transmit it to the fetus. Considering that most pregnant women infected with syphilis have non-specific symptoms, it is necessary to strengthen prenatal health education, especially concerning sexually transmitted diseases. This will promote regular prenatal care visits and the detection and effective treatment of syphilis in a timely manner.

Conclusion

The case presented in this article shows that mother-to-child transmission of syphilis still occurs in countries with high coverage rates of prenatal syphilis screening. The incidence of congenital syphilis is related to not only the syphilis infection rate but also the antenatal care coverage rate. The extensive clinical manifestations of syphilis infection mimic those of many other diseases during pregnancy, which may lead to delayed diagnosis and serious consequences. Therefore, the doctor should exclude the possibility of *T. pallidum* infection in pregnant women with a rash with no obvious cause, even if the early syphilis screening result was negative. Otherwise, this preventable infectious disease is easily overlooked. Additionally, it is very important to promote prenatal care, increase prenatal health awareness for pregnant women and their spouses, and encourage regular syphilis screening in all women during pregnancy. This could minimize the adverse influence of syphilis on pregnant women and their infants.

Data availability statement

The original contributions presented in the study are included in the article/supplementary material, further inquiries can be directed to the corresponding author.

Ethics statement

Written informed consent was obtained from the individual(s) legal guardian for the publication of any potentially identifiable images or data included in this article.

Author contributions

Y-JG analyzed the data. L-WP wrote the manuscript. Z-XG revised the manuscript. Y-lC and HX collected the data. All authors contributed to the discussion of the article and agreed to be accountable for the content of the work.

Funding

This work was supported by the Foundation (No. 21H1219) and the Science and Technology Department of Sichuan Province (No. 2022YFS0239). The funders played no role in the

study design, data collection and analyses, decision to publish, or manuscript preparation.

Conflict of interest

The authors declare that the research was conducted in the absence of any commercial or financial relationships that could be construed as a potential conflict of interest.

Publisher's note

References

1. Rowley J, Vander Hoorn S, Korenromp E, Low N, Unemo M, Abu-Raddad LJ, et al. Chlamydia, gonorrhoea, trichomoniasis and syphilis: global prevalence and incidence estimates, 2016. *Bull World Health Organ.* (2019) 97:548–62. doi: 10.2471/BLT.18.228486

2. Rodriguez PJ, Roberts DA, Meisner J, Sharma M, Owiredu MN, Gomez B, et al. Cost-effectiveness of dual maternal HIV and syphilis testing strategies in high and low HIV prevalence countries: a modelling study. *Lancet Global Health.* (2021) 9:E61–71. doi: 10.1016/S2214-109X(20)30395-8

3. Nathan L, Bohman VR, Sanchez PJ, Leos NK, Twickler DM, Wendel GD Jr. *In utero* infection with *Treponema pallidum* in early pregnancy. *Prenat Diagn.* (2015) 17:119–23. doi: 10.1002/(sici)1097-0223(199702)17:2<119::aid-pd39>3.0.co;2-t

4. Gomez GB, Kamb ML, Newman LM, Mark J, Broutet N, Hawkes SJ, et al. Untreated maternal syphilis and adverse outcomes of pregnancy: a systematic review and meta-analysis. *Bull World Health Organ.* (2013) 91:217–26. doi: 10.2471/BLT.12.107623

5. Kittipornpechdee N, Hanamornroongruang S, Lekmak D, Treetipsatit J. Fetal and placental pathology in congenital syphilis: a comprehensive study in perinatal autopsy. *Fetal Pediatr Pathol.* (2018) 37:231–42. doi: 10.1080/15513815.2018.1485798

6. Temmerman M, Gichangi P, Fonck K, Apers L, Claeys P, Van Renterghem L, et al. Effect of a syphilis control programme on pregnancy outcome in Nairobi, Kenya. *Sex Transm Infect.* (2000) 76:117–21. doi: 10.1136/sti.76.2.117

7. Korenromp EL, Rowley J, Alonso M, Mello MB, Wijesooriya NS, Mahiané SG, et al. Global burden of maternal and congenital syphilis and associated adverse birth outcomes—Estimates for 2016 and progress since 2012. *PLoS ONE.* (2019) 14:e0219613. doi: 10.1371/journal.pone.0219613

8. Centers for Disease Control and Prevention. *Sexually Transmitted Infections Treatment Guidelines.* (2021). Available online at: https://wwwcdcgov/std/treatment-guidelines/congenital-syphilishtm (accessed September 8, 2022).

9. European Centre for Disease Prevention and Control (ECDC). *Congenital syphilis - Annual Epidemiological Report for 2019.Stockholm: ECDC.* (2022). Available online at: https://www.ecdc.europa.eu/en/publications-data/congenital-syphilis-annual-epidemiological-report-2019 (accessed September 8, 2022).

10. Xiangdong G, Xiaoli Y, Fei T, Ning J, Peixuan M. Syphilis in China from 2000 to 2013: epidemiological trends and characteristics. *Chin J Dermatol.* (2014) 47:310–5. doi: 10.3760/cma.j.issn.0142-4030.2014.05.002

11. Xiaoli Y, Xiangdong G, Jing L, Jiahui Z. Epidemiological trends and features of syphilis in China, 2014—2019. *Chin J Dermatol.* (2021) 54:668–72. doi: 10.35541/cjd.20210098

12. WHO. *Global Guidance on Criteria and Processes for Validation: Elimination of Mother-to-child transmission of HIV and syphilis, 2nd edn.* (2017). Available online at: https://www.who.int/reproductivehealth/publications/emtct-hiv-syphilis/en/ (accessed September 8, 2022).

13. Braccio S, Sharland M, Ladhani SN. Prevention and treatment of mother-to-child transmission of syphilis. *Curr Opin Infect Dis.* (2016) 29:268–74. doi: 10.1097/QCO.0000000000000270

14. Chapel AT. The signs and symptoms of secondary syphilis. *Sex Transm Dis.* (1980) 7:161–4. doi: 10.1097/00007435-198010000-00002

15. Baughn RE, Musher DM. Secondary syphilitic lesions. *Clin Microbiol Rev.* (2005) 18:205–16. doi: 10.1128/CMR.18.1.205-216.2005

16. Alexander JM, Sheffield JS, Sanchez PJ, Mayfield J, Wendel GD Jr. Efficacy of treatment for syphilis in pregnancy. *Obstet Gynecol.* (1999) 93:5–8. doi: 10.1097/00006250-199901000-00002

17. Wijesooriya NS, Rochat RW, Kamb ML, Turlapati P, Temmerman M, Broutet N, et al. Global burden of maternal and congenital syphilis in 2008 and 2012: a health systems modelling study. *Lancet Global Health.* (2016) 4:E525–33. doi: 10.1016/S2214-109X(16)30135-8

18. Roberts CP, Raich A, Stafylis C, Klausner JD. Alternative treatments for syphilis during pregnancy. *Sex Transm Dis.* (2019) 46:637–40. doi: 10.1097/OLQ.0000000000001050

19. Theel ES, Katz SS, Pillay A. Molecular and direct detection tests for treponema pallidum subspecies pallidum: a review of the literature, 1964-2017. *Clin Infect Dis.* (2020) 71:S4–12. doi: 10.1093/cid/ciaa176

20. *Australian Government Department of Health Syphilis.* (2019). Available online at: https://wwwhealthgovau/resources/pregnancy-care-guidelines/part-f-routine-maternal-health-tests/syphilis (accessed September 12, 2022).

21. Satyaputra F, Hendry S, Braddick M, Sivabalan P, Norton R. The laboratory diagnosis of syphilis. *J Clin Microbiol.* (2021) 59: e0010021. doi: 10.1128/JCM.00100-21

22. Gaspar PC, Bigolin Á, Alonso Neto JB, Pereira ED, Bazzo ML. Brazilian protocol for sexually transmitted infections 2020: syphilis diagnostic tests. *Rev Soc Bras Med Trop.* (2021) 54:e2020630. doi: 10.1590/0037-8682-630-2020

23. National Health Commission of the People 's Republic of China. *Guidelines for the Prevention of Mother-to-Child Transmission of AIDS, Syphilis and Hepatitis B.* (2020). Available online at: http://www.nhc.gov.cn/cms-search/xxgk/getManuscriptXxgk.htm?id=fc7b46b2b48b45a69bd390ae3a62d065 (accessed September 12, 2022).

24. Lithgow KV, Cameron CE. Vaccine development for syphilis. *Expert Rev Vaccines.* (2017) 16:37–44. doi: 10.1080/14760584.2016.1203262

25. Centers for Disease Control and Prevention. *Sexually Transmitted Infections Treatment Guidelines.* (2021). Available online at: https://wwwcdcgov/std/treatment-guidelines/syphilis-pregnancyhtm (accessed September 12, 2022).

26. Ishaque S, Yakoob MY, Imdad A, Goldenberg RL, Eisele TP, Bhutta ZA. Effectiveness of interventions to screen and manage infections during pregnancy on reducing stillbirths: a review. *BMC Public Health.* (2011) 11(Suppl. 3):S3. doi: 10.1186/1471-2458-11-S3-S3

27. Cheng JQ, Zhou H, Hong FC, Zhang D, Zhang YJ, Pan P, et al. Syphilis screening and intervention in 500,000 pregnant women in Shenzhen, the People's Republic of China. *Sex Transm Infect.* (2007) 83:347–50. doi: 10.1136/sti.2006.023655

28. Zhong S, Ou Y, Zhang F, Lin Z, Huang R, Nong A, et al. Prevalence trends and risk factors associated with HIV, syphilis, and hepatitis C virus among pregnant women in Southwest China, 2009-2018. *AIDS Res Ther.* (2022) 19:31. doi: 10.1186/s12981-022-00450-7

29. Keuning MW, Kamp GA, Schonenberg-Meinema D, Dorigo-Zetsma JW, van Zuiden JM, Pajkrt D. Congenital syphilis, the great imitator-case report and review. *Lancet Infectious Diseases.* (2020) 20:E173–9. doi: 10.1016/S1473-3099(20)30268-1

30. Khafaja S, Youssef Y, Darjani N, Youssef N, Fattah CM, Hanna-Wakim R. Case report: a delayed diagnosis of congenital syphilis-too many missed opportunities. *Front Pediatr.* (2021) 8:499534. doi: 10.3389/fped.2020.499534

frontiers | Frontiers in Medicine

TYPE Case Report
PUBLISHED 06 January 2023
DOI 10.3389/fmed.2022.1092879

OPEN ACCESS

EDITED BY
Francesco Paolo Bianchi,
University of Bari Aldo Moro, Italy

REVIEWED BY
Utpal Anand,
All India Institute of Medical Sciences, India
Dalong Yin,
University of Science and Technology of China, China
Hairui Wang,
Shengjing Hospital of China Medical University, China

*CORRESPONDENCE
Hiroaki Shimizu
✉ h-shimizu@med.teikyo-u.ac.jp

SPECIALTY SECTION
This article was submitted to Infectious Diseases: Pathogenesis and Therapy, a section of the journal Frontiers in Medicine

RECEIVED 08 November 2022
ACCEPTED 15 December 2022
PUBLISHED 06 January 2023

CITATION
Nojima H, Shimizu H, Murakami T, Yamazaki M, Yamazaki K, Suzuki S, Shuto K, Kosugi C, Usui A and Koda K (2023) Successful hepatic resection for invasive *Klebsiella pneumoniae* large multiloculated liver abscesses with percutaneous drainage failure: A case report.
Front. Med. 9:1092879.
doi: 10.3389/fmed.2022.1092879

Successful hepatic resection for invasive *Klebsiella pneumoniae* large multiloculated liver abscesses with percutaneous drainage failure: A case report

Hiroyuki Nojima[1], Hiroaki Shimizu[1]*, Takashi Murakami[1], Masato Yamazaki[1], Kazuto Yamazaki[2], Seiya Suzuki[2], Kiyohiko Shuto[1], Chihiro Kosugi[1], Akihiro Usui[1] and Keiji Koda[1]

[1]Department of Surgery, Teikyo University Chiba Medical Center, Ichihara, Japan, [2]Department of Pathology, Teikyo University Chiba Medical Center, Ichihara, Japan

Background: Invasive *Klebsiella*-associated liver abscesses can progress rapidly and cause severe metastatic infections such as meningitis and hydrocephalus, which are associated with high morbidity and mortality. In patients with large multiloculated liver abscesses after failure of percutaneous drainage, rapid diagnosis of the abscess followed by hepatic resection is necessary for early recovery and to prevent severe secondary metastatic complications.

Case presentation: An 84-year-old woman with a large liver abscess and in septic shock was transferred to our hospital. Abdominal CT showed multiloculated liver abscesses 15 cm in diameter in the right lobe of the liver. We first performed percutaneous liver abscess drainage. The patient was managed in the intensive care unit, as well as treated with intravenous administration of meropenem followed by cefozopran according to the antibiogram. *Klebsiella pneumoniae* with invasive infection was confirmed by a string test in an isolated colony of *K. pneumoniae*; the K1 serotype with the *rmpA* and *magA* genes was determined by polymerase chain reaction and Sanger sequencing. Additional percutaneous liver abscess drainage was performed due to initial inadequate drainage. Although the abscess had shrunk to a diameter of 8 cm after drainage in 4 weeks, the patient recovered from sepsis, but still had low-grade fever (occasionally 38°C) and continued to have symptoms of chronic inflammation with persistent hyper mucus discharge from the liver abscess. Surgical resection was chosen to prevent prolonged hospitalization and ensure early recovery. A right posterior sectionectomy of the liver, including liver abscess, was performed. The post-operative course was uneventful, with no complications, and she was discharged after 18 days. There were no signs of abscess recurrence 1 year after surgery.

Conclusion: We present a case of successful hepatic resection after percutaneous drainage failure in a patient with invasive *K. pneumoniae* multiloculated liver abscess.

KEYWORDS

Klebsiella*-associated multiloculated liver abscess, percutaneous drainage failure, K1 serotype, hyper mucus discharge, *K. pneumoniae

1. Introduction

Klebsiella pneumoniae is the most common causative organism of bacterial liver abscesses and is classified into two groups, classical *K. pneumoniae* and hypervirulent *K. pneumoniae* (1). Hypervirulent *K. pneumoniae* was first identified in Taiwan in 1986 as a liver abscess associated with septic endophthalmitis in young and immunocompetent hosts (2). Hypervirulent strains have a higher potential to resist phagocytosis and metastasize to distant sites forming highly mucoid colonies with capsule polysaccharide, leading to a hypermucoviscous colony phenotype. Accordingly, it is also called hypermucoviscous *K. pneumoniae* (1). Hypermucoviscosity has been mostly associated with serotype K1, followed by serotype K2, and is associated with the hypervirulence phenotype of *Klebsiella* regulated by the mucoviscosity-associated gene A (magA) and regulator of mucoid phenotype A (rmpA) (3). *Klebsiella*-associated invasive liver abscess syndrome with the hypermucoviscous phenotype can progress rapidly and cause severe metastatic infections such as meningitis and hydrocephalus, which are associated with high morbidity and mortality (4, 5). A rapid diagnosis followed by treatment, such as percutaneous drainage and antibiotic therapy, is the standard for improving patient outcomes with hypermucoviscous *K. pneumoniae* (6). For large multiloculated abscesses with percutaneous drainage failure, surgical resection is necessary for early recovery and to prevent severe secondary metastatic lesions. Herein, we present a case of successful hepatic resection in a patient with an invasive *K. pneumoniae* multiloculated drainage-resistant liver abscess.

2. Case description

An 84-year-old woman, weighing 54 kg with a height of 150 cm, was urgently admitted to the previous hospital with a diagnosis of liver abscess. Antimicrobial agents for 1 week did not improve symptoms at the previous hospital, and she was transferred to our hospital with septic shock. The patient had an implant stem after a left femur fracture and a history of asthma. There was no history of diabetes or cancer, and no history of smoking, drinking alcohol, or drug allergies. On arrival at our hospital, her initial vital signs were as follows: body temperature, 38°C; heart rate, 122 beats/min; blood pressure, 64/50 mmHg; respiratory rate, 26 breaths/min; and oxygen saturation, 91%. Her blood test revealed an increased ammonia level of 127 μg/dl, decreased serum albumin level of 1.5 g/dl, and a bilirubin level of 0.8 mg/dl. Her white blood cell count was 18200/μL, PT-INR was 1.54, d-dimer was 27.4 ng/mL, and FDP was 32.3 U/mL. Her disseminated intravascular coagulation (DIC) score was 5 points. Abdominal computed tomography showed a multiloculated liver abscess 15 cm in diameter in the right lobes of the liver extending across the right hepatic vein (**Figure 1**). Extrahepatic infections, such as infections of the lungs and brain, were not detected.

First, we performed percutaneous liver abscess drainage with two drainage tubes. Following transfer to the intensive care unit, intravenous meropenem followed by cefozopran was administered, according to the antibiogram. *K. pneumoniae* with invasive infection was confirmed by a string test in an isolated colony of *K. pneumoniae*, and invasive *K. pneumoniae* large liver abscess was diagnosed. We carried out polymerase chain reaction (PCR) with DNA from the aspirated fluid to detect the presence of hypermucoviscous *K. pneumoniae* as previously described (7). The PCR determined the amplification of specific genes for serotype K1, a regulator of mucoid phenotype A (rmpA), and mucoid associated gene A (magA), which was confirmed by Sanger sequencing (**Figure 2**). The additional abscess drainage was performed 1 week after the initial drain placement due to inadequate drainage, and finally, five drainage tubes were placed into the multiloculated liver abscess (**Supplementary Figure 1**). Although the abscess in the posterior segments of the liver had shrunk to a diameter of 8 cm at 4 weeks after drainage, the patient recovered from sepsis, but still had low-grade fever (occasionally 38°C), an elevated white blood cell count of 10,300/μL, C-reactive protein level of 6 U/L (**Supplementary Figure 2**), and continued to have symptoms of a chronic inflammation with persistent hyper mucus discharge from the liver abscess *via* five drainage tubes (**Figure 3**). We also checked for other causes of fever such as pneumonia and urinary tract infection, but no other infection related to fever was identified other than the liver abscess. We decided that further drainage treatment would be insufficient due to the multiloculated liver abscess with

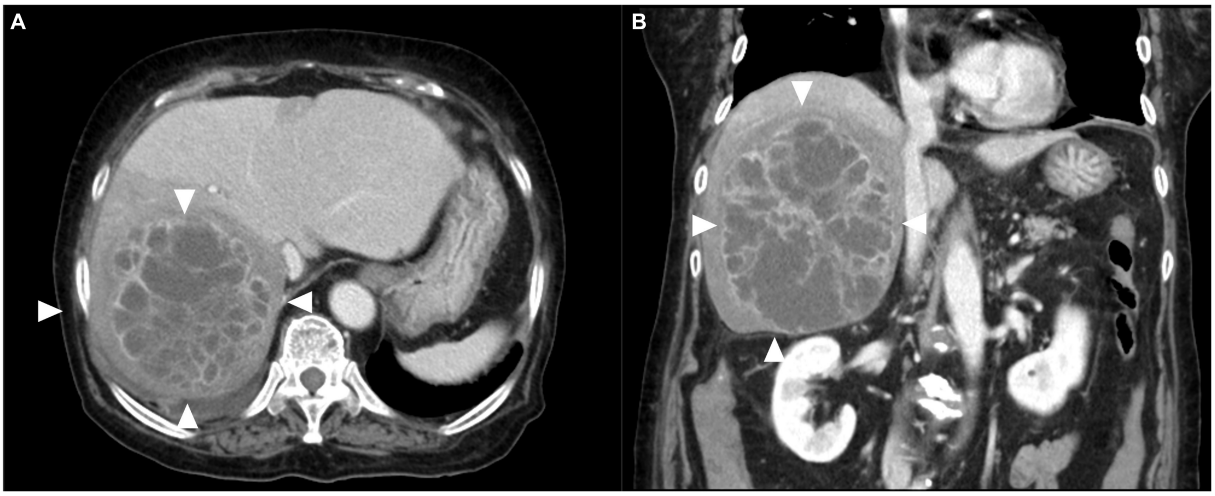

FIGURE 1
Contrast-enhanced computed tomography images of the liver. **(A)** Multiloculated liver abscess (white arrows) occupying the right lobes of the liver extending across the right hepatic vein. **(B)** Coronal image revealing multiloculated liver abscess (white arrows) 15 cm in diameter.

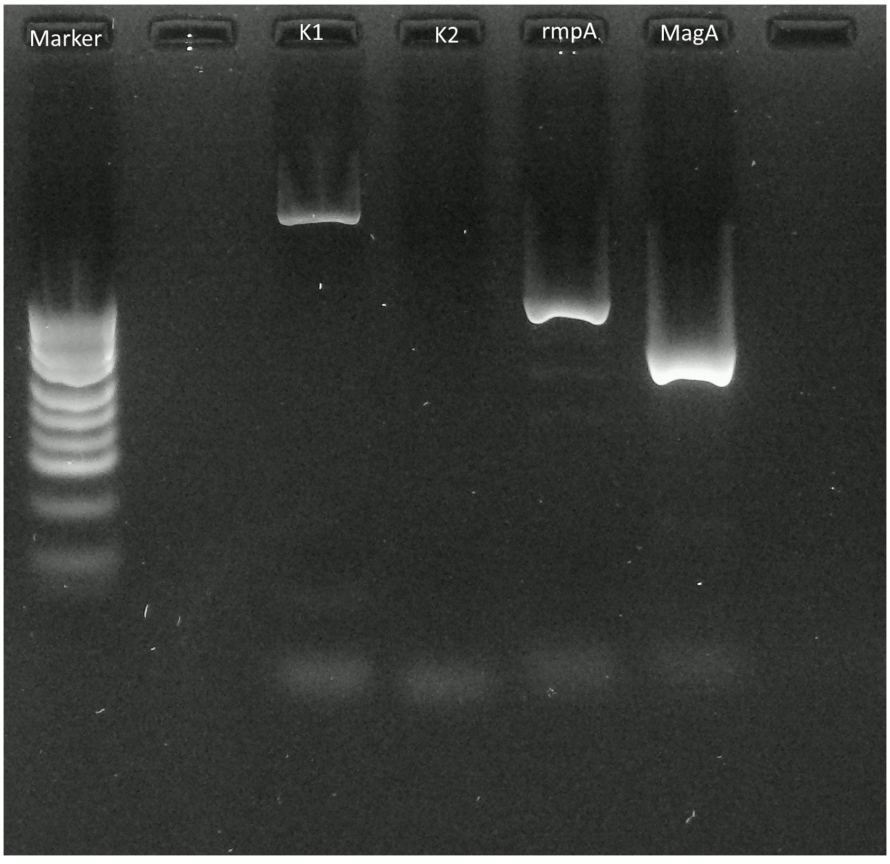

FIGURE 2
Polymerase chain reaction (PCR) applied to the pus of the liver abscess. PCR with extracted DNA from the pus of the abscess revealed amplification of the *Klebsiella pneumoniae* serotype K1 specific locus *(wzyKPK1), rmpA, and magA* fragments that were detected by electrophoresis on 2.0% agarose.

hyper mucus components and prolonged hospitalization with her advanced age. After explaining the patient's condition and treatment options, a right posterior sectionectomy of the liver, including hepatic abscess, was performed. Although the abscess was not perforated, severe adhesions between the liver abscess and the right diaphragm were observed. The abscess was close to the root of Glisson's sheath of the right posterior section; therefore, the right posterior sectionectomy of the liver, including the liver abscess, was performed (**Supplementary Figure 3**).

The operative time was 4 h and 48 min, and the total blood loss was 723 ml. The resected right posterior section of the liver revealed a multiloculated and necrotic liver abscess. Histological examination showed a pyogenic liver abscess with areas of necrosis, inflammatory granulation, and a few fluid components, composed of a chronic inflammatory

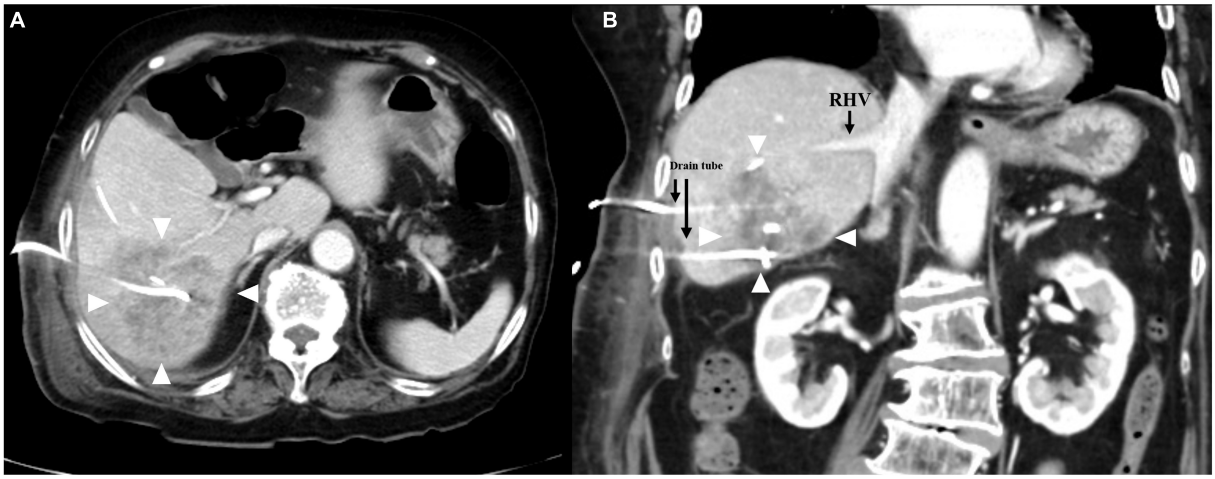

FIGURE 3
Contrast-enhanced computed tomography images of the liver. **(A)** Right hepatic vein separated from the multiloculated liver abscess (white arrows). **(B)** Coronal image revealing multiloculated liver abscess (white arrows) with drainage tubes 8 cm in diameter.

TABLE 1 Reported cases of hepatectomy for *Klebsiella pneumoniae* abscesses.

Cases	Age (year)	Sex	Abscess	Surgery	Reason for surgical treatment	Outcome
Shiba et al. (28)	84	Female	A gas-containing abscess (S2/3)	Lateral segmentectomy	Ruptured gas-containing liver abscess	Discharged 31 days after surgery
Morii et al. (13)	69	Female	A multiloculated abscess more than 10 cm in diameter (S7/8)	Partial segment S7/8 resection	Failure of antibiotic therapy and abscess perforation	Discharged 8 weeks after surgery
Maybury et al. (27)	74	Female	A multiloculated abscess (S2/3)	Left lateral sectionectomy	Failure of abscess drainage	Good recovery following surgery
Maybury et al. (27)	51	Male	A multiloculated abscess (S2)	Partial segment 2 resection	Failure of antibiotic therapy	Good recovery following surgery
Chan et al. (19)	41	Female	A multiloculated abscess 10 cm in diameter (S6/7)	Segment 6/7 resection	Failure of antibiotic therapy and abscess drainage	Discharged 6 weeks after surgery
Pais-Costa et al. (29)	54	Female	A multiloculated abscess 12 cm in diameter (Rt lobe)	Right hepatectomy	–	Discharged 23 days after surgery
Pais-Costa et al. (29)	66	Male	A multiloculated abscess 20 cm in diameter (Rt lobe)	Right hepatectomy	–	Discharged 25 days after surgery
Pais-Costa et al. (29)	73	Male	An abscess 7 cm in diameter (Lt lobe)	Laparoscopic left hepatectomy	–	Discharged 5 days after surgery
Sato et al. (28)	80	Male	A multiloculated abscess more than 10 cm in diameter (S2/3)	Left hepatectomy	Failure of antibiotic therapy and abscess drainage	Discharged 30 days after surgery
Our case	84	Female	A multiloculated abscess more than 15 cm in diameter (S6/7)	Right posterior sectionectomy	Failure of antibiotic therapy and abscess drainage	Discharged 15 days after surgery

infiltrate consisting of lymphocytes, epithelioid macrophages, eosinophils, and neutrophils. The adjacent hepatocytes appeared atrophic (**Supplementary Figure 4**). The post-operative course was uneventful, with no complications. The patient was discharged on post-operative day 18. Follow-up examinations using ultrasonography showed no signs of abscess recurrence 1 year after surgery.

3. Discussion

Liver abscesses can be divided into bacterial and amoebic liver abscesses; most of them are bacterial in origin, with *K. pneumoniae* reported to be the most common causative organism in bacterial liver abscesses (8). Invasive liver abscess syndrome caused by *K. pneumoniae* has been reported in Taiwan since the 1980s (2). *K. pneumoniae* is a mucoid-producing bacterium, and serotype K1 is the most common mucoid-producing strain of *K. pneumoniae*, followed by serotype K2 (3). In particular, *magA* has been identified as a gene associated with liver abscesses and metastatic lesions in K1 strains (3). Microbiological definitions of invasive liver abscess syndrome are described as *K pneumoniae* liver abscess caused by the K1 or K2 serotype (3). According to previous reports, some mucoid-producing strains of the genus *Klebsiella* are highly viscous, resistant to phagocytosis, and can spread hematogenously, resulting in secondary abscesses such as meningitis, hydrocephalus, endophthalmitis, and metastatic lung lesions (4, 5). Among these metastatic infections, endophthalmitis is the most serious complication and a poor prognostic factor for visual acuity (8). Rapid and accurate diagnosis of *K. pneumoniae*, such as the string test, and identification of the pathogen by metagenomic next-generation sequencing, is the key to start appropriate treatment immediately (9, 10). In our case, the patient had a positive string test, and PCR revealed amplification of the *K. pneumoniae* serotype K1 specific locus (*wzyKPK1*), *rmpA,* and *magA* fragments. Invasive liver abscess syndrome involving K1 strains is associated with an absence of immunodeficiency disorders; however, recent studies have shown that diabetes mellitus is recognized as an important risk factor for the development of the disease, as well as a poor prognostic factor for visual acuity (11). The frequency of spontaneous liver abscess rupture is as low as 3.8% (12). However, liver abscesses larger than 8 cm tend to rupture easily because of the high pressure of the contents, and ruptures presenting with peritonitis require emergency surgery (13, 14). In addition, an abscess larger than 6 cm is reported to be a significant independent risk factor for metastatic infections (15). Currently, combined antibiotic therapy based on the antibiogram and percutaneous catheter drainage of liver abscesses is the first choice of treatment for liver abscesses (16). Although many treatment strategies have been proposed for pyogenic liver abscesses, the indications for hepatic resection have not been systematically studied (17, 18). Surgical resection should be considered when there is no clinical improvement with antimicrobial therapy and percutaneous drainage, or if the liver abscess ruptures (19–21). Regarding multiloculated liver abscesses, the failure rate of percutaneous catheter drainage is high (22). Previous studies suggested that large multiloculated abscesses should be treated surgically (23). For large multiple liver abscesses with hyper mucus components, surgical resection should be performed if percutaneous drainage is inadequate, which may lead to improved prognosis and earlier recovery (24). In a report of 10 liver resections for *K. pneumoniae* liver abscess, including our case, 8 cases were multiloculated liver abscesses, 4 cases were operated due to failure of percutaneous abscess drainage, and 2 cases were due to abscess perforation. The post-operative course was reported to be uneventful in all cases (**Table 1**) (13, 19, 25–28). Regarding to the recurrence rate of liver abscess, the K1 serotype is known to be an important risk factor that influences liver abscess recurrence (29). This case report have some limitations. This was just a single case report, further accumulation of cases is necessary to establish the best therapeutic strategy for invasive *K. pneumoniae* liver abscess.

In conclusion, in large multiloculated abscesses after drainage failure, such as in our case, complete liver abscess resection should be performed to ensure earlier recovery and prevent metastatic disease recurrence or secondary metastatic lesions.

Data availability statement

The original contributions presented in this study are included in the article/**Supplementary material**, further inquiries can be directed to the corresponding author.

Ethics statement

Ethics approval was obtained from the Ethical Review Board for Clinical Studies at Teikyo University Chiba Medical Center. Written informed consent was obtained from the patient for the publication of any potentially identifiable images or data included in this article.

Author contributions

HS was the major contributor to the writing of the manuscript. HS and HN supervised the manuscript and performed the surgical therapy. TM and MY were involved in surgical therapy and patient care. KY and SS supported the pathological examination results. KS, CK, AU, and KK supported the clinical examinations. All authors have read and approved the final manuscript.

Acknowledgments

We would like to thank Editage (www.editage.com) for English language editing.

Conflict of interest

The authors declare that the research was conducted in the absence of any commercial or financial relationships that could be construed as a potential conflict of interest.

Publisher's note

All claims expressed in this article are solely those of the authors and do not necessarily represent those of their affiliated organizations, or those of the publisher, the editors and the reviewers. Any product that may be evaluated in this article, or claim that may be made by its manufacturer, is not guaranteed or endorsed by the publisher.

Supplementary material

The Supplementary Material for this article can be found online at: https://www.frontiersin.org/articles/10.3389/fmed.2022.1092879/full#supplementary-material

SUPPLEMENTARY FIGURE 1
Percutaneous liver abscess drainage. Percutaneous drainage of the liver abscess was performed twice. The additional drainage of the liver abscess with two tubes (white arrowhead) was carried out following drainage with three tubes (black arrowhead).

SUPPLEMENTARY FIGURE 2
Clinical course of the present case. The patient still had low-grade fever, occasionally 38°C, accompanied by elevated C-reactive protein (CRP) levels.

SUPPLEMENTARY FIGURE 3
(A) Intraoperative appearance of the abscess surrounded liver parenchyma (white arrowhead). **(B)** Intraoperative view of raw surface of the liver after hepatectomy.

SUPPLEMENTARY FIGURE 4
Gross image of resected specimen and histopathological microscopy of the liver abscess. **(A)** Resected right posterior section of the liver, revealing the multiloculated and necrotic liver abscess. **(B)** Pyogenic liver abscess with areas of necrosis and inflammatory granulation, composed of a chronic inflammatory infiltrate consisting of lymphocytes, epithelioid macrophages, eosinophils, and neutrophils. The adjacent hepatocytes appeared atrophic.

References

1. Jun J. *Klebsiella pneumoniae* Liver Abscess. *Infect Chemother.* (2018) 50:210–8. doi: 10.3947/ic.2018.50.3.210

2. Liu Y, Cheng D, Lin C. *Klebsiella pneumoniae* liver abscess associated with septicendophthalmitis. *Arch Intern Med.* (1986) 146:1913–6. doi: 10.1001/archinte.1986.00360220057011

3. Siu L, Yeh K, Lin J, Fung C, Chang F. *Klebsiella pneumoniae* liver abscess: a new invasive syndrome. *Lancet Infect Dis.* (2012) 12:881–7. doi: 10.1016/S1473-3099(12)70205-0

4. Sun R, Zhang H, Xu Y, Zhu H, Yu X, Xu J. *Klebsiella pneumoniae*-related invasive liver abscess syndrome complicated by purulent meningitis: a review of the literature and description of three cases. *BMC Infect Dis.* (2021) 21:15. doi: 10.1186/s12879-020-05702-3

5. Chou D, Wu S, Chung K, Han S. Septic pulmonary embolism caused by a *Klebsiella pneumoniae* liver abscess: clinical characteristics, imaging findings, and clinical courses. *Clinics (Sao Paulo).* (2015) 70:400–7. doi: 10.6061/clinics/2015(06)03

6. Li F, Zheng W, Yu J, Zhao L. *Klebsiella pneumoniae* liver abscess with purulent meningitis and endogenous endophthalmitis: A case report. *Front Surg.* (2022) 9:894929. doi: 10.3389/fsurg.2022.894929

7. Compain F, Babosan A, Brisse S, Genel N, Audo J, Ailloud F, et al. Multiplex PCR for detection of seven virulence factors and K1/K2 capsular serotypes of *Klebsiella pneumoniae*. *J Clin Microbiol.* (2014) 52:4377–80. doi: 10.1128/JCM.02316-14

8. Fung C, Chang F, Lee S, Hu B, Kuo B, Liu C, et al. A global emerging disease of *Klebsiella pneumoniae* liver abscess: is serotype K1 an important factor for complicated endophthalmitis? *Gut.* (2002) 50:420–4. doi: 10.1136/gut.50.3.420

9. Zeng S, Yan W, Wu X, Zhang H. Case report: diagnosis of *Klebsiella pneumoniae* invasive liver abscess syndrome with purulent meningitis in a patient from pathogen to lesions. *Front Med (Lausanne).* (2021) 8:714916. doi: 10.3389/fmed.2021.714916

10. Russo T, Olson R, Fang C, Stoesser N, Miller M, Macdonald U, et al. Identification of biomarkers for differentiation of hypervirulent *Klebsiella pneumoniae* from classical K. pneumoniae. *J Clin Microbiol.* (2018) 56:e776–718. doi: 10.1128/JCM.00776-18

11. Zheng S, Florescu S, Mendoza M. *Klebsiella pneumoniae* invasive syndrome in a diabetic patient with gallbladder abscess. *Clin Case Rep.* (2020) 8:1940–2. doi: 10.1002/ccr3.3038

12. Jun C, Yoon J, Wi J, Park S, Lee W, Jung S, et al. Risk factors and clinical outcomes for spontaneous rupture of pyogenic liver abscess. *J Dig Dis.* (2015) 16:31–6. doi: 10.1111/1751-2980.12209

13. Morii K, Kashihara A, Miura S, Okuhin H, Watanabe T, Sato S, et al. Successful hepatectomy for intraperitoneal rupture of pyogenic liver abscess caused by *Klebsiella pneumoniae*. *Clin J Gastroenterol.* (2012) 5:136–40. doi: 10.1007/s12328-012-0293-6

14. Pham Van T, Vu Ngoc S, Nguyen Hoang N, Hoang Huu D, Dinh Duong T. Ruptured liver abscess presenting as pneumoperitoneum caused by *Klebsiella pneumoniae*: a case report. *BMC Surg.* (2020) 20:228. doi: 10.1186/s12893-020-00858-w

15. Shin S, Park C, Lee Y, Kim E, Kim S, Goo J. Clinical and radiological features of invasive *Klebsiella pneumoniae* liver abscess syndrome. *Acta Radiol.* (2013) 54:557–63. doi: 10.1177/0284185113477400

16. Serraino C, Elia C, Bracco C, Rinaldi G, Pomero F, Silvestri A, et al. Characteristics and management of pyogenic liver abscess: A European experience. *Med (Baltim).* (2018) 97:e0628. doi: 10.1097/MD.0000000000010628

17. Rismiller K, Haaga J, Siegel C, Ammori J. Pyogenic liver abscesses: a contemporary analysis of management strategies at a tertiary institution. *HPB (Oxford).* (2017) 19:889–93. doi: 10.1016/j.hpb.2017.06.005

18. Lo J, Leow J, Ng P, Lee H, Mohd Noor N, Low J, et al. Predictors of therapy failure in a series of 741 adult pyogenic liver abscesses. *J Hepato-Bil Pancreat Sci.* (2015) 22:156–65. doi: 10.1002/jhbp.174

19. Chan T, Lauscher J, Chan A, Law C, Karanicolas P. Hypermucoviscous *Klebsiella pneumoniae* liver abscess requiring liver resection. *BMJ Case Rep.* (2018) 2018:bcr2018226490. doi: 10.1136/bcr-2018-226490

20. Onder A, Kapan M, Böyük A, Gümüş M, Tekbaş G, Girgin S, et al. Surgical management of pyogenic liver abscess. *Eur Rev Med Pharmacol Sci.* (2011) 15:1182–6.

21. Hsieh H, Chen T, Yu C, Wang N, Chu H, Shih M, et al. Aggressive hepatic resection for patients with pyogenic liver abscess and Apache II score > or =15. *Am J Surg.* (2008) 196:346–50. doi: 10.1016/j.amjsurg.2007.09.051

22. Nham E, Lee J, Huh K, Ko J, Cho S, Kang C, et al. Predictive and prognostic factors associated with unliquefied pyogenic liver abscesses. *J Microbiol Immunol Infect*. (2022):S1684-1182-00109-8. doi: 10.1016/j.jmii.2022.07.010

23. Ferraioli G, Garlaschelli A, Zanaboni D, Gulizia R, Brunetti E, Tinozzi F, et al. Percutaneous and surgical treatment of pyogenic liver abscesses: observation over a 21-year period in 148 patients. *Dig Liver Dis.* (2008) 40:690–6. doi: 10.1016/j.dld.2008.01.016

24. Tan Y, Chung A, Chow P, Cheow P, Wong W, Ooi L, et al. An appraisal of surgical and percutaneous drainage for pyogenic liver abscesses larger than 5 cm. *Ann Surg.* (2005) 241:485–90. doi: 10.1097/01.sla.0000154265.14006.47

25. Maybury B, Powell-Chandler A, Kumar N. Two cases of *Klebsiella pneumoniae* liver abscess necessitating liver resection for effective treatment. *Ann R Coll Surg Engl.* (2015) 97:e37–8. doi: 10.1308/003588414X14055925060037

26. Shiba H, Aoki H, Misawa T, Kobayashi S, Saito R, Yanaga K. Pneumoperitoneum caused by Ruptured gas-containing liver abscess. *J Hepatobiliary Pancreat Surg.* (2007) 14:210–1. doi: 10.1007/s00534-006-1136-y

27. Pais-Costa S, Araujo S, Figueiredo V. Hepatectomy for pyogenic liver abscess treatment: Exception Approach? *Arq Bras Cir Dig.* (2018) 31:e1394. doi: 10.1590/0102-672020180001e1394

28. Sato K, Takahashi K, Kusuta T. A case of hypermucoviscosity phenotype of *Klebsiella Pneumoniae* liver abscess saved by damage control strategy. *Case Rep Surg.* (2022):6019866. doi: 10.1155/2022/6019866

29. Yang Y, Siu L, Yeh K, Fung C, Huang S, Hung H, et al. Recurrent *Klebsiella pneumoniae* liver abscess: clinical and microbiological characteristics. *J Clin Microbiol.* (2009) 47:3336–9. doi: 10.1128/JCM.00918-09

frontiers | Frontiers in Medicine

TYPE Case Report
PUBLISHED 06 January 2023
DOI 10.3389/fmed.2022.1099408

OPEN ACCESS

EDITED BY
Francesco Paolo Bianchi,
University of Bari Aldo Moro, Italy

REVIEWED BY
Carla Ramalho,
University of Porto, Portugal
Carolyn Jones,
Victoria University of Manchester, United Kingdom
Drucilla Jane Roberts,
Massachusetts General Hospital and Harvard Medical School, United States

*CORRESPONDENCE
Hannah A. Bullock
ocr3@cdc.gov

†These authors have contributed equally to this work and share first authorship

SPECIALTY SECTION
This article was submitted to Infectious Diseases: Pathogenesis and Therapy, a section of the journal Frontiers in Medicine

RECEIVED 15 November 2022
ACCEPTED 13 December 2022
PUBLISHED 06 January 2023

CITATION
Bullock HA, Fuchs E, Martines RB, Lush M, Bollweg B, Rutan A, Nelson A, Brisso M, Owusu-Ansah A, Sitzman C, Ketterl L, Timmons T, Lopez P, Mitchell E, McCutchen E, Figliomeni J, Iwen P, Uyeki TM, Reagan-Steiner S and Donahue M (2023) Probable vertical transmission of Alpha variant of concern (B.1.1.7) with evidence of SARS-CoV-2 infection in the syncytiotrophoblast, a case report. *Front. Med.* 9:1099408. doi: 10.3389/fmed.2022.1099408

Probable vertical transmission of Alpha variant of concern (B.1.1.7) with evidence of SARS-CoV-2 infection in the syncytiotrophoblast, a case report

Hannah A. Bullock[1*†], Erika Fuchs[1,2†], Roosecelis B. Martines[1], Mamie Lush[2], Brigid Bollweg[1], Alyssa Rutan[3], Amy Nelson[3], Mark Brisso[3], Albert Owusu-Ansah[3], Craig Sitzman[3], Laurie Ketterl[3], Tim Timmons[4], Patricia Lopez[4], Elizabeth Mitchell[5,6], Emily McCutchen[5,6], Jonathan Figliomeni[2], Peter Iwen[5,6], Timothy M. Uyeki[1], Sarah Reagan-Steiner[1] and Matthew Donahue[2]

[1]Centers for Disease Control and Prevention, Atlanta, GA, United States, [2]Nebraska Department of Health and Human Services, Lincoln, NE, United States, [3]Bryan Health, Lincoln, NE, United States, [4]Lincoln-Lancaster County Health Department, Lincoln, NE, United States, [5]Nebraska Public Health Laboratory, Omaha, NE, United States, [6]University of Nebraska Medical Center, Omaha, NE, United States

Introduction: Definitive vertical transmission of severe acute respiratory syndrome coronavirus-2 (SARS-CoV-2) infection has been rarely reported. We present a case of a third trimester pregnancy with fetal distress necessitating cesarean section that demonstrated maternal, placental, and infant infection with the SARS-CoV-2 Alpha variant/B.1.1.7.

Methods: CDC's Influenza SARS-CoV-2 Multiplex RT-PCR Assay was used to test for SARS-CoV-2 in a maternal NP swab, maternal plasma, infant NP swab, and formalin-fixed paraffin-embedded (FFPE) placental tissue specimens. Whole genome sequencing (WGS) was performed on maternal plasma, infant, and placental specimens to determine the SARS-CoV-2 genotype. Histopathological evaluation, SARS-CoV-2 immunohistochemistry testing (IHC), and electron microscopy (EM) analysis were performed on placenta, umbilical cord, and membrane FFPE blocks.

Results: All specimens tested positive for SARS-CoV-2 by RT-PCR. WGS further revealed identical SARS-CoV-2 sequences from clade 20I/501Y.V1 (lineage Alpha/B.1.1.7) in maternal plasma, infant, and placental specimens. Histopathologic evaluation of the placenta showed histiocytic and neutrophilic intervillositis with fibrin deposition and trophoblast necrosis with positive SARS-CoV-2 immunostaining in the syncytiotrophoblast and electron microscopy evidence of coronavirus.

Discussion: These findings suggest vertical transmission of SARS-CoV-2, supported by clinical course timing, identical SARS-CoV-2 genotypes from

maternal, placental, and infant samples, and IHC and EM evidence of placental infection. However, determination of the timing or distinction between prepartum and peripartum SARS-CoV-2 transmission remains unclear.

KEYWORDS

SARS-CoV-2, vertical transmission, electron microscopy, histopathology, immunohistochemistry, case report

Introduction

Confirmed cases of vertical transmission of severe acute respiratory syndrome coronavirus-2 (SARS-CoV-2) appear to be rare (1), but case series and reports have described instances of possible transplacental SARS-CoV-2 transmission (2–6). However, timely ascertainment of laboratory evidence has been a barrier to confirmation (1, 2, 4). In this report, we present findings of SARS-CoV-2 infection in a symptomatic individual in the third trimester of pregnancy and infant delivered by cesarean section.

Case description

A 27-year-old pregnant female (G2P1001 at 35 weeks, 5 days gestation) with an early childhood history of acute lymphocytic leukemia and no previous COVID-19 vaccination developed COVID-19 symptoms (Table 1), including chest pain and shortness of breath, and tested positive for SARS-CoV-2 by rapid antigen test on day 3 after onset of symptoms. Cough, severe dyspnea, and pleuritic chest pain developed on day 9. Computed tomography scan revealed a mild patchy ground-glass density in the lateral right middle lung lobe. A fetal non-stress test to evaluate heart rate and responsiveness was reassuring. Fever resolved on day 10 with improvement of dyspnea and chest pain on day 11, but cough and pleuritic chest pain continued. The mother expressed concern over reduced fetal movement and hospital evaluation was recommended. After a nonreactive fetal non-stress test with several fetal deceleration events, a cesarean section was performed the same day and was complicated by postpartum hemorrhage. The mother remained afebrile with improving cough and pleuritic chest pain and was discharged after 2 days on illness day 14.

Apgar scores of the infant at birth were 7, 6, and 7, at 1, 5, and 10 min, respectively. Birthweight was 2,475 g and placental weight was 516 grams trimmed. The umbilical artery had a pH of 7.2. Meconium-stained amniotic fluid and double nuchal cord were present at delivery. The infant was in respiratory distress and brought to post-anesthesia care unit (PACU) for resuscitation. Suctioning revealed large amounts of meconium-stained fluid. The infant required continuous positive airway pressure (CPAP) with 5+cm H_2O positive end expiratory pressure (PEEP) at 30% fraction of inspired oxygen (FiO_2) at 4 min of life with an oxygen saturation (SpO_2) of 58%. Due to increased work of breathing (SpO_2 70–80%), PEEP was increased to 6+cm H_20 and FiO_2 was increased to 40% around 7 min of life. SpO_2 improved to 88–90% and the infant was transported to the neonatal intensive care unit (NICU).

In the NICU, CPAP was switched to noninvasive neurally-adjusted ventilatory assist. Chest x-ray revealed a right pneumothorax and bilateral ground glass densities, and the infant was switched back to conventional CPAP at 6 h of life. The infant's respiratory status quickly improved and was weaned to room air on day 1 after birth. Nasal swabs collected 1 and 2 days after delivery tested negative and positive, respectively, by SARS-CoV-2 antigen test. A reverse transcription polymerase chain reaction (RT-PCR) test on a nasopharyngeal (NP) swab collected day 3 after birth was positive for SARS-CoV-2 and negative for a panel of other respiratory viruses. Delivery and neonatal care staff wore facemasks over N-95 respirators, or powered air-purifying respirators. The mother was masked throughout the delivery and did not have contact with the infant prior to NICU transfer.

The infant's pneumothorax resolved without chest tube placement. Routine hematologic and clinical chemistry testing on blood were normal for age. The infant was in airborne isolation for 10 days and was discharged at 13 days old feeding appropriately and gaining weight. Subsequently, identical SARS-CoV-2 Alpha/B.1.1.7 genotypes were identified in specimens from mother, infant, and placenta. Placenta histology was consistent with previous reports of placental SARS-CoV-2 infection (1, 4, 7, 8). Additionally, immunostaining for SARS-CoV-2 and electron microscopy (EM) analysis of the placenta found evidence of coronavirus in the syncytiotrophoblast.

Materials and methods

This study was reviewed by the Centers for Disease Control and Prevention (CDC) and was conducted consistent with applicable federal law and CDC policy.[§] Written informed consent for this work was obtained from the mother for herself and from both parents for the infant. Nebraska Public Health Laboratory (NPHL) received four specimens

TABLE 1 Case timeline: Maternal and neonatal symptom development, clinical care, and sample collection.

Day	Patient	Event	Result of testing
1	Mother	Onset of symptoms, including chest pain and shortness of breath	N/A
3	Mother	SARS-CoV-2 antigen test performed	Positive
9	Mother	Developed cough, severe dyspnea, and pleuritic chest pain; computed tomography (CT) scan with contrast performed, patient discharged	Chest CT scan negative for pulmonary embolism, mild patchy ground glass density was identified in the lateral right middle lobe
10	Mother	Fever resolved	N/A
11	Mother	Improved dyspnea and chest pain, cough and pleuritic chest pain continued, noted reduced fetal movement, cesarean delivery performed	Maternal plasma collected before cesarean delivery and placental tissue subsequently test positive for SARS-CoV-2 (see Results)
11	Neonate	In respiratory distress after birth, transported to the neonatal intensive care unit; chest X-ray performed	Right pneumothorax, bilateral ground glass densities, and other radiologic findings consistent with prematurity
12	Neonate	Respiratory status improved; SARS-CoV-2 nasal swab antigen test (collected 24 h after birth)	Negative
13	Neonate	SARS-CoV-2 nasal swab antigen test (collected 48 h after birth)	Positive
14	Mother	Discharged from hospital	N/A
14	Neonate	Reverse transcription polymerase chain reaction (RT-PCR) test on a nasopharyngeal (NP) swab (collected 72 h after birth)	Positive for SARS-CoV-2; negative for a panel of other respiratory viruses
16	Mother and Neonate	NP swabs collected from each individual	Swabs subsequently test positive for SARS-CoV-2 (see Results)
24	Neonate	Discharged from hospital	N/A

for analysis: maternal NP swab collected 5 days post-delivery, maternal plasma collected approximately 30 min before delivery, infant NP swab collected 5 days post-birth, and formalin-fixed, paraffin-embedded (FFPE) placental tissue. Nucleic acid isolation was performed using the MagMAX™ Viral/Pathogen II Nucleic Acid Isolation Kit and KingFisher Flex System (Thermo Fisher Scientific) for NP swabs, QIAamp Viral RNA Mini Kit (QIAGEN) and QIAcube Connect for serum, and RNeasy FFPE Kit (QIAGEN) for RNA isolation from FFPE tissue. All specimens underwent RT-PCR testing using CDC's Influenza SARS-CoV-2 Multiplex Assay on the Applied Biosystems™ 7500 Fast Dx RT-PCR Instrument (Thermo Fisher Scientific).

Whole genome sequencing (WGS) was performed using the Clear Dx™ WGS SARS-CoV-2 kit and Clear Labs Dx™ System (Clear Labs), composed of a GridION (Oxford Nanopore) and Hamilton STAR liquid handler. The Clear View WGS application (https://wgs.app.clearlabs.com) was used for assembly and sequencing coverage analysis. RNA mutation identification used Nextclade version v0.14.2 (https://clades.nextstrain.org). Sample lineages were assigned using the Pangolin COVID-19 Lineage Assigner (https://pangolin.cog.uk.io). Clonality between samples was determined *via* single nucleotide polymorphism (SNP) analysis using SNP-sites/2.5 with default parameters (https://github.com/sanger-pathogens/snp-sites).

The CDC Infectious Diseases Pathology Branch performed histopathological evaluation and SARS-CoV-2 immunohistochemical (IHC) and EM analysis of placenta, umbilical cord, and membrane FFPE blocks. Placenta, umbilical cord, and membrane tissues had been received fresh by the pathologist in Nebraska and fixed in 10% neutral buffered formalin and embedded in paraffin to create FFPE blocks. IHC assays used a rabbit polyclonal antibody raised against SARS-CoV-2 nucleocapsid (GenTex-GTX635686) at 1:100 dilution and a mouse monoclonal SARS-CoV-2 spike (GeneTex-GTX632604) at dilution 1:250 with a Mach 4 Universal AP Polymer Kit (Biocare Medical) with Permanent Red Chromogen (Cell Marque). Slides were pretreated with heat-induced epitope retrieval with citrate-based buffer (Biocare Medical). Negative controls, run in parallel, used normal rabbit, or mouse serum in place of the primary antibody. FFPE samples for EM were processed as described in Martines et al. (9).

Results

RT-PCR detected SARS-CoV-2 RNA in the maternal NP swab, maternal plasma, infant NP swab, and FFPE placental tissue specimens. Cycle threshold (Ct) values, identified from graphical outputs, were 29.8, 25.7, 16.5, and 14.4 for the maternal NP swab, maternal plasma, infant NP swab, and

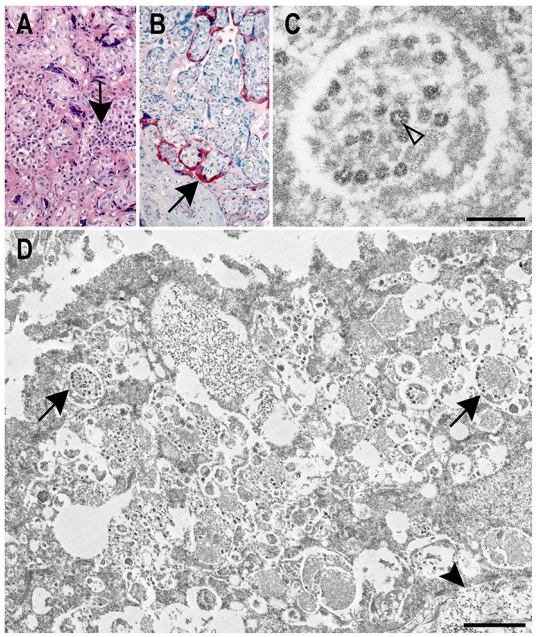

FIGURE 1
Correlative histology, immunohistochemistry, and ultrastructural findings in a SARS-CoV-2 positive placenta. **(A)** Placenta showing histiocytic intervillositis (arrow) with villous trophoblast necrosis and fibrin (H&E, original magnification 20X). **(B)** Immunostaining of SARS-CoV-2 nucleocapsid protein (arrow) in the syncytiotrophoblast of the placenta (IHC, original magnification 20X). **(C)** Electron microscopy image displaying a membrane bound accumulation of coronavirus particles in the syncytiotrophoblast. Cross sections through the viral nucleocapsid visible (open arrowhead). Scale bar: 200 nm. **(D)** Vacuolar, membrane bound accumulations of coronavirus particles (arrows) in the syncytiotrophoblast of the placenta as seen by electron microscopy. A cytotrophoblast (arrowhead) is visible below the syncytiotrophoblast. Scale bar: 1 μm.

placental tissue, respectively. The test's Ct cutoff value was 40. WGS performed on the maternal plasma, infant, and placental specimens revealed all SARS-CoV-2 sequences belonged to clade 20I/501Y.V1 (lineage Alpha/B.1.1.7) and were 100% identical along the 29902-bps analyzed with no SNP differences. Sequencing was not performed on the maternal NP swab due its high Ct value (29.8).

Placenta histology displayed prominent histiocytic and neutrophilic intervillositis with fibrin deposition and trophoblast necrosis (Figure 1A). Umbilical cord and membranes showed no significant histopathologic findings. IHC assays using antibodies against SARS-CoV-2 nucleocapsid and spike proteins showed extensive staining in villous syncytiotrophoblast and intervillous inflammatory cells (Figure 1B).

EM revealed particles morphologically consistent with coronavirus in the syncytiotrophoblast (Figures 1C, D). Areas for EM analysis were identified from IHCs showing positive staining for the SARS-CoV-2 spike protein (Figure 1B). Membrane-bound viral particles displayed visible cross-sections through the viral nucleocapsid and were on average 66 nm in diameter (range 56–81 nm; Figure 1C). The size of these particles was smaller than is typical of a coronavirus due to the use of FFPE tissues. Spikes were not readily apparent on the viral particles; viral spikes are typically not visible on intracellular coronavirus viral particles. Though the ultrastructure of the specimen was diminished due to the use of FFPE tissues, margins of the syncytiotrophoblast and adjacent cytotrophoblast were discernable as were vacuolar accumulations of viral particles within the syncytiotrophoblast cytoplasm (Figure 1D).

Discussion

Though rare, vertical transmission of SARS-CoV-2 has been reported (1, 3, 5, 6, 8, 10, 11), however, conclusive cases remain elusive. This report presents evidence indicating probable vertical transmission of SARS-CoV-2, supported by clinical course timing, lack of contact between mother and infant postpartum, and identical genotypes of SARS-CoV-2 identified from both patients' specimens, including maternal plasma before cesarean delivery. However, determination of the timing or distinction between prepartum and peripartum SARS-CoV-2 transmission remains unclear due partially to specimen availability.

Previous SARS-CoV-2 studies indicate placental infection is necessary before fetal infection and *in utero* infection requires that virus crosses the maternal-placental interface to access fetal vessels (12). We demonstrated placental SARS-CoV-2 infection by IHC, as recommended by Roberts et al. (7), showing localization of SARS-CoV-2 nucleocapsid and spike proteins in the syncytiotrophoblast, consistent with published reports (13, 14). Positive staining has been reported in Hofbauer cells and villous capillary endothelial cells (14), but was not observed in this case. EM further verified coronavirus infection of the syncytiotrophoblast. The presence of numerous membrane bound collections of coronavirus particles within the syncytiotrophoblast suggest the virus is replicating in this cell type. As the syncytiotrophoblast is the initial defense against pathogens attempting to cross the placental barrier and is in direct contact with maternal blood, the virus observed in this cell type is further evidence of maternal viremia. Since coronavirus was not identified by EM in other areas of the placenta, whether the virus entered fetoplacental circulation cannot be determined. Even now, accurate reports of coronavirus particles in the placenta have been rare (15, 16) with several articles misidentifying common subcellular structures as coronavirus in the placenta as well as other tissues (17).

Placental histopathologic evaluation further revealed chronic histiocytic intervillositis, trophoblastic necrosis, and increased perivillous fibrin deposition, all described

as hallmarks of SARS-CoV-2 placental infection (7, 8, 11). However, the intervillositis observed may be an incidental finding or SARS-CoV-2 infection may have exacerbated existing intervillositis. The potential causes of intervillositis are varied and not well understood, though the condition is hypothesized to result from excessive maternal inflammation toward the placenta, possibly due to maternal infection in some cases (18, 19). Intervillositis has been reported in other placentas from SARS-CoV-2 positive individuals (13, 20, 21), but has also been observed with other infectious diseases including dengue (22) and cytomegalovirus (23). Larger cohort studies are necessary to determine any correlation between SARS-CoV-2 infection and adverse pregnancy outcomes including intervillositis.

Together, the data presented enable this case to meet the definition for probable SARS-CoV-2 vertical transmission (12) and serve as an example of the importance of comprehensive sample collection. Detection of SARS-CoV-2 RNA in maternal plasma before cesarean delivery suggests viremia, while RT-PCR, IHC, and EM results indicated the presence of SARS-CoV-2 in placental tissues. SARS-CoV-2 infection in the neonate was confirmed on days 2 and 3 after delivery, by antigen test and RT-PCR, respectively. Unfortunately, a specimen from the infant on the day of delivery was not available for RT-PCR testing. Meconium-stained amniotic fluid was present at delivery and a large amount of meconium-stained fluid was suctioned from the infant's lungs. However, for meconium aspiration to be the route of transmission, SARS-CoV-2 would need to be present in the meconium either prior to birth or present in amniotic fluid the infant aspirated along with meconium during delivery. While amniotic fluid and meconium were not available for testing in this case, other studies have noted a higher viral load in placental tissue than in amniotic fluid (20) and amniotic fluid from 43 SARS-CoV-2 positive pregnant mothers tested negative for SARS-CoV-2 by RT-PCR (24). Additionally, a systematic review by Allotey et al., found infection of amniotic fluid or placental tissue with SARS-CoV-2 did not necessarily correlate with fetal infection (1). Still, the lack of a specimen from the infant on the day of delivery or an amniotic fluid or meconium specimen limit definitive conclusions about the timing of vertical transmission.

Thankfully, this case had a positive outcome with the full recovery of both mother and infant. At the time of this delivery, maternal SARS-CoV-2 vaccination was an individual decision. CDC, the American College of Obstetricians and Gynecologists, and the Society for Maternal-Fetal Medicine now strongly recommend vaccination to prevent SARS-CoV-2 infection before or during pregnancy (25).

Ethics statement

This activity was reviewed by CDC and was conducted consistent with applicable federal law and CDC policy.[§] Written informed consent was obtained. [§]See e.g., 45 C.F.R. part 46, 21 C.F.R. part 56; 42 U.S.C. §241(d); 5 U.S.C. §552a; 44 U.S.C. §3501 et seq. Written informed consent to participate in this study was provided by the participants' legal guardian/next of kin. Written informed consent was obtained from the individual(s), and minor(s)' legal guardian/next of kin, for the publication of any potentially identifiable images or data included in this article.

Author contributions

HB and EF contributed equally to conceptualization, design, and drafting of the manuscript. HB, EF, RM, TU, SR-S, and MD contributed to study design, data review, and manuscript revision. AR, AN, and MB participated in patient treatment. AO-A and LK participated in neonate care. Initial investigation and gathering of case information was performed by ML, TT, PL, and MD. MD, PI, CS, and JF participated in specimen and testing coordination. CS participated in specimen collection. Laboratory testing and review of results was performed by HB, BB, RM, EMi, and EMc. ML, HB, MD, EMi, EMc, RM, BB, and TU contributed to the interpretation of laboratory results. All authors reviewed and approved of the final manuscript.

Funding

This work was supported by the Epidemiology and Laboratory Capacity for Prevention and Control of Emerging Infectious Diseases (ELC) Cooperative Agreement and through contractual mechanisms, including the Local Health Department Initiative. This study was performed as regular work of the Centers for Disease Control and Prevention.

Acknowledgments

We thank the participants and family involved in this case report. We thank Cynthia Goldsmith for her guidance with electron microscopy. We are thankful for the leadership and mentorship of Dr. Sherif Zaki and dedicate this report to his lasting memory.

Conflict of interest

The authors declare that the research was conducted in the absence of any commercial or financial relationships

that could be construed as a potential conflict of interest.

Publisher's note

All claims expressed in this article are solely those of the authors and do not necessarily represent those of their affiliated organizations, or those of the publisher, the editors and the reviewers. Any product that may be evaluated in this article, or claim that may be made by its manufacturer, is not guaranteed or endorsed by the publisher.

Author disclaimer

The findings and conclusions in this report are those of the authors and do not necessarily represent the official position of the Centers for Disease Control and Prevention (CDC).

References

1. Allotey J, Chatterjee S, Kew T, Gaetano A, Stallings E, Fernández-García S, et al. SARS-CoV-2 positivity in offspring and timing of mother-to-child transmission: living systematic review and meta-analysis. *BMJ.* (2022) 376:e067696. doi: 10.1136/bmj-2021-067696

2. Woodworth KR, Olsen EO, Neelam V, Lewis EL, Galang RR, Oduyebo T, et al. Birth and infant outcomes following laboratory-confirmed SARS-CoV-2 infection in pregnancy — SET-NET, 16 Jurisdictions, March 29–October 14, 2020. *MMWR Morb Mortal Wkly Rep.* (2020) 69:1635–40. doi: 10.15585/mmwr.mm6944e2

3. Alamar I, Abu-Arja MH, Heyman T, Roberts DJ, Desai N, Narula P, et al. A possible case of vertical transmission of SARS-CoV-2 in a newborn with positive placental in situ hybridization of SARS-CoV-2 RNA. *J Pediatric Infect Dis Soc.* (2020) 9:636–9. doi: 10.1093/jpids/piaa109

4. Shook LL, Brigida S, Regan J, Flynn JP, Mohammadi A, Etemad B, et al. SARS-CoV-2 placentitis associated with B.1.617.2 (Delta) variant and fetal distress or demise. *J Infect Dis.* (2022) 225:754–8. doi: 10.1093/infdis/jiac008

5. Kotlyar AM, Grechukhina O, Chen A, Popkhadze S, Grimshaw A, Tal O, et al. Vertical transmission of coronavirus disease 2019: a systematic review and meta-analysis. *Am J Obstet Gynecol.* (2021) 224:35–53. doi: 10.1016/j.ajog.2020.07.049

6. Patanè L, Morotti D, Giunta MR, Sigismondi C, Piccoli MG, Frigerio L, et al. Vertical transmission of coronavirus disease 2019: severe acute respiratory syndrome coronavirus 2 RNA on the fetal side of the placenta in pregnancies with coronavirus disease 2019–positive mothers and neonates at birth. *Am J Obstet Gynecol.* (2020) 2:100145. doi: 10.1016/j.ajogmf.2020.100145

7. Roberts DJ, Edlow AG, Romero RJ, Coyne CB, Ting DT, Hornick JL, et al. A standardized definition of placental infection by severe acute respiratory syndrome coronavirus 2 (SARS-CoV-2), a consensus statement from the National Institutes of Health/Eunice Kennedy Shriver National Institute of Child Health and Human Development SARS-CoV-2 Placental Infection Workshop. *Am J Obstet Gynecol.* (2021) 225:593–9. doi: 10.1016/j.ajog.2021.07.029

8. Schwartz DA, Morotti D. Placental pathology of COVID-19 with and without fetal and neonatal infection: trophoblast necrosis and chronic histiocytic intervillositis as risk factors for transplacental transmission of SARS-CoV-2. *Viruses.* (2020) 12:1308 doi: 10.3390/v12111308

9. Martines RB, Ritter JM, Matkovic E, Gary J, Bollweg BC, Bullock H, et al. Pathology and pathogenesis of SARS-CoV-2 associated with fatal coronavirus disease, United States. *Emerg Infect Dis.* (2020) 26:2005–15. doi: 10.3201/eid2609.202095

10. Reagan-Steiner S, Bhatnagar J, Martines RB, Milligan NS, Gisondo C, Williams FB, et al. Detection of SARS-CoV-2 in neonatal autopsy tissues and placenta. *Emerg Infect Dis.* (2022) 28:510–7. doi: 10.3201/eid2803.211735

11. Watkins JC, Torous VF, Roberts DJ. Defining severe acute respiratory syndrome coronavirus 2 (SARS-CoV-2) Placentitis: a report of 7 cases with confirmatory in situ hybridization, distinct histomorphologic features, and evidence of complement deposition. *Arch Pathol Lab Med.* (2021) 145:1341–9. doi: 10.5858/arpa.2021-0246-SA

12. World Health Organization. *Definition and Categorization of the Timing of Mother-to-Child Transmission of SARS-CoV-2.* (2021). Available online at: https://www.who.int/publications/i/item/WHO-2019-nCoV-mother-to-child-transmission-2021.1

13. Schwartz DA, Baldewijns M, Benachi A, Bugatti M, Collins RRJ, De Luca D, et al. Chronic histiocytic intervillositis with trophoblast necrosis is a risk factor associated with placental infection from coronavirus disease 2019 (COVID-19) and intrauterine maternal-fetal Severe Acute Respiratory Syndrome Coronavirus 2 (SARS-CoV-2) transmission in live-born and stillborn infants. *Arch Pathol Lab Med.* (2021) 145:517–28. doi: 10.5858/arpa.2020-0771-SA

14. Schwartz DA, Baldewijns M, Benachi A, Bugatti M, Bulfamante G, Cheng K, et al. Hofbauer cells and COVID-19 in pregnancy molecular pathology analysis of villous macrophages, endothelial cells, and placental findings from 22 placentas infected by SARS-CoV-2 with and without fetal transmission. *Arch Pathol Lab Med.* (2021) 145:1328–40. doi: 10.5858/arpa.2021-0296-SA

15. Birkhead M, Glass AJ, Allan-Gould H, Goossens C, Wright CA. Ultrastructural evidence for vertical transmission of SARS-CoV-2. *Int J Infect Dis.* (2021) 111:10–1. doi: 10.1016/j.ijid.2021.08.020

16. Rakheja D, Treat K, Timmons CF, Carrillo D, Miller SE, Stroberg E, et al. SARS-CoV-2 immunohistochemistry in placenta. *Int J Surg Pathol.* (2022) 30:393–6. doi: 10.1177/10668969211067754

17. Bullock HA, Goldsmith CS, Miller SE. Detection and identification of coronaviruses in human tissues using electron microscopy. *Microsc Res Tech.* (2022) 85:2740–7. doi: 10.1002/jemt.24115

18. Brady CA, Williams C, Sharps MC, Shelleh A, Batra G, Heazell AEP, et al. Chronic histiocytic intervillositis: a breakdown in immune tolerance comparable to allograft rejection? *Am J Reprod Immunol.* (2021) 85:e13373. doi: 10.1111/aji.13373

19. Capuani C, Meggetto F, Duga I, Danjoux M, March M, Parant O, et al. Specific infiltration pattern of FOXP3+ regulatory T cells in chronic histiocytic intervillositis of unknown etiology. *Placenta.* (2013) 34:149–54. doi: 10.1016/j.placenta.2012.12.004

20. Vivanti AJ, Vauloup-Fellous C, Prevot S, Zupan V, Suffee C, Cao J, et al. Transplacental transmission of SARS-CoV-2 infection. *Nat Commun.* (2020) 11:3572. doi: 10.1038/s41467-020-17436-6

21. Debelenko L, Katsyv I, Chong AM, Peruyero L, Szabolcs M, Uhlemann AC. Trophoblast damage with acute and chronic intervillositis: disruption of the placental barrier by severe acute respiratory syndrome coronavirus 2. *Hum Pathol.* (2021) 109:69–79. doi: 10.1016/j.humpath.2020.12.004

22. Ribeiro CF, Lopes VGS, Brasil P, Pires ARC, Rohloff R, Nogueira RMR. Dengue infection in pregnancy and its impact on the placenta. *Int J Infect Dis.* (2017) 55:109–12. doi: 10.1016/j.ijid.2017.01.002

23. Taweevisit M, Sukpan K, Siriaunkgul S, Thorner PS. Chronic histiocytic intervillositis with cytomegalovirus placentitis in a case of hydrops fetalis. *Fetal Pediatr Pathol.* (2012) 31:394–400. doi: 10.3109/15513815.2012.659405

24. Arora D, Rajmohan KS, Dubey S, Dey M, Singh S, Nair VG, et al. Assessment of materno-foetal transmission of SARS-CoV-2: a prospective pilot study. *Med J Armed Forces India.* (2021) 77(Suppl 2):S398–403. doi: 10.1016/j.mjafi.2021.01.007

25. ACOG. *ACOG and SMFM Recommend COVID-19 Vaccination for Pregnant Individuals.* (2021). Available online at: https://www.acog.org/news/news-releases/2021/07/acog-smfm-recommend-covid-19-vaccination-for-pregnant-individuals

frontiers | Frontiers in Medicine

TYPE Case Report
PUBLISHED 12 January 2023
DOI 10.3389/fmed.2022.1094347

OPEN ACCESS

EDITED BY
Francesco Paolo Bianchi,
University of Bari Aldo Moro, Italy

REVIEWED BY
Chenguang Shen,
Southern Medical University, China
Yanqun Wang,
Guangzhou Medical University, China
Xiangpeng Chen,
Beijing Children's Hospital, Capital Medical University, China

*CORRESPONDENCE
Yang Yang
✉ young@mail.sustech.edu.cn
Yingxia Liu
✉ yingxialiu@hotmail.com
Haibin Gao
✉ 315219232@qq.com

†These authors have contributed equally to this work

SPECIALTY SECTION
This article was submitted to Infectious Diseases: Pathogenesis and Therapy, a section of the journal Frontiers in Medicine

RECEIVED 10 November 2022
ACCEPTED 14 December 2022
PUBLISHED 12 January 2023

CITATION
Jiang C, Xu Z, Li J, Zhang J, Xue X, Jiang J, Jiang G, Wang X, Peng Y, Chen T, Liu Z, Xie L, Gao H, Liu Y and Yang Y (2023) Case report: Clinical and virological characteristics of aseptic meningitis caused by a recombinant echovirus 18 in an immunocompetent adult. *Front. Med.* 9:1094347. doi: 10.3389/fmed.2022.1094347

Case report: Clinical and virological characteristics of aseptic meningitis caused by a recombinant echovirus 18 in an immunocompetent adult

Chunmei Jiang[1†], Zhixiang Xu[2†], Jin Li[3†], Jiaqi Zhang[2†], Xingkui Xue[1], Jingxia Jiang[1], Guihua Jiang[1], Xisheng Wang[1], Yun Peng[2], Tian Chen[1], Zhenzhen Liu[1], Liu Xie[1], Haibin Gao[1*], Yingxia Liu[2*] and Yang Yang[2*]

[1]Department of Infectious Disease, The People's Hospital of Longhua, Shenzhen, China, [2]Shenzhen Key Laboratory of Pathogen and Immunity, State Key Discipline of Infectious Disease, Shenzhen Third People's Hospital, Second Hospital Affiliated to Southern University of Science and Technology, Shenzhen, China, [3]Shenzhen Polytechnic, Shenzhen, China

Echovirus 18 has been recognized as an important causative pathogen of aseptic meningitis in young children worldwide, and echovirus 18-induced meningitis is rarely found in adults with immunocompetence. In this case study, we report the clinical and virological characteristics of aseptic meningitis caused by recombinant echovirus 18 in an adult with immunocompetence. A 31-year-old woman with immunocompetence was admitted to our hospital with fever, dizziness, severe headache, nausea, and vomiting for the past 1 day and was diagnosed with viral meningitis based on the clinical manifestations and laboratory results from cerebrospinal fluid (CSF). The patient received antiviral treatment with ribavirin and interferon as soon as the enterovirus infection was identified using qRT-PCR and was cured after 4 days. From the oropharyngeal swab and CSF samples, two echovirus 18 strains were isolated with a single nucleotide difference located at the 5′ UTR. Phylogenetic analyses based on the VP1 gene showed that the two strains belonged to the subgenotype C2 and were clustered with sequences obtained from China after 2015, while the results from the 3D polymerase region showed that the two strains were closely related to the E30 strains. Bootscanning results using the 5′ UTR to 2A region and the 2B to 3′ UTR region showed that potential intertypic recombination had occurred in the 2B gene. Recombination analyses further confirmed that the two strains (echovirus 18) presented genome recombination with echovirus 30 in the nucleotide regions of the 2B gene. To the best of our knowledge, this is the first report of echovirus 18-induced meningitis in an adult with immunocompetence from mainland China, highlighting the need for close surveillance of echovirus 18 both in children and adults in the future.

KEYWORDS

aseptic meningitis, echovirus 18, immunocompetent adult, recombination < evolution, case report

Introduction

Meningitis is inflammation of the meninges characterized by an abnormal number of white blood cells (WBC) in cerebrospinal fluid (CSF) with few or no focal neurological findings or brain abnormalities on imaging and accompanied by the acute onset of fever, headache, and neck stiffness (1, 2). Infectious agents, including viruses, bacteria, and fungi, are the most common causes of meningitis (3). Viral meningitis is associated with the acute onset of meningeal symptoms and fever, pleocytosis of the cerebrospinal fluid, and no growth on routine bacterial cultures, usually affecting young children (1, 4). Many viruses have been shown to cause viral meningitis, such as enteroviruses (EVs), parechovirus, herpesviruses, influenza viruses, arboviruses, and coronaviruses, and viral etiology varies according to age and country (3).

Human enteroviruses belong to the Enterovirus genus of the Picornaviridae family and are characterized as non-enveloped, positive-sense, single-stranded RNA viruses with ∼7,500 nucleotides (5). The enteroviruses contain four enterovirus species (A to D) and three rhinovirus species (A to C) and infect millions of people worldwide every year with mostly mild and self-limited symptoms, such as hand-foot-and-mouth disease, herpangina, pleurodynia, rashes, and rhinitis (5, 6). Moreover, an increasing number of enteroviruses have been found to infect the central nervous system and result in various neurological diseases, of which non-polio human enteroviruses (NPEV) have become the leading recognizable cause of viral meningitis (5, 6). Notably, Enterovirus B (EV-B), a species of the genus Enterovirus, particularly echovirus 6, 9, 13, 14, 16, and 30, accounted for the majority of meningitis cases with worldwide distribution (5). As a member of EV-B, echovirus 18 was first discovered in 1955 (7), and since then, it has been reported as a pathogen causing aseptic meningitis in many countries of the world (8–14). Most of the patients in these reports were young children, and an outbreak of encephalitis/meningitis caused by echovirus 18 in children has been reported in 2015 in mainland China (9). There was no report of echovirus 18-induced meningitis in adults with immunocompetence in mainland China and scant report in other countries of world (10–12). In the present study, we report the clinical and virological characteristics of aseptic meningitis caused by the recombinant echovirus 18 in an adult with immunocompetence from Shenzhen, China.

Materials and methods

Sample collection and virus isolation

Oropharyngeal swabs and CSF samples were collected from the patient on the first and second days following admission, respectively. All specimens positive for enterovirus infection by qRT-PCR were cultured in Rhabdomyosarcoma (RD) cells for virus isolation. The study was performed in accordance with guidelines approved by the ethics committees of Shenzhen People's Hospital Longhua Branch and the Shenzhen Third People's Hospital. Written informed consent was obtained from the patient for the publication of any potentially identifiable images or data included in this article.

Quantitative reverse transcriptase PCR (qRT-PCR)

Nucleic acids were extracted from 140 μl of the oropharyngeal swab, CSF, and cell culture supernatant samples using the QIAamp RNA Viral Kit (Qiagen, Germany) according to the instructions of the manufacturer. Nucleic acids were eluted in 50 μl of AVE buffer and stored at −80°C for subsequent use. Nucleic acids samples were tested by quantitative reverse transcription polymerase chain reaction (qRT-PCR) in an ABI QuantStudio Dx Real-Time cycler (Applied Biosystems, USA), using commercial kits targeting the common pathogens that induce meningitis (Mabsky Biotech Co., Ltd.), including herpes simplex virus (HSV)-1, HSV-2, varicella-zoster virus (VZV), human cytomegalovirus (HCMV), Epstein-Barr virus (EBV), human herpes virus 6 (HHV-6), HHV7, JC virus (JCV), human parechovirus (HPeV), enterovirus (EV), mumps virus, measles virus, *Haemophilus influenzae*, *Streptococcus pneumoniae*, *Staphylococcus aureus*, *Listeria monocytogenes*, *Neisseria meningitidis*, *Streptococcus agalactiae*, *Cryptococcus neoformans*, and *Escherichia coli*.

Full-length genome amplification

The amplification and sequencing of our two echovirus strains were performed, as previously reported with some modifications (15). Three long-distance PCR amplifications were performed using a PrimeScriptTM One-Step RT-PCR Kit Version 2 (Takara, China). The primers used for RT-PCR and sequencing of the full-length genome were designed using a "primer-walking" strategy and are listed in **Supplementary Table 1**. The PCR products were purified using the QIAquick PCR purification kit (Qiagen, Germany) and sequenced (Sangon, China).

Phylogenetic analysis

The phylogenetic analyses were done as previously reported with slight modifications (16). Sequence alignment was performed using MEGA software version 7.0. Phylogenetic trees of the 5′ UTR to 2A region, the 2B to 3′ UTR regions, and the 3D gene were constructed by the neighbor-joining method, with bootstrap values obtained from 1,000 replicates and bootstrap values of >80% were shown. The phylogenetic tree of the VP1 gene and the evolution rates were constructed and determined with Bayesian Evolutionary Analysis Sampling Trees (BEAST) software version 1.8 using a lognormal relaxed clock, a constant-size tree prior, and the GTR + G substitution model. Each Bayesian MCMC analysis was run for 100 million generations. Bootstrap testing with 1,000 replicates was used to estimate the strength of the phylogenetic trees.

Recombination analysis

The recombination analyses were done as described in the previous report (16). A potential recombination within the complete genome sequences of echovirus 18 was assessed using the similarity plot and the bootscanning method with the neighbor-joining method and the Kimura 2-parameter substitution model with a window size

of 500 nucleotides (nt) and a step size of 20 nt. The value of the permuted trees of > 80% indicated potential recombination events.

Results

Case presentation

A 31-year-old immunocompetent woman was admitted to our hospital in May 2019 and presented with fever (37.8°C), dizziness, severe headache, nausea, and vomiting for 1 day (Figure 1). Upon admission, the patient had a normal heart rate (71 bpm) and blood pressure (116/76 mmHg). There were no abnormalities in the skin, in muscle tension, and during defecation, and there was no manifestation of Babinski's sign but of nuchal rigidity. She was primarily diagnosed as having an intracranial infection based on the clinical manifestations above and hospitalized (4). Serum laboratory tests revealed leukopenia (WBC count: 3.28×10^9/L) and lymphopenia (LYM count: 0.97×10^9/L). Furthermore, pleocytosis (WBC in CSF: 40×10^6/L) (17, 18), moderately increased levels of protein (564 mg/dl), and normal glucose (2.93 mmol/L) were found in CSF (4) (Table 1). Based on the manifestations and laboratory results, viral meningitis was diagnosed. To reduce the intracranial pressure, an empirical therapy with intravenous acyclovir for antiviral treatments and mannitol and glycerol fructose injections was used (Figure 1). A panel of common pathogens that induce meningitis was detected using commercial qRT-PCR kits, and the results showed that EV was positive in both the oropharyngeal swab and the CSF samples. Then, ribavirin and interferon were used as soon as possible instead of acyclovir. The fever lasted for another 3 days with a higher body temperature of 38.4°C, and the headache also resolved completely 3 days after the therapy. The treatment with interferon, mannitol, and glycerol fructose injections was stopped after 12 h of the fever breaks. Meanwhile, the result of the Gram staining smear test was negative 1 day after submission, and the bacterial culture with CSF was also negative during the cultivation time, which further confirmed aseptic meningitis.

Isolation and identification of echovirus 18

The product of qRT-PCR was sequenced using Sanger sequencing, and the results of BLAST showed the highest similarity with echovirus 18. Then, the oropharyngeal swab and CSF samples were subjected to virus isolation using RD cells. After two rounds of passage, both the supernatant from the oropharyngeal swab and the CSF samples showed typical cytopathic effects (CPEs) and positive qRT-PCR results of EV, indicating the successful isolation of the virus (data not shown). Overlapping fragments covering the entire genome of the virus were amplified and then sequenced by Sanger sequencing. The assembled genome sequences were submitted to the GenBank database with strain names LJ/0530/2019 (GenBank accession no. MN215884) and LJ/0601/2019 (GenBank accession no. MN337405) from oropharyngeal swab and CSF samples, respectively. Only one nucleotide at the 5′ UTR differed between the two strains with C in the CSF and T in the oropharyngeal swab, and this difference was confirmed using the original specimens. The complete genomes of the two strains showed an identity of 89.07% with the prototype strain of echovirus 18 strain Metcalf (GenBank accession no. AF317694). Meanwhile, the two strains showed the highest similarity of approximately 99% with the two sequences collected in Beijing, China, in 2018 (GenBank accession no. MN815810.1 and MN815811.1).

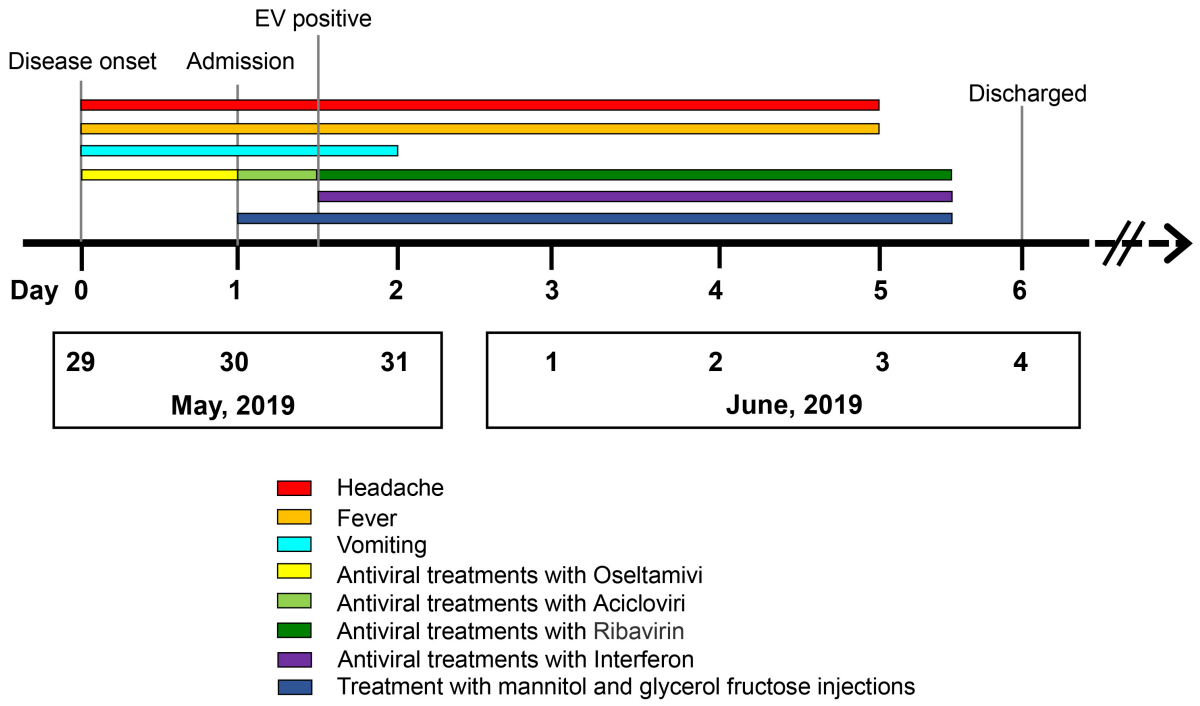

FIGURE 1
The timeline of the patients with echovirus 18-induced aseptic meningitis.

TABLE 1 Laboratory results of the serum and cerebrospinal fluid.

Parameter	Sample type	Laboratory results	Reference range	Interpretation of result
WBC ($\times 10^9$/L)	Serum	3.28	3.5–9.5	Decreased
LYM ($\times 10^9$/L)	Serum	0.97	1.1–3.2	Decreased
LYM (%)	Serum	29.6	20–50	Normal
NEU ($\times 10^9$/L)	Serum	1.78	1.8–6.3	Decreased
NEU (%)	Serum	54.3	40–75	Normal
MONO ($\times 10^9$/L)	Serum	0.51	0.1–0.6	Normal
MONO (%)	Serum	15.5	3–10	Increased
EO ($\times 10^9$/L)	Serum	0.01	0.02–0.52	Decreased
EO (%)	Serum	0.3	0.4–0.8	Decreased
BASO ($\times 10^9$/L)	Serum	0.01	0.00–0.06	Normal
BASO (%)	Serum	0.3	0.1–1	Normal
PLT ($\times 10^9$/L)	Serum	227	125–350	Normal
WBC ($\times 10^6$/L)	CSF	40	0–8	Increased
RBC ($\times 10^6$/L)	CSF	0	0	Normal
GLU (mmol/L)	CSF	2.93	2.8–4.5	Normal
CI (mmol/L)	CSF	125.9	120–130	Normal
PRO (mg/dL)	CSF	564	0–500	Increased

WBC, white blood cell; LYM, lymphocyte; NEU, neutrophil; MONO, monocyte; EO, eosinophils; BASO, basophilic granulocyte; PLT, platelet; RBC, red blood cell; GLU, glucose; CI, chloridion; PRO, protein.

Phylogenetic characteristics of the isolated echovirus 18

To analyze the evolutionary relationship of the two strains to the other 18 echovirus strains in our study, phylogenetic analyses based on the VP1 coding region and 3D polymerase genes were performed. A total of 95 representative complete VP1 gene sequences of echovirus 18, including the 14 strains dated in 2019 and 2020, were downloaded from GenBank and analyzed using MEGA7.0 and BEAST software. As previously reported (9), all the strains were divided into three genotypes (genotypes A, B, and C), and genotype C was further divided into the C1 and C2 subgroups (**Figure 2**). The mean genetic distance between genotypes A and B was 0.17 (ranging from 0.15 to 0.21), between genotypes A and C was 0.22 (ranging from 0.19 to 0.25), and between genotypes B and C was 0.19 (ranging from 0.15 to 0.24). The two strains in our study belonged to the subgenotype C2 and were clustered with sequences obtained in China after 2015. Phylogenetic analysis of 3D the polymerase region was conducted using sequences obtained from the 3D gene of the LJ-0601 and its first 100 hits obtained from a BLAST search in GenBank (**Supplementary Figure 1**). Our two strains were also found to be closely related to the E30 strain (GenBank accession no. MW080372, MW080377, and MK238483), which differs from the results with the VP1 gene, indicating that possible recombination has occurred. Notably, strains E18-221, E18-398, and E18-314 were also found to be recombinants based on our analysis, which is consistent with a previous report (16).

Moreover, phylogenetic relationship analyses based on the bootscanning results were performed using the 5′ UTR to 2A region (**Figure 3A**) and the 2B to 3′ UTR region (**Figure 3B**) of our two strains and the other 79 EV-B strains available in GenBank. The results showed that the 5′ UTR to 2A region of our two strains was closely clustered with other echovirus 18 strains, especially the strains found in Hebei, China, in 2015 (**Figure 3**), which is consistent with the preliminary molecular typing results. However, for the 2B to 3′ UTR region, our two strains did not cluster with other echovirus 18 strains while showing high similarity with the two echovirus E30 strains (GenBank accession no. MW080372 and MW080377), as shown in **Supplementary Figure 1**, suggesting that potential intertypic recombination had occurred in the 2B gene.

Recombination analysis of the isolated echovirus 18

First, the RDP V4.1 software was used to analyze the potential recombinant sequences (19). The results showed that the most possible major and minor parent strains were echovirus 18 isolate E18-393/HeB/CHN/2015 (GenBank accession no. MG720258) and echovirus E30 isolate TL7C/NM/CHN/2016 (GenBank accession no. MW080377), respectively, and other possible parent strains include echovirus 18 isolate Metcalf (GenBank accession no. AF317694) and echovirus E30 isolate TL7C/NM/CHN/2016 (GenBank accession no. MW080377) (data not shown). By combining the results of the phylogenetic and RDP analyses, four potential parental strains were subjected to similarity plots and bootscanning analyses using Simplot v3.1 software (**Figure 4**). Consistent with the results in **Figure 3**, our two strains showed the highest similarity with the echovirus 18 isolate E18-393/HeB/CHN/2015 in the 5′ UTR to 2A region and with the echovirus E30 isolate TL7C/NM/CHN/2016 in the 2B to 3′ UTR region. Furthermore, the bootscanning results further confirmed that the intratypic recombination site was in the 2B gene (**Figure 4**).

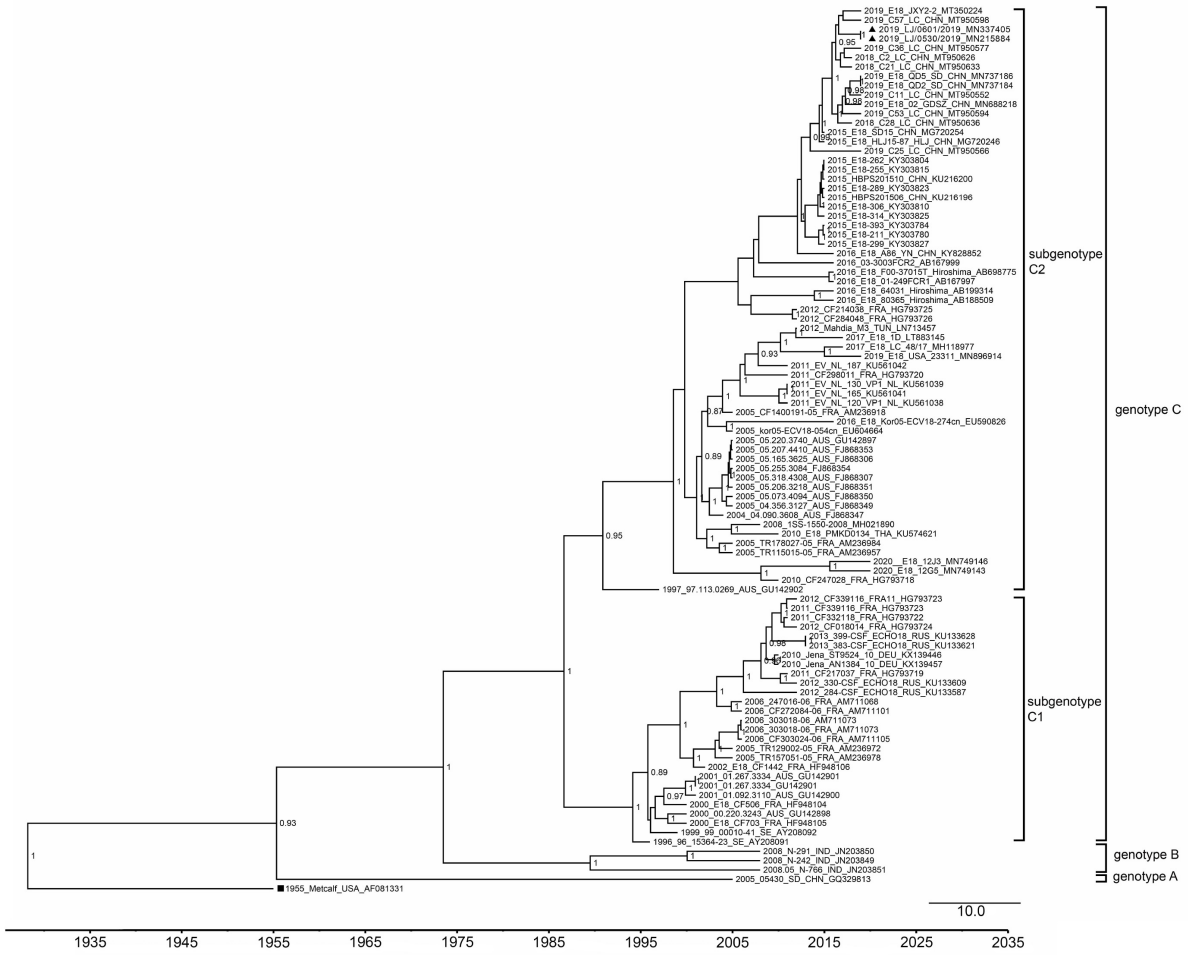

FIGURE 2
Phylogenetic tree based on the VP1 gene of echovirus 18. The phylogenetic tree was constructed using BEAST software. The posterior probabilities from the MrBayes analyses supporting the trees are indicated at the nodes. The triangle indicates the two strains in our study. The scale bar indicates years. The strain name, year of sampling, and GenBank accession numbers are shown.

Discussion

For the clinical diagnosis of meningitis, clinical symptoms are always not typical enough, as fever, chills, abdominal pain, nausea, and headaches are common in patients with meningitis, and short and fast breathing, loss of appetite, neck stiffness and pain, and sensitivity to bright light were also found in some patients (2, 20). Meanwhile, the presence of Brudzinski's sign, Kering's sign, or nuchal rigidity indicates that these bedside tests can be used by physicians to assess whether a patient should have a lumbar puncture (20). WBC, the proportion of neutrophils, glucose, and concentration of lactic acid in the CSF are key for differentiating the different types of meningitis (20–23). Although bacterial meningitis is usually characterized as a high WBC count ($\geq$ 500 cells/μl) with a large proportion of neutrophils (>80%), studies also found that patients with bacterial meningitis may present with normal CSF leukocyte counts (24, 25), which is of concern for the diagnosis based on a lumbar puncture. Moreover, with few exceptions, the clinical manifestations and symptoms associated with viral meningitis are similar despite different causative viruses, making it difficult to choose antiviral agents (1, 4). Currently, molecular diagnosis methods, including nested-PCR, multiplex PCR, and qRT-PCR assays targeting specific viruses, serve as the new golden standard tool for the diagnosis of viral meningitis with high sensitivity and specificity, which enables healthcare providers to rapidly diagnose certain infections and therefore allow clinical management decisions (4, 26). In our study, the patient received empirical antiviral therapy with intravenous acyclovir upon admission, which is effective for Herpesviridae family members but not for enteroviruses (27). The antiviral agents were changed into ribavirin and interferon as soon as the EV infection was identified using qRT-PCR, which could significantly improve the antiviral treatment efficiency with the rapid cure of this patient.

Aseptic meningitis encompasses broad differential diagnoses related to inflammation of the meninges not caused by pyogenic bacteria with both infective and noninfective causes, while viral pathogens are the most common causative agents (20). Notably, the viral etiology varies by age, the immune status of the host, geographic location, season, and exposure history (2). For example, arbovirus-induced meningitis was highly correlated with geographical location and season; Herpesviridae family members, including CMV, VZV, HHV-6, and EBV-induced meningitis, were mainly found in patients who were immunocompromised but rarely in individuals with immunocompetence (28); mumps, measles, and VZV-induced CNS

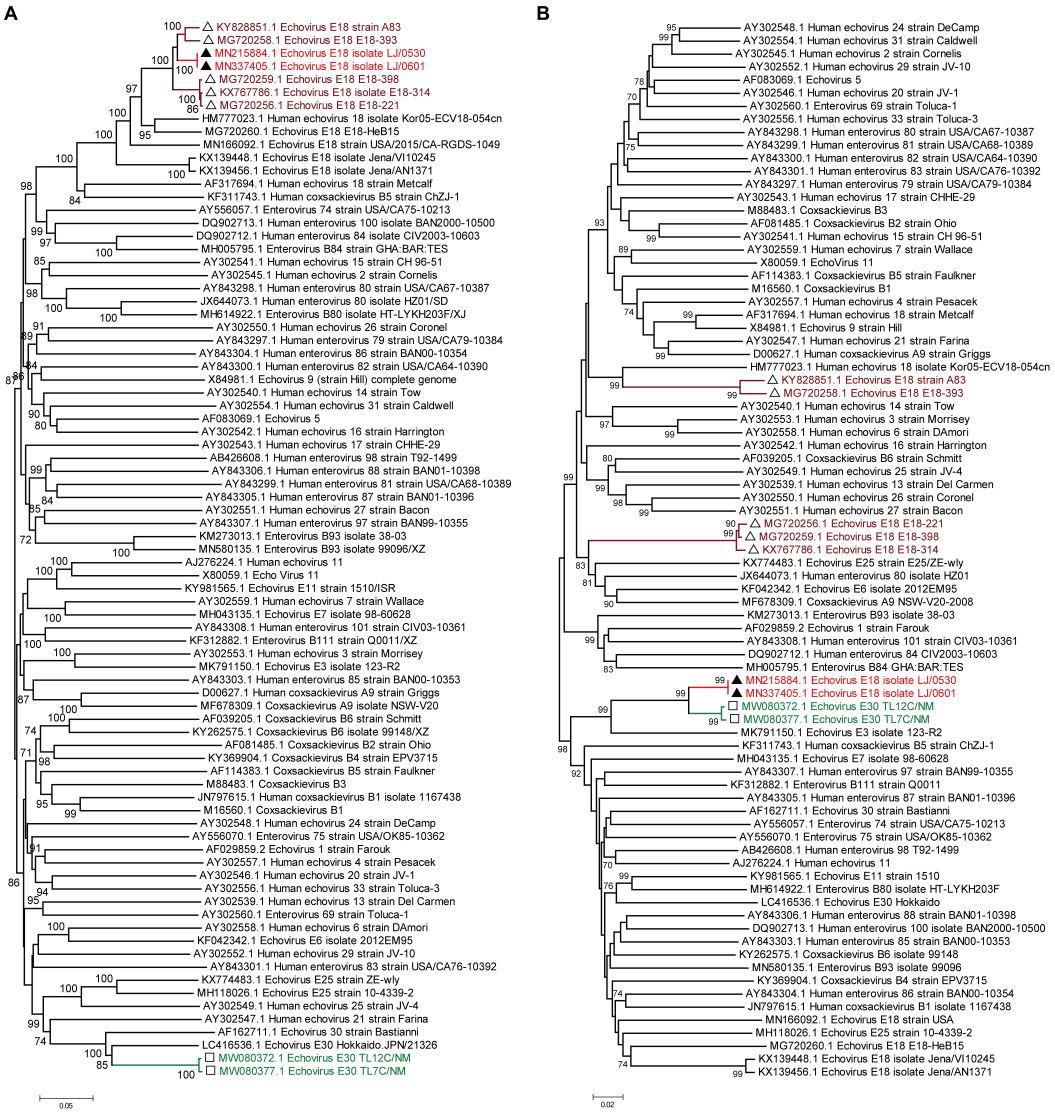

FIGURE 3
Phylogenetic relationships based on the 5′ UTR to 2A region and the 2B region to 3′ UTR of EV-B strains. Panels **(A,B)** show the phylogenetic trees of the representative 5′ UTR to 2A region **(A)** and the 2B to 3′ UTR region of the EV-B strains. Numbers at the nodes indicate bootstrap support for that node (percentage of 1,000 bootstrap replicates). The scale bars represent the genetic distance. Red indicates the two strains in our study. Brown indicates the echovirus 18 strains that are highly homologous to our strains in the 5′ UTR to 2A region. Green indicates the echovirus 30 strains that are highly homologous to our strains in the 2B region to 3′ UTR.

infections significantly declined after effective vaccines became available (2). Enteroviruses are the most common viruses that could cause meningitis in children and adults (5, 29). Studies showed that approximately 58.6% of the infected children and 51.6% of the infected adults diagnosed with meningitis/encephalitis were due to enterovirus (30, 31). One recent nationwide active surveillance study in China showed that EVs accounted for approximately 64.14% of acute meningitis/encephalitis in children and 25.19% in adults (32).

Echovirus 18-induced aseptic meningitis was mainly found in children, from sporadic infection to outbreak in various countries (12, 14, 15, 33–36), and the most recent outbreak in children has been reported in 2015 in mainland China (9). Adult patients with echovirus 18-induced aseptic meningitis have been previously reported in a limited number of cases (10, 12, 14), while severe manifestations and possibly long-term neurofunctional disability were also found to be associated (37, 38). Studies showed that the echovirus 18 strains were phylogenetically divided into three genotypes (16), and our strain belonged to the C1 subgroup, clustered with strains from China found after 2015. Moreover, the results based on the bootscanning analyses using the 5′ UTR to 2A region and the 2B to 3′ UTR region suggested a potential intratypic recombination had occurred in the 2B gene, and this was further confirmed by the recombination analysis. Recombination and mutations in enteroviruses have been recognized as the main mechanisms for the observed high rate of evolution and subsequently lead to changes in the tropism and virulence of enterovirus (39, 40). Similar to other enteroviruses, recombination was also found to be frequent for echovirus 18 (15, 16). Previous studies suggested that the current echovirus 18 strains were potential multiple-recombinant viruses containing many other EV-B donor sequences, and recombination was frequently detected in the 5′ UTR, P2, and P3 regions (15, 16). Consistent with previous studies, the recombination site of our

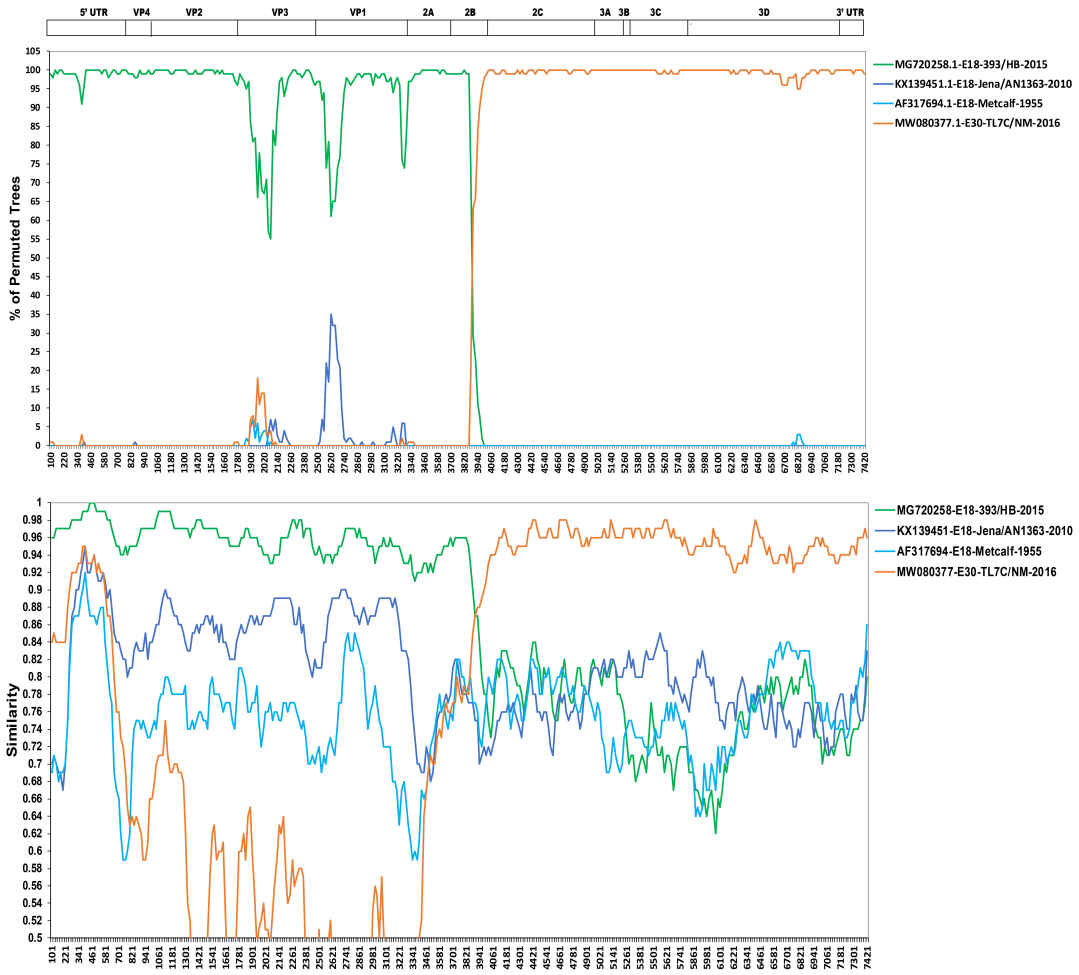

FIGURE 4
Similarity plot and bootscanning analyses of the two echovirus 18 strains based on their full-length genomes. Four potential parental strains of echovirus 18 and echovirus 30 were subjected to similarity plots and bootscanning analyses using Simplot v3.1 software.

strain was also in the 2B protein of the P2 region. Moreover, as studies showed that mutations and deletions in the UTR of some viruses are associated with replication and virulence (41–45), the single nucleotide difference between the two strains from the CSF and oropharyngeal swab samples in the 5′ UTR of echovirus 18 merits further investigation.

Conclusion

Although echovirus 18 has been circulating in mainland China for years, induced aseptic meningitis by echovirus 18 was only found in children previously. To the best of our knowledge, this is the first report of echovirus 18 in an adult with immunocompetence from mainland China, highlighting the need for close surveillance of echovirus 18 both in children and adults in the future.

Data availability statement

The datasets presented in this study can be found in online repositories. The names of the repository/repositories and accession number (s) can be found in the Genbank database: MN215884 and MN337405.

Ethics statement

This study was performed in accordance with guidelines approved by the Ethics Committees from the People's Hospital of Longhua and Shenzhen Third People's Hospital. Written informed consent was obtained from the patient for the publication of any potentially identifiable images or data included in this article.

Author contributions

YY, YL, and HG contributed to the conception and design of the study. CJ, ZX, JL, JZ, and XX enrolled the patient, performed the experiments, and analyzed the clinical data and sequences. JJ, GJ, XW, YP, TC, ZL, and LX collected the clinical data and performed some of the experiments. JL and YY drafted the manuscript. CJ, HG, and YL contributed to the critical revision of the manuscript. All authors reviewed and revised the manuscript and approved the final version.

Funding

This study was supported by the National Science and Technology Major Project (grant no. 2021YFC2301803), the Shenzhen Science and Technology Research and Development Project (grant no. JSGG20201103153802007), and the Shenzhen High-Level Hospital Construction Fund. The funding bodies had no role in the design of the study; the collection, analysis, and interpretation of data; or the writing of the manuscript.

Conflict of interest

The authors declare that the research was conducted in the absence of any commercial or financial relationships that could be construed as a potential conflict of interest.

Publisher's note

Supplementary material

The Supplementary Material for this article can be found online at: https://www.frontiersin.org/articles/10.3389/fmed.2022.1094347/full#supplementary-material

References

1. Logan SA, MacMahon E. Viral meningitis. *BMJ.* (2008) 336:36–40. doi: 10.1136/bmj.39409.673657.AE

2. Polage CR, Cohen SH. State-of-the-Art microbiologic testing for community-acquired meningitis and encephalitis. *J Clin Microbiol.* (2016) 54:1197–202. doi: 10.1128/jcm.00289-16

3. Al-Qahtani SM, Shati AA, Alqahtani YA, Ali AS. Etiology, clinical phenotypes, epidemiological correlates, laboratory biomarkers and diagnostic challenges of pediatric viral meningitis: descriptive review. *Front Pediatr.* (2022) 10:923125. doi: 10.3389/fped.2022.923125

4. Wright WF, Pinto CN, Palisoc K, Baghli S. Viral (aseptic) meningitis: a review. *J Neurol Sci.* (2019) 398:176–83. doi: 10.1016/j.jns.2019.01.050

5. Chen BS, Lee HC, Lee KM, Gong YN, Shih SR. Enterovirus and encephalitis. *Front Microbiol.* (2020) 11:261. doi: 10.3389/fmicb.2020.00261

6. Huang HI, Shih SR. Neurotropic enterovirus infections in the central nervous system. *Viruses.* (2015) 7:6051–66. doi: 10.3390/v7112920

7. Eichenwald HF, Ababio A, Arky AM, Hartman AP. Epidemic diarrhea in premature and older infants caused by ECHO virus type 18. *J Am Med Assoc.* (1958) 166:1563–6. doi: 10.1001/jama.1958.02990130023005

8. Baek K, Park K, Jung E, Chung E, Park J, Choi H, et al. Molecular and epidemiological characterization of enteroviruses isolated in Chungnam, Korea from 2005 to 2006. *J Microbiol Biotechnol.* (2009) 19:1055–64. doi: 10.4014/jmb.0810.584

9. Chen X, Li J, Guo J, Xu W, Sun S, Xie Z. An outbreak of echovirus 18 encephalitis/meningitis in children in Hebei Province, China, 2015. *Emerg Microbes Infect.* (2017) 6:e54. doi: 10.1038/emi.2017.39

10. Krumbholz A, Egerer R, Braun H, Schmidtke M, Rimek D, Kroh C, et al. Analysis of an echovirus 18 outbreak in Thuringia, Germany: insights into the molecular epidemiology and evolution of several enterovirus species B members. *Med Microbiol Immunol.* (2016) 205:471–83. doi: 10.1007/s00430-016-0464-z

11. Miyamura K, Yamashita K, Yamadera S, Kato N, Akatsuka M, Yamazaki S. An epidemic of echovirus 18 in 1988 in Japan–high association with clinical manifestation of exanthem. a report of the national epidemiological surveillance of infectious agents in Japan. *Jpn J Med Sci Biol.* (1990) 43:51–8. doi: 10.7883/yoken1952.43.51

12. Turabelidze G, Lin M, Butler C, Fick F, Russo T. Outbreak of echovirus 18 meningitis in a rural Missouri community. *Mo Med.* (2009) 106:420–4.

13. Wang SM, Ho TS, Shen CF, Wang JR, Liu CC. Echovirus 18 meningitis in southern Taiwan. *Pediatr Infect Dis J.* (2011) 30:259–60. doi: 10.1097/INF.0b013e3181f7cb69

14. Wilfert CM, Lauer BA, Cohen M, Costenbader ML, Myers E. An epidemic of echovirus 18 meningitis. *J Infect Dis.* (1975) 131:75–8. doi: 10.1093/infdis/131.1.75

15. Zhang H, Zhao Y, Liu H, Sun H, Huang X, Yang Z, et al. Molecular characterization of two novel echovirus 18 recombinants associated with hand-foot-mouth disease. *Sci Rep.* (2017) 7:8448. doi: 10.1038/s41598-017-09038-y

16. Chen X, Ji T, Guo J, Wang W, Xu W, Xie Z. Molecular epidemiology of echovirus 18 circulating in Mainland China from 2015 to 2016. *Virol Sin.* (2019) 34:50–8. doi: 10.1007/s12250-018-0080-8

17. Centers for Disease Control and Prevention (CDC). Outbreaks of aseptic meningitis associated with echoviruses 9 and 30 and preliminary surveillance reports on enterovirus activity–United States, 2003. *MMWR Morb Mortal Wkly Rep.* (2003) 52:761–4.

18. Khetsuriani N, Lamonte-Fowlkes A, Oberst S, Pallansch MA. Enterovirus surveillance–United States, 1970-2005. *MMWR Surveill Summ.* (2006) 55:1–20.

19. Martin D, Rybicki E. RDP detection of recombination amongst aligned sequences. *Bioinformatics.* (2000) 16:562–3. doi: 10.1093/bioinformatics/16.6.562

20. Kohil A, Jemmieh S, Smatti MK, Yassine HM. Viral meningitis: an overview. *Arch Virol.* (2021) 166:335–45. doi: 10.1007/s00705-020-04891-1

21. Davis LE. Acute bacterial meningitis. *Continuum (Minneap Minn).* (2018) 24:1264–83. doi: 10.1212/con.0000000000000660

22. Dumaidi K, Al-Jawabreh A. Molecular detection and genotyping of enteroviruses from CSF samples of patients with suspected sepsis-like illness and/or aseptic meningitis from 2012 to 2015 in West Bank, Palestine. *PLoS One.* (2017) 12:e0172357. doi: 10.1371/journal.pone.0172357

23. Shahan B, Choi EY, Nieves G. Cerebrospinal fluid analysis. *Am Fam Physician.* (2021) 103:422–8.

24. Lambert HP. Diagnosing viral meningitis: other important diagnoses must be excluded. *BMJ.* (2008) 336:110. doi: 10.1136/bmj.39458.446551.3A

25. van Soest TM, Chekrouni N, van Sorge NM, Brouwer MC, van de Beek D. Bacterial meningitis presenting with a normal cerebrospinal fluid leukocyte count. *J Infect.* (2022) 84:615–20. doi: 10.1016/j.jinf.2022.02.029

26. Ramanan P, Bryson AL, Binnicker MJ, Pritt BS, Patel R. Syndromic panel-based testing in clinical microbiology. *Clin Microbiol Rev.* (2018) 31:e00024-17. doi: 10.1128/cmr.00024-17

27. Meyfroidt G, Kurtz P, Sonneville R. Critical care management of infectious meningitis and encephalitis. *Intensive Care Med.* (2020) 46:192–201. doi: 10.1007/s00134-019-05901-w

28. Poplin V, Boulware DR, Bahr NC. Methods for rapid diagnosis of meningitis etiology in adults. *Biomark Med.* (2020) 14:459–79. doi: 10.2217/bmm-2019-0333

29. Le Govic Y, Demey B, Cassereau J, Bahn YS, Papon N. Pathogens infecting the central nervous system. *PLoS Pathog.* (2022) 18:e1010234. doi: 10.1371/journal.ppat.1010234

30. Balada-Llasat JM, Rosenthal N, Hasbun R, Zimmer L, Bozzette S, Duff S, et al. Cost of managing meningitis and encephalitis among infants and children in the United States. *Diagn Microbiol Infect Dis.* (2019) 93:349–54. doi: 10.1016/j.diagmicrobio.2018.10.012

31. Hasbun R, Rosenthal N, Balada-Llasat JM, Chung J, Duff S, Bozzette S, et al. Epidemiology of meningitis and encephalitis in the United States, 2011-2014. *Clin Infect Dis.* (2017) 65:359–63. doi: 10.1093/cid/cix319

32. Wang LP, Yuan Y, Liu YL, Lu QB, Shi LS, Ren X, et al. Etiological and epidemiological features of acute meningitis or encephalitis in China: a nationwide active surveillance study. *Lancet Reg Health West Pac.* (2022) 20:100361. doi: 10.1016/j.lanwpc.2021.100361

33. Chen XP, Sun SZ, Guo JY, Li JJ, Xie ZD. Complete genome sequence analysis of echovirus 18 associated with aseptic meningitis in hebei province, China, in 2015. *Genome Announc.* (2016) 4:e01165-16. doi: 10.1128/genomeA.01165-16

34. McLaughlin JB, Gessner BD, Lynn TV, Funk EA, Middaugh JP. Association of regulatory issues with an echovirus 18 meningitis outbreak at a children's summer camp in Alaska. *Pediatr Infect Dis J.* (2004) 23:875–7. doi: 10.1097/01.inf.0000136867.18026.22

35. Tsai HP, Huang SW, Wu FL, Kuo PH, Wang SM, Liu CC, et al. An echovirus 18-associated outbreak of aseptic meningitis in Taiwan: epidemiology and diagnostic and genetic aspects. *J Med Microbiol.* (2011) 60(Pt. 9):1360–5. doi: 10.1099/jmm.0.027698-0

36. Wang J, Meng M, Xu H, Wang T, Liu Y, Yan H, et al. Analysis of enterovirus genotypes in the cerebrospinal fluid of children associated with aseptic meningitis in Liaocheng, China, from 2018 to 2019. *BMC Infect Dis.* (2021) 21:405. doi: 10.1186/s12879-021-06112-9

37. Bodilsen J, Mens H, Midgley S, Brandt CT, Petersen PT, Larsen L, et al. Enterovirus meningitis in adults: a prospective nationwide population-based cohort study. *Neurology.* (2021) 97:e454–63. doi: 10.1212/wnl.0000000000012294

38. McGill F, Griffiths MJ, Bonnett LJ, Geretti AM, Michael BD, Beeching NJ, et al. Incidence, aetiology, and sequelae of viral meningitis in UK adults: a multicentre prospective observational cohort study. *Lancet Infect Dis.* (2018) 18:992–1003. doi: 10.1016/s1473-3099(18)30245-7

39. Lukashev AN, Shumilina EY, Belalov IS, Ivanova OE, Eremeeva TP, Reznik VI, et al. Recombination strategies and evolutionary dynamics of the human enterovirus a global gene pool. *J Gen Virol.* (2014) 95(Pt. 4):868–73. doi: 10.1099/vir.0.060004-0

40. Lukashev AN, Lashkevich VA, Ivanova OE, Koroleva GA, Hinkkanen AE, Ilonen J. Recombination in circulating human enterovirus B: independent evolution of structural and non-structural genome regions. *J Gen Virol.* (2005) 86(Pt. 12):3281–90. doi: 10.1099/vir.0.81264-0

41. Zhang QY, Liu SQ, Li XD, Li JQ, Zhang YN, Deng CL, et al. Sequence duplication in 3′ UTR modulates virus replication and virulence of Japanese encephalitis virus. *Emerg Microbes Infect.* (2022) 11:123–35. doi: 10.1080/22221751.2021.2016354

42. Xiong J, Cui X, Zhao K, Wang Q, Huang X, Li D, et al. Novel motif in the 3′-UTR of PRRSV-2 is critical for viral multiplication and contributes to enhanced replication ability of highly pathogenic or L1 PRRSV. *Viruses.* (2022) 14:166. doi: 10.3390/v14020166

43. Wang D, Yang C, Deng Y, Cao X, Xu W, Han Z, et al. Conserved RNA secondary structure in Cherry virus A 5′-UTR associated with translation regulation. *Virol J.* (2022) 19:91. doi: 10.1186/s12985-022-01824-z

44. Ben Youssef A, Gharbi J, George B, Das S, Ben M'hadheb MA. Single mutation in the cryptic AUG (cAUG) affects in vitro translation and replication efficiencies and in vivo virulence of coxsackievirus B3 (CVB3). *Curr Microbiol.* (2022) 79:288. doi: 10.1007/s00284-022-02986-3

45. Xu Z, Yang D, Wang L, Demongeot J. Statistical analysis supports UTR (untranslated region) deletion theory in SARS-CoV-2. *Virulence.* (2022) 13:1772–89. doi: 10.1080/21505594.2022.2132059

frontiers | Frontiers in Public Health

TYPE Case Report
PUBLISHED 13 January 2023
DOI 10.3389/fpubh.2022.1046666

OPEN ACCESS

EDITED BY
Ana Afonso,
Universidade NOVA de Lisboa, Portugal

REVIEWED BY
Steven De Keukeleire,
Regionaal Ziekenhuis Heilig Hart Tienen, Belgium
Bistra Blagova,
UMHATEM N. I. Pirogov, Bulgaria

*CORRESPONDENCE
Radeyah Waseem
✉ radeyahwaseem@hotmail.com

SPECIALTY SECTION
This article was submitted to Infectious Diseases: Epidemiology and Prevention, a section of the journal Frontiers in Public Health

RECEIVED 16 September 2022
ACCEPTED 05 December 2022
PUBLISHED 13 January 2023

CITATION
Waseem R, Seher M, Ghazal S, Shah HH and Habiba U (2023) Cat scratch disease in a 23-year-old male–Case report.
Front. Public Health 10:1046666.
doi: 10.3389/fpubh.2022.1046666

Cat scratch disease in a 23-year-old male–Case report

Radeyah Waseem*, Muskan Seher, Sohiba Ghazal, Hussain Haider Shah and Ume Habiba

Dow University of Health Sciences, Karachi, Sindh, Pakistan

Cat-scratch disease (CSD) is an infectious disease that usually presents with fever, headache, loss of appetite, weight loss, tender lymphadenopathy, and other symptoms. CSD is also the most common cause of infectious lymphadenitis in children, adolescents, and young adults. This contagious disease most often results from a scratch or bite of a cat. The course of this disease depends on the patient's immune status. CSD sometimes presents as a systemic disease and leads to various disease entities. In this study, we describe the case of a 23-year-old man exhibiting fever, generalized weakness, and neck swelling. The patient was unconscious when presented to the Emergency Department. He was given at least 3–4 liters IV bolus of 0.9% normal saline, but it failed to raise the blood pressure. He was then given an inotropic drug (noradrenaline) for low blood pressure and antibiotics (azithromycin) for fever. Venereal disease research laboratory (VDRL) and human immunodeficiency virus (HIV) serology came out negative. Histopathology ruled out tuberculosis and malignancy and confirmed necrotizing/suppurative granulomatous inflammation. These features favor the diagnosis of CSD.

KEYWORDS

cat scratch disease, *Bartonella henselae*, fever, lymphadenopathy, infection

Background

Principally caused by the Gram-negative rod *Bartonella henselae*, cat-scratch disease (CSD) is one of the most common causes of chronic lymphadenopathy in adolescents and children. It has obscure international incidence despite cases being reported globally, and seropositive prevalence rates show wide fluctuations between 0.6 and 37%. An association with warm, humid climates has been established (1). As depicted in a study conducted by Nelson et al. (2) spanning the time period between 2005 and 2013, the incidence peaked in 2005 (5.7/100,000 population) and gradually tapered to 4.0/100,000 in 2013 (2).

While CSD classically comes to clinical attention with a distinct inoculum site and regional lymphadenopathy, 10% of patients can present with atypical features which embody multi-system involvement. These include the cardiovascular system, musculoskeletal system, and neurological, dermal, and other regional sites, coupled with bacteremia. A prototypical case manifesting these findings has been reported in a previous case report by De Keukeleire et al. (3).

Cat-scratch disease has been barely reported in Pakistan, with the first documented case being reported in Rawalpindi in 2018 and published in 2020 (4). A new case has now been found in Karachi on 29 May 2022.

Case presentation

A 23-year-old man with no known co-morbidities presented in the Emergency Department at a Tertiary Care Hospital in Karachi with multiple complaints of neck swelling for 1 year, fever for 1 month, and generalized weakness for 1 week. He was a resident of Khuzdar, unmarried, and a final-year student of Doctor of Veterinary Medicine. On detailed history, the single neck swelling presented anteriorly and was not associated with any joint swelling, morning stiffness, or tenderness in small joints. It also regressed with time. However, he then noticed another static swelling on the right side of the neck in close proximity to the previous one. Fever was reported as intermittent and documented up to 104°F. It was associated with rigors and chills but subsided after oral paracetamol. It was associated with severe body aches and joint pain involving the wrists, elbows, and knees bilaterally. No diurnal variation or night sweats were accounted for, nor was any rash or oral ulcer. There was no history of Raynaud's phenomenon, burning micturition, cough, or loose stools. On further inquiry, it was revealed that he had a pet cat for a duration of 1 year in 2020 and is a student of Doctor of Veterinary Medicine (DVM), reports positive for exposure to various animals. His personal history revealed no addictions, but there was a history of sexual contact. On examination, three to four swellings were accounted for in the right posterior cervical region, the largest one having dimensions of ~2.0 × 1.0 cm. They were non-tender, non-erythematous, firm, and immobile, with no discharging sinus. Two small swellings were also noted bilaterally in the inguinal region. These were also found to be non-tender, non-erythematous, firm, and immobile with no discharging sinus. They measured ~1.0 × 1.0 cm. Blood pressure was recorded as 80/40 mm Hg, pulse 92 beats/min, oxygen saturation 98% on room air, and temperature as afebrile in the Emergency Department. On systemic examination, the abdomen was found to be soft and non-tender, with no visceromegaly noted; the chest, cardiovascular system, and central nervous system were also found to be unremarkable. The hospital course was initiated by giving IV fluids and commencing ionotropic drugs (noradrenaline) to raise his blood pressure, and he was hospitalized. Meropenem 1 g was started IV three times a day (TDS) secondary to high total leukocyte count (TLC = 49) and procalcitonin (PCT = 8.17). As the diagnosis was uncertain and the patient presented with fever, to rule out infective endocarditis and vegetation, echocardiography was scheduled, which was found to be unremarkable. Next, the general surgery team was consulted for an excisional biopsy of the right cervical lymph node. He was then stepped down to a private room as blood pressure started to show improvement, and ionotropic support was eventually tapered off. Azithromycin 500 mg was added to the treatment regime as there was no improvement in fever. The Infectious Diseases Department next advised VDRL and HIV serology (which came out to be negative), and azithromycin was switched to an injection of ciprofloxacin 500 mg IV twice daily. Histopathology ruled out tuberculosis and malignancy, and as fever started to space out, meropenem and ciprofloxacin were continued. After about 5–6 days, the histopathology department came up with the diagnosis of cat-scratch disease. The patient was fever-free for 2 days, clinically and vitally stable, and discharged on doxycycline 100 mg and rifampicin 300 mg twice daily for 6 weeks. Figure 1 shows a section of a lymph node showing areas of necrosis and abscess surrounded by palisading histiocytes along with capsular and subcapsular granulomas. Table 1 highlights results of important laboratory investigations to reach a diagnosis.

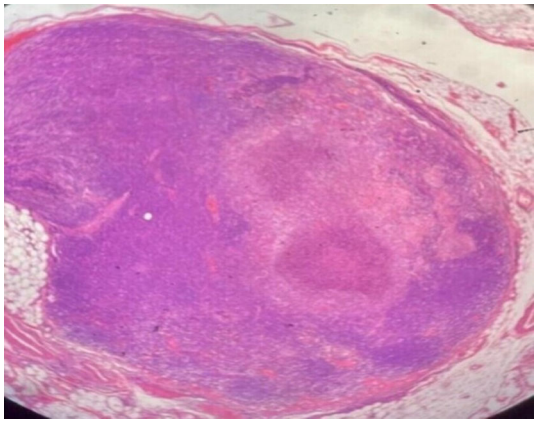

FIGURE 1
Section examined reveals lymph node showing areas of necrosis and abscess surrounded by palisading histiocytes along with capsular and subcapsular granulomas.

Discussion

CSD is a feline infection that is transmitted to humans by a scratch, bite, or contamination of a wound or mucous membrane, especially by young cats (kittens) (5). It is also referred to as cat-scratch fever or subacute regional lymphadenitis. The disease commonly resolves spontaneously in the majority of immunocompetent patients; however, rare cases have been identified where it may progress to present atypical, systemic features, such as oculoglandular syndrome, neuroretinitis, pneumonia, arthralgia, arthritis, encephalitis, and thrombotic thrombocytopenic purpura (6). Hepatic and splenic involvement is occasionally reported and warrants investigation to exclude more conventional causes. It was reported by Rocco

10.3389/fpubh.2022.1046666

TABLE 1 Results of laboratory investigations.

Laboratory investigation	Results	Normal reference range
Hematology		
Hemoglobin (gm/dl)	13	13–18
TLC (per liter)	49.7	4–10 × 10^9
PCV (%)	39.7	36–54
Platelet count (×10^9 /L)	235	150–400 × 10^9
PT (seconds)	12	11–13.5
APTT (seconds)	22	21–35
INR	1.21	0.8–1.1
Renal profile		
Urea (mg%)	35	10–50
Creatinine (mg%)	1.15	0.5–1.5
Chloride (mmol/L)	105	0–111
Potassium (mmol/L)	2.7	3.5–5.3
Sodium (mmol/L)	138	137–150
Bicarbonate (mmol/L)	21	22–34
Magnesium (mg%)	1–2.9	1.9–2.5
Calcium (mg%)	7–8.3	8.1–10.4
Phosphorus (mg%)	3.84	2.5–1.5
Liver profile		
Bilirubin total (mg%)	0.68	0.2–1.2
Bilirubin direct (mg%)	0.40	0.0–0.25
Bilirubin indirect	0.28	
SGPT/ALT (Units/L)	65	Upto 40
Alkaline phosphatase (Units/L)	54	117
Gamma-GT (Units/L)	64	7–22
Amylase (Units/L)	75	28–100
Lipase (Units/L)	35	0–160

TLC, Total Leucocyte Count; PCV, Packed Cell Volume; PT, Prothrombin Time; APTT, Activated Partial Thromboplastin Time; INR, International Normalized Ratio.

et al. (7) on a black, 16-year-old man who presented with disseminated signs, neck swelling, and hepatosplenomegaly (7). Involvement is in the form of granulomas that appear on ultrasound as multiple, rounded, well-circumscribed, hypoechoeic lesions with diameters ranging from 0.5 to 3 cm (8). Probable diagnosis comprises an exhaustible list of bacterial diseases inclusive of *M. tuberculosis*, *M. avium*, *F. tularensis*, *T. whippelii*, *C. burnetti*, *L. monocytogenes*, and *C. psittaci*, among others (9). Infection in an immunocompetent host is usually self-relenting, resolving within a few weeks. The initial stage of infection presents as papules or pustules at the site of the inoculum, and erythema nodusum accompanied by prodromal features such as fever and fatigue. Regional lymphadenopathy concurrently develops, characteristically unilaterally and involving a solitary node in half of the population reporting, with the other half progressing to involve multiple nodes or discrete regions. CSD may also disseminate systemically, with eyes being most frequently involved. Eye involvement may report clinically with a plethora of presentations, including neuroretinitis, anterior uveitis, choroiditis, Parinaud syndrome, retinal vessels occlusion, and inflammatory disc edema, among others (10, 11). The disease may also present atypically in immunocompetent patients precipitating deleterious consequences including cardiac complications (endocarditis), respiratory manifestation (pneumonia and pleural effusion), musculoskeletal involvement (osteomyelitis and paravertebral abscess), and CNS involvement (aseptic meningitis and encephalopathy) (12). Infection in an immunocompromised host follows a very different course, manifesting as bacillary angiomatosis–peliosis, which is symbolized by angioproliferative lesions mimicking those of Kaposi sarcoma in various sites amalgamating the skin, the liver, the spleen, the bone, and various others (1). The most notable causative agents of the disease are the *Bartonella* species, namely *Bartonella henselae*, *Bartonella quintana*, *Bartonella elizabethae*, and *Bartonella vinsonii*. *B. henselae* and *B. quintana* are habitually associated with human disease, while *B. elizabethae* infrequently harbors infection in immunocompromised patients. No cases have been reported of *B. vinsonii* in humans (13). In some cases, treatment with antibiotics such as azithromycin can be helpful. Other standard antibiotics used for treating CSD include clarithromycin, rifampin, trimethoprim-sulfamethoxazole, and ciprofloxacin. CSD classically follows a variable clinical course, initially presenting at the site of inoculation, extending to involve multiple lymph nodes, and finally presenting general, systemic symptoms. It commences as lone or multiple erythematous papules 3–4 days after inoculation at the site of infection, and a detailed history is vital to a proper diagnosis. The papule undergoes different stages from erythematous to vesicular to papular and finally to the crusted stage. Typically, this is followed by regional lymphadenopathy 1–3 weeks after the initiating cause and frequently involves a single node, relapsing after several months. Axillary and epitrochlear nodes and lymph nodes of the head, neck, and groin may also be involved asymmetrically. The nodes are found to be hyperechoic, multiple, and highly vascularised when visualized under an ultrasound examination (14). Approximately half of the reported cases may develop mild systemic symptoms constituting abdominal and generalized pain, malaise, and anorexia (15). Histopathological examination of the lymph nodes reveals a granulomatous picture alongside microabscesses and focal necrosis (16). Atypical involvement of CSD involves hepatosplenic CSD, cardiopulmonary CSD, CSD-associated

osteomyelitis, central nervous system involvement, and systemic and bacteremic CSD. The diagnosis of CSD is conventionally made when three of four criteria are met: (1) positive history of contact supported with a primary inoculation site, (2) a supporting CSD skin test result, (3) exclusion of other potential causes of subacute lymphadenopathy, and (4) biopsy results showing the specific histopathological features (13).

Conclusion

With the second case of CSD being documented in the country, it is crucial that a proper diagnosis is made as the clinical picture of the disease imitates various chronic illnesses like tuberculosis or malignancy. Pakistan is endemic to tuberculosis which has profound similarities in regard to the clinical presentation of CSD, emphasizing the need for a proper diagnosis. The differential diagnosis of a patient presenting with lymphadenopathy should consider cat-scratch disease a potential cause, especially in children. Due to its uncommon incidence in Pakistan, clinicians rarely consider CSD a possible cause of a patient's symptoms. However, the recent reporting of two cases in different provinces (Punjab and Sindh) and age groups (8 and 23 years) highlights the importance of being cognizant of the possibility of the disease whenever a patient presents with symptoms like lymphadenopathy syndrome, undifferentiated arthritis, and a fever with no underlying cause. Immaculate history and examination need to be conducted, and relevant expertise must be sought to make the proper diagnosis and treat the patient accordingly to prevent iatrogenic compromise in the quality of life of the afflicted.

Data availability statement

The raw data supporting the conclusions of this article will be made available by the authors, without undue reservation.

Ethics statement

Ethical review and approval was not required for the study on human participants in accordance with the local legislation and institutional requirements. The patients/participants provided their written informed consent to participate in this study. Written informed consent was obtained from the individual(s) for the publication of any potentially identifiable images or data included in this article.

Author contributions

RW and MS: conceptualization and writing—original draft. SG: writing—original draft. HS and UH: writing—review and editing. All authors contributed to the article and approved the submitted version.

Conflict of interest

The authors declare that the research was conducted in the absence of any commercial or financial relationships that could be construed as a potential conflict of interest.

Publisher's note

All claims expressed in this article are solely those of the authors and do not necessarily represent those of their affiliated organizations, or those of the publisher, the editors and the reviewers. Any product that may be evaluated in this article, or claim that may be made by its manufacturer, is not guaranteed or endorsed by the publisher.

References

1. Schwartz RA. Cat Scratch Disease (Cat Scratch Fever): Background, Pathophysiology, Etiology. *Medscape*. (2022). Available online at: https://emedicine.medscape.com/article/214100-overview

2. Nelson CA, Saha S, Mead PS. Cat-Scratch Disease in the United States, 2005-2013. *Emerg Infect Dis*. (2016) 22:1741–6. doi: 10.3201/eid2210.160115

3. De Keukeleire S, Geldof J, De Clerck F, Vandecasteele S, Reynders M, Orlent M. Prolonged course of hepatic granulomatous disease due to *Bartonella henselae* infection. *Acta Gastroenterol Belg*. (2016) 79:497–9.

4. Khan M, Safdar RM, Ishaq M, Akhtar M, Farooq U, Arif K, et al. Experience of Cat Scratch Disease (CSD) in Rawalpindi, Pakistan – Could Physician's vigilance help in detection and case management? *Int J Infect Dis*. (2020) 101:398. doi: 10.1016/j.ijid.2020.09.1043

5. Hozáková L, RoŽnovský L, Janout V. *Cat scratch Disease – A Neglected Zoonosis | proLékare.cz. Epidemiology, Microbiology, Immunology*. (2017). Available online at: https://www.prolekare.cz/en/journals/epidemiology-microbiology-immunology/2017-2-4/cat-scratch-disease-a-neglected-zoonosis-61280?hl=en (accessed September 15, 2022).

6. Carithers HA. Cat-scratch Disease. *Am J Dis Children*. (1985) 139:1124. doi: 10.1001/archpedi.1985.02140130062031

7. Rocco VK, Roman RJ, Eigenbrodt EH. Cat scratch disease. Report of a case with hepatic lesions and a brief review of the literature. *Gastroenterology*. (1985) 89:1400–6. doi: 10.1016/0016-5085(85)90661-4

8. Talenti E, Cesaro S, Scapinello A, Perale R, Zanesco L. Disseminated hepatic and splenic calcifications following cat-scratch disease. *Pediatr Radiol*. (1994) 24:342–43. doi: 10.1007/BF02012123

9. Stacey R. Vlahakis, Hepatic Granulomas. In: Leonard R, editor. *Johnson, Encyclopedia of Gastroenterology*. Elsevier. (2004). p309–10.

10. Oray M, Önal S, Koç Akbay A, Tugal Tutkun I. Diverse clinical signs of ocular involvement in cat scratch

disease. *Turk J Ophthalmol.* (2017) 47:9–17. doi: 10.4274/tjo.28009

11. Ormerod LD, Dailey JP. Ocular manifestations of cat-scratch disease. *Curr Opin Ophthalmol.* (1999) 10:209–16. doi: 10.1097/00055735-199906000-00010

12. Biancardi AL, Curi AL. Cat-scratch disease. *Ocul Immunol Inflamm.* (2014) 22:148–54. doi: 10.3109/09273948.2013.833631

13. Lamps LW, Scott MA. Cat-scratch disease. *Pathol Patterns Rev.* (2004) 121:S71–80. doi: 10.1309/JC8YM53L4E0L6PT5

14. Rohr A, Saettele MR, Patel SA, Lawrence CA, Lowe LH. Spectrum of radiological manifestations of paediatric cat-scratch disease. *Pediatr Radiol.* (2012) 42:1380–4. doi: 10.1007/s00247-012-2451-x

15. Florin TA, Zaoutis TE, Zaoutis LB. Beyond cat scratch disease: widening spectrum of *Bartonella henselae* Infection. *Pediatrics.* (2008) 121:e1413–25. doi: 10.1542/peds.2007-1897

16. Mancino P, Ucciferri C, Falasca K, Racciatti D, di Girolamo A, Vecchiet J, et al. Inguinal lymphadenopathy due to *Bartonella henselae*. *Infez Med.* (2008) 16:91–3.

frontiers | Frontiers in Medicine

TYPE Case Report
PUBLISHED 17 January 2023
DOI 10.3389/fmed.2022.1111830

OPEN ACCESS

EDITED BY
Francesco Paolo Bianchi,
University of Bari Aldo Moro, Italy

REVIEWED BY
Julián Solís García Del Pozo,
Complejo Hospitalario Universitario de Albacete, Spain
Hasan Tahsin Gozdas,
Abant Izzet Baysal University, Türkiye

*CORRESPONDENCE
Yi Zhou
✉ zhouyi390@stu.xjtu.edu.cn
Xiaojing Liu
✉ xiaojing406@163.com

SPECIALTY SECTION
This article was submitted to Infectious Diseases: Pathogenesis and Therapy, a section of the journal Frontiers in Medicine

RECEIVED 30 November 2022
ACCEPTED 30 December 2022
PUBLISHED 17 January 2023

CITATION
Zhou M, Wang K, Liu H, Ran R, Wang X, Yang Y, Han Q, Zhou Y and Liu X (2023) Case report: Brucellosis with rare multiple pulmonary nodules in a depressed patient.
Front. Med. 9:1111830.
doi: 10.3389/fmed.2022.1111830

Case report: Brucellosis with rare multiple pulmonary nodules in a depressed patient

Mingjing Zhou, Ke Wang, Haoyuan Liu, Ran Ran, Xuan Wang, Yuqian Yang, Qunying Han, Yi Zhou* and Xiaojing Liu*

The First Affiliated Hospital of Xi'an Jiaotong University, Xi'an, China

Background: Brucellosis is a zoonotic disease that threatens public health and creates an economic burden. Unfortunately, it is often overlooked in developing countries, with misdiagnosis causing negative impacts on those with low income. Although the symptoms of brucellosis are commonly reported as fever and fatigue, rare pulmonary, and psychiatric involvements should also be considered. We present the first brucellosis patient in China with multiple pulmonary nodules and depression. Furthermore, this report highlights the importance of collecting patient history in epidemic areas of brucellosis.

Case presentation: We report the case of a 40-year-old woman with intermittent fever for 2 months and gradually accompanied by chills, dry cough, arthralgia, and fatigue. The patient was also diagnosed with depression after fever. She received symptomatic treatment at a regional hospital; however, there was no significant symptom relief. She suddenly developed hemoptysis 1 day prior to arrival at our hospital, where we discovered that her liver, spleen, neck, and axillary lymph nodes were enlarged, and there were multiple nodules in both lungs. The patient was eventually diagnosed with brucellosis after the serum agglutination test and received antibiotic therapy, which provided symptom relief.

Conclusion: This report describes a case of brucellosis with uncommon multipulmonary nodules and depression in China. This study has widened the evidence of respiratory involvement due to brucellosis. Second, it demonstrates the importance of collecting a comprehensive medical history, especially in epidemic areas. In conclusion, for febrile patients with pulmonary nodules and depression, especially in endemic areas, brucellosis should be considered.

KEYWORDS

brucellosis, pulmonary nodules, depression, developing countries, case report

1. Introduction

Brucellosis is a common universal zoonosis caused by *Brucella*, a gram-negative bacterium that affects sheep, cattle, and pigs, and is transmitted to humans through the skin mucosa, respiratory tract, and digestive tract (1). Patients with brucellosis generally present with fever, fatigue, chills, and swelling. Occasionally, the bacterium can invade the nerve systems, which

may cause various neuropsychiatric manifestations (2, 3). However, pulmonary involvement is a rare complication of brucellosis (4, 5).

More than 500,000 new cases are reported annually, especially in developing countries (6). Similar to China, the prevalence of brucellosis tends to be higher in northern cities and was closely associated with livestock during 2004–2018 (7). However, owing to lack of financial and medical resources, brucellosis remains neglected in developing countries. Misdiagnosis of brucellosis will significantly impose heavy economic burden on public health systems (1, 8, 9). In this report, we describe a Chinese depressed patient with rare multi-pulmonary nodule brucellosis and present the medical history, symptoms, signs, and results of a series of examinations. The patient was diagnosed with brucellosis and received effective antibiotic therapy. This report highlights the importance of clinical-epidemiological suspicion as well as early diagnosis of brucellosis.

2. Case description

On July 10, 2022, a 40-year-old woman was admitted to the first affiliated hospital of Xi'an Jiaotong University due to intermittent fever for 2 months. Two months prior, her temperature fluctuated between 37.4 and 38.4°C in the afternoons, and chills and a dry cough accompanied this symptom. She had previously undergone examination and symptomatic treatment at a regional hospital. However, the treatment was ineffective. Furthermore, arthralgia and fatigue gradually appeared, with no chest pain and tightness, or rash. A month and a half prior, she was diagnosed with depression and treated with escitalopram oxalate, and magnesium valproate sustained-release tablets at a hospital. The symptoms slightly improved after treatment. Half a month prior, a B-ultrasonic examination showed lymphadenopathy throughout her body. Therefore, lymphoma was suspected but she did not get any treatment. One day prior to her arrival at our hospital, the patient suddenly developed hemoptysis of approximately 2 ml, which occurred four times for no reason. Past medical history revealed that she was diagnosed with chronic hepatitis B (CHB) in 2014 and developed cirrhosis a year later. Her CHB was well-controlled by a long-term oral antiviral treatment with Entecavir. In addition, she had lost 5 kg over the past 3 months.

On admission, her temperature was 37°C, respiratory rate was 19 breathe·min^{-1}, heart rate was 70 beat·min^{-1}, and blood pressure was 103/72 mmHg. The liver, spleen, lymph nodes of the neck, and axillary lymph nodes were enlarged with moderate activity and no tenderness. Rough breath sounds were detected in both lungs with dry and wet rales. All other clinical examination results were negative.

Laboratory examination revealed inflammation and liver dysfunction: red cell count, 4.27 × 10^{12}/L (4–4.5 × 10^{12}/L); white cell count, 4.87 × 10^{9}/L (5–12 × 10^{9}/L); platelet count 89 × 10^{9}/L (125–350 × 10^{9}/L), hypersensitive C-reactive protein 9.81 mg/L (0–3 mg/L), direct bilirubin 6.2 μmol/L (0–3.4 μmol/L), aspartate aminotransferase, 54 U/L (13–45 U/L); alanine aminotransferase, 20 U/L (7–40 U/L); alkaline phosphatase, 164 U/L (35–100 U/L); γ-glutamyl transpeptidase, 82 U/L (7–45 U/L), albumin 33.8 g/L (40–55 g/L).

Abbreviations: CHB, chronic hepatitis B; CT, computed tomography; SAT, serum agglutination test; RBPT, rose bengal plate agglutination test.

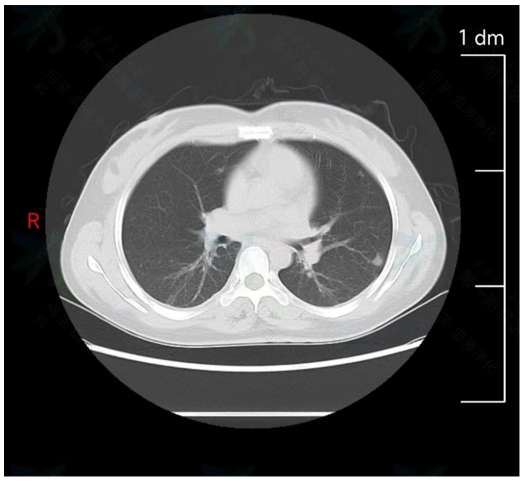

FIGURE 1
Chest computed tomography (CT) revealed multiple pulmonary nodules in both lungs.

B-scan ultrasonography revealed bilateral cervical and axillary lymphadenopathies. Chest computed tomography (CT) revealed multiple pulmonary nodules in both lungs, with a small amount of pleural effusion (Figure 1) and enlarged lymph nodes in the bilateral axilla. To effectively confirm the nature of the lesion, we performed needle biopsies of pulmonary nodules and lymph nodes. The results implied an infectious disease, while the detection of T cells in tuberculosis infection was negative. Therefore, suspicions of tumors and tuberculosis were excluded.

Interestingly, we noticed that the patient came from Ningxia province, which is famous for animal husbandry. The patient reluctantly informed us that she raised cattle and had come into contact with neighboring sheep without vaccination. Consequently, *Brucella* infection was suspected. On the fourth day of admission, the serum agglutination test (SAT) result was 1:800, and the rose-bengal plate agglutination test (RBPT) result was positive. Furthermore, the blood culture for *Brucella melitensis* was positive on the tenth day after admission. Characteristic rod-shaped gram-negative bacteria could be observed under a microscope. Subsequently, the patient was definitively diagnosed with brucellosis.

Following the brucellosis diagnosis, she received antibiotic therapy with rifampicin (600 mg/dose, once a day) and doxycycline (100 mg/dose, twice a day) for 3 months from the fourth day of the course. Furthermore, due to the poor medical conditions of the patient's residence and excessive complications, including multipulmonary nodules, arthralgia, hepatosplenomegaly, and lymphadenopathy, moxifloxacin and ceftriaxone sodium were added from the sixth day of the course to prevent the possibility of developing drug-resistant brucellosis after discharge. During treatment, the patient and her family were highly cooperative. At discharge, fever, cough, arthralgia, depression and fatigue were relieved. After 2 months of follow-up, the fever and cough were gone, as was fatigue and arthralgia. In addition, the number of multiple nodules in both lungs was reduced. At the same time, liver function test results also indicated that the patient was recovering well. After 3 months of follow-up, her weight had increased and her depression symptoms were alleviated. The entire process of diagnosis, treatment, and outcomes is shown in Figure 2.

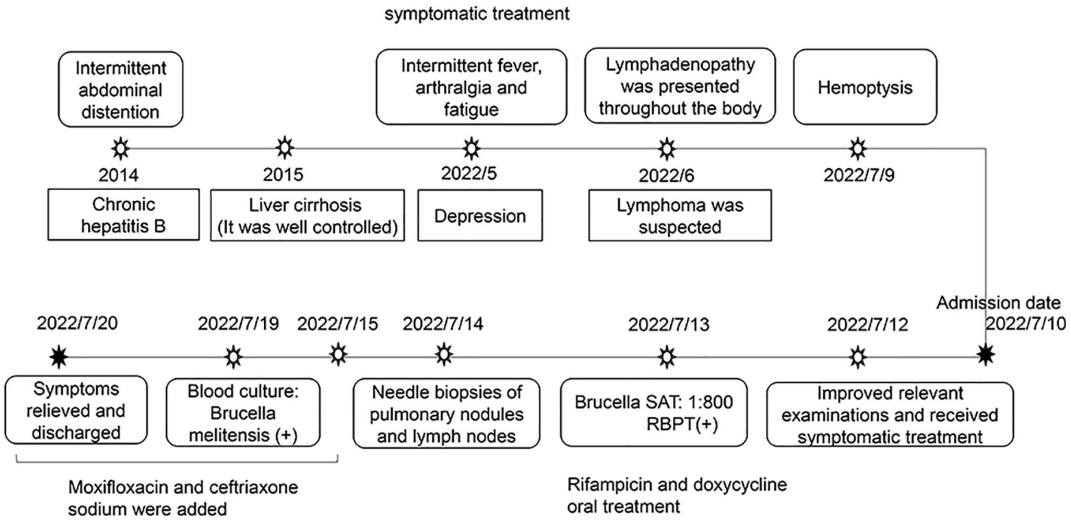

FIGURE 2
The entire process of diagnosis, treatment, and outcome.

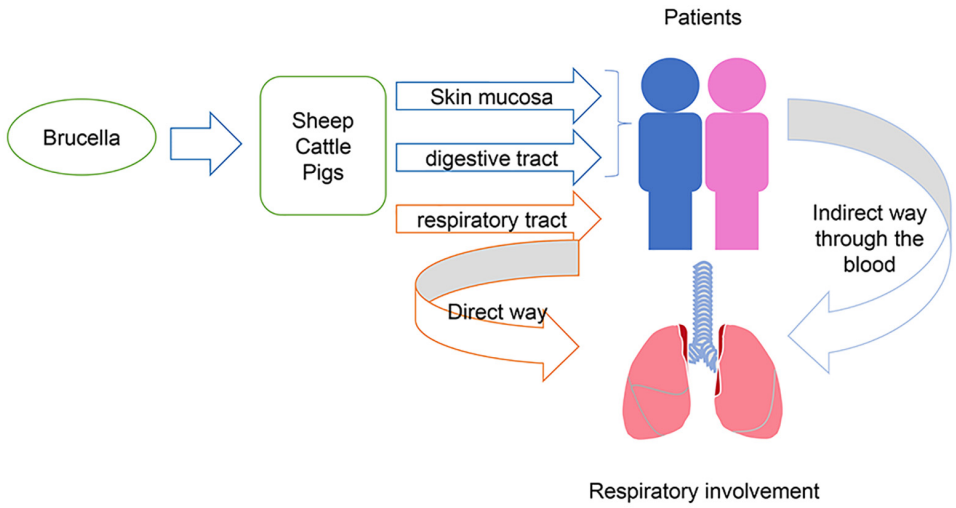

FIGURE 3
Mechanism of respiratory involvement by *Brucella*.

3. Discussion and conclusion

Brucellosis is a zoonosis with more than half a million newly reported cases worldwide each year, posing a threat to public health and increasing economic burdens (1, 9). In particular, owing to a lack of resources, this remains a neglected disease in developing countries. In China, brucellosis cases continue to increase and have appeared in all provinces (10, 11). Severe epidemic areas include Jilin, Xinjiang, Qinghai, Ningxia, and Henan, and April to June is considered to be peak epidemic periods (11). In this report, we present the first publicly reported brucellosis patient in China with multiple pulmonary nodules and depression. More importantly, due to signs of multipulmonary nodules and lymphadenopathy, the patient was misdiagnosed with a tumor, which increased her economic and psychological burden.

In general, brucellosis causes fever, fatigue, and chills. However, an expanded understanding of the disease has led to reporting of an increasing number of complications. These include respiratory (4), ocular (12), nerve (13), and reproductive systems (14). Regarding respiratory involvement, brucellosis can present with bronchitis, pleural effusion, and pulmonary nodules (15–17). These symptoms may be directly caused by the transmission of bacteria through the respiratory tract to the respiratory system, or they can be caused by the transmission of bacteria through the blood after infecting the human body in other ways (**Figure 3**). Respiratory involvement due to brucellosis in China has rarely been reported. A previous study found that the percentage of respiratory involvement in Chinese brucellosis patients was only 13% (18). This is insufficient to provide comprehensive evidence for an accurate diagnosis of brucellosis in the future.

Pulmonary nodules are mostly benign and can be caused by many factors, including cancer, infection, and inflammation (19). Pulmonary metastatic carcinoma is the most common cause

of cancer and is usually accompanied by cachexia. Etiological and immunological tests often provide evidence of infection and inflammation. To make a clear diagnosis, we performed needle biopsies of pulmonary nodules under CT guidance, and the results suggested an infectious disease. Blood cultures for *Brucella*, SAT, and RBPT were also positive. By combining the patient's symptoms, signs, and epidemic history, a diagnosis of brucellosis was confirmed.

Interestingly, the patient was diagnosed with depression after presenting with fever, arthralgia, and fatigue. Several studies have reported that depression was one of the rare symptoms of brucellosis infection (20, 21). In this case, the patient's emotional changes such as mood disorder, feelings of sadness and loss of interest were slightly improved after anti-depression therapy while were alleviated by antibiotic therapy. Considering her epidemiological history and psychiatric manifestations after intermittent fever, we presumed that her depression might be caused by brucellosis. Her head MRI scans and neurological signs were both negative. Unfortunately, further examinations to evaluate her neuropsychiatric manifestations were not carried out, which is a major limitation in our study.

Antimicrobial therapy is usually chosen for the treatment of brucellosis. Doxycycline combined with rifampicin is considered the most common combination choice in the treatment of pulmonary brucellosis (22–24). In cases with complications, treatment should be appropriately extended. In this report, considering the lung involvement and multiple lymphadenopathies throughout the body, the patient was treated with quadruple antibacterial treatment, including rifampicin, doxycycline, ceftriaxone sodium, and moxifloxacin. Due to lack of a definite diagnosis of neurobrucellosis, we decided to give this patient the 3 months standard treatment regimen. Her symptoms were alleviated a lot and did not recur after 3 months antibiotic therapy.

In conclusion, we reported a case of brucellosis with multipulmonary nodules in a depressed patient. Our report adds to the literature on the complications of brucellosis, which is often neglected in developing countries. During the process of diagnosis, we demonstrated the importance of obtaining a complete personal history of patients from disease-endemic areas. In addition, we suggest that examinations of *Brucella* should be carried out among patients with fever, pulmonary involvement and depression in endemic areas.

Data availability statement

The original contributions presented in this study are included in this article/supplementary material, further inquiries can be directed to the corresponding authors.

Ethics statement

The studies involving human participants were reviewed and approved by the Ethical Review Committee of Xi'an Jiaotong University. The patients/participants provided their written informed consent to participate in this study. Written informed consent was obtained from the individual(s) for the publication of any potentially identifiable images or data included in this article.

Author contributions

MZ, QH, YZ, and XL designed the study. KW and HL collected the clinical data. RR, XW, and YY analyzed the data and provided the materials. MZ wrote the first draft of the manuscript. All authors participated in the diagnosis and treatment of the patient, read, and approved the final manuscript.

Funding

This work was supported by the Instructional Reform Fund of the First Affiliated Hospital of Xi'an Jiaotong University (JG2022-0302). The funder was responsible for drafting the manuscript.

Acknowledgments

We sincerely thank all the medical workers who contributed to this treatment.

Conflict of interest

The authors declare that the research was conducted in the absence of any commercial or financial relationships that could be construed as a potential conflict of interest.

Publisher's note

References

1. Franco M, Mulder M, Gilman R, Smits H. Human brucellosis. *Lancet Infect Dis.* (2007) 7:775–86. doi: 10.1016/S1473-309970286-4

2. Eren S, Bayam G, Ergönül O, Celikbaş A, Pazvantoğlu O, Baykam N, et al. Cognitive and emotional changes in neurobrucellosis. *J Infect.* (2006) 53:184–9. doi: 10.1016/j.jinf.2005.10.029

3. Esmael A, Elsherif M, Elegezy M, Egilla H. Cognitive impairment and neuropsychiatric manifestations of neurobrucellosis. *Neurol Res.* (2021) 43:1–8. doi: 10.1080/01616412.2020.1812805

4. Pappas G, Bosilkovski M, Akritidis N, Mastora M, Krteva L, Tsianos E. Brucellosis and the respiratory system. *Clin Infect Dis.* (2003) 37:e95–9. doi: 10.1086/378125

5. Hatipoglu C, Bilgin G, Tulek N, Kosar U. Pulmonary involvement in brucellosis. *J Infect.* (2005) 51:116–9. doi: 10.1016/j.jinf.2004.10.004

6. Pappas G, Papadimitriou P, Akritidis N, Christou L, Tsianos E. The new global map of human brucellosis. *Lancet Infect Dis.* (2006) 6:91–9. doi: 10.1016/S1473-309970382-6

7. Wang Y, Wang Y, Zhang L, Wang A, Yan Y, Chen Y, et al. An epidemiological study of brucellosis on mainland China during 2004-2018. *Transbound Emerg Dis.* (2021) 68:2353–63. doi: 10.1111/tbed.13896

8. Franc K, Krecek R, Häsler B, Arenas-Gamboa A. Brucellosis remains a neglected disease in the developing world: a call for interdisciplinary action. *BMC Public Health.* (2018) 18:125. doi: 10.1186/s12889-017-5016-y

9. Dean A, Crump L, Greter H, Schelling E, Zinsstag J. Global burden of human brucellosis: a systematic review of disease frequency. *PLoS Negl Trop Dis.* (2012) 6:e1865. doi: 10.1371/journal.pntd.0001865

10. Jiang H, O'Callaghan D, Ding J. Brucellosis in China: history, progress and challenge. *Infect Dis Poverty.* (2020) 9:55. doi: 10.1186/s40249-020-00673-8

11. Deqiu S, Donglou X, Jiming Y. Epidemiology and control of brucellosis in China. *Vet Microbiol.* (2002) 90:165–82. doi: 10.1016/s0378-113500252-3

12. Rolando I, Olarte L, Vilchez G, Lluncor M, Otero L, Paris M, et al. Ocular manifestations associated with brucellosis: a 26-year experience in peru. *Clin Infect Dis.* (2008) 46:1338–45. doi: 10.1086/529442

13. Shehata G, Abdel-Baky L, Rashed H, Elamin H. Neuropsychiatric evaluation of patients with brucellosis. *J Neurovirol.* (2010) 16:48–55. doi: 10.3109/13550280903586386

14. Yang H, Feng J, Zhang Q, Hao R, Yao S, Zhao R, et al. A case report of spontaneous abortion caused by brucella melitensis biovar 3. *Infect Dis Poverty.* (2018) 7:31. doi: 10.1186/s40249-018-0411-x

15. Papiris S, Maniati M, Haritou A, Constantopoulous S. Brucella haemorrhagic pleural effusion. *Eur Respir J.* (1994) 7:1369–70.

16. Zhang T, Wang C, Niu R, Wang X. Pulmonary brucellosis on FDG PET/CT. *Clin Nucl Med.* (2014) 39:222–3. doi: 10.1097/RLU.0000000000000327

17. Sevilla López S, Quero Valenzuela F, Piedra Fernández I. Bilateral pulmonary nodules due to brucellosis. *Arch Bronconeumol.* (2011) 47:320–1. doi: 10.1016/j.arbres.2011.02.003

18. Zheng R, Xie S, Lu X, Sun L, Zhou Y, Zhang Y, et al. A systematic review and meta-analysis of epidemiology and clinical manifestations of human brucellosis in China. *Biomed Res Int.* (2018) 2018:5712920. doi: 10.1155/2018/5712920

19. Beigelman-Aubry C, Hill C, Grenier P. Management of an incidentally discovered pulmonary nodule. *Eur Radiol.* (2007) 17:449–66. doi: 10.1007/s00330-006-0399-7

20. Shoaei S, Bidi N. Serologic evaluation of brucellosis in patients with psychiatric disorders. *Caspian J Intern Med.* (2012) 3:557–8.

21. Elzein F, Al Sherbini N, Alotaibi M, Al-Hassan W. Brucellosis accompanied by haemophagocytic lymphohistiocytosis and multiple splenic abscesses in a patient with depression. *BMJ Case Rep.* (2018) 2018:224018. doi: 10.1136/bcr-2017-224018

22. Solera J, Martínez-Alfaro E, Espinosa A. Recognition and optimum treatment of brucellosis. *Drugs.* (1997) 53:245–56. doi: 10.2165/00003495-199753020-00005

23. Solera J, Solís García del Pozo J. Treatment of pulmonary brucellosis: a systematic review. *Expert Rev Anti Infect Ther.* (2017) 15:33–42. doi: 10.1080/14787210.2017.1254042

24. Erdem H, Inan A, Elaldi N, Tekin R, Gulsun S, Ataman-Hatipoglu C, et al. Respiratory system involvement in brucellosis: the results of the kardelen study. *Chest.* (2014) 145:87–94. doi: 10.1378/chest.13-0240

frontiers | Frontiers in Medicine

TYPE Case Report
PUBLISHED 02 February 2023
DOI 10.3389/fmed.2023.1071239

OPEN ACCESS

EDITED BY
Francesco Paolo Bianchi,
University of Bari Aldo Moro, Italy

REVIEWED BY
Kin Israel Notarte,
Johns Hopkins Medicine, Johns Hopkins University, United States
Giuseppe Murdaca,
University of Genoa, Italy
Leena Sulaibeekh,
Mohammed Bin Khalifa Bin Sulman Al Khalifa Cardiac Centre, Bahrain

*CORRESPONDENCE
Roberto Badaró
✉ Roberto.badaro@fieb.ba.org.br
Milena Botelho Pereira Soares
✉ milena.soares@fiocruz.br

SPECIALTY SECTION
This article was submitted to Infectious Diseases: Pathogenesis and Therapy, a section of the journal Frontiers in Medicine

RECEIVED 16 October 2022
ACCEPTED 02 January 2023
PUBLISHED 02 February 2023

CITATION
Badaró R, Novaes G, Andrade AC, de Araujo Neto CA, Machado BA, Barbosa JDV and Soares MBP (2023) Myocardial infarction or myocarditis? A case report and review of a myocardial adverse event associated with mRNA vaccine.
Front. Med. 10:1071239.
doi: 10.3389/fmed.2023.1071239

Myocardial infarction or myocarditis? A case report and review of a myocardial adverse event associated with mRNA vaccine

Roberto Badaró[1,2]*, Gustavo Novaes[3], Ana Cristina Andrade[2], Cesar Augusto de Araujo Neto[4], Bruna Aparecida Machado[1], Josiane Dantas Viana Barbosa[1] and Milena Botelho Pereira Soares[1,5]*

[1]SENAI Institute of Innovation (ISI) in Health Advanced Systems, University Center SENAI/CIMATEC, Salvador, Brazil, [2]Allmed Specialized Clinic, Salvador, Brazil, [3]UNIMED Hospital, Feira de Santana, Brazil, [4]Image Diagnosis, Salvador, Brazil, [5]Gonçalo Moniz Institute, Oswaldo Cruz Foundation (FIOCRUZ), Salvador, Brazil

A 23-year-old man started with chest pain 8 h after his first Pfizer-BioNTech COVID-19 vaccination. ECG evaluation showed sinus tachycardia with ST-segment elevation in D1, AVL, V5, and V6, the findings compatible with acute subepicardial myocardial damage. However, cardiac MRI documented myocardial fibrosis, with cardiac late enhancement non-ischemic pattern with diffuse edema. He had no other symptoms to suggest another etiology than the vaccination. The patient was hospitalized and received corticosteroid (prednisolone) daily. Then, 2 weeks after hospitalization, all laboratory parameters and ECG were normal and the patient was discharged from the hospital. The patient had a history of Wolf-Parkinson White that was corrected with ablation when he was 11 years old. This report calls attention to myocardial adverse reaction risk for mRNA COVID-19 vaccines for people with a previous cardiac disease history.

KEYWORDS

COVID-19, mRNA vaccine, cardiotoxicity, cardiac disease, adverse event

Introduction

Heart inflammation, such as endocarditis, myocarditis, and pericarditis, is the adverse reaction associated with mRNA vaccination reported in several countries during the COVID-19 vaccination development and after the onset of the vaccination campaign (1–6). Overall, six cases of myocarditis after the BNT162b2 vaccination were reported by Abu Mouch and Roguin et al. (1), with five patients presenting myocarditis after the second and one after the first dose of the vaccine. The six patients were men, with a median age of 23 years. Additional cases of myocarditis were also reported in individuals who received the Moderna mRNA COVID-19 vaccine (1). In adolescents and young adults, the reports of myocarditis and pericarditis were higher in frequency after the second dose than the first dose of one mRNA COVID-19 vaccine (Pfizer-BioNTech or Moderna) (1, 4, 6).

Overall, a review by the Centers for Disease Control and Prevention (CDC) of the Vaccine Adverse Events Reporting System (VAERS) identified a total of 1,226 cases of myocarditis as of 11 June 2021 (4). From 29 December 2020 to 11 June 2021, about 296 million doses of mRNA COVID-19 vaccines were administered in the USA, being 52 million to persons aged 12–29 years, receiving 30 and 22 million as first and second doses, respectively (4). The cases reported using the electronic VAERS CDC reporting system should be carefully evaluated (7), since a report to VAERS does not mean that a vaccine caused a myocardial adverse event, which should fit the diagnostic criteria for myocarditis, following the classification of the Brighton Collaboration (8). The revision of myocarditis cases reported to VAERS by the cardiologists in persons aged below 30 years reported from 1 May to 11 June 2021, and 323 cases (among 484 records) met the CDC criteria in case definitions for myocarditis, myopericarditis, or pericarditis (4).

Recently, a retrospective review of data from 5,125,696 Israeli residents which received two doses of the BNT162b2 mRNA vaccine (Pfizer-BioNTech) showed 283 having definitive or probable myocarditis attributed to the vaccination among 304 reported cases, including one fulminant fatal case (9). However, in most cases (95%—129 recipients), the myocarditis was mild, occurring in 142 persons after the first dose or a month following the second dose. In another report from Israel, the authors estimated an incidence of myocarditis of 2.13 cases/100,000 persons who had received at least one dose of vaccine [95% confidence interval (CI), 1.56–2.70], and the highest incidence (10.69 cases per 100,000 persons; 95% CI, 6.93–14.46) was reported in young male patients (aged between 16 and 29 years) (10).

The occurrence of myocarditis associated with the mRNA vaccine, on an overall risk difference between the first and second doses, has been estimated as 1.76 per 100,000 persons [95% confidence interval (CI), 1.33–2.19], with the most considerable difference among male aged between 16 and 19 years (difference, 13.73 per 100,000 persons; 95% CI, 8.11–19.46) (4, 10, 11).

In this report, we call the attention of public health services to include an advertisement for individual selection of COVID-19 type of vaccine for persons with a history of previous cardiac diseases.

Case description

A 23-year-old man presented with oppressive chest pain that started 6–8 h after being administered with his first Pfizer-BioNTech COVID vaccination dose. His initial vital signs were a temperature of 38.7^{o}C, blood pressure of 130/70 mmHg, heart rate of 128 bmp, and 100% oxygen saturation at the emergency room. The initial levels of cardiac enzymes evaluated were troponin $I > 15$ ng/ml ($N = 0.04$ ng/ml), CK = 1,894 U/L ($N = 294$ U/L), and CK-MB = 65.74 ng/ml ($N = 5.0$ ng/ml). Troponin I and CK-MB levels dropped to normal values 5 days later (**Table 1**).

The electrocardiogram (ECG) 8 h after BNT162b2 messenger RNA (mRNA) vaccine (Pfizer-BioNTech) administration on 15 August 2021 showed sinus tachycardia with ST-segment elevation in D1, AVL, V5, and V6, abnormalities compatible with acute subepicardial myocardial infarction (LV) left ventricular lateral wall (LV) (**Figure 1A**), whereas the ECG was normalized 13 days after vaccination (**Figure 1B**).

His echocardiogram with the Doppler findings at admission was a mild-to-moderate left ventricular dysfunction associated with mild pericardial effusion with a left ventricular ejection fraction of 56% and, at discharge, was 65%. Nevertheless, the cardiac magnetic resonance image (**Figure 2**) documented myocardial non-ischemic fibrosis 5 days later, with a cardiac enhancement non-ischemic pattern with diffuse edema. During the hospitalization, the patient received corticosteroid (prednisolone) on the following schedule: 120 mg for 3 days, 60 mg for 3 days, and 30 and 20 mg until visiting the doctor of infectious disease (ID). Then 2 weeks after hospitalization, all laboratory parameters and ECG were normal. The patient was discharged from the hospital, and during the visit to the ID doctor, the steroid therapy was suspended after performing a new ECG, which gave a normal result.

Additional evaluations by computerized tomography of the chest showed no evidence of pulmonary embolism or any identifiable pathology. The patient was not under stress, did not consume a significant amount of caffeine, and denied using any drugs or taking any over-the-counter medications (including herbals or supplements). He had no additional symptoms indicative of possible causes for the myocarditis other than the vaccine taken. He has a familiar history of Wolf-Parkinson White syndrome which was corrected with ablation when he was 11 years old. Moreover, he had a documented myocarditis of unknown cause 8 years previous to this episode. His father died of a sudden cardiac attack at the age of 50 years. A timeline of events is presented in **Figure 3**.

Discussion

The SARS-CoV-2 vaccination disrupted the COVID-19 pandemic. An estimated 3.6 billion (47.6%) people in the world had received at least one dose of the COVID-19 vaccine, and the number of global COVID-19 cases and deaths dropped to less than 10% in developed countries, whereas overall, at least 40% of the population were vaccinated. In contrast, only 2.5% of people in low-income countries received at least one dose of vaccine (12). Unquestionable is the benefit of COVID-19 vaccination. By 9 October 2021, the world data reported that SARS-CoV-2S-based mRNA vaccine types were administered to 233.39 million people for the Pfizer-BioNTech and 152.84 million for the Moderna vaccine. This type of vaccine is indicated for frail patients, such as those with autoimmune diseases, transplant recipients, and patients living with HIV since they showed higher efficacy and higher estimated effectiveness (13–15). Thus, knowing predisposition factors that could determine the development of severe cardiac adverse events upon mRNA vaccination is of great relevance for vaccination programs.

Overall, solicited systemic adverse events were reported during the trials for dose definitions of the Moderna vaccine (16). The adverse reaction to this mRNA vaccine, such as local adverse events, which were nearly all mild or moderate, and pain at the injection site, was most frequently reported with a higher dose and, more frequently, after the second dose. Solicited systemic and local adverse events occurred in most adults and adolescents across both vaccinations with the Pfizer-BioNTech mRNA vaccine, including high fever, fatigue, chills, headache, myalgia, and pain at the injection site (16, 17). Among the recipients of the Pfizer-BioNTech, four serious adverse events related to the vaccine were reported (shoulder injury related to vaccine administration, right axillary lymphadenopathy, paroxysmal ventricular arrhythmia, and

TABLE 1 Laboratory results of cardiac enzymes.

		Date of examination					
Examination	Ref. value	08/15/2021 10:00 PM	08/16/2021 02:00 AM	08/17/2021 05:00 AM	08/18/2021 05:00 AM	08/19/2021 06:00 AM	08/20/2021 06:00 AM
CPK	294 U/L	121.25	121.25	121.25	121.25	121.25	121.26
CK-MB	0.03 ng/ml	47.73	65.76	10.14	2.30	2.08	1.17
Troponin I	0.03 ng/ml	> 15	14.42	8.24	3.54	1.08	0.18

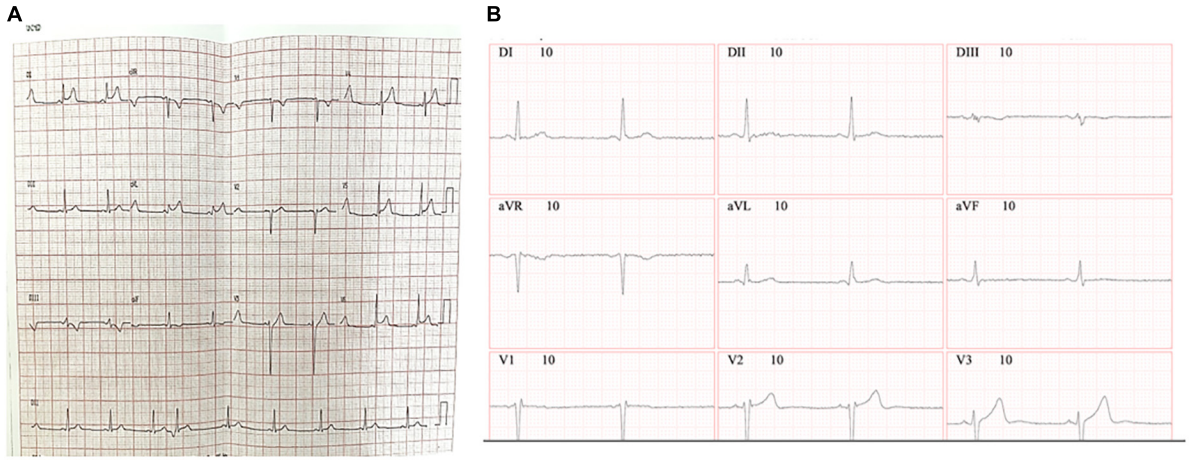

FIGURE 1
Electrocardiogram results. ECG was recorded with a set of 12-lead ECG electrodes connected to a central unit software. ECG was taken 8 h **(A)** or 13 days **(B)** after the administration of the BNT162b2 messenger RNA (mRNA) (Pfizer-BioNTech) vaccine.

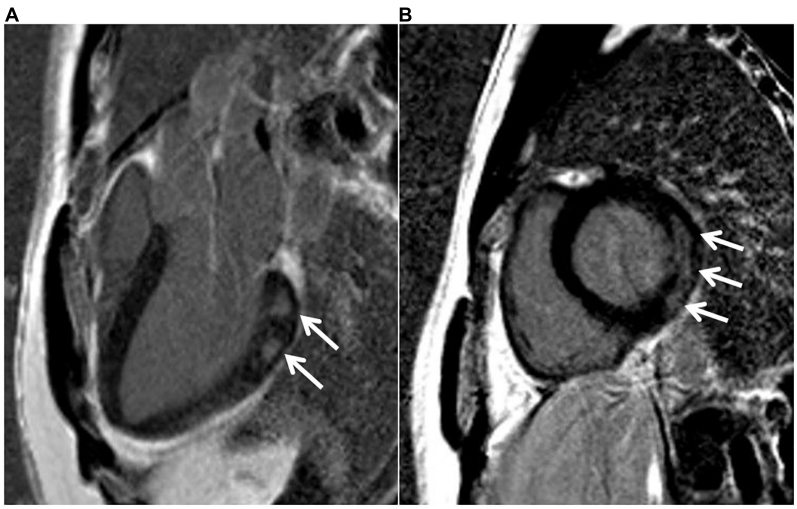

FIGURE 2
MRI results. Cardiac MRI 16 days after the administration of the BNT162b2 messenger RNA (mRNA) (Pfizer-BioNTech) vaccine, 1.5-T MR system. Delayed enhancement sequence in the long axis **(A)** and short axis **(B)**. Arrows indicate an area of myocardial fibrosis with a non-ischemic pattern in the basal lateral wall, compatible with myocarditis.

right leg paresthesia). Myocarditis is unquestionably a serious adverse reaction and, following mRNA vaccination, it is estimated to occur, following a second dose, at a rate of 12.6–24 cases per million, more often in adolescents and young adults at the age of 18–29 years (10, 11).

In total, two persons vaccinated with BNT162b2 died in the phase 2/3 study, one due to arteriosclerosis, and the other, by cardiac arrest (18). In another study, histopathological analysis in heart samples obtained from an autopsy of 25 individuals who were vaccinated with the mRNA vaccine for COVID-19 showed the presence of acute myocarditis with focal inflammatory foci in four persons without any signs of other possible causes of death (19). Previous cardiac diseases associated with cardiovascular adverse events were not related to the recipient's age of the mRNA vaccine. Our patient is a young

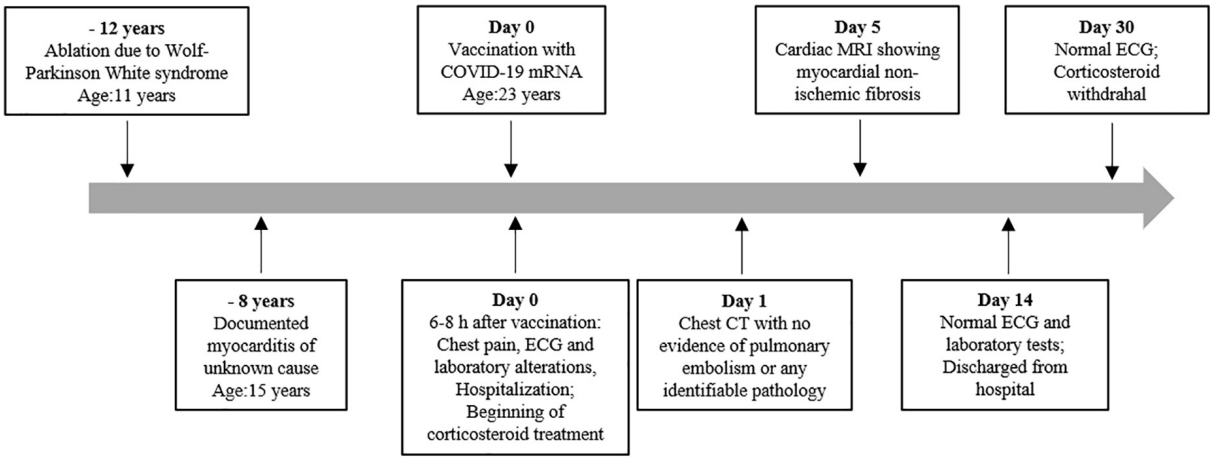

FIGURE 3
Timeline of the patient's previous cardiac diseases, myocarditis, and pericarditis post-BNT162b2 messenger RNA (mRNA) (Pfizer-BioNTech) vaccine.

TABLE 2 Reports on cardiotoxicity of SARS-CoV2 mRNA vaccines.

References	Vaccine	Number of cases	Manifestation	Country
Abu Mouch et al. (1)	BNT162b2	6	Myocarditis established by cardiac MRI	Israel
D'Angelo et al. (2)	BNT162b2	1	Myopericarditis by laboratory and cardiac MRI	Italy
Deb et al. (3)	mRNA-1273	1	Myocarditis	USA
Gargano et al. (4)	BNT162b2 and mRNA-1273	323 confirmed of 484 < 30 years	Myocarditis, pericarditis, myopericarditis confirmed by revision of cases	USA
Khogali and Abdelrahman (5)	mRNA-1273	1	Acute perimyocarditis	Qatar
Mevorach et al. (9)	BNT162b2	136	Myocarditis (definitive or probable)	Israel
Witberg et al. (10)	BNT162b2	54	Myocarditis	Israel
Larson et al. (26)	BNT162b2 and mRNA-1273	8	Myocarditis by laboratory and cardiac MRI	USA and Italy
Marshall et al. (27)	BNT162b2	7	Acute myocarditis or myopericarditis	USA
Verma et al. (28)	BNT162b2 and mRNA-1273	2	Myocarditis	USA
Freise et al. (29)	BNT162b2 and mRNA-1273	8	Cardiac symptoms compatible with myocarditis	Germany
Meier et al. (30)	BNT162b2 and mRNA-1273	1	Subclinical pericarditis established by cardiac MRI	Germany
Saadi et al. (31)	BNT162b2	1	Myocarditis	Saudi Arabia
Kim et al. (32)	BNT162b2 and mRNA-1273	4	Myocarditis by laboratory and cardiac MRI	USA
Montgomery et al. (33)	BNT162b2 and mRNA-1273	21	Myocarditis by laboratory and cardiac MRI	USA
Schwab et al. (19)	BNT162b2 and mRNA-1273	4	Acute (epi-) myocarditis by histopathological analysis	Germany
Schneider et al. (34)	BNT162b2	1	Myocarditis	Germany

adult with previous history of cardiac arrhythmia and presented a myocarditis simulating myocardial infarction event. His ventricular dysfunction, cardiac enzyme elevations, and ECG suggested acute subepicardial myocardial infarction, which the cardiac MRI could not confirm. However, transient myocardial non-ischemia fibrosis without necrotic consequences could be shown by cardiac MRI. Moreover, myopericarditis can be associated with atrioventricular (AV) dissociation, a condition of desynchrony of electrical activity between atria and ventricles associated with ST elevation in the anterior, leading to the altered ECG and raised troponin I levels (20, 21). One limitation of this case investigation was the lack of coronary angiography, which could help to rule out myocardial infarction.

The presence of histological changes compatible with myopericarditis was shown in an experimental study after the first priming dose by intravenous route in mice. The myopericarditis persisted for 2 weeks and was aggravated by a second booster dose by intramuscular or intravenous routes (22). In addition, the gene expression of pro-inflammatory cytokines such as IL-1β, IFN-β, IL-6, and TNF-α in the hearts was significantly increased after the mRNA vaccine injection by intravenous route. Lipid nanoparticles are the most commonly utilized carriers for *in vivo* RNA delivery due to their ability to protect mRNA molecules from degradation, bring mRNA to the negatively charged cell membranes, and mediate endocytosis and endosomal escape (23, 24).

Indeed, there is no doubt that mRNA vaccines affect myocardial cells, possibly by inducing and increase in IL-18 levels (25). The CDC surveillance committee for COVID-19 vaccine adverse reactions previously recommended a precaution for the administered mRNA-based vaccine (7). **Table 2** summarizes the studies describing the cardiotoxicity of SARS-CoV-2 mRNA vaccination. Importantly, a systematic literature review highlights that protective immune responses elicited by COVID-19 mRNA vaccines decline within 90–180 days, indicating the need to continuously boost the population (35).

We conclude that, even though the mRNA COVID-19 vaccine appears to be very safe, a careful selection of the type of COVID-19 vaccine should be done for young males with a history of cardiac disease. Additionally, chest pain with ECG alteration suggests myocarditis in patients that report being vaccinated with the mRNA COVID-19 vaccine may not necessarily be cardiac ischemic disease.

Data availability statement

The raw data supporting the conclusions of this article will be made available by the authors, without undue reservation.

Ethics statement

The studies involving human participants were reviewed and approved by the Ethics Committee of SENAI CIMATEC. The patients/participants provided their written informed consent to participate in this study. Written informed consent was obtained from the individual(s) for the publication of any potentially identifiable images or data included in this article.

Author contributions

RB, GN, AA, and CA conducted the diagnostics and medical assistance. RB wrote the original draft. BM, JB, and MS edited and contributed to the literature quoted in this manuscript. All authors read and approved the submitted version.

Funding

This work was supported by the SENAI Institute of Innovation (ISI) in Health Advanced Systems, University Center SENAI/CIMATEC research funding. BM, JB, and MS are the recipients of fellowships from the Brazilian National Council (CNPq).

Acknowledgments

We would like to thank the patient for agreeing to publish his myocarditis mRNA vaccine-related case in the study.

Conflict of interest

The authors declare that the research was conducted in the absence of any commercial or financial relationships that could be construed as a potential conflict of interest.

Publisher's note

References

1. Abu Mouch S, Roguin A, Hellou E, Ishai A, Shoshan U, Mahamid L, et al. Myocarditis following COVID-19 mRNA vaccination. *Vaccine.* (2021). 39:3790–3. doi: 10.1016/j.vaccine.2021.05.087

2. d'Angelo T, Cattafi A, Carerj M, Booz C, Ascenti G, Cicero G, et al. Myocarditis after SARS-CoV-2 vaccination: a vaccine-induced reaction? *Can J Cardiol.* (2021) 37:1665–7. doi: 10.1016/j.cjca.2021.05.010

3. Deb A, Abdelmalek J, Iwuji K, Nugent K. Acute myocardial injury following COVID-19 vaccination: a case report and review of current evidence from vaccine adverse events reporting system database. *J Prim Care Community Health.* (2021) 12:21501327211029230. doi: 10.1177/21501327211029230

4. Gargano J, Wallace M, Hadler S, Langley G, Su J, Oster M, et al. Use of mRNA COVID-19 vaccine after reports of myocarditis among vaccine recipients: update from the advisory committee on immunization practices – United States, June 2021. *MMWR Morb Mortal Wkly Rep.* (2021) 70:977–82. doi: 10.15585/mmwr.mm7027e2

5. Khogali F, Abdelrahman R. Unusual presentation of acute perimyocarditis following SARS-COV-2 mRNA-1237 moderna vaccination. *Cureus.* (2021) 13:e16590. doi: 10.7759/cureus.16590

6. Rose J, McCullough P. A report on myocarditis adverse events in the U.S. Vaccine Adverse Events Reporting System (VAERS) in association with COVID-19 injectable biological products. *Curr Probl Cardiol.* (2021) [Epub ahead of print]. doi: 10.1016/j.cpcardiol.2021.101011

7. Different COVID-19 Vaccines. *Vaccine Adverse Events Reporting System (VAERS) by the Centers for Disease Control and Prevention.* Atlanta, GA: Centers for Disease Control and Prevention (2021).

8. Brighton Collaboration. *Myocarditis/pericarditis case definition.* Atlanta, GA: The Task Force for Global Health (2021).

9. Mevorach D, Anis E, Cedar N, Bromberg M, Haas E, Nadir E, et al. Myocarditis after BNT162b2 mRNA vaccine against Covid-19 in Israel. *N Engl J Med.* (2021) 385:2140–9. doi: 10.1056/NEJMoa2109730

10. Witberg G, Barda N, Hoss S, Richter I, Wiessman M, Aviv Y, et al. Myocarditis after Covid-19 vaccination in a large health Care Organization. *N Engl J Med.* (2021) 385:2132–9. doi: 10.1056/NEJMoa2110737

11. Shay D, Shimabukuro T, DeStefano F. Myocarditis occurring after immunization with mRNA-based COVID-19 vaccines. *JAMA Cardiol.* (2021) 6:1115–7. doi: 10.1001/jamacardio.2021.2821

12. Coronavirus Our World in data. *Covid vaccine doses administered Our World Data.* New Delhi: Linear Logistics (2021). Available online at: https://ourworldindata.org/covid-vaccinations

13. Murdaca G, Noberasco G, Olobardi D, Lunardi C, Maule M, Delfino L, et al. Current take on systemic sclerosis patients'. vaccination

recommendations. *Vaccines.* (2021) 9:1426. doi: 10.3390/vaccines9121426

14. Milano E, Ricciardi A, Casciaro R, Pallara E, De Vita E, Bavaro D, et al. Immunogenicity and safety of the BNT162b2 COVID-19 mRNA vaccine in PLWH: a monocentric study in Bari. *Italy. J Med Virol.* (2022) 94:2230–6. doi: 10.1002/jmv.27629

15. Dib M, Le Corre N, Ortiz C, García D, Ferrés M, Martinez-Valdebenito C, et al. CoV-2 vaccine booster in solid organ transplant recipients previously immunised with inactivated versus mRNA vaccines: a prospective cohort study. *Lancet Reg Health Am.* (2022) 16:100371. doi: 10.1016/j.lana.2022.100371

16. Jackson L, Anderson E, Rouphael N, Roberts P, Makhene M, Coler R, et al. An mRNA Vaccine against SARS-CoV-2 – preliminary report. *N Engl J Med.* (2020) 383:1920–31. doi: 10.1056/NEJMoa2022483

17. Frenck R Jr, Klein N, Kitchin N, Gurtman A, Absalon J, Lockhart S, et al. Safety, immunogenicity, and efficacy of the BNT162b2 Covid-19 vaccine in adolescents. *N Engl J Med.* (2021) 385:239–50. doi: 10.1056/NEJMoa2107456

18. Polack F, Thomas S, Kitchin N, Absalon J, Gurtman A, Lockhart S, et al. Safety and efficacy of the BNT162b2 mRNA Covid-19 vaccine. *N Engl J Med.* (2020) 383:2603–15. doi: 10.1056/NEJMoa2034577

19. Schwab C, Domke L, Hartmann L, Stenzinger A, Longerich T, Schirmacher P. Autopsy-based histopathological characterization of myocarditis after anti-SARS-CoV-2-vaccination. *Clin Res Cardiol.* (2022) [Epub ahead of print]. doi: 10.1007/s00392-022-02129-5

20. Rajiah P, Desai M, Kwon D, Flamm SD. MR imaging of myocardial infarction. *Radiographics.* (2013) 33:1383–412. doi: 10.1148/rg.335125722

21. Ata F, Chaudhry H, Bilal A, Lopez M. Myopericarditis presenting as acute ST-Elevation myocardial infarction with atrioventricular dissociation. *Heart Views.* (2020) 21:284–8.

22. Li C, Chen Y, Zhao Y, Lung D, Ye Z, Song W, et al. Intravenous injection of COVID-19 mRNA vaccine can induce acute myopericarditis in mouse model. *Clin Infect Dis.* (2021) 74:1933–50. doi: 10.1093/cid/ciab707

23. Reichmuth A, Oberli M, Jaklenec A, Langer R, Blankschtein D. mRNA vaccine delivery using lipid nanoparticles. *Ther Deliv.* (2016) 7:319–34. doi: 10.4155/tde-2016-0006

24. Whitehead K, Langer R, Anderson D. Knocking down barriers: advances in siRNA delivery. *Nat Rev Drug Discov.* (2009) 8:129–38. doi: 10.1038/nrd2742

25. Won T, Gilotra N, Wood M, Hughes D, Talor M, Lovell J, et al. Increased interleukin 18-dependent immune responses are associated with myopericarditis After COVID-19 mRNA vaccination. *Front Immunol.* (2022) 13:851620. doi: 10.3389/fimmu.2022.851620

26. Larson K, Ammirati E, Adler ED, Cooper L Jr, Hong K, Saponara G, et al. Myocarditis After BNT162b2 and mRNA-1273 Vaccination. *Circulation.* (2021) 144:506–8. doi: 10.1161/CIRCULATIONAHA.121.055913

27. Marshall M, Ferguson I, Lewis P, Jaggi P, Gagliardo C, Collins J, et al. Symptomatic acute myocarditis in 7 Adolescents after pfizer-BioNTech COVID-19 vaccination. *Pediatrics.* (2021) 148:e2021052478. doi: 10.1542/peds.2021-052478

28. Verma A, Lavine K, Lin C. Myocarditis after Covid-19 mRNA vaccination. *N Engl J Med.* (2021) 385:1332–4. doi: 10.1056/NEJMc2109975

29. Freise N, Kivel M, Grebe O, Meyer C, Wafaisade B, Peiper M, et al. Acute cardiac side effects after COVID-19 mRNA vaccination: a case series. *Eur J Med Res.* (2022) 27:80. doi: 10.1186/s40001-022-00695-y

30. Meier C, Korthals D, Bietenbeck M, Chamling B, Drakos S, Vehof V, et al. Serial cardiovascular magnetic resonance studies prior to and after mRNA-Based COVID-19 booster vaccination to assess booster-associated cardiac effects. *Front Cardiovasc Med.* (2022) 9:877183. doi: 10.3389/fcvm.2022.877183

31. Saadi S, Bossei A, Alsulimani L. Acute myocarditis after COVID-19 vaccination. *Saudi Med J.* (2022) 43:1270–5. doi: 10.1093/eurheartj/ehac239

32. Kim H, Jenista E, Wendell D, Azevedo C, Campbell M, Darty S, et al. Patients With Acute Myocarditis Following mRNA COVID-19 Vaccination. *JAMA Cardiol.* (2021) 6:1196–201. doi: 10.1001/jamacardio.2021.2828

33. Montgomery J, Ryan M, Engler R, Hoffman D, McClenathan B, Collins L, et al. Myocarditis Following Immunization With mRNA COVID-19 Vaccines in Members of the US Military. *JAMA Cardiol.* (2021) 6:1202–6. doi: 10.1001/jamacardio.2021.2833

34. Schneider J, Sottmann L, Greinacher A, Hagen M, Kasper H, Kuhnen C, et al. Postmortem investigation of fatalities following vaccination with COVID-19 vaccines. *Int J Legal Med.* (2021) 135:2335–45. doi: 10.1007/s00414-021-02706-9

35. Notarte K, Guerrero-Arguero I, Velasco J, Ver A, Santos de Oliveira M, Catahay J, et al. Characterization of the significant decline in humoral immune response six months post-SARS-CoV-2 mRNA vaccination: a systematic review. *J Med Virol.* (2022) 94:2939–61. doi: 10.1002/jmv.27688

frontiers | Frontiers in Medicine

TYPE Original Research
PUBLISHED 08 February 2023
DOI 10.3389/fmed.2023.1122529

OPEN ACCESS

EDITED BY
Francesco Paolo Bianchi,
University of Bari Aldo Moro, Italy

REVIEWED BY
Soumya Panigrahi,
Case Western Reserve University, United States
Marta Massanella,
IrsiCaixa, Spain

*CORRESPONDENCE
Ram Yogendra
✉ ryogendramd@gmail.com

†These authors share senior authorship

SPECIALTY SECTION
This article was submitted to Infectious Diseases: Pathogenesis and Therapy, a section of the journal Frontiers in Medicine

RECEIVED 13 December 2022
ACCEPTED 23 January 2023
PUBLISHED 08 February 2023

CITATION
Patterson BK, Yogendra R, Guevara-Coto J, Mora-Rodriguez RA, Osgood E, Bream J, Parikh P, Kreimer M, Jeffers D, Rutland C, Kaplan G and Zgoda M (2023) Case series: Maraviroc and pravastatin as a therapeutic option to treat long COVID/Post-acute sequelae of COVID (PASC). *Front. Med.* 10:1122529. doi: 10.3389/fmed.2023.1122529

Case series: Maraviroc and pravastatin as a therapeutic option to treat long COVID/Post-acute sequelae of COVID (PASC)

Bruce K. Patterson[1], Ram Yogendra[2]*, Jose Guevara-Coto[3], Rodrigo A. Mora-Rodriguez[4], Eric Osgood[5], John Bream[6], Purvi Parikh[7], Mark Kreimer[8], Devon Jeffers[9], Cedric Rutland[10], Gary Kaplan[11†] and Michael Zgoda[12†]

[1]IncellDX Inc., San Carlos, CA, United States, [2]Department of Anesthesiology, Beth Israel Lahey Health, Burlington, MA, United States, [3]Centro de Investigación en Cirugía y Cáncer (CICICA), Universidad de Costa Rica, San Jose, Costa Rica, [4]Lab of Tumor Chemosensitivity, CIET/DC Lab, Faculty of Microbiology, Universidad de Costa Rica, San Jose, Costa Rica, [5]Department of Medicine, St. Francis Medical Center, Trenton, NJ, United States, [6]Department of Emergency Medicine, Novant Health Kernersville Medical Center, Kernersville, NC, United States, [7]Department of Allergy and Immunology, NYU Langone Tisch Hospital, New York, NY, United States, [8]Department of Emergency Medicine, New York Presbyterian Hospital, Brooklyn, NY, United States, [9]Department of Anesthesiology, Stamford Hospital, Stamford, CT, United States, [10]Rutland Medical Group, Newport Beach, CA, United States, [11]Department of Community and Family Medicine, Georgetown University Medical Center, Washington, DC, United States, [12]Department of Medicine, Creighton University School of Medicine, Phoenix, AZ, United States

Post-acute sequelae of COVID (PASC), or long COVID, is a multisystem complication of SARS-CoV-2 infection that continues to debilitate millions worldwide thus highlighting the public health importance of identifying effective therapeutics to alleviate this illness. One explanation behind PASC may be attributed to the recent discovery of persistent S1 protein subunit of SARS-CoV-2 in CD16+ monocytes up to 15 months after infection. CD16+ monocytes, which express both CCR5 and fractalkine receptors (CX3CR1), play a role in vascular homeostasis and endothelial immune surveillance. We propose targeting these receptors using the CCR5 antagonist, maraviroc, along with pravastatin, a fractalkine inhibitor, could disrupt the monocytic-endothelial-platelet axis that may be central to the etiology of PASC. Using five validated clinical scales (NYHA, MRC Dyspnea, COMPASS-31, modified Rankin, and Fatigue Severity Score) to measure 18 participants' response to treatment, we observed significant clinical improvement in 6 to 12 weeks on a combination of maraviroc 300 mg per oral twice a day and pravastatin 10 mg per oral daily. Subjective neurological, autonomic, respiratory, cardiac and fatigue symptoms scores all decreased which correlated with statistically significant decreases in vascular markers sCD40L and VEGF. These findings suggest that by interrupting the monocytic-endothelial-platelet axis, maraviroc and pravastatin may restore the immune dysregulation observed in PASC and could be potential therapeutic options. This sets the framework for a future double-blinded, placebo-controlled randomized trial to further investigate the drug efficacy of maraviroc and pravastatin in treating PASC.

KEYWORDS

long COVID, maraviroc, CCR5 antagonist, PASC, statins, fractalkine (CX3CR1)

Introduction

Post-acute sequelae of COVID (PASC), commonly referred to as long COVID, is an emerging public health syndrome that continues to devastate and debilitate adult and pediatric survivors of acute SARS-CoV-2 infection. The World Health Organization (WHO)-led Delphi consensus defined PASC as a syndrome starting 3 months from onset of probable infection with symptoms lasting over 2 months and could not be explained by an alternative diagnosis (1). Over 200 symptoms have been attributed to PASC (2) thus posing an enormous challenge clinically. The multi-organ involvement causes cognitive impairment, debilitating neuropathy, chronic migraines, autonomic dysfunction, cardiac dysrhythmias, dyspnea at rest, severe fatigue, and myalgias (3). Presently, minimal therapeutic options are available to treat PASC which can be attributed to the pathology not yet being fully described. However, we recently reported that the S1 protein subunit of SARS-CoV2 is retained in both non-classical (CD14− CD16+) and intermediate (CD14+ CD16+) monocytes several months after acute infection. Typically, these monocytes persist only for a few days, but in PASC patients, the S1 containing monocytes can persist for months and years (4), which we propose contributes to the pathophysiology behind PASC. Non-classical monocytes are involved in phagocytosis and vascular adhesion by patrolling the endothelium under homeostatic and inflammatory conditions through B2 integrin, lymphocyte function-associated antigen-1 (LFA-1) and high levels of fractalkine receptors (CX3CR1) (5, 6). On the other hand, CD14+ CD16+ monocytes express high levels of C-C chemokine receptor type 5 (CCR5) and fractalkine receptors and are involved in antigen presentation, cytokine secretion and apoptosis regulation (6, 7). Since CCR5 and fractalkine receptors have been studied for various chronic inflammatory pathologies, we hypothesized that both these receptors may also be therapeutic targets for PASC. CD16+ monocytes also produce high levels of various pro-inflammatory cytokines which could be an explanation for the heterogenous symptomatology in PASC. Specifically, elevations in C-C chemokine ligand 5 (CCL5)/RANTES (Regulated on Normal T-cell Expression and Secretion), IL-2, IL-6, IFN-gamma and Vascular Endothelial Growth Factor (VEGF), along with decrease in CCL4 have been observed in patients and are hypothesized to be contributing to the pathophysiology of PASC (8).

Here, we describe an 18 participant case series investigating the combination of the CCR5 receptor antagonist maraviroc, and pravastatin, which targets fractalkine, as a potential therapeutic approach in addressing and treating the potential pathology of PASC. The CCR5 receptor is a seven-transmembrane G protein-coupled receptor (GPCR) that is found on macrophages and T-lymphocytes and functions to regulate trafficking and effector functions of these cells (9). The role of CCR5 as a co-receptor for human immunodeficiency virus (HIV) entry was discovered in 1996. Maraviroc is the first and only US Food and Drug Administration (FDA) and European Medical Agency (EMA) approved CCR5 receptor antagonist available to date. Maraviroc is a negative allosteric modulator of the CCR5 receptor, and by binding to the CCR5 receptor, it induces receptor conformational changes that prevent the chemokine binding of RANTES (CCL5) and CCR5-mediated signaling (10). While this mechanism has been researched and studied extensively in HIV infection, there is increasingly greater recognition and appreciation of the CCR5-CCL5 axis in many other conditions and pathologies such as cancer, autoimmune disorders and endothelial dysfunction. This signaling is central to the pathophysiology of inflammation by directing immune cells through a process called chemotaxis. These actions are mediated through RANTES, which is produced by platelets, macrophages, eosinophils, fibroblasts, endothelial, epithelial and endometrial cells (11). The effects of RANTES have been implicated in respiratory tract infections, especially viruses possessing RNA genome (including coronavirus, influenza, RSV, and adenovirus), asthma, neuroinflammation, and atherosclerosis (12, 13). Maraviroc has also been documented to restore the homeostasis of regulatory T-cells (Treg), increase CD4 and CD8 positive counts, and inhibit HIV-associated chronic inflammation and activation (14, 15). Interestingly, CD4 and CD8 positive T-cells expressing PD-1 and T-regs have been observed to be significantly lower in PASC patients compared to healthy controls (8), thus suggesting maraviroc could restore the immune dysregulation seen in PASC. The commonly known mechanism of action of statins is inhibition of hydroxymethylglutaryl-CoA (HMG-CoA) reductase enzyme in lowering cholesterol. However, statins have also been implicated in reducing inflammation, suppressing fractalkine, and lowering VEGF and IL-6 (16), and as such, may play a role in the pathophysiology of PASC. We targeted fractalkine using pravastatin since CD16+ monocytes express high levels of the fractalkine receptor believing this may address the elevations in vascular markers seen in PASC.

Materials and methods

The records and immunological lab reports from 18 adult PASC patients treated with maraviroc 300 mg per oral twice daily and pravastatin 10 mg per oral daily from our virtual medical clinic were collected and analyzed.

TABLE 1 Patient information and demographics.

	Sex	Age	Months from positive COVID test to testing	Weeks on maraviroc and pravastatin	Hospitalized Y/N
P1	F	50	9	10	N
P2	M	59	10	8	N
P3	F	43	8	6	N
P4	F	27	7	8	N
P5	F	33	5	8	N
P6	M	30	14	6	N
P7	F	46	14	8	N
P8	M	50	10	6	N
P9	F	53	4	6	N
P10	F	53	14	12	N
P11	M	57	17	6	N
P12	M	47	9	10	Y
P13	F	46	6	8	N
P14	F	40	8	8	N
P15	M	45	17	8	N
P16	M	63	10	7	N
P17	M	18	8	6	N
P18	F	43	16	12	N

The 18 participants selected for this case series were from a pool of patients who reported symptom improvement while on maraviroc and pravastatin and who fit the inclusion and exclusion criteria we set below.

Inclusion criteria

All the participants in the case series were COVID-19 survivors with documented FDA EUA approved RT-PCR SARS-CoV2 positive test and/or were positive for anti-SARS-CoV2 antibodies using FDA EUA approved tests. All participants had one or more new onset symptoms that persisted greater than 3 months after the diagnosis of acute COVID-19 infection. These symptoms included cognitive impairment (brain fog), migraines, post exertional malaise (PEM), myalgias, arthralgias, severe fatigue, tachyarrhythmias, postural orthostatic tachycardia syndrome (POTS), and shortness of breath. All participants displayed either isolated or combinations of elevated pro-inflammatory markers: RANTES, TNF-alpha, IFN-gamma, sCD40L, VEGF, IL-6, IL-2, and IL-8 on the IncellKINE panel. The IncellKINE cytokine panel is a set of 14 cytokines that was constructed from a previous machine-based learning algorithm that identified potential markers of PASC (8).

Exclusion criteria

We excluded participants with a pre-COVID history of migraines, neuropathy, inflammatory bowel disease, depression and anxiety disorders, chronic fatigue syndrome, Epstein-Barr infection, Lyme disease, fibromyalgia, arthritis, COPD, asthma, chronic kidney disease, chronic heart failure (CHF), arrhythmias, bleeding disorders, and anticoagulation therapy.

Treatment endpoints

When patients reported that their post-COVID symptoms improved by 80% of greater, we initiated discontinuation of both maraviroc and pravastatin. Bi-monthly follow-ups were conducted for 12 weeks post-treatment to monitor if symptoms reappeared or worsened.

Validated scoring system for patient assessment before and after treatment

A challenge in studying and defining PASC is the heterogenous clinical presentation and multisystem involvement. Thus, we categorized the main participant symptoms into 5 groups: neurological/autonomic function, cardiac, respiratory, overall functionality, and fatigue. Since there are no validated scales for PASC, we used five validated scales for other organ systems [New York Heart Association (NYHA), Modified Rankin Scale for Neurologic Disability, Fatigue Severity Scale (FSS), COMPASS-31 and Medical Research Council (MRC) Dyspnea Scale, respectively] to measure subjective participant responses to treatment (Tables 1–5). Participants were administered validated self-questionnaires about their PASC symptoms before and after treatment with maraviroc and pravastatin treatment. The length of duration of treatment varied based on repeat immune markers and participant-reported symptom improvement. Since many of these participants were on other medications and anti-inflammatories prior to starting maraviroc and pravastatin, the biomarkers and subjective data presented are from the onset of this combination. Phone interviews were conducted with each participant before and after subjective responses to the medications.

The **New York Heart Association (NYHA) functional classification** was used to classify severity of PASC associated cardiac symptoms.

The **Composite Autonomic Symptom Scale 31 (COMPASS 31)**, a self-rating questionnaire consisting of 31 items and evaluating orthostatic intolerance, vasomotor, secretomotor, gastrointestinal, bladder, and pupillomotor function, was used to measure autonomic dysfunction and the subsequent therapeutic effects of maraviroc and pravastatin. A sub raw score for each of the six domains was calculated and converted into a weighted sub-score. The sum of this weighted sub-score gave a total score which ranged from 0 to 100, with 0 meaning no autonomic symptoms and 100 reflecting the most severe autonomic symptoms.

Medical Research Council (MRC) Dyspnea scale is a validated method comprised of five statements that aims to measure perceived feeling of breathlessness.

The **Modified Rankin scale for neurologic disability** is a validated scale to measure degree of disability after suffering a stroke or neurological insult.

The **Fatigue Severity Scale (FSS) questionnaire** is a nine-statement validated scale that rates the severity of fatigue symptoms. Participants were asked how accurately each statement reflected their condition before and after treatment with maraviroc and pravastatin and the extent to which they agreed or disagreed based on a scale of 1 (strongly disagree) to 7 (strongly agree).

Serum cytokine measurements from participants: Multiplex cytokine quantification

Fresh plasma was used for cytokine quantification using a customized 14-plex bead based flow cytometric assay (IncellKINE,

TABLE 2 New York Heart Association (NYHA) functional classification.

Class 1	No limitation of physical activity. Ordinary physical activity does not cause undue fatigue, palpitation, dyspnea (shortness of breath).	**Class 2**	Slight limitation of physical activity. Comfortable at rest. Ordinary physical activity results in fatigue, palpitation, dyspnea (shortness of breath).	**Class 3**	Marked limitation of physical activity. Comfortable at rest. Less than ordinary activity causes fatigue, palpitation, or dyspnea.	**Class 4**	Unable to carry on any physical activity without discomfort. Symptoms of heart failure at rest. If any physical activity is undertaken, discomfort increases.

TABLE 3 Medical Research Council (MRC) dyspnea scale.

Grade 1	Are you ever troubled by breathlessness except on strenuous exertion?	**Grade 2**	Are you short of breath when hurrying on the level or walking up a slight hill?	**Grade 3**	Do you have to walk slower than most people on the level? Do you have to stop after a mile or so (or after 15 min) on the level at your own pace?	**Grade 4**	Do you have to stop for breath after walking about 100 yds. (or after a few minutes) on the level?	**Grade 5**	Are you too breathless to leave the house, or breathless after undressing?

TABLE 4 Modified Rankin scale.

0	No symptoms	**1**	No significant disability despite symptoms; able to carry out all usual duties and activities	**2**	Slight disability; unable to carry out all previous activities, but able to look after own affairs without assistance	**3**	Moderate disability; requiring some help, but able to walk without assistance	**4**	Moderately severe disability; unable to walk without assistance and unable to attend to own bodily needs without assistance	**5**	Severe disability; bedridden, incontinent and requiring constant nursing care and attention

TABLE 5 Fatigue Severity scale.

1	My motivation is lower when I am fatigued.	2	Exercise brings on excessive fatigue.	3	I am easily fatigued.	4	Fatigue interferes with my physical functioning.	5	Fatigue causes frequent problems for me.	6	My fatigue prevents sustained physical functioning.
7	Fatigue interferes with carrying out certain duties and responsibilities.	8	Fatigue is among my three most disabling symptoms.	9	Fatigue interferes with my work, family, or social life.						

IncellDx, Inc., San Carlos, CA, United States) on a CytoFlex flow cytometer as previously described (8) using the following analytes: "TNF-α," "IL-4," "IL-13," "IL-2," "GM-CSF," "sCD40L," "CCL5 (RANTES)," "CCL3 (MIP-1α)," "IL-6," "IL-10," "IFN-γ," "VEGF," "IL-8," and "CCL4 (MIP-1β)". For each participant sample, 25 μL of plasma was used in each well of a 96-well plate.

End points for the study were when the patients reported improvement in post-COVID symptoms that led to increases in daily functionality and quality of life. We checked in with the patients every 2 weeks to monitor progress.

Data acquisition and preprocessing

In total there were 18 unique individuals, with each individual being represented in duplicate for before and after treatment. The presence of a pre and post treatment for each individual categorized as PASC allowed us the possibility to separate the data set into a before and after data sets for the required statistical comparisons. To separate the before and after groups, we used the *python* programming language (version 3.9) and the *pandas* library (17, 18), which allowed us to group the samples according to before and after treatment. Once we separated the data in the two data sets, we then conducted the necessary comparative statistical analysis, including the statistical test to determine if there were significant differences between the two groups.

Wilcoxon's paired test to compare the before and after treatment groups

To determine if there were differences between the biomarker's levels of the two groups (before and after) we compared the datasets by implementing the non-parametric Wilcoxon's paired test. The implementation of this test was done using the python library *scipy* (19). The selection of the Wilcoxon test was based on the assumption that this non-parametric test does not assume normal distribution of the variables. Additionally, in contrast to parametric tests like ANOVA, Wilcoxon's paired test does not base its comparison on the mean but median values. For our data we compared group *before* and group *after* with two alternative hypotheses. The first was a two-sided test, which resulted in a p-value less than 0.05. Subsequently, we tested for an alternative hypothesis "*greater,*" resulting in a p-value of less than 0.05.

Correlation analysis between biomarker levels and subjective scores

In order to identify potential statistically significant relationships between the biomarkers present in the dataset and the subjective scores, we imported the full dataset into the R programming language (version 4.1.1) (20) and conducted a correlation analysis. The correlation analysis was calculated using the Pearson correlation coefficient, which allows the measurement of both strength and direction of the linear relationship between two variables.

The Pearson correlation coefficient has the advantage that its values are highly interpretable, always ranging from −1 (strong negative correlation) to +1 (strong positive correlation). Correlation coefficients were calculated for both the before and after data points, and to validate their statistical significance, their p-value was calculated. We defined that correlation coefficients were statistically significant if their p-value was equal or less than 0.05. In order to properly interpret and convey the correlation relationships and their statistical significances, we constructed a modified correlation matrix using a dot plot with the python programming language. We implemented additional functions and arguments that allowed us create a diagram only showing statistically significant correlations. Additionally, because correlation plot is constructed using a matrix,

there is a mirror-image effect between the left and right side of the diagonal. We used the arguments of the plot to avoid this effect, in order to improve plot interpretability.

The dot plot implemented a color and size code. In this system, positive correlation coefficient were associated with shades of blue, whereas negative correlation values where associated with red correlation values. Regarding the size of the dot, it represented statistical significance, with greater sizes being indicative of greater statistical significance, smaller dots representing lesser values of significance, and no dots indicating no significance.

Validation of long hauler status using a machine learning classifier

To determine the state of individuals in the dataset as Post-acute sequelae SARS-CoV-2 (PASC) we classified them using a machine learning model. This model, which consisted of a random forest classifier, developed in a previous report (8) and used to determine if samples belonged to disease state (Normal/Control, Mild-Moderate, Severe or PASC), was given the dataset as a prediction set. The implementation of this model was to confirm the disease status of individuals in the dataset as PASC. The random forest classifier was trained using a dataset consisting of 224 instances representing Normal/Control, Mild-Moderate, Severe or PASC. The classes in the dataset were imbalanced, and to address this, we implementing synthetic oversampling of the minority class (SMOTE) (21), which creates minority class instances by interpolation. The model using a balanced trainings set, was subsequently implemented in the unseen the dataset. The predictions of before and after individuals were outputted as an array, with a number indicating the predicted class.

Results

Comparison between "before" and "after" treatment demonstrates statistical differences between groups

The Wilcoxon paired test to contrast the before and after treatment groups using a two-sided hypothesis revealed the existence of statistically significant differences (p-value = 2.20e-17) between the cytokine profiles of the two treatment groups (before and after). Group 1 was defined as the before treatment and group 2 was after treatment. These results support that the medians of both groups are different and that a one-sided test was required to define the difference between group 1 and group 2. For the one-sided test, we focused on determining if the medians values for the biomarkers in treatment group 1 (before) were greater than those of group 2 (after). The results indicated that before treatment had statistically significant greater (p-value = 1.10e-17) magnitudes for the cytokines than the after-treatment group. The statistical analysis using a two-tailed and a one-tailed Wilcoxon test of the individuals from the maraviroc and pravastatin group indicated that there were statistically significant differences between the before and after treatment. The two-tailed test indicated that there were differences in the medians of these two groups (p-value = 2.20e-17). The one-sided test (p-value = 1.10e-17) indicated that before treatment had greater magnitudes for the cytokines (biomarkers) than the after treatment.

Correlation analysis indicates the presence of positive correlations between cytokine biomarkers and subjective scores

The correlation dot plot indicates the presence of significant correlations based on color and size of the dot (circle) on the right of the diagonal. The correlation value is indicative of the joint correlation for both the before and after treatment groups when compared to each variable. The diagonal correlation values are the values of each marker or subjective score compared against itself, and thus the coefficient will be equal to 1 (dark blue) and have the largest size possible dot. For the observed correlation coefficients, the intensity of the color was indicative of values of r (correlation coefficients) including various negligible positive and negative correlations, and instances ranging from low positive to moderate positive correlation, however we also identified the presence of negative correlation. Identification of correlation values was done by comparing with color scale in **Figure 1**, where dark blue indicated highly positive correlation (+1), and dark red indicated highly negative correlation (−1). The dot plot omitted non-significant correlations, which are represented as blank spaces. This permitted us to focus on the statistically significant relationships, and more specifically those between cytokines and subjective scores.

Additionally, it is possible to see that for the subjective scores (NYHA, MRC Dyspnea, Rankin, COMPASS 31 and Fatigue) there were multiple significant correlations with biomarkers. These significant correlations followed the trend of being mostly low positive or moderate positive, as indicated by the color of the dot (**Figure 1**). The presence of these cytokines and their significance values can be referenced in **Figure 2** and **Table 6**, where positive significant correlations are reported. As indicated, we identified low negative correlation values, which were found for between CCL5 and both the subjective scores NYHA and MRC Dyspnea.

We analyzed the linear relationship between the cytokine biomarkers and the modified Rankin score (22). In brief, this is a 6-point disability scale that ranges from 0 (individual has no residual symptoms) to 5 (the individual is bedridden, incontinent and requires continuous care). According to the documentation an additional value of 6 is included for deceased or "expired" individuals. For the Rankin subjective score, we identified a low positive correlation with statistical significance for two biomarkers, VEGF and sCD40L (**Table 6**). Finally, we did the correlation analysis for the COMPASS 31 score (23). This scale was developed as a robust statistical instrument to determine autonomic symptoms, thus providing relevant severity scores for clinical assessment. For this scale, we identified that several cytokines had statistically significant relationships to the subjective score (**Figure 1**). TNF-alpha and GM CSF had low positive correlations, while VEGF and sCD40L showed moderate positive correlation (**Table 6**).

Applying the New York Heart Association (NYHA) Functional Classification, which labels individuals in one of four categories, we were able to identify two statistically significant biomarkers in the joint correlation (**Figure 3** and **Table 6**). The cytokines IL-8 and GM-CSF showed a low positive correlation to the NYHA score, with both having r values between 0.30 and 0.50. The linear association between IL-8 and GM-CSF indicates that there appears to be a weak linear association between both treatment groups (before and after) where the levels of both cytokines appear to be positively associated with the NYHA score. When subsequently analyzed the correlation

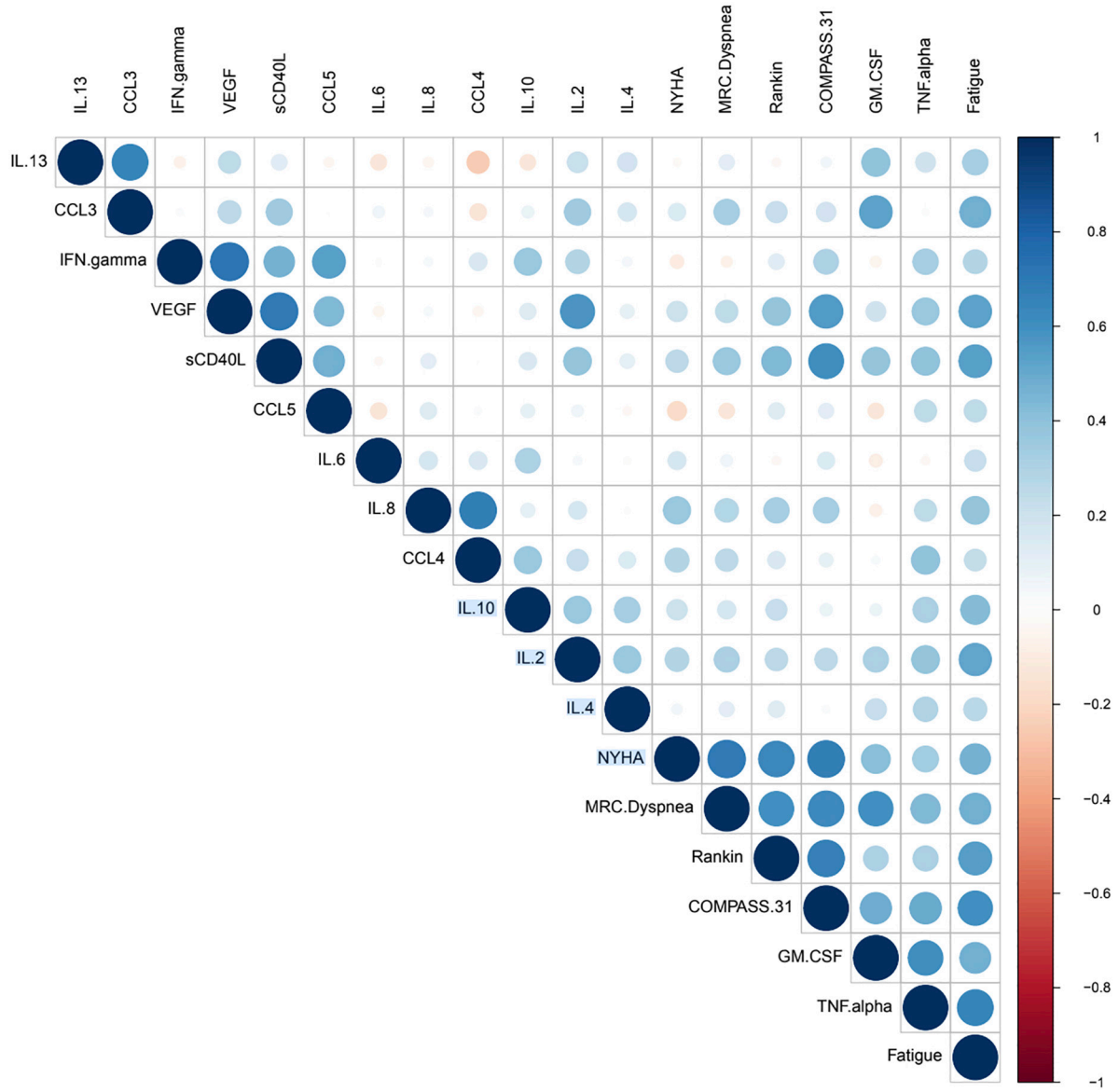

FIGURE 1
Correlation dot plot.

values for the Medical Research Council (MRC) Dyspnea scale score (Figure 3), which is a simple scale allowing participants to indicate the effects of breathlessness on mobility, we were able to identify that for both treatment groups (joint correlation), the biomarkers GM-CSF, TNF-alpha and sCD40L presented statistically correlations. In the case of GM-CSF, the linear association between the cytokine and the subjective score was 0.593, which makes it a moderate positive correlation. For TNF-alpha and sCD40L there correlation values were in ranges between 0.30 and 0.50, indicating their association with the MRC Dyspnea score were low positive.

In addition, the correlation analysis of the Fatigue score from the Shirley Ryan Ability Lab at the Rehabilitation Institute of Chicago[1] provides a 9-item scale allowing the measurement of the effects of fatigue on an individual. The scores range from a value of 9 (lowest possible score) to 63 (highest fatigue effects). Our analysis identified that various biomarkers showed statistically significant correlations (Figure 3). These linear associations were present in both the before and after treatment groups (joint correlation). The cytokines IL-2, sCD40L, TNF alpha and VEGF presented a positive correlation, with *r* values ranging between 0.50 and 0.70, as shown in Figure 1. In addition to these biomarkers, IL-8, IL-10, and GM CSF presented low positive correlations, with *r* values ranging between 0.30 and 0.50.

Our results suggest that there are a number of biomarkers that appear to be positively associated in varying degrees with the various subjective scores. The most common cytokine was sCD40L, positively associated to all scores except for the NYHA Functional Classification score. Another interesting finding is the relationship of GM-CSF to a wide variety of subjective scores. This cytokine had significant positive association to all scales except for the modified Rankin score. Finally, both VEGF and TNF-alpha were correlated with 3 of the 5 subjective scores, with VEGF not having a significant relation to NHYA and MRC Dyspnea, while TNF-alpha not correlating

1 https://www.sralab.org/rehabilitation-measures/fatigue-severity-scale

10.3389/fmed.2023.1122529

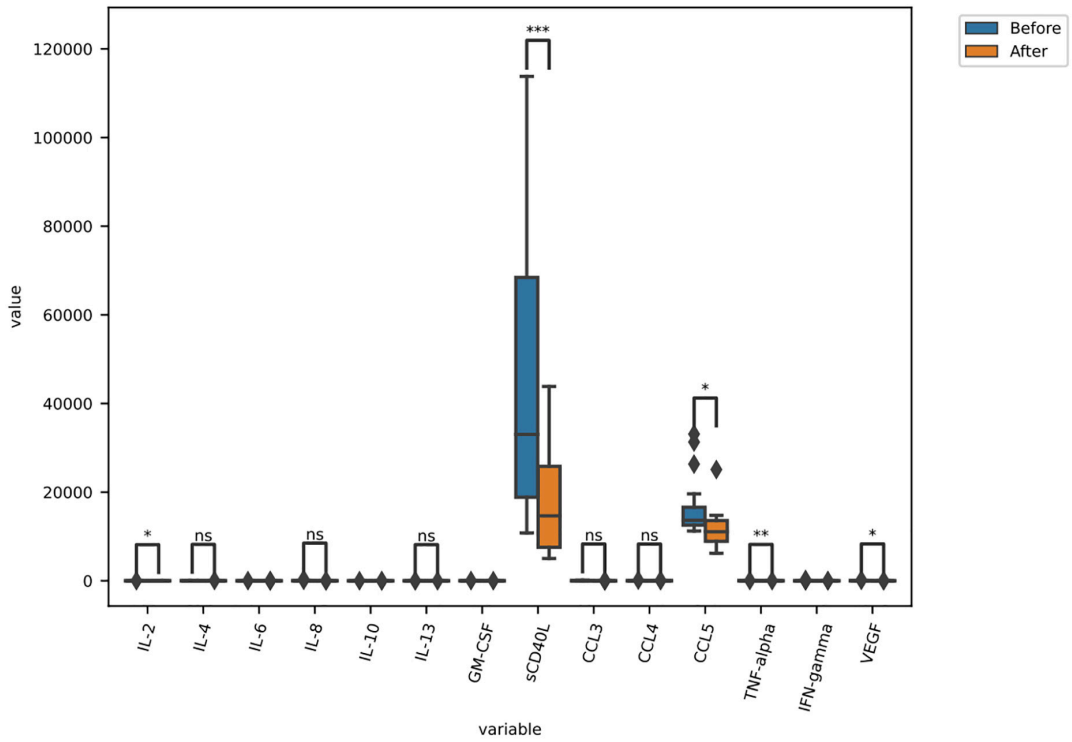

FIGURE 2
Before and after treatment individual cytokine measurement comparisons. The bar plot represent the statistical comparison using the Wilcoxon paired test between the two treatment groups (before and after). Statistical significance intervals are represented with asterisks (*), where ns indicates non-significant. *1.00e-02 $< p \leq$ 5.00e-02, **1.00e-03 $< p \leq$ 1.00e-02, ***1.00e-04 $< p \leq$ 1.00e-03, and ****$p \leq$ 1.00e-04.

to NYHA and Rankin. These results suggest that many cytokine biomarkers possess for both the before and after treatment groups positive levels of statistically significant relationship.

TABLE 6 Statistically significant positive Pearsons correlation coefficients between subjective scores and cytokines.

Score	Biomarker correlation		
Rankin	sCD40L	CC: 0.42	$p = 0.01$
	VEGF	CC: 0.40	$p = 0.02$
COMPASS-31	sCD40L	CC: 0.6	$p = 0.0001$
	VEGF	CC: 0.6	$p = 0.0005$
	GM = CSF	CC: 0.5	$p = 0.002$
	TNF-alpha	CC: 0.5	$p = 0.0026$
NYHA	IL-8	CC: 0.4	$p = 0.03$
	GM-CSF	CC: 0.4	$p = 0.01$
MRC Dyspnea	sCD40L	CC: 0.4	$p = 0.04$
	IL-2	CC: 0.4	$p = 0.05$
	TNF-alpha	CC: 0.4	$p = 0.01$
	GM-CSF	CC: 0.6	$p = 0.0002$
Fatigue Severity	sCD40L	CC: 0.5	$p = 0.001$
	IL-2	CC: 0.6	$p = 0.0005$
	TNF-alpha	CC: 0.7	$p = 4 \times 10^{-5}$
	VEGF	CC: 0.5	$p = 0.001$
	GM-CSF	CC: 0.5	$p = 0.004$

Machine learning classifier validates the labeling of individuals in the dataset group as PASC using cytokine profiles

The individuals in the dataset (data points for the before and after treatment condition) were classified as belonging to the PASC class. This labeling or classification was achieved using the random forest classifier previously published (8) and described in brief in the corresponding methods section. The 36 datapoints of the dataset (18 individuals for each treatment) were labeled with the numeric value of 3, which corresponded to PASC (0 = Normal, 1 = Mild-Moderate, 2 = Severe, and 3 = PASC). Classification off individuals using the random forest model is based on their cytokine profiles. The subjective scores were dropped as the model did not account for these. In addition, because the model was constructed using the 4 states (Normal/Unaffected, Mild-Moderate, Severe and PASC), datapoints can only be classified within one of these states.

Although we observed differences between the before and after treatment conditions (as indicated by the significance of our statistical analysis), with the one tailed-test indicating that the magnitudes in the before condition are greater than after, these changes are not sufficient to lead to a difference in classification using the machine learning model. Although the before and after groups are different when undertaking a statistical comparison, the magnitude in the shift between the groups could not be large enough to be captured as change in state, reflected by the statistical comparison and the subjective scores. Additionally, it is possible that individuals in the after group presented cytokines patterns similar top PASC at the time of sample collection, but if we were to analyze the progression of

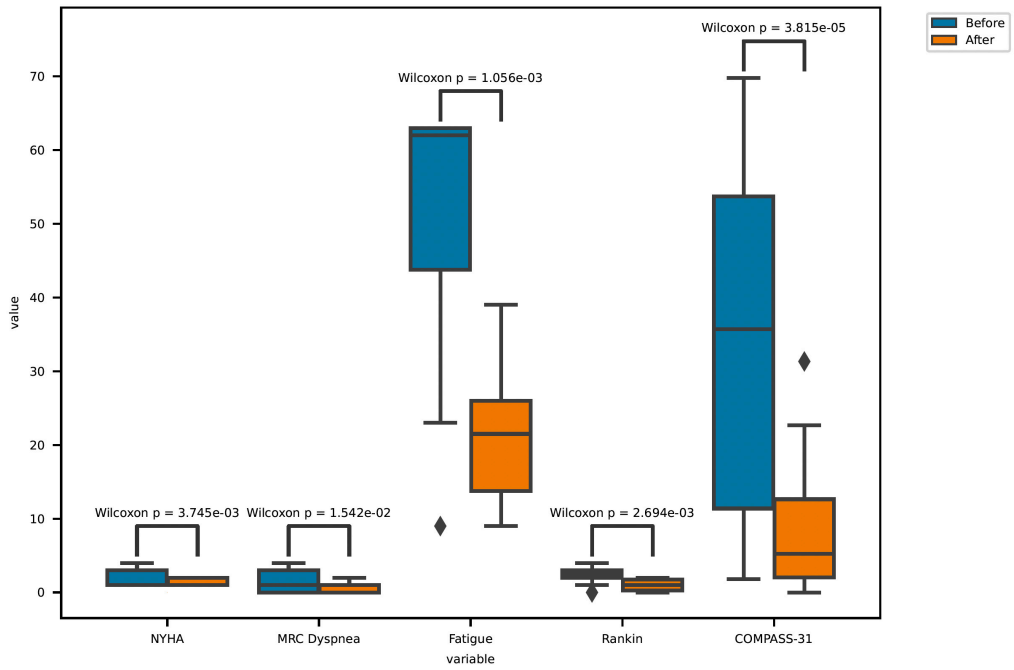

FIGURE 3
Before and after treatment individual subjective score comparisons. The bar plot represents the statistical comparison using the Wilcoxon paired test between the two treatment groups (before and after). Statistical significance intervals are represented with asterisks (*), where ns indicates non-significant. *1.00e-02 < $p \leq$ 5.00e-02, **1.00e-03 < $p \leq$ 1.00e-02, ***1.00e-04 < $p \leq$ 1.00e-03, and ****$p \leq$ 1.00e-04.

these samples in a defined time period, we could potentially observe a change in classification, as cytokine profiles continue to change.

Discussion

The discovery of CD16+ monocytes containing persistent S1 proteins from PASC patients may help further understand its pathophysiology and identify targets for therapy (4). Both CD16+ monocytes subsets, intermediate (CD14+ CD16+) and non-classical (CD14− CD16+), respectively, are known to interact significantly with the endothelium and platelets *via* the fractalkine pathway (24). This suggests that the pathophysiology of PASC may lie with the monocytic-endothelial-platelet axis. Fractalkine, which mediates cell adhesion and leucocyte recruitment, is a transmembrane protein expressed in the brain, colon, heart, and lung, along with endothelial cells and astrocytes. Intermediate monocytes express high levels of both CCR5 and fractalkine receptors, whereas non-classical monocytes express high levels of fractalkine receptors (6, 7). This interaction between fractalkine and fractalkine receptors have been involved in the pathogenesis of atherosclerosis, vasculitis, vasculopathies, and inflammatory brain disorders (5) and could also be contributing to vascular endothelialitis in PASC. Vascular endothelialitis leads to collagen exposure along with platelet activation and adherence *via* glycoprotein 1b-IX-V-receptor (GPIb-IX-V) with collagen-bound von Willebrand factor (vWF) (25). Activated platelets release soluble CD40 ligand (sCD40L) to recruit both neutrophils and monocytes to the vascular lesions (26), thus activating the coagulation cascade. Stimulated platelets also release RANTES which binds to endothelial cells and encourages monocyte adhesion to inflamed endothelial tissues (27) and acts as a chemotactic agent for inflammatory cells. Activated platelets and endothelial cells can also secrete VEGF which induces angiogenesis and microvascular hyperpermeability. VEGF is a diagnostic marker for vasculitic neuropathy and also contributes to a pro-inflammatory-prothrombotic environment (28). While the vascular effects of statins have been well-documented (29), the protective role of maraviroc on the endothelium has also been similarly published (30). Hence, we targeted CCR5 and fractalkine receptors using maraviroc and pravastatin, respectively, hypothesizing that this combination could be therapeutically effective in treating vascular endothelialitis and resolving symptoms associated with PASC.

Neurological symptoms associated with PASC include severe headaches and cognitive impairment (brain fog), along with neuropathy and weakness, necessitating the need for assistance in performing daily tasks. CD14+ CD16+ monocytes are known to transmigrate across the blood brain barrier and play an important role in central nervous system (CNS) immune surveillance. These monocytes were implicated as HIV reservoirs in the CNS causing neuroinflammation, neuronal damage, and cognitive defects (31). We hypothesize that the S1 protein containing CD14+ CD16+ monocytes in PASC patients are also crossing the blood brain barrier and triggering neuroinflammation and inducing neurological symptoms. Both maraviroc and statins are known to cross the blood-brain-barrier, and more specifically, maraviroc has been suggested as treatment for Parkinson's, neurocognitive impairment, and strokes (32). Interestingly, after the introduction of maraviroc and pravastatin, participants showed a decrease in modified Rankin scale scores (**Figure 3**) and reported improvement in neurological function and ability. These findings were correlated with a statistically significant decrease in VEGF (r = 0.4, p = 0.02) and sCD40L (r = 0.42, p = 0.01) (**Table 6**), suggesting treatment targeting cytokines associated with vascular endothelialitis correlated with improvement in neurological symptoms.

Autonomic dysfunction such as postural orthostatic tachycardia syndrome (POTS) and light sensitivity has also been associated with PASC. POTS is a syndrome consisting of unexplained tachycardia, dizziness, light-headedness, fainting, and abdominal pain. While the true etiology of POTS has yet to be defined, endothelial dysfunction has been suggested as the pathophysiology (33). There is also evidence that POTS maybe be associated with G-protein-coupled receptor autoantibodies (34). Interestingly, since CCR5 and fractalkine receptor are also G-protein-coupled receptors (9, 35), it is possible that antagonism of these receptors could also inhibit the autonomic effects of these autoantibodies. We observed a statistically significant decrease in COMPASS-31 (**Figure 3**) scores correlating with statistically significant decreases in VEGF (r = 0.6, p = 0.0005), sCD40L (r = 0.6, p = 0.0001), and TNF-alpha (r = 0.5, p = 0.0026), suggesting that pro-inflammatory macrophage activation may be triggering vascular endothelialitis. Interestingly, elevations in sCD40L have also been associated with sympathoadrenal activation and targeting these vascular markers may address PASC associated dysautonomia (36).

Cardiorespiratory complaints leading to exertional intolerance and limitation of physical activity are very commonly reported by PASC patients. Many PASC patients with cardiac and pulmonary symptoms have undergone extensive workup (EKG, echocardiogram, stress test, pulmonary function testing, etc.) which has not detected any abnormalities or pathologies. Subsequently, current clinical approaches have only been used to treat symptoms with antiarrhythmics, bronchodilators or alpha-adrenergics, instead of addressing the underlying pathophysiology. We observed an improvement in exertional tolerance and physical activity as evidenced by a decrease in NYHA functional classification (**Figure 3**). This improvement was associated with statistically significant decreases in IL-8 (r = 0.4, p = 0.03) and GM-CSF (r = 0.4, p = 0.01). Interestingly, endothelial cells are main producers of IL-8 (37) and statins are known to decrease IL-8 (38). Additionally, maraviroc has been suggested as reducing the cardiovascular risk for acute coronary disease by protecting the endothelium from pro-inflammatory macrophage infiltration (39). These mechanisms potentially support their use in addressing PASC associated cardiac symptoms. We also observed improvement in respiratory symptoms after initiating maraviroc and pravastatin therapy. Participants reported improvements as reflected by a statistically significant decrease in the MRC Dyspnea scale (**Figure 3**). These responses and improvements correlated with statistically significant decreases in IL-2 (r = 0.4, p = 0.05), GM-CSF (r = 0.6, p = 0.0002), sCD40L (r = 0.4, p = 0.04), and TNF-alpha (r = 0.4, p = 0.01). Intriguingly, CD16+ monocytes are known to produce large quantities of TNF-alpha and could be activated by the retained S1 proteins (40), causing vascular endothelialitis *via* the fractalkine-fractalkine receptor interaction in pulmonary vasculature. Elevations in sCD40L have been associated with pulmonary arterial hypertension (PAH) (41), while IL-2 can induce pulmonary microvasculature injury and generate an asthma-like bronchoconstriction (42). We previously published a multi-class model score that described an increase IL-2 as a characteristic specific to PASC (8), thus confirming the clinical significance of IL-2 in PASC. Both maraviroc and statins can decrease IL-2 and TNF-alpha (38, 43), which may explain the observed improvements in PASC associated respiratory symptoms. The patient Fatigue Severity Score (FSS) also significantly decreased (**Figure 3**) after maraviroc and pravastatin which correlated with decrease in sCD40L (r = 0.5, p = 0.001), VEGF (r = 0.5, p = 0.001), TNF-alpha (r = 0.7, p = 4e-5), IL-2 (r = 0.6, p = 0.0005), and GM-CSF (r = 0.5, p = 0.004), again suggesting that targeting the monocytic-platelet-endothelial axis can alleviate PASC associated fatigue.

Despite a black box warning for hepatoxicity, maraviroc has demonstrated a strong safety profile in adult, pediatric, and neonatal populations (44, 45). Analysis of the MOTIVATE study demonstrated a low incidence of hepatoxicity with maraviroc even after 96 weeks of treatment at the FDA approved dose of 300 mg B.I.D (46). This influenced our decision to treat with this dose. Hepatic safety was monitored in all the participants by measuring and evaluating AST, ALT, and total bilirubin (LFTs) prior to commencing treatment with maraviroc and every 2 weeks while on treatment. None of participants presented here experienced any clinical signs of hepatotoxicity or elevated liver function serologies while on, or after, treatment. Maraviroc is metabolized by CYP3A4, and we chose to avoid any CYP3A4 metabolizing statins to mitigate any potential drug interactions. This approach guided our decision to treat with pravastatin 10 mg PO daily over the other statins since it is metabolized *via* glucuronidation. However, the therapeutic benefits with other statins have also been observed and should be considered.

Due to rising numbers of post-COVID symptoms and lack of studies and approved therapeutics, many patients have been on different therapeutics. This was reflected in the participants of this case series where some were previously on other therapeutics including ivermectin, fluvoxamine, and prednisone. This presents a significant limitation in this case series because what is unknown is whether these patients were already getting better from these medications before commencing maraviroc and pravastatin. After starting maraviroc and pravastatin, some participants saw symptom relief after 6 weeks, while others needed treatment up to 12 weeks before discontinuing medications. We recognize that studies will need to be conducted to understand this variation in length of treatment between participants. We followed up bi-monthly with these 18 patients for up to 12 weeks post-treatment and no one reported that their symptoms worsened or returned during this period.

Other limitations and weakness of the study were no in-person, objective assessments due to the virtual nature of our clinic, the lack of the control arm and the open label nature of the study. Since immune subset assays were not available for this study, in the future, we would also like to study CD4/CD8 ratios and the amount of S1 proteins in CD16+ monocytes before and after treatment. The results we present in this case series do not replace the need for a double-blinded placebo controlled randomized trial to understand drug efficacy. However, we do believe this study sets the framework for our future clinical trial designs to further investigate the efficacy and usefulness of maraviroc and pravastatin to treat PASC.

Data availability statement

The original contributions presented in this study are included in the article/supplementary material, further inquiries can be directed to the corresponding author.

Ethics statement

The studies involving human participants were reviewed and approved by CCTC Ethics and IRB Committee. The

patients/participants provided their written informed consent to participate in this study.

Author contributions

RY, EO, and MZ conceptualized the study. RY organized the study. JG-C and RM-R performed the bioinformatics. RY, JG-C, and RM-R wrote the draft of the manuscript. All authors contributed to revising the manuscript and approved the submitted version.

Acknowledgments

The authors would like to acknowledge the work of Brittany McKenney RN, Amy White RN, Surlin Chadha RN, Amanda Robinson, and Christine Meda in assisting in the study and interacting with the patients.

Conflict of interest

IncellDX holds the patent for the use of CCR5 antagonists (maraviroc) in COVID and long COVID. BP was employed by IncellDX Inc. BP, RY, PP, JB, EO, DJ, CR, and MK were independent contractors of the CCTC.

The remaining authors declare that the research was conducted in the absence of any commercial or financial relationships that could be construed as a potential conflict of interest.

Publisher's note

References

1. Soriano J, Murthy S, Marshall J, Relan P, Diaz J, Who Clinical Case Definition Working Group on Post-Covid-19 Condition. A clinical case definition of Post-COVID-19 condition by a Delphi consensus. *Lancet Infect Dis.* (2021) S1473-3099:703–9.

2. Davis H, Assaf G, McCorkell L, Wei H, Low R, Re'em Y, et al. Characterizing long COVID in an international cohort: 7 months of symptoms and their impact. *EClinicalMedicine.* (2021) 38:101019. doi: 10.1016/j.eclinm.2021.101019

3. Novak P, Mukerji S, Alabsi H, Systrom D, Marciano S, Felsenstein D, et al. multisystem involvement in post-acute sequelae of coronavirus disease 19. *Ann Neurol.* (2021) 91:367–79.

4. Patterson B, Francisco E, Yogendra R, Long E, Pise A, Rodrigues H, et al. Persistence of SARS-CoV2-2 S1 protein in CD16+ monocytes in post-acute sequelae of covid-19 (PASC) up to 15 months post-infection. *Front Immunol.* (2022) 12:746021. doi: 10.3389/fimmu.2021.746021

5. Thomas G, Tacke R, Hedrick C, Hanna R. Nonclassical patrolling monocyte function in the vasculature. *Arterioscler Thromb Vasc Biol.* (2015) 35:1306–16.

6. Kapellos T, Bonaguro L, Gemünd I, Reusch N, Saglam A, Hinkley E, et al. Human monocyte subsets and phenotypes in major chronic inflammatory diseases. *Front Immunol.* (2019) 10:2035. doi: 10.3389/fimmu.2019.02035

7. Weber C, Belge KU, Hundelshausen P v, Draude G, Steppich B, Mack M, et al. Differential chemokine receptor expression and function in human monocyte subpopulations. *J Leukoc Biol.* (2000) 67:699–704.

8. Patterson BK, Guevara-Coto J, Yogendra R, Francisco EB, Long E, Pise A, et al. Immune-based prediction of COVID-19 severity and chronicity decoded using machine learning. *Front Immunol.* (2021) 12:700782. doi: 10.3389/fimmu.2021.700782

9. Oppermann M. Chemokine receptor CCR5: insights into structure, function, and regulation. *Cell Signal.* (2004) 16:1201–10.

10. Vangelista L, Vento S. The expanding therapeutic perspective of CCR5 blockade. *Front Immunol.* (2018) 8:1981. doi: 10.3389/fimmu.2017.01981

11. Marques R, Guabiraba R, Russo R, Teixeira M. Targeting CCL5 in inflammation. *Expert Opin Ther Targets.* (2013) 17:1439–60.

12. Patterson BK, Seethamraju H, Dhody K, Corley MJ, Kazempour K, Lalezari J, et al. CCR5 inhibition in critical COVID-19 patients decreases inflammatory cytokines, increases CD8 T-cells, and decreases SARS-CoV2 RNA in plasma by day 14. *Int J Infect Dis.* (2021) 103:25–32. doi: 10.1016/j.ijid.2020.10.101

13. Bowen G, Borgland S, Lam M, Libermann T, Wong N, Muruve D. Adenovirus vector-induced inflammation: capsid-dependent induction of the C-C chemokine RANTES requires NF-kappa B. *Hum Gene Ther.* (2002) 13:367–79. doi: 10.1089/10430340252792503

14. Arberas H, Guardo AC, Bargalló ME, Maleno MJ, Calvo M, Blanco JL, et al. In vitro effects of the CCR5 inhibitor maraviroc on human T cell function. *J Antimicrob Chemother.* (2013) 68:577–86. doi: 10.1093/jac/dks432

15. Pozo-Balado MM, Rosado-Sánchez I, Méndez-Lagares G, Rodríguez-Méndez MM, Ruiz-Mateos E, Benhnia MR, et al. Maraviroc contributes to the restoration of the homeostasis of regulatory T-cell subsets in antiretroviral-naive HIV-infected subjects. *Clin Microbiol Infect.* (2016) 22:e1–5. doi: 10.1016/j.cmi.2015.12.025

16. Cimato T, Palka B. Fractalkine (CX3CL1), GM-CSF and VEGF-A levels are reduced by statins in adult patients. *Clin Transl Med.* (2014) 3:14. doi: 10.1186/2001-1326-3-14

17. Sanner MF. Python: a programming language for software integration and development. *J Mol Graph Model.* (1999) 17:57–61.

18. Mckinney W. *pandas: a foundational python library for data analysis and statistics.* (2021). Available online at: http://pandas.sf.net (accessed April 17, 2021)

19. Virtanen P, Gommers R, Oliphant T, Haberland M, Reddy T, Cournapeau D, et al. SciPy 1.0: fundamental algorithms for scientific computing in Python. *Nat Methods.* (2020) 17:261–72. doi: 10.1038/s41592-019-0686-2

20. Ihaka R, Gentleman RR. A language for data analysis and graphics. *J Comput Graph Stat.* (1996) 5:299–314. doi: 10.1080/10618600.1996.10474713

21. Chawla NV, Bowyer K, Hall L, Kegelmeyer WP. SMOTE: synthetic minority over-sampling technique. *J Artif Intell Res* (2002) 16:321–57. doi: 10.1613/jair.953

22. Modified Rankin Score (MRS). *Specifications manual for joint commission national quality measures (v2018A).* (2022). Available online at: https://manual.jointcommission.org/releases/TJC2018A/DataElem0569.html (accessed February 3, 2022).

23. Sletten D, Suarez G, Low P, Mandrekar J, Singer W. COMPASS 31: a refined and abbreviated composite autonomic symptom score. *Mayo Clin Proc.* (2012) 87:1196–201. doi: 10.1016/J.MAYOCP.2012.10.013

24. Kasama T, Wakabayashi K, Sato M, Takahashi R, Isozaki T. Relevance of the CX3CL1/Fractalkine-CX3CR1 pathway in vasculitis and vasculopathy. *Transl Res.* (2010) 155:20–6. doi: 10.1016/j.trsl.2009.08.009

25. Varga-Szabo D, Pleines I, Nieswandt B. Cell adhesion mechanisms in platelets. *Arterioscler Thromb Vasc Biol.* (2008) 28:403–12.

26. Flierl U, Bauersachs J, Schäfer A. Modulation of platelet and monocyte function by the chemokine fractalkine (CX3CL1) in cardiovascular disease. *Eur J Clin Invest.* (2015) 45:624–33. doi: 10.1111/eci.12443

27. Hundelshausen P v, Weber KS, Huo Y, Proudfoot AE, Nelson PJ, Ley K, et al. RANTES deposition by platelets triggers monocyte arrest on inflamed and atherosclerotic endothelium. *Circulation.* (2001) 103:1772–7.

28. Cuadrado MJ, Buendía P, Velasco F, Aguirre MA, Barbarroja N, Torres LA, et al. Vascular endothelial growth factor expression in monocytes from patients with primary antiphospholipid syndrome. *J Thromb Haemost.* (2006) 4:2461–9.

29. Liberale L, Carbone F, Montecucco F, Sahebkar A. Statins reduce vascular inflammation in atherogenesis: a review of underlying molecular mechanisms. *Int J Biochem Cell Biol.* (2020) 122:105735. doi: 10.1016/j.biocel.2020.105735

30. Francisci D, Pirro M, Schiaroli E, Mannarino MR, Cipriani S, Bianconi V, et al. Maraviroc intensification modulates atherosclerotic progression in HIV-suppressed patients at high cardiovascular risk. A randomized, crossover pilot study. *Open Forum Infect Dis.* (2019) 6:ofz112. doi: 10.1093/ofid/ofz112

31. Veenstra M, León-Rivera R, Li M, Gama L, Clements J, Berman J. Mechanisms of CNS viral seeding by HIV+ CD14+ CD16+ monocytes: establishment and reseeding of viral reservoirs contributing to HIV-associated neurocognitive disorders. *mBio.* (2017) 8:e1280–1217. doi: 10.1128/mBio.01280-17

32. Mondal S, Rangasamy S, Roy A, Dasarathy S, Kordower J, Pahan K. Low-dose maraviroc, an antiretroviral drug, attenuates the infiltration of T-cells into the central nervous system and protects the nigrostriatum in hemiparkinsonian monkeys. *J Immunol.* (2019) 202:3412–22. doi: 10.4049/jimmunol.1800587

33. Liao Y, Chen S, Liu X, Zhang Q, Ai Y, Wang Y, et al. Flow-mediated vasodilation and endothelium function in children with postural orthostatic tachycardia syndrome. *Am J Cardiol.* (2010) 106:378–82. doi: 10.1016/j.amjcard.2010.03.034

34. Gunning W, Stepkowski S, Kramer P, Karabin B, Grubb B. Inflammatory biomarkers in postural orthostatic tachycardia syndrome with elevated G-Protein-coupled receptor autoantibodies. *J Clin Med.* (2021) 10:623. doi: 10.3390/jcm10040623

35. Poniatowski ŁA, Wojdasiewicz P, Krawczyk M, Szukiewicz D, Gasik R, Kubaszewski Ł, et al. Analysis of the role of CX3CL2(Fractalkine) and its receptor CX3CR1 in traumatic brain and spinal cord injury: insight into recent advances in actions of neurochemokine agents. *Mol Neurobiol.* (2017) 54:2167–88. doi: 10.1007/s12035-016-9787-4

36. Johansson PI, Sørensen AM, Perner A, Welling K, Wanscher M, Larsen CF, et al. High sCD40L levels early after trauma are associated with enhanced shock, sympathoadrenal activation, tissue and endothelial damage, coagulopathy and mortality. *J Thromb Haemost.* (2012) 10:207–16. doi: 10.1111/j.1538-7836.2011.04589.x

37. Oude Nijhuis C, Vellenga E, Daenen S, Kamps W, De Bont E. Endothelial cells are main producers of interleukin 8 through toll-like receptor 2 and 4 signaling during bacterial infection in leukopenic cancer patients. *Clin Diagn Lab Immunol.* (2003) 10:558–63. doi: 10.1128/cdli.10.4.558-563.2003

38. Sakoda K, Yamamoto M, Negishi Y, Liao J, Node K, Izumi Y. Simvastatin decreases IL-6 and IL-8 production in epithelial cells. *J Dent Res.* (2006) 85:520–3.

39. Cipriani S, Francisci D, Mencarelli A, Renga B, Schiaroli E, D'Amore C, et al. Efficacy of the CCR5 antagonist maraviroc in reducing early, ritonavir-induced atherogenesis and advanced plaque progression in mice. *Circulation.* (2013) 127:2114–24. doi: 10.1161/CIRCULATIONAHA.113.001278

40. Belge K, Dayyani F, Horelt A, Siedlar M, Frankenberger M, Frankenberger B, et al. The proinflammatory CD14+CD16+DR++ monocytes are a major source of TNF. *J Immunol.* (2002) 168:3536–42. doi: 10.4049/jimmunol.168.7.3536

41. Damås JK, Otterdal K, Yndestad A, Aass H, Solum NO, Frøland SS, et al. Soluble CD40 ligand in pulmonary arterial hypertension. *Circulation.* (2004) 110:999–1005.

42. Rabinovici R, Sofronski MD, Borboroglu P, Spirig AM, Hillegas LM, Levine J, et al. Interleukin-2-induced lung injury. The role of complement. *Circ Res.* (1994) 74:329–35. doi: 10.1161/01.res.74.2.329

43. Kim S, Kang H, Jhon M, Kim J, Lee J, Walker A, et al. Statins and inflammation: new therapeutic opportunities in psychiatry. *Front Psychiatry.* (2019) 10:103. doi: 10.3389/fpsyt.2019.00103

44. Giaquinto C, Mawela MP, Chokephaibulkit K, Negra MD, Mitha IH, Fourie J, et al. Pharmacokinetics, safety and efficacy of maraviroc in treatment-experienced pediatric patients infected with CCR5-tropic HIV-1. *Pediatr Infect Dis J.* (2018) 37:459–65. doi: 10.1097/INF.0000000000001808

45. Gulick RM, Fatkenheuer G, Burnside R, Hardy WD, Nelson MR, Goodrich J, et al. Five-year safety evaluation of maraviroc in HIV-1–infected treatment-experienced patients. *J Acquir Immune Defic Syndr.* (2014) 65:78–81. doi: 10.1097/QAI.0b013e3182a7a97a

46. Ayoub A, Alston S, Goodrich J, Heera J, Hoepelman A, Lalezari J, et al. Hepatic safety and tolerability in the maraviroc clinical development program. *AIDS.* (2010) 24:2743–50. doi: 10.1097/QAD.0b013e32833f9ce2

frontiers | Frontiers in Medicine

TYPE Case Report
PUBLISHED 03 May 2023
DOI 10.3389/fmed.2023.1117474

OPEN ACCESS

EDITED BY
Francesco Paolo Bianchi,
University of Bari Aldo Moro, Italy

REVIEWED BY
Lei Huang,
First Hospital, Peking University, China
Roberto Spina,
Gosford Hospital, Australia
Rimjhim Kanaujia,
Post Graduate Institute of Medical Education and Research (PGIMER), India

*CORRESPONDENCE
Jian Lu
✉ szlujian@szu.edu.cn
Yitao He
✉ heyitaovv@126.com

†These authors have contributed equally to this work

RECEIVED 06 December 2022
ACCEPTED 04 April 2023
PUBLISHED 03 May 2023

CITATION
Yang M, Lin Y, Peng X, Wu J, Hu B, He Y and Lu J (2023) *Abiotrophia defectiva* causing infective endocarditis with brain infarction and subarachnoid hemorrhage: a case report. *Front. Med.* 10:1117474. doi: 10.3389/fmed.2023.1117474

Abiotrophia defectiva causing infective endocarditis with brain infarction and subarachnoid hemorrhage: a case report

Miaojuan Yang[1,2,3†], Yanxia Lin[4†], Xin Peng[5], Jingsong Wu[6], Bo Hu[1,2,3], Yitao He[1,2,3*] and Jian Lu[4*]

[1]Department of Neurology, The Second Clinical Medical College of Jinan University, Shenzhen, Guangdong, China, [2]The First Affiliated Hospital of Southern University of Science and Technology, Shenzhen, Guangdong, China, [3]Shenzhen Clinical Research Center for Geriatrics, Shenzhen People's Hospital, Shenzhen, China, [4]Department of Infectious Diseases, Shenzhen University General Hospital, Shenzhen, China, [5]Department of Cardiology, Huazhong University of Science and Technology Union Shenzhen Hospital, Shenzhen, Guangdong, China, [6]Department of Laboratory Medicine, Shenzhen People's Hospital, Shenzhen, China

Introduction: A rare pathogen of Infective Endocarditis (IE), the *Abiotrophia defectiva,* has been known to trigger life-threatening complications. The case discussed here is of a teenager with brain infarction and subarachnoid hemorrhage caused by IE due to *A. defectiva*.

Case report: A 15-year-old girl with movement disorders involving the left limbs and intermittent fevers was admitted to the hospital. A head CT scan revealed cerebral infarction in the right basal ganglia and subarachnoid hemorrhage. Moreover, vegetation on the mitral valve were confirmed by echocardiography. The blood cultures were found to be positive for Gram-positive streptococcus and identified by Vitek mass spectrometry as *A. defectiva*. She was prescribed vancomycin antibacterial therapy and underwent a surgical mitral valve replacement.

Conclusion: This case is suggestive of the fact that *A. defectiva* is a rare but crucial pathogen of IE-associated stroke. Obtaining early blood cultures and using microbial mass spectrometry could help achieve an accurate diagnosis. Moreover, reasonable anti-infective medications and surgical interventions need to be combined to avoid and/or manage severe complications.

KEYWORDS

***Abiotrophia defectiva*, infective endocarditis, brain infarction, subarachnoid hemorrhage, microbial mass spectrometry**

Introduction

Abiotrophia defectiva (*A. defectiva*), was originally known to be a Nutritionally Variant Streptococci (NVS). This NVS was subsequently reclassified as *Abiotrophia defectiva*, *Granulicatella adiacens*, *Granulicatella elegans*, and *Granulicatella balaenopterae* through 16S rRNA gene sequencing. These organisms are normal colonization bacteria of the human body. *A. defectiva* needs L-cysteine, pyridoxal, and other such factors for its proper growth. In earlier case reports, the subacute IE were the most frequently reported cases of *A. defectiva* due to their indolent clinical course. Nevertheless, *A. defectiva* led to severe complications including valvular damage, congestive heart failure, and events of embolisation. Thus, early diagnosis and effective treatment strategy for *A. defectiva* become crucial in clinical practice.

Case description

A 15-year-old girl was admitted to Shenzhen People's Hospital Neurology Intensive Care Unit (NICU) due to the sudden onset of a left-sided movement disorder. She experienced a sudden episode of weakness in her left lower limb one and a half months prior to hospitalization, which resolved spontaneously 3 days later. A month ago, she developed weakness in her left upper extremity, which disappeared after 5 days. Intermittent fevers of 39°C started 1 week ago, along with mild shortness of breath but no chills, cough, diarrhea, or bladder irritation symptoms. She noticed the sudden onset of a persistent left-limb movement disorder 3 h before being admitted to the NICU. She claimed to have lost 7.5 kilograms (17 percent of her body weight) in 3 months. She underwent orthodontic treatment a year ago and subsequently wore braces. She denied having a history of hypertension, diabetes, cigarette smoking, alcohol consumption, intravenous drug use, immunosuppressant use, atrial fibrillation, and inherited diseases.

She was conscious on physical examination, and her verbal responses to questions were appropriate. Her face was pale, her left lower limb muscle strength was grade II, her left upper limb muscle strength was grade III, and both Babinski and Brudzinski's signs were positive. In addition, a grade 4–6 systolic murmur was heard in the mitral region, splenomegaly was confirmed by abdominal palpation, and clubbed fingers were observed upon careful inspection of the hands.

Laboratory analysis showed the following: a normal leukocyte count, but mild normocytic anemia (hemoglobin, 91 g/L); an elevated C-reactive protein level of 32.05 mg/L (normal range, 0–5 mg/L); and a slightly elevated procalcitonin level (0.07 ng/mL; normal range, < 0.05 ng/mL). The NT-proBNP level was 1,123 pg/m (normal range, < 125 pg/mL). The cerebrospinal fluid (CSF) was red, the pressure was 180 mm H_2O, the glucose level decreased (1.79 mmol/L; normal range, 3.9–6.1 mmol/L), the protein concentration increased (0.55 g/L; normal range, 0.15-0.45 g/L), the nucleated cell number increased (280 /μL; normal range, < 20 /μL), and the CSF culture was negative.

A head CT scan urgently performed revealed a cerebral infarction in the right basal ganglia and a subarachnoid hemorrhage (Figure 1). A transthoracic echocardiogram (TTE) revealed vegetation on the mitral leaflets measuring 2.3 × 1.3 cm (Figure 2). Before administering ceftriaxone to the patient, three blood cultures (aerobic and anaerobic bottles from peripheral blood once every half an hour) were obtained. After 9.5 h, the blood culture was positive for facultative anaerobic Gram-positive streptococcus, which was immediately identified as *A. defectiva* (Figure 3) with the Vitek MS using library v3.2 (bioMérieux, Marcy-l'Étoile, France) and the percent of identity is 99.9%. According to antimicrobial susceptibility testing (Supplementary Figure 1), the bacteria were susceptible to vancomycin, clindamycin, and linezolid but resistant to penicillin, ceftriaxone, and cefepime. All three blood cultures tested positive for *A. defectiva*. The girl met two of the modified Duke diagnostic criteria for IE. Based on the susceptibility test results, the antibiotic therapy was immediately changed to vancomycin, 3 days later, the girl's temperature turned normal. The girl was transferred to a higher-level hospital for cardiovascular surgery on the tenth hospital day. Three weeks later, she underwent mitral valve replacement surgery. Upon discharge, two months after the onset of symptoms, her left lower limb muscle strength was grade V, while the left upper limb muscle showed a strength of grade IV.

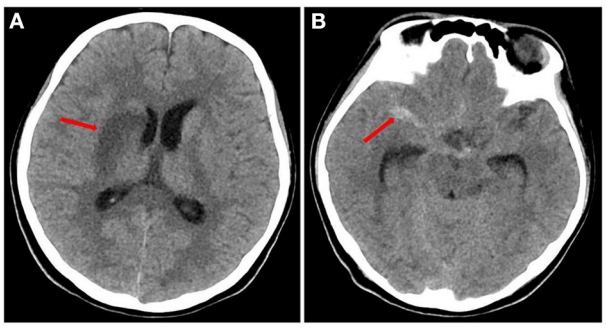

FIGURE 1
Head CT of the patient **(A)** the red arrow indicates infarction of the right basal ganglia. **(B)** The red arrow indicates subarachnoid hemorrhage.

Discussion

A. defectiva is a facultative anaerobic Gram-positive coccus that was first reported in a case of IE in 1961 (1). *A. defectiva* normally afflicts the respiratory, urogenital, and gastrointestinal tracts (2). The IE caused by *A. defectiva* usually occurs in patients with congenital heart disease or a history of previous cardiac surgery (3). Moreover, oral hygiene, and a dental procedure could also be important causes of *A. defectiva* related IE (4, 5). In the pertinent case, the girl had a history of an orthodontics procedure, which could have contributed to IE. Compared to other pathogens leading to IE, *A. defectiva* is more likely to form valvular vegetations and lead to cardiogenic emboli (6, 7). Literature suggests that due to the production of a considerable amount exopolysaccharides, the organism has a higher affinity for the endocardium and the ability to bind with fibronectin in the extracellular matrix, further contributes to their virulence (8, 9). Colonization and infection of corneas, joints and heart valves may indicate a significant tendency of the bacterium to colonize vascular free collagen tissue (10). Besides, *A. defectiva* endocarditis has an indolent course and is often culture-negative, contributing to a delayed diagnosis, with high mortality, and complication rates (6). The NVS are estimated to cause approximately 5%−6% of all cases of IE (11), the mortality rate of NVS IE is 9.2% (12). In the patient in the pertinent case, the disease course continued for 6 weeks. Unfortunately, the IE was complicated by heart failure, a brain infarction, and subarachnoid hemorrhage when diagnosed.

The patient, in this case, the young girl, was admitted to the NICU with symptoms associated with brain infarction, hence, urgent brain imaging was essential to confirm the stroke diagnosis and guide the therapy strategies. Moreover, the etiology of brain infarction determines the subsequent prevention strategies. Stroke, cardioembolic causes, and arterio-pathic causes are the most frequent etiologies in childhood (defined as 29 days to 18 years of

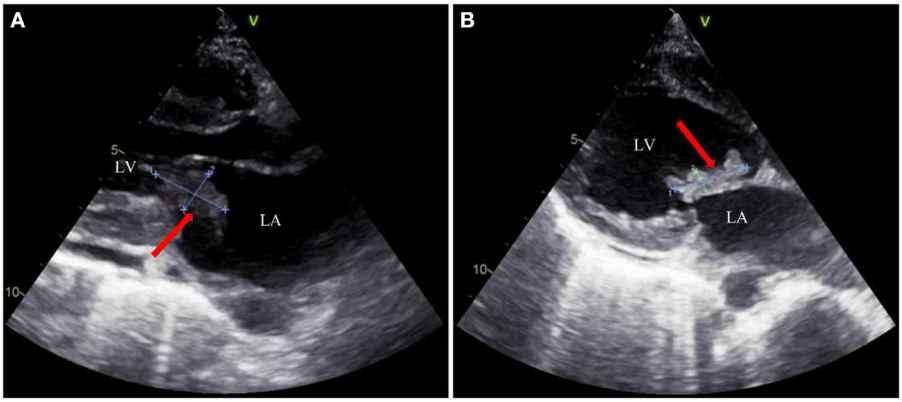

FIGURE 2
Transthoracic echocardiography examination of the heart in the patient. **(A)** THE red arrow indicates the vegetation (2.3 × 1.3 cm) on the mitral valve. **(B)** The red arrow indicates another position of the vegetation (2.3 × 0.7 cm) on the mitral valve. LA: left atrium; LV: left ventricle.

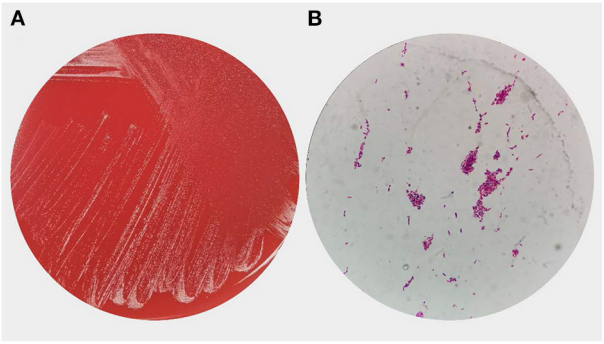

FIGURE 3
Overview of *Abiotrophia defectiva* of growth morphology **(A)** Colony growth of *A. defectiva* on blood agar. **(B)** Smear showing gram-positive cocci in chains.

age). The reasons for arterial ischemic stroke include congenital or acquired heart disease, non-atherosclerotic arteriopathies (arterial dissection, focal cerebral arteriopathy, and Moyamoya), and sickle cell diseases (13).

For the diagnosis of IE, an echocardiogram and laboratory testing (especially blood cultures) would be needed. In the current case, timely blood cultures and bacterial mass spectrometry facilitated the rapid identification of a rare pathogen, like *A. defectiva*. The 16S rRNA sequencing also played an important role in verification of *A. defective* (14). Moreover, Metagenomic Next-Generation Sequencing (mNGS) has been reported in the clinical diagnosis of IE (15). Compared to conventional cultures, the mNGS has been found to be more sensitive and particularly suitable for rare or culture-negative pathogens (16). Recently, Du reported a case of IE caused by *A. defectiva*, with the diagnosis being assisted by mNGS (17).

The administration of proper antibiotics is the foundation of the IE treatment. According to the 2015 European Society of Cardiology (ESC) guidelines, penicillin G, ceftriaxone, or vancomycin need to be used for 6 weeks, combined with an aminoglycoside for at least 2 weeks (18). The American Heart Association guidelines recommend the administration of a combination regimen that includes ampicillin (12 g/d in divided doses) or penicillin (18–30 million U/D in divided doses or by continuous infusion) plus gentamicin (3 mg/kg/day in 2–3 divided doses) with infectious diseases consultation to determine the duration of the therapy (19). Almost all susceptibility studies have reported that *A. defectiva* was susceptible to vancomycin. Although *A. defectiva* susceptibility to ceftriaxone was 92%–100% (20), in this case study, the bacteria were resistant to ceftriaxone. In IE caused by *A. defectiva*, approximately 27% of patients need prosthetic valve replacement (21). Due to the large mitral valve vegetations (>1 cm) and severe embolic events, the pertinent patient had to undergo surgical mitral valve replacement.

Conclusion

This case study indicated that *A. defectiva* is an important cause of IE, which could lead to severe complications. Thus, timely application of blood cultures and rapid identification of *A. defectiva* would enable the proper prescription of antibiotics. Moreover, effective anti-infective medications and surgical interventions need to be combined to avoid and/or manage serious complications.

Data availability statement

The original contributions presented in the study are included in the article/Supplementary material, further inquiries can be directed to the corresponding authors.

Ethics statement

Written informed consent was obtained from the individual(s), and minor(s)' legal guardian/next of kin, for the publication

of any potentially identifiable images or data included in this article. Written informed consent was obtained from the participant/patient(s) for the publication of this case report.

Author contributions

MY: diagnosis and treatment of the patient and conception and creation of the manuscript. YL: conceptualization and original draft preparation. XP: writing. JW: microbial identification. BH: clinical consultation. YH: reviewing. JL: supervision and reviewing. All authors contributed to the article and approved the submitted version.

Funding

This study was supported by Shenzhen Basic Research Key projects, Shenzhen Science and Technology Innovation Commission (JCYJ20200109144220704), and Natural Science Foundation of Shenzhen University General Hospital (SUGH2018QD047).

Conflict of interest

The authors declare that the research was conducted in the absence of any commercial or financial relationships that could be construed as a potential conflict of interest.

Publisher's note

Supplementary material

The Supplementary Material for this article can be found online at: https://www.frontiersin.org/articles/10.3389/fmed.2023.1117474/full#supplementary-material

SUPPLEMENTARY FIGURE 1
Antimicrobial susceptibility test results of *Abiotrophia defectiva* according to CLSI M45 criterion. MIC, Minimum Inhibitory Concentration; KB, Kirby-Bauer Test; I, Intermediate; R, Resistant; S, Susceptible.

References

1. Frenkel A, Hirsch W. Spontaneous development of L forms of streptococci requiring secretions of other bacteria or sulphydryl compounds for normal growth. *Nature.* (1961) 191:728–30. doi: 10.1038/191728a0

2. Al-Jasser AM, Enani MA, Al-Fagih MR. Endocarditis caused by *Abiotrophia defectiva*. *Libyan J Med.* (2007) 2:43–5. doi: 10.3402/ljm.v2i1.4691

3. Baltimore RS, Gewitz M, Baddour LM, Beerman LB, Jackson MA, Lockhart PB, et al. Infective endocarditis in childhood: 2015 update: a scientific statement from the american heart association. *Circulation.* (2015) 132:1487–515. doi: 10.1161/CIR.0000000000000298

4. Blochowiak KJ. Dental treatment and recommended management in patients at risk of infective endocarditis. *Kardiochir Torakochirurgia Pol.* (2019) 16:37–41. doi: 10.5114/kitp.2019.83944

5. Birlutiu V. and Birlutiu RM, Endocarditis due to Abiotrophia defectiva, a biofilm-related infection associated with the presence of fixed braces: a case report. *Medicine (Baltimore).* (2017) 96:e8756. doi: 10.1097/MD.0000000000008756

6. Kalogeropoulos AS, Siva A, Anderson L. *Abiotrophia defectivus* infectious endocarditis: think beyond the heart. *Lancet.* (2015) 385:1044. doi: 10.1016/S0140-6736(15)60090-3

7. Tellez A, Ambrosioni J, Llopis J, Pericas JM, Falcas C, Almela M, et al. Epidemiology, clinical features, and outcome of infective endocarditis due to abiotrophia species and granulicatella species: report of 76 Cases, 2000-2015. *Clin Infect Dis.* (2018) 66:104–11.

8. Park S, Ann H, Ahn J, Ku N, Han S, Hong G, et al. A case of infective endocarditis caused by *Abiotrophia defectiva* in Korea. *Infect Chemother.* (2016) 48:229–33. doi: 10.3947/ic.2016.48.3.229

9. Pinkney JA, Nagassar RP, Green KJ, Ferguson T. Abiotrophia defectiva endocarditis. *BMJ Case Rep.* (2014) 201:bcr20142073614. doi: 10.1136/bcr-2014-207361

10. Abry F, Sauer A, Riegel P, Saleh M, Gaucher D, Schatz C, et al. Infectious crystalline keratopathy caused by Streptococcus *Abiotrophia defective. Cornea.* (2010) 29:934–6. doi: 10.1097/ICO.0b013e3181ca2e8f

11. Ruoff KL. Nutritionally variant streptococci. *Clin Microbiol Rev.* (1991) 4:184–90. doi: 10.1128/CMR.4.2.184

12. Garcia-Granja PE, Lopez J, Vilacosta I, Sarria C, Ladroon R, Olmos C, et al. Nutritionally variant streptococci infective endocarditis: a different view. *Clin Infect Dis.* (2018) 67:1800–1. doi: 10.1093/cid/ciy444

13. Sporns PB, Fullerton H, Lee S, Kim H, Lo W, Mackay M, et al. Childhood stroke. *Nat Rev Dis Primers.* (2022) 8:12. doi: 10.1038/s41572-022-00337-x

14. Rozemeijer W, Jiya TU, Rijnsburger M, Heddema E, Savelkoul P, Ang W. Abiotrophia defectiva infection of a total hip arthroplasty diagnosed by 16S rRNA gene sequencing. *Diagn Microbiol Infect Dis.* (2011) 70:142–4. doi: 10.1016/j.diagmicrobio.2010.11.016

15. Tattevin P, Watt G, Revest M, Arvieux C, Fournier P-E. Update on blood culture-negative endocarditis. *Med Mal Infect.* (2015) 45:1–8. doi: 10.1016/j.medmal.2014.11.003

16. Fukui Y, Aoki K, Okuma S, Sato T, Ishii Y, Tateda K. Metagenomic analysis for detecting pathogens in culture-negative infective endocarditis. *J Infect Chemother.* (2015) 21:882–4. doi: 10.1016/j.jiac.2015.08.007

17. Du Y, Zhang Z, Chen C, Xia H, Zhang H, Guo Z, et al. Case report: report of infective endocarditis caused by *Abiotrophia defectiva* and literature review. *Front Pediatr.* (2022) 10:894049. doi: 10.3389/fped.2022.894049

18. Habib G, Lancellotti P, Antunes MJ, Bongiomi MG, Casalta J, Zotti F, et al. 2015 ESC Guidelines for the management of infective endocarditis: The Task Force for the Management of Infective Endocarditis of the European Society of Cardiology (ESC). Endorsed by: European Association for Cardio-Thoracic Surgery (EACTS), the European Association of Nuclear Medicine (EANM). *Eur Heart J.* (2015) 36:3075–128. doi: 10.1093/eurheartj/ehv319

19. Baddour LM, Wilson W, Bayer A, Fowler V, Tleyjeh I, Rybak M, et al. Infective endocarditis in adults: diagnosis, antimicrobial therapy, and management of complications: a scientific statement for healthcare professionals from the american heart association .*Circulation.* (2015) 132:1435–86.

20. Dumm RE, Wing A, Richterman A, Jacob J, Glaser L, Rodino K. Closing the brief case: a variant on a classic-abiotrophia *Defectiva endocarditis* with discitis. *J Clin Microbiol.* (2021) 59:e0309420. doi: 10.1128/JCM.03094-20

21. Kiernan TJ, O'Flaherty N, Gilmore R, Ho E, Hickey M, et al. Abiotrophia defectiva endocarditis and associated hemophagocytic syndrome–a first case report and review of the literature. *Int J Infect Dis.* (2008) 12:478–82. doi: 10.1016/j.ijid.2008.01.014

Frontiers in Medicine

Translating medical research and innovation into improved patient care

A multidisciplinary journal which advances our medical knowledge. It supports the translation of scientific advances into new therapies and diagnostic tools that will improve patient care.

Discover the latest Research Topics

See more →

Frontiers

Avenue du Tribunal-Fédéral 34
1005 Lausanne, Switzerland
frontiersin.org

Contact us

+41 (0)21 510 17 00
frontiersin.org/about/contact